ROLL RATE BASED STABILITY CONTROL - THE ROLL STABILITY CONTROL ™ SYSTEM

Jianbo Lu
Dave Messih
Albert Salib
Ford Motor Company
United States
Paper Number 07-136

ABSTRACT

This paper presents the Roll Stability Control ™ system developed at Ford Motor Company. It is an active safety system for passenger vehicles. It uses a roll rate sensor together with the information from the conventional electronic stability control hardware to detect a vehicle's roll condition associated with a potential rollover and executes proper brake control and engine torque reduction in response to the detected roll condition so as to mitigate a vehicular rollover.

INTRODUCTION

The traditional electronic stability control (ESC) systems aim to control the yaw and sideslip angle of a moving vehicle through individual wheel braking and engine torque reduction such that the desired path of a vehicle determined through the driver's inputs (e.g., steering input) can be maintained. That is, ESC systems help the vehicle to follow the driver's intent such that the driver maintains good control of the vehicle regardless of the variation of road conditions.

Beyond yaw and sideslip control, brake controls in ESC systems have been pursued to mitigate vehicular rollovers in recent years. For example, [1] describes an enhanced system over Driver Stability Control systems for commercial trucks. [2] proposes a stand-alone function called Anti-Rollover Braking (ARB) when an impending rollover of a vehicle is sensed. In [3], engineers from Bosch describe a rollover mitigation function over its ESP system. Continental Teves has developed an Active Rollover Prevention (ARP) system. [4] proposes a Rollover Control Function (RCF). Note that the aforementioned systems use only ESC hardware. In addition to ESC-based brake controls, other chassis control systems have been pursued to mitigate rollovers, see [5], [6], [7], [8] and [9] for more details.

In order to achieve smooth rollover control without sacrificing other vehicle dynamics performance attributes with respect to road and driving condition variations, precise detection or prediction of a potential rollover event is critical. Due to the lack of precise detection of potential rollover conditions and driving conditions such as road bank and vehicle loading, the aforementioned approaches need to conduct necessary trade-offs between control sensitivity and robustness.

In this paper, a system referred to as Roll Stability Control™ (RSC), is presented. Such a system is designed specifically to mitigate vehicular rollovers. The idea of RSC, first documented in [10], was developed at Ford Motor Company and has been implemented on various vehicles within Ford Motor Company since its debut on the 2003 Volvo XC90. The RSC system adds a roll rate sensor and necessary control algorithms to an existing ESC system. The roll rate sensor, together with the information from the ESC system, help to effectively identify the critical roll conditions which could lead to a potential vehicular rollover. Such critical roll conditions need to be discriminated from those due to road bank variations and to be characterized with respect to vehicle loading variations. RSC then applies pressure to the brake(s) on the wheel(s) of the outside of the turn. This reduces lateral force and helps keep the inside wheels firmly on the ground, thus reducing the likelihood of a rollover event.

Although a complete RSC system includes many algorithm modules such as sensor off-set compensation, sensor signal filtering and processing, sensor plausibility, active wheel lift detection, software enhancement of brake hydraulics, longitudinal velocity computation, etc., this paper focuses on vehicle roll dynamics and state estimation as well as the RSC control strategy. Interested readers may find more details on those topics from various patents granted to Ford Motor Company such as (but not limited to) [11],[12],[13],[14],[15] and [16].

This paper is organized as follows. The vehicle roll stability and state estimation are discussed in the next section. The sequential section provides a brief description of vehicle loading estimation. Wheel lift detection is discussed in the next section. The last two sections focus on various RSC control strategies and the conclusions.

VEHICLE ROLL DYNAMICS SENSING AND STATE ESTIMATION

Vehicular roll instability (rollover) is the condition where a vehicle has divergent roll motion along its roll axis.

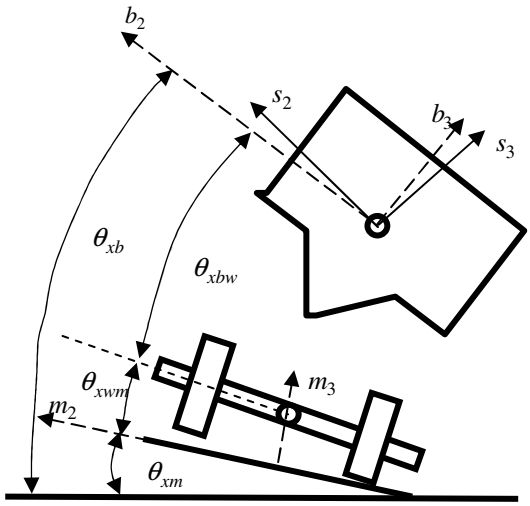

Figure 1. The roll angle definitions for a vehicle driven on a banked road.

Consider a vehicle driven on a general road surface. Figure 1 shows a rear view of the vehicle. Its roll instability can be identified and characterized by using the vertical travel of the wheel centers with respect to the smooth road surface. That is, it is said to be roll instable if it has sustainable two wheel lift from the road surface (both wheels are on the inside of a turn).

The roll instability can also be determined by using various roll information. In order to define the various roll angles, we define two coordinate systems: a body-fixed coordinate system b with axes b_1, b_2 and b_3 (called the body frame) and a road coordinate system m with axes m_1, m_2 and m_3 which is attached to the road surface but moves and yaws with the vehicle body (called a moving road frame). The roll angle of the vehicle body with respect to the sea level is denoted as θ_{xb}, the road bank angle with respect to the sea level is denoted as θ_{xm}, the roll angle between the wheel axle and the road surface is denoted as θ_{xwm} (which is called a wheel departure angle), and the roll angle between the body and the axle of the wheels is denoted as θ_{xbw} (which is called a chassis roll angle).

The critical roll angle defining a potential rollover event is the relative roll angle θ_{xbm} between the vehicle body and the moving road, which is defined as

$$\theta_{xbm} = \theta_{xbw} + \theta_{xwm} \quad (1)$$

or

$$\theta_{xbm} = \theta_{xb} - \theta_{xm} \quad (2)$$

If the magnitude of θ_{xbm} is greater than a threshold for a certain duration, the vehicle is likely to be roll-instable.

The relative roll angle θ_{xbm} may be determined through laser height sensors which measure the distances of the vehicle body at the sensor mounting locations from the road surface along the direction of the laser beams. However using them in mass production for rollover detection purpose is generally cost prohibitive with the current technology. Therefore using the other sensors equipped with the vehicle is desired.

			RSC→→→→→→→→→→→→→	
		ESC→→→→→→→→→→→→→→→→→→→→		
	Traction Control→→→→→→→→→→→→→→→→→→→→			
ABS→→→→→→→→→→→→→→→→→→→→→→→→→→→→→→→→				
1988	**1998**	**2001**	**2003**	**2005 -**
Key Sensor Inputs: Wheel Speeds	Key Sensor Inputs: Same as ABS	Key Sensor Inputs: Steering Wheel Angle, Yaw Rate, Lateral Acceleration, MC Pressure, Longitudinal Acceleration	Key Sensor Inputs: Roll Rate The RSC System was first available on the 2003 Volvo XC90	AdvanceTrac® with RSC is standard on Explorer, Mountaineer, Aviator and Navigator since the 2005 MY, E-350 Econoline Extended Passenger vans since the 2006 MY, and Expedition, Escape, Edge, Explorer SportTrac, Lincoln MKX, Mazda CX – 9, Land Rover LR2, Mazda Tribute and Mercury Mariner for 2007 MY

Figure 2. The evolution of the sensors used in vehicle stability control systems.

The sensor set used in the RSC system evolved from the initial sensors equipped on an anti-lock brake system (ABS), see Figure 2. It includes a centralized motion sensor cluster called the RSC sensor cluster, a steering wheel angle sensor, four wheel speed sensors, a master cylinder pressure sensor, etc. The RSC sensor cluster adds a roll rate senor to the ESC motion sensor cluster, i.e., it is composed of a roll rate sensor, a yaw rate sensor, a lateral accelerometer and a longitudinal accelerometer, which are packaged together along the three orthogonal directions.

Since the measuring directions of the RSC sensor cluster do not always coincide with the directions of the body frame b, it is necessary to define a sensor frame s. The angular differences between frame b and frame s are called the sensor misalignments, which are usually generated due to the mounting errors when the RSC sensor cluster is attached to the vehicle body. Although the sensor misalignments are relatively small, they may need to be corrected in order to avoid potential signal contamination. In addition to the sensor misalignments, oftentimes the misalignment between the vehicle body and the road surface due to unevenly distributed loading inside the vehicle may also need to be corrected. For example, a vehicle with heavy loading near the rear axle might cause the RSC sensor cluster to be tilted with a pitch angle relative to the road surface. These misalignments can be conditionally determined based on the sensor and the calculated signals and the driving conditions.

The kinematics of the RSC sensor cluster can be expressed as in the following equations after small angle approximations and neglecting the vehicle's vertical velocity [17]

$$\begin{aligned} \dot{\theta}_{xs} &\approx \omega_{xs} + \omega_{zs}\theta_{ys} \\ \dot{v}_{xs} &\approx a_{xs} + \omega_{zs}v_{ys} + g\theta_{ys} \\ \dot{v}_{ys} &\approx a_{ys} - \omega_{zs}v_{xs} - g\theta_{xs} \end{aligned} \quad (3)$$

where ω_{xs} and ω_{zs} are the angular rates along the longitudinal and vertical directions, a_{xs} and a_{ys} are the longitudinal and lateral accelerations of the origin of the sensor frame attached to the RSC sensor cluster, v_{xs} and v_{ys} are the longitudinal and lateral velocities of the origin of the sensor frame. θ_{xs} and θ_{ys} are the roll and pitch angles of the sensor frame with respect to the sea level. Notice that v_{xs} in (3) can be related to the vehicle reference velocity calculated based on the wheel speed sensor signals.

Based on (3), it is not hard to find the following:

(i) the roll rate sensor only provides global information of the sensor frame with respect to the sea level, $\dot{\theta}_{xb}$ as in Figure 1, which cannot be directly used as a control variable to drive the RSC system;

(ii) the global roll and pitch angles can be determined from the accelerometers if the lateral velocity v_{ys} is known, however in reality, it is unknown;

(iii) the lateral velocity or sideslip angle can be determined from the lateral acceleration sensor signal if the global roll angle can be determined;

(iv) the roll rate sensor will have non-zero output even if there is no roll attitude change when there is yaw rate on a pitched road.

Since there are uncertainties in the roll rate sensor signal and in the computation of the pitch angle, direct integration of the first equation in (3) is not practical due to the potential of integration drift. Therefore, in order to use the roll rate sensor information to determine critical roll angles and roll conditions used for RSC, various computations are required.

Chassis Roll Angle Estimation

Let's first consider computing the roll angle θ_{xbw} between the body-fixed frame and the axle of the wheels, which is called the chassis roll angle.

Let F_{yf} and F_{yr} be the resultant forces along the lateral direction of the RSC sensor cluster but applied to the vehicle body through the front and rear roll centers of the vehicle. Let the vertical distance from the vehicle body c.g. location to the front and rear roll centers be h_f and h_r. Let l_{s2cg} be the longitudinal distance between the origin of the RSC sensor cluster and the c.g. of vehicle body. Using Newton's law in the sensor frame s, we obtain the following equations of motion

$$
\begin{aligned}
M_s(a_{ys} + l_{s2cg}\dot{\omega}_{zs}) &= F_{yf} + F_{yr} \\
I_z\dot{\omega}_{zs} &= F_{yf}b_f - F_{yr}b_r \\
I_x\dot{\omega}_{xs} &= F_{yf}h_f + F_{yr}h_r - K_{roll}\theta_{xbw} - D_{roll}\dot{\theta}_{xbw}
\end{aligned} \quad (4)
$$

where I_x and I_z are the moments of inertia of the vehicle body with respect its longitudinal and vertical body axes; K_{roll} and D_{roll} are the equivalent roll stiffness and damping rate for the suspension system; b_f and b_r are the distance of the vehicle body c.g. to the front and rear axles with $b = b_f + b_r$.

Based on equations in (4) and using the Laplace transformation, the chassis roll angle can be computed as in the following

$$\theta_{xbw} = T_1(s)a_{ycgs} + T_2(s)\omega_{sx} + T_3(s)\omega_{zs} \quad (5)$$

where $T_1(s), T_2(s)$ and $T_3(s)$ are three transfer functions which can be obtained through the inertia parameters, their formulas can be found in [18], and

$$a_{ycgs} = a_{ys} + l_{s2cg}\dot{\omega}_{zs}$$

is the lateral acceleration of the vehicle body at its c.g. location but projected along the lateral direction of the frame s.

Notice that the above calculated chassis roll angle is based on a linear model with a fixed vehicle body roll axis, hence it will deviate from the true value if the vehicle has wheel lift and if the vehicle enters into the nonlinear suspension operation region. Such a computation can be sensitive to the vehicle's loading due to the variation of the center of gravity and roll moment of inertia. However if there is no wheel-lift, θ_{xbw} closely models the true relative roll angle between the vehicle body and the road if the vehicle parameters, such as the sprung mass and height of the c.g. are accurate. Hence a small magnitude of θ_{xbw} is a good indication of a roll-stable situation.

Global Roll Angle Estimation

The aforementioned chassis roll angle will be saturated when one side of the vehicle is about to lift from the ground due to the suspension saturation and it is independent of the wheel departure angle θ_{xwm}. Therefore θ_{xbw} can no longer characterize the relative roll between the vehicle body and the road during a potential rollover event.

In order to overcome this, a roll angle based on the roll rate sensor signal is pursued. Based on the analysis before, roll angle obtained through the roll rate sensor is a global roll angle and includes various components as shown in Figure 1.

Since θ_{xs} computed based on the roll rate sensor signal is the sum of the road bank, the wheel departure angle, and the chassis roll angle, it provides a means to confirm certain variables if the other variables are known. On the other hand, if the vehicle is driven on level ground without wheel lift, the global roll angle θ_{xs} matches the chassis roll angle θ_{xbw}. Such a global roll angle can also be used in determining the road camber status which could have a significant influence on the roll stability of the vehicle.

As mentioned before, there are various uncertainties when trying to capture the velocity of the global roll angle θ_{xb}. Denote the uncertainties due to sensor off-sets, drifts and misalignments in roll and yaw rate sensors as $\Delta\omega_{xs}$ and $\Delta\omega_{zs}$, the chassis pitch angle due to suspension motion as θ_{ybw} and a steady state characterization of the global pitch angle as θ_{ybss}, then the velocity of the global roll angle can be related to the estimated value from the sensor signal $\dot{\hat{\theta}}_{xb}$ as

$$\dot{\hat{\theta}}_{xb} = \dot{\theta}_{xb} - \Delta\dot{\theta}_{xb} \quad (6)$$

and the uncertainties $\Delta\dot{\theta}_{xb}$ can be expressed as

$$\Delta\dot{\theta}_{xb} = \Delta\omega_{xs} + \omega_{zs}\theta_{ybss} + \Delta\omega_{zs}\theta_{ybss} + \Delta\omega_z\theta_{ybw} \quad (7)$$

And $\dot{\hat{\theta}}_{xb}$ can be calculated from the known variables as in the following

$$\dot{\hat{\theta}}_{xb} = \omega_{xs} + \omega_{zs}\theta_{ybw} \quad (8)$$

where θ_{ybw} is the chassis pitch angle (see [6] for detail).

If the steady state capture of the vehicle body's global pitch angle θ_{ybss} can be estimated, such as in [19],

$\Delta\dot{\theta}_{xb}$ and $\dot{\hat{\theta}}_{xb}$ can be alternatively computed as in the following

$$\begin{aligned}\Delta\dot{\theta}_{xb} &= \Delta\omega_{xs} + \Delta\omega_{zs}\theta_{ybss} + \Delta\omega_z\theta_{ybw} \\ \dot{\hat{\theta}}_{xb} &= \omega_{xs} + \omega_{zs}(\theta_{ybw} + \theta_{ybss})\end{aligned} \quad (9)$$

Since the uncertainties in $\Delta\dot{\theta}_{xb}$ defined in (7) are usually dominated by low frequency content, an anti-drift integration filter $T_{adi}(s)$ is used to integrate $\dot{\hat{\theta}}_{xb}$ to obtain the dynamic content of the true global roll angle. Notice that, in critical roll instable situations, such a roll velocity $\dot{\hat{\theta}}_{xb}$ defined in (8) or (9) together with $T_{adi}(s)$ can be used to characterize the roll conditions that might lead to a potential rollover.

Since $T_{adi}(s)$ removes both the low frequency content of the uncertainty and the low frequency content of the true global roll angle, a steady-state recovery term is used. This leads to the following estimation of the global roll angle

$$\hat{\theta}_{xb} = T_{adi}(s)\dot{\hat{\theta}}_{xb} + T_{ss}(s)\theta_{xbss} \quad (10)$$

where θ_{xbss} is the steady state capture the roll angle. One computation of θ_{xbss} is

$$\theta_{xbw} + \theta_{xwm}$$

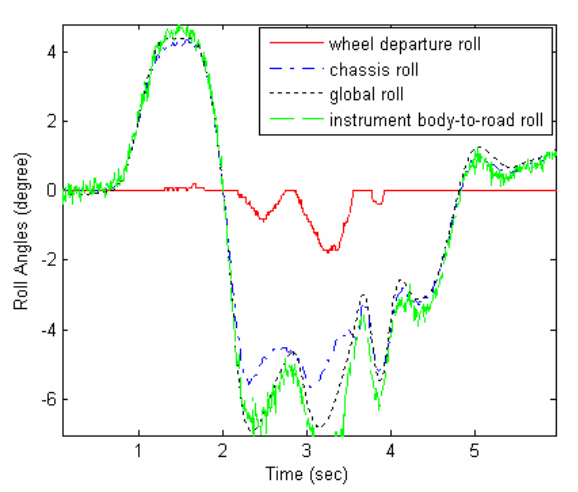

Figure 3. A comparison of the measured roll angle and the calculated roll angle when the vehicle is driven on a level ground.

Another computation of θ_{xbss} is the global roll angle from the 3rd equation of (3) by setting $\dot{v}_{ys} = 0$ or setting $\dot{v}_{ys}$ to the computation generated from the linear sideslip angle. Further details regarding the computation of θ_{xb} can be found in [20].

Figure 3 provides a comparison between the computed global roll angle estimation $\hat{\theta}_{xb}$ using (10) and the relative roll angle between the vehicle body and the moving road using laser height sensors, for a vehicle driven on level ground during a lane change maneuver. Since the road is level, the bank angle θ_{xm} of the moving road is zero. Hence the global roll angle should match the relative roll angle between the body and the road.

Wheel Departure Angle Estimation

The global roll angle together with the chassis roll angle discussed in the previous sections can quantify the axle angle, which is the sum of the road bank angle and the wheel departure angle, but can not determine the magnitude of each.

By utilizing the roll dynamics of the vehicle and wheel lift detection methods to be described later, the conditional determination of the wheel departure angle is obtained.

Let's denote the axle velocity as

$$\dot{\theta}_{xaxle} = \dot{\hat{\theta}}_{xb} - \dot{\theta}_{xbw} \quad (11)$$

then the velocity of the wheel departure angle is

$$\dot{\theta}_{xwm} = \dot{\theta}_{xaxle} - \dot{\theta}_{xm} \quad (12)$$

Integrating (12) gives

$$\theta_{xwm}(t) = \int_0^t \dot{\theta}_{xaxle}(\tau)d\tau - \theta_{xm}(t) \quad (13)$$

Since θ_{xwm} becomes non-zero when there is wheel lift, it is obvious that the integration should be conducted whenever wheel lift is initiated. Assume at time instant t_0, there is a detected wheel lift. Let the road bank angle at time t_0 be θ_{xm0}. Then, (13) implies

$$0 = \int_0^{t_0} \dot{\theta}_{xaxle}(\tau) d\tau - \theta_{xm0} \quad (14)$$

At time instant t such that $t_0 \le t \le t_f$ (t_f is the time instant when the lifted wheels come back in contact with the road surface), we subtract (14) from (13) and obtain the following

$$\theta_{xwm}(t) = \int_{t_0}^{t} \dot{\theta}_{xaxle}(\tau) d\tau - [\theta_{xm}(t) - \theta_{xm0}] \quad (15)$$

If the vehicle is driven on level ground or on a constant road bank, (15) leads to

$$\theta_{xwm}(t) = \hat{\theta}_{xwm}(t) = \int_{t_0}^{t} \dot{\theta}_{xaxle}(\tau) d\tau \quad (16)$$

Notice that $\hat{\theta}_{xwm}$ is a good approximation of θ_{xwm} if the change in road bank is small, i.e., if

$$\Delta\theta_{xm}(t) = \theta_{xm}(t) - \theta_{xm0} \quad (17)$$

is close to zero or negligible with respect to $\hat{\theta}_{xwm}$. This is true for the following conditions:

(i) the vehicle is driven on a level ground;

(ii) the vehicle is not driven on a transient road bank;

(iii) during the time when there is wheel lift the road bank doesn't change much in comparison with the road bank at the time when the wheel lifting starts;

(iv) during the time when there is wheel lift, the vehicle is driven very aggressively such that the roll velocity due to the road bank is much smaller than the roll velocity due to the wheel departure and the chassis roll.

Notice that the afore-mentioned cases cover a large portion of the scenarios where wheel lift could occur, especially since wheel lift is often short in duration (typically less than 1 second). During this time the magnitude of change of the road bank is typically very small. Therefore, the magnitude of change in road bank should be much less than the magnitude of $\hat{\theta}_{xwm}$. A detailed computation regarding wheel departure angle can be found in [21].

Figure 3 shows the computed chassis roll angle, global roll angle, wheel departure angle and the instrumented roll angle between the body and the moving road for a vehicle driven on level ground in a double lane change maneuver (with detuned control). It is not hard to see that the wheel departure angle fills the gap between the true relative roll between the body and the moving road, and the chassis roll angle.

Road Bank Angle Estimation

The relative roll angle between the vehicle body and the road surface can be computed based on (1) using the variables calculated in the previous sections and it can also be computed based on (2) using the road bank angle information. The advantage of using (2) is that it relies on the known characterization of the road bank based on the computed variables and its influence on the vehicle's roll tendency.

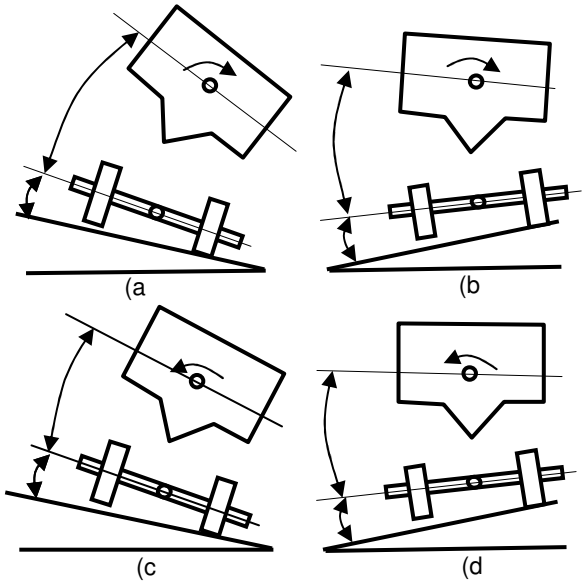

Figure 4. The 4 cases for a vehicle turning left on a banked road.

Figure 4 shows the 4 patterns of the interaction between the vehicle dynamics and the road bank when a vehicle turns to the left on banked roads. (a) and (c) are the off-camber turns and (b) and (d) are on-camber turns.

In the off-camber turns, (a) indicates the worst case scenario where the vehicle roll motion is amplified by the road bank, while in (c) the vehicle rolls in the opposite direction of the road bank, hence the vehicle has less tendency to rollover. In the on-camber turns (b) and (d), the vehicle roll motions are either

reduced or increase in the direction which does not cause rollover at all.

Based on the computed wheel departure angle, chassis roll angle and the global roll angle, and the physical meaning of road bank, a road bank adjustment in order to generate favorable control variable θ_{xbm} for RSC using (2) can be conducted as in [22,23].

Rear Sideslip Angle Estimation

Based on the third equation in (3), the lateral velocity of the vehicle at the origin of the sensor frame can be calculated if the global roll angle is available. Further analysis shows that such a lateral velocity is the only unknown if using the RSC sensor cluster signals, which satisfied a second order differential equation without involving the other unknowns such as the global roll and pitch angles. Therefore, using the RSC sensor set the lateral velocity can be computed which is robust to road bank and slope and the driving conditions, see [24] for a detailed discussion.

The sideslip angle defined at the rear axle of the vehicle can be determined as in the following

$$\beta_{ra} = \frac{v_{ys} - \omega_{zs} l_{xs2ra}}{\max(v_x, \underline{v}_x)} \quad (18)$$

where $\underline{v}_x$ is the minimum lateral velocity threshold and l_{xs2ra} is the distance between the sensor location and the rear axle location.

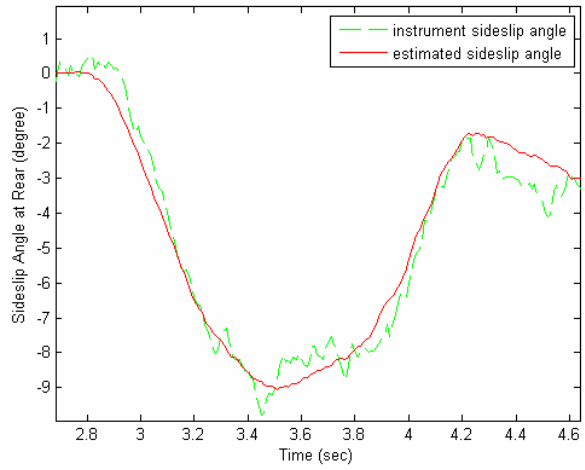

Figure 5. A comparison of the calculated sideslip angle and the measured sideslip angle.

Figure 5 shows a comparison between the measured sideslip angle and the calculated sideslip angle during a maneuver. The measured sideslip angle is calculated based on the velocity sensors equipped with the vehicle which measures the longitudinal and lateral velocities of the vehicle body at the velocity sensor mounting location.

VEHICLE LOADING DETECTION

One of the important control variables used in the RSC system is the relative roll angle θ_{xbm} between the vehicle body and the road surface, which directly measures the potential of a rollover event. Such an angle can be computed as in (1). Hence the accuracy of the chassis roll angle θ_{xbw} can influence the RSC control performance.

Since chassis roll angle is calculated through a linear roll model, the parameters used in the model are functions of characteristics such as the height of the c.g. and the sprung mass. One challenge with using these parameters in computing θ_{xbw} is that they vary with the vehicle loading conditions.

For example, a 150 pound roof load for a typical SUV with a curb weight of 5000 pounds may cause a 30% error in the chassis roll angle calculations if computed assuming no load. Note that a 150 pound load accounts for only a 3% mass variation over the vehicle curb weight. If the above parameters are fixed at certain nominal values in the RSC system, it is conceivable that optimal control performance may not be achieved under a different loading condition. For example, if the parameters in the chassis roll angle model are determined based on nominal vehicle loading condition assumptions, without considering variations due to loading, the chassis roll angle may be under estimated for vehicles with load that raises the c.g. On the other hand, if the parameters in the chassis roll angle model are determined based on a certain loading condition that raises the c..g., it may be over estimated for vehicles without load.

In order to improve the overall performance of the RSC system, it is desirable to estimate and update the vehicle parameters periodically or adaptively adjust them in real time based on the actual behavior of the vehicle.

The loading condition of the vehicle can be determined based on the fact that during level road driving the chassis roll angle must match the vehicle's

global roll angle when the vehicle doe not have wheel lift.

By equating (5) and (10), the composite parameters used to determine the chassis roll angle can be learned through a real-time least-square parameter identification algorithm. Such information is used to adjust the feedback control gains so as to request more aggressive brake pressure when appropriate.

WHEEL LIFT DETECTION

In order to confirm when the vehicle wheels are firmly on the ground and when the vehicle has wheel lift, wheel-lift detection is conducted in RSC. Wheel-lift status is also used in estimating wheel departure angle by determining when to conduct the integration in (16). The wheel lift detection includes an active wheel lift detection (AWLD) logic and a passive wheel lift detection (PWLD) logic. The integrated wheel lift detection (IWLD) integrates AWLD and PWLD to provide the final wheel-lift status. The wheel lift status for each wheel is set to one of 5 levels which assume values of 2, 4, 8, 16 and 32 that indicate the wheel being absolutely grounded, possibly grounded, no indication, possibly lifted and absolutely lifted, respectively.

AWLD is used to determine if a wheel is lifted or grounded by checking the wheel rotation in response to a given brake pressure. More specifically, it sends a small brake pressure to an inside wheel, then checks the response of that lightly braked wheel. If the vehicle lateral acceleration sensor indicates a hard cornering of the vehicle on a high mu surface and the inside wheel experiences a longitudinal slip ratio larger than a threshold in response to a relatively small brake pressure, then this inside wheel is likely to be lifted from the ground. Due to the reactive nature of this strategy, a lifted conclusion based on AWLD suffers a potential time delay.

The intent of PWLD is to determine if a wheel is lifted or grounded by checking the vehicle dynamics and wheel speed behavior without actively requesting brake pressures. Namely, it passively monitors the wheel speeds together with the other key vehicle dynamics variables to determine if the speeds indicate a potential wheel lift condition.

In order to capitalize on the benefits of AWLD during steady-state driving conditions and the instantaneous nature of PWLD during dynamic maneuvers, an integration of AWLD and PWLD is required. Figure 6 illustrates such an integration. A detailed description of the above wheel lift detection methods can be found in [25].

Figure 7 shows the final wheel lift detection status for a wheel during a J-turn maneuver with a detuned control. The brake pressure due to the AWLD request and the wheel speed response are also included in the figure.

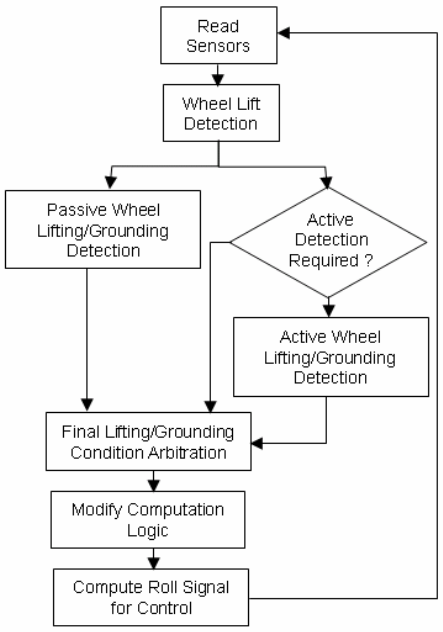

Figure 6. The integration between AWLD and PWLD.

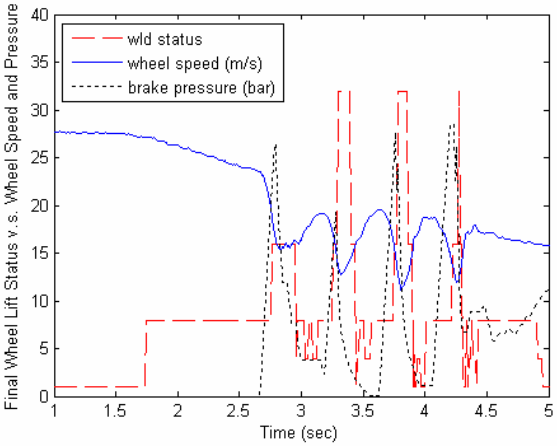

Figure 7. The wheel lift detection flag for an inside wheel during a J-turn maneuver (with detuned control).

RSC CONTROL STRATEGY

The RSC control strategies are designed to utilize all the available information to overcome the delays in the brake hydraulics and to provide effective brake torques to counteract the vehicle body roll motion which may lead to a rollover. It includes a Transition Control module which performs control for the transitional portion of a dynamic maneuver, and a Quasi-steady State Feedback Control which performs control for less dynamic maneuvers. The interaction between those two strategies provides an effective control for mitigating vehicular rollovers, see [26], [27], [28] and [29] for more details.

Transition Control

In order to execute the RSC function, a large brake pressure is requested on the front outside wheel during potentially roll-instable events. When the RSC function requests the maximum pressure build rate, significant delays in brake pressure buildup can occur due to limitations in the hydraulic capabilities. Therefore, if a brake pressure buildup is requested after the roll instability is underway, there may not be sufficient time to build an adequate control pressure to mitigate the roll-instable event. To deal with such a brake pressure build delay, the first control strategy used in the Transition Control module is a feedforward control that is used to pre-charge the hydraulic system. Such a feedforward control utilizes the prediction information based on the driver's steering and the other vehicle state information to provide a pressure build prior to the roll instability. Note that this pre-charge is designed to minimize pressure build delay, and therefore is a relatively small pressure to overcome the inertia in the brake controls pump and to reduce the caliper knockback.

The other control strategy used in the Transition Control module is a feedback control which is the coordination and combination of three feedback control commands based on three different control signals so as to achieve three different control objectives.

One of the feedback control signals used in RSC is θ_{xbw}. The brake pressure command from θ_{xbw} uses a PD feedback control where the control gains and deadbands are functions of various measured and computed signals. Notice that θ_{xbw} is adjusted to adapt to various vehicle loading conditions. Since for sufficiently aggressive transitional maneuvers, the roll momentum can result in a lifting of the center of gravity of the vehicle at the end of the transition. It is an objective of this θ_{xbw} based PD feedback control to introduce effective roll damping before the occurrence of wheel lift by rounding off the buildup of lateral force when needed as it approaches its peak level in the final phase of the transition.

Due to the limitation in hydraulic capabilities, a leading indicator of θ_{xbw} is needed to effectively utilize the roll feedback so as to sufficiently mitigate potential rollovers. Therefore another control signal used in the Transition Control module is the model-based linear sideslip angle, β_{falin}, at the front axle, which is the front tire lateral force divided by the front tire cornering stiffness

$$\beta_{falin} = \frac{F_{yf}}{C_f} \quad (19)$$

where F_{yf} is the front cornering force which can be obtained from (4) and C_f is the cornering stiffness for the front wheels.

The control based on β_{falin} significantly leads the θ_{xbw} control. However, β_{falin} also has the potential to be relatively erratic, potentially leading to a premature reduction in control effort. Therefore, a robust signal is needed to fill in the resulting control gap between β_{falin} and θ_{xbw} control. A yaw rate-based PD controller can accomplish this. Notice that such a yaw rate-based PD control also provides adequate yaw damping to minimize the occurrence of excessive yaw rate overshoot in limit maneuvers, which further reduces the occurrence of excessive sideslip angle and lateral forces that significantly exceed the steady state cornering capacity of the vehicle. Hence it can increase the roll stability margin of the vehicle especially during aggressive maneuvers. A goal in such a yaw rate-based PD control is to provide as much yaw damping as possible without inhibiting the responsiveness of the vehicle or becoming intrusive.

In such a control structure including three feedback controllers and a feedforward controller, the phasing in a fishhook maneuver would be such that a particular controller is dominant as the transitional maneuver progresses (see Figure 8), which supports smooth intervention and reduces the potential for exciting pitch dynamics in the vehicle.

Because the transition control is designed to lead the roll PID control intervention used in the Quasi-steady State Feedback Control module (to be discussed in the next subsection) in a given maneuver, the roll PID control can then be initiated at a significantly higher pressure level, requiring less magnitude of the feedback signal to achieve the critical pressure level required to stabilize the vehicle.

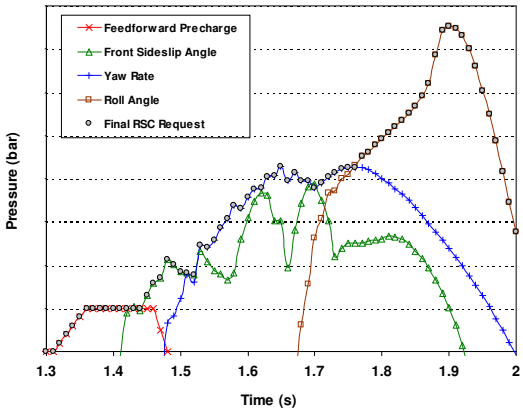

Figure 8. Pressure profile of the transition control during a fishhook maneuver.

In addition to the feedforward control such as the caliper pre-charge functionality, pressure build prediction and actuator delay compensation have also been introduced in the Transition Control module. Limitations in pressure build rates are compensated for by projecting forward when a pre-determined pressure level is likely to be requested, based on the chassis roll angle, roll rate, roll acceleration, and estimated caliper pressure. Pressure is built during the transition so that the desired peak pressure can be achieved when it is needed so as to reduce the effects of limited pressure build rates.

A detailed description regarding the Transition Control module can be found in [27].

Quasi-Steady State Feedback Control

During a quasi-steady state dynamic condition (usually in the non-linear dynamic region but with less dynamic content), a vehicle could experience slow buildup but extended wheel lift or sideslip angle. For example, during a J-turn maneuver for a vehicle with roof loading which raises its c.g., the vehicle could have one- or two-wheel lift before building up a large sideslip angle at the vehicle's rear axle. Note that the rate of change of the roll rate, yaw rate and the driver's steering wheel angle are all small. In this case the aforementioned transition control is no longer effective enough. While for the same maneuver if the vehicle has a lower c.g., the vehicle might slowly build up sideslip angle before one- or two-wheel lift occurs. A similar event could occur in a decreasing radius turn, such as those on some freeway on- or off-ramps.

These quasi-steady state conditions cannot be effectively captured by the computations used in ESC systems due to sensing limitation of the ESC sensor set. Under these driving conditions, the ability to detect and accurately estimate the slow build up of wheel departure angle and rear sideslip angle of the vehicle becomes critical for providing appropriately timed stabilizing torque. Using the RSC sensor cluster, the proper computation of the wheel departure angle θ_{xwm} and the rear sideslip angle β_{ra} referenced in the previous sections are possible. Hence the RSC system can provide the incremental ability to control the vehicle in the quasi-steady state region in addition to the highly dynamic rolling and yawing conditions.

Roll Angle Based Feedback Control

The relative roll angle θ_{xbm} between the vehicle body and the moving road is the main feedback control variable in this feedback controller structure.

For vehicles with a high c.g. and driven with rather steady state steering input, the wheel lift could build up at relatively low lateral accelerations (i.e., before a large rear sideslip angle is built up), thus leading to the buildup of the wheel departure angle. Since the Transition Control module described earlier does not address this scenario, the wheel departure angle based θ_{xbm} provides a unique characterization of such quasi-steady state conditions, hence an effective roll angle based feedback is possible. Therefore a PID feedback structure based on the relative roll angle between the body and the road (including wheel departure angle) θ_{xbm} is proposed.

The PID controller deadbands and gains are established at a level such that an appropriately progressive brake torque level is requested during periods of increasing wheel departure angle, while allowing for vehicle to do well in limit handling maneuvers without unnecessary brake interventions whenever the wheel departure angle is minor or non-existent.

Rear Sideslip Angle Based Feedback Control

For cases where a vehicle is operating with a low c.g. and is being driven in a near limit steady state maneuver, such as a J-turn, the vehicle may experience abrupt wheel lift if the vehicle's sideslip angle at the rear axle builds up to a certain threshold, i.e., the rear sideslip angle can slowly build up before a large wheel departure angle can build up.

In those cases, the roll-angle feedback control will be non-existent; yet buildup of rear side slip angle can occur at a slow rate. If such a condition is left undetected, the slowly growing rear sideslip angle can potentially lead to a sudden roll instability. Hence in this case, the calculated rear sideslip angle provides the ability to measure this slowly building sideslip angle.

A PD feedback controller structure using the calculated rear sideslip angle as the control variable is devised to control such diverging sideslip angle tendency.

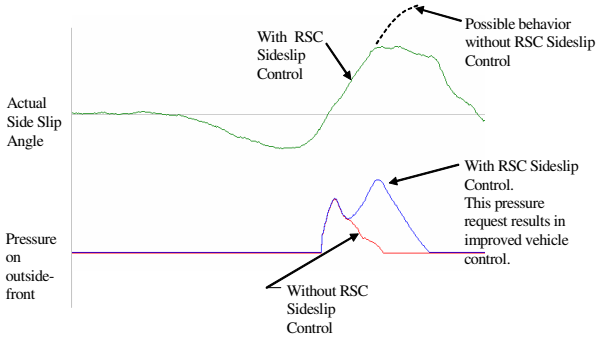

Figure 9. The RSC Sideslip Control brake pressure profile during a quasi-steady state maneuver.

Figure 9 shows, during a J-turn maneuver for a vehicle with nominal load, how RSC sideslip angle control requests brake pressure on the outside front wheel that extends beyond the ESC pressure request. Such control leads to reduced vehicle sideslip angle, which further reduces the tire lateral force helping to mitigate a potential rollover during such a quasi-steady state condition.

Control Integration inside RSC

The control strategies discussed in the previous subsections include the feedforward control within the Transition Control module which aims to prepare the brake hydraulics so as to eliminate delays in the brake pressure buildup, the feedback control within the Transition Control module which aims to mitigate rollover occurring during very dynamic conditions such as fishhooks and double lane changes, and the Quasi-steady State Feedback Control module which aims to mitigate rollovers occurring during non-dynamic conditions such as J-turn and decreasing radius turns.

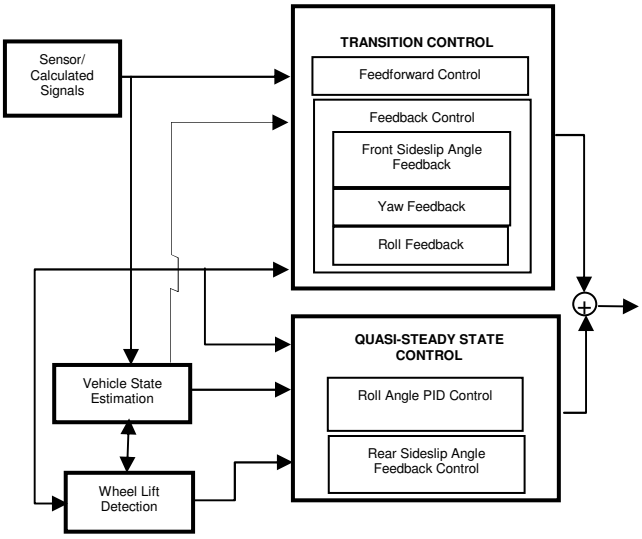

Figure 10. RSC Algorithm Integration.

In order to achieve a coordinated or combined control strategy, an integration among the afore-mentioned control strategies are conducted. Figure 10 provides a schematic overview of such integration.

RSC Interfacing with the Other Functions

The ESC system gives a driver the full ability to control the vehicle, but with intervention when needed to help the vehicle follow the driver's intent. One of the biggest differentiators between ESC and RSC is that the brake control in RSC is no longer solely in response to driver intent.

It is possible that the RSC system may cause the vehicle to reduce the lateral force at the outside tire patches, which could lead to the activation of the ESC system to request understeer control during a RSC activation, i.e., the RSC function is counteracted by the ESC understeer control. For this reason, it is important to integrate the RSC and ESC functions.

On the other hand, if during an RSC activation ESC oversteer control is also activated, the arbitrated

brake pressure should pick the maximum between the ESC oversteer control pressure command and the RSC control pressure command together with a slip control function.

Notice that RSC function must also be integrated with the ABS function. While ABS aims to maintain a certain slip target to optimize stopping distance and steerability when in an ABS event, RSC will likely request an alternate slip target, so as to modulate lateral forces and subsequently reduce the resulting roll moment.

Since the active wheel lift detection is checking if a potentially lifted inside wheel will develop slip as a result from a small brake pressure build, the wheel can enter ABS event. Therefore, the active wheel lift detection used in RSC will also need to interact with the ABS function.

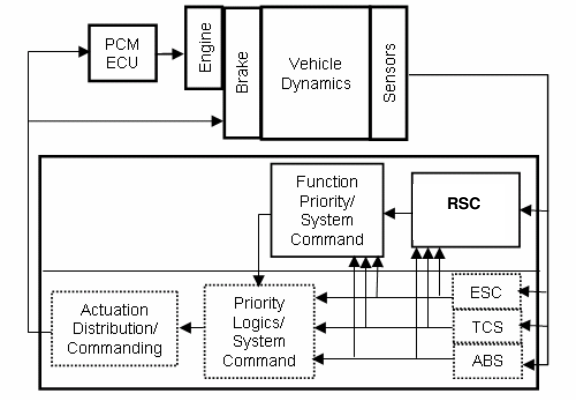

Figure 11. Function partition in a brake control Electronic Control Unit (ECU)

The RSC system resides in the brake ECU where the ABS, TCS and ESC functions reside, such that the integration between RSC and the existing brake control functions can be easily implemented. A block diagram for such an integration is shown in Figure 11, where the lower block depicts the brake ECU which is divided into two parts: the lower portion contains the existing functions and their priority and arbitration logic together with all the fail-safe and interface logic; the upper portion includes the RSC function and its priority and arbitration logic.

CONCLUSION

The Roll Stability Control ™ system discussed in this paper provides a system to mitigate vehicular rollovers, which works in harmony with and compliments the other functions existing in the current ESC systems. The addition of a roll rate sensor allows the RSC system to detect imminent rollover events regardless of variations of the vehicle loading condition and the road condition in both transition maneuvers and quasi-steady state maneuvers. The road bank determination conducted in the RSC system can also be used to improve ESC sideslip angle control during a slow sideslip buildup or on banked roads.

ACKNOWLEDGEMENT

There are many people involved in the development and implementation of the Roll Stability Control ™ system. The authors would like to thank all of them for their contributions.

REFERENCES

[1] Palkovics, L., A. Semsey and E. Gerum, "Rollover prevention system for commercial vehicles – additional sensorless function of the electronic brake system." Vehicle System Dynamics, Vol. 32, pp. 285-297, 1999.

[2] Wielenga, T. J., "A method for reducing on-road rollovers – anti-rollover braking." SAE 1999-01-0123.

[3] Liebemann, E. K., K. Meder, J. Schuh and G. Nenninger, "Safety and Performance Enhancement: the Bosch Electronic Stability Control (ESP)." SAE 2004-21-0060.

[4] Lu, J., D. Messih, A. Salib and D. Harmison, “An Enhancement to an Electronic Stability Control System to Include a Rollover Control Function.” SAE 2007-01-0809, to appear.

[5] Ackermann, J. and D. Odenthal, "Robust steering control for active rollover avoidance of vehicles with elevated center of gravity." Proc. International Conference on Advances in Vehicle Control and Safety, Amiens, France, July 1998.

[6] Hac, A., "Influence of active chassis systems on vehicle propensity to maneuver-induced rollovers." SAE 2002-01-0967.

[7] Lee, Y., "Control methodology to alter automobile rollover tendencies." NASA Tech Brief, vol. 24, No. 4, 2000.

[8] Shim, T. and D. Toomey, "Investigation of active steering/wheel torque control at rollover limit maneuver." SAE 2004-01-2097.

[9] Yoon, S., J. Jung, B. Koo and D. Kim, "Development of rollover prevention system using unified chassis control of ESP and CDC systems." SAE 2006-01-1276.

[10] T. Brown and D. Rhode, "Roll over stability control for an automotive vehicle." US Patent 6263261.

[11] Samuel, S. and T. Brown, "Method and system for correcting sensor offsets." US Patent 7085642.

[12] Hrovat, D., H. E. Tseng and L. Xu, "System and method for detecting roll rate sensor fault." US Patent 6941205.

[13] J. Meyers and T. Brown, "Wheel lift identification for an automotive vehicle." US Patent 6356188.

[14] Brewer, M. and T. Brown, "System and method for controlling a hydraulic system." US Patent 6997524.

[15] Joyce, J. and T. Brown, "Hydraulic control unit with ambient temperature compensation during fluid pressure delivery." US Patent 5971503.

[16] Lu, J. and T. Brown, "Method for determining a longitudinal vehicle velocity by compensating individual wheel speeds using pitch attitude.",US6915193.

[17] Greenwood, D. T., *Principle of Dynamics*, 2nd Edition, Prentice-hall, Inc., Englewood Cliffts, 1998.

[18] Lu, J. and T. Brown, "Attitude sensing system of an automotive vehicle relative to the road." US Patent 6556908.

[19] Hrovat, D., H. E. Tseng and T. Brown, "Method for road grade/vehicle pitch estimation." US Patent 6714851.

[20] Lu, J. and T. Brown, "Attitude sensing system for an automotive vehicle." US Patent 6631317.

[21] Lu, J., T. Brown, E. Chubb and A. Salib, "System and method for determining a wheel departure angle for a rollover control system with respect to road roll rate and loading misalignment." US Patent 7079928.

[22] Lu, J. and T. Brown, "System for detecting surface profile of a driving road." US Patent 6718248.

[23] Lu, J., S. Samuel and T. Brown, "System and method for characterizing the road bank for vehicle roll stability control." US Patent 7085639.

[24] Lu, J. and T. Brown, "Method and apparatus for determining lateral velocity of a motor vehicle in closed form for all road and driving conditions." US Patent 6725140.

[25] Lu, J., J. Meyers, K. Mattson and T. Brown, "Wheel lift identification for an automotive vehicle using passive and active detection." US Patent 7132937.

[26] Salib, A., H. Ghani, M. Geurink and T. Brown, “System and method for determining an amount of control for operating a rollover control system.” US Patent 6961648.

[27] Salib, A., H. Ghani, M. Geurink and T. Brown, “System and method for operating a rollover control system in a transition to a rollover condition.” US Patent 7120528.

[28] Salib, A., H Ghani, M. Geurink and T. Brown, “System and method for operating a rollover control system during an elevated condition.” US Patent 7096103.

[29] Salib, A. and J. Lu, “System and method for desensitizing the activation criteria of a rollover control system.” US Patent 6961648.

ENHANCEMENT OF CAR SAFETY USING IMPROVED ESC AND TYRE DEVELOPMENT METHOD

Eric Fenaux
PSA Peugeot Citroen
France
eric.fenaux@mpsa.com
Jeremy Buisson
MICHELIN
France
jeremy.buisson@fr.michelin.com

Paper number 07-0138

ABSTRACT

ESC efficiency to reduce accident is now well proven. To obtain this accident reduction tests employed for the tuning of a car equipped with an ESC must be related to real world accident cases. With accident statistics obtained in France, two main categories of accidents are defined: loss of control in a curve and accidents in a straight line or at an intersection. For each of these categories, thanks to detailed analyses of real accidents, we can define tests scenarios that are related to real world. Several examples are given.
To measure the performance of a car equipped with an ESC during these tests, stability criteria are defined. In addition criteria to assess the quality of ESC intervention are defined. These tests pointed some limitations of ESCs. Some improvements of ESCs algorithms were specified to overcome these problems. Examples are given.
During this ESC tuning, it is decided if a rollover prevention module is necessary or not. This decision process, which includes both real tests and HIL (Hardware In the Loop) tests is described. One of the conditions that may lead to a rollover is a contact between the rim and the ground. This process also enables us to define test conditions to check there is no risk of rim contact on the ground.
A test method of a tyre on a bench to check these conditions are satisfied is described. It is also shown that the risk to have a contact of the rim on the ground is not significantly modified during the brake activation by the ESC.

1. INTRODUCTION

1.1 Efficiency of ESC's and pertinent accidents

ESC is an efficient equipment to avoid accident. A lot of studies have been published and show a statistically significant reduction of accident for cars equipped with ESC [1] [2] [3] [4].
The later is very interesting as it distinguishes the different accident scenarios.

Then it identifies accident situations for which the ESC is pertinent or not. For example ESC is pertinent for loss of control accidents while it is not for cars pulling out of a junction. According to this paper, the accidents for which the ESP is pertinent are related to loss of control or guidance problems. The given list is:

- Single car accident. Loss of control or guidance problem on a straight road outside junction
- Loss of control or guidance problem on a straight road outside junction. Collision with an opponent
- Single car accident. Loss of control or guidance problem in a bend outside junction
- Loss of control or guidance problem in a bend. Collision with an opponent
- Single car accident. Loss of control or guidance problem at a junction.

Then it is interesting to test the ESC's with driving conditions that are related to these pertinent accidents.
In this paper we will only deal with the loss of control that is initiated by a driver manoeuvre on a dry road: namely action on the steering wheel, the brake or the gas pedal.

1.2 Selection of the test procedures

The detailed method to select the procedures and the initial conditions is given in [5]. The test procedures are derived from ISO standard. The initial conditions are the one observed in the detailed analysis of real world accidents.
In the following different tests examples are given:

- Braking in a curve ISO 7975
- Power off in a curve ISO 9816
- Severe lane change manoeuvre ISO 3888-2

For these tests we give an example of a metric used to enhance the tuning of an ESC.

2. BRAKING IN A CURVE

2.1 Desired improvement

For our test the initial radius is 150 m and the initial longitudinal speed is 120 km/h. In [5] a metric was proposed to assess the stability performance of a car during a brake in turn test. In this metric the yaw speed variation and the side slip angle value were considered. But there is a need to improve this metric when the car is equipped with an ESC. This is because the yaw speed variation is only considered at given times after the beginning of the braking t_0. For a car equipped with ESC, the yaw speed variation may show a time history like the one of figure 1.

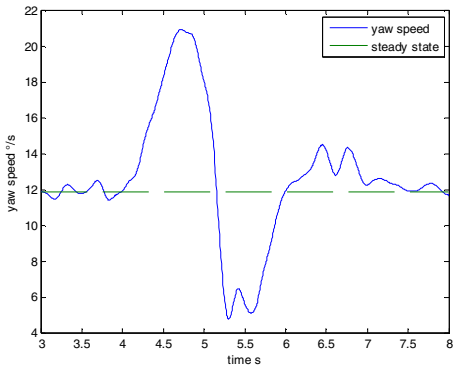

Figure 1: Example of yaw speed time history during a braking in a curve with an ESC intervention

In this case, the braking is initiated at time t_0=4s. With a measurement of yaw speed variation between t_0 and $t_0 + 1$ s, the oscillation will not be penalised.
The yaw speed oscillation is clearly something to avoid, it generates a sudden variation of the trajectory and significant yaw acceleration. The variation of trajectory is an objective stability problem and the yaw acceleration that is very well perceived by the driver is more a subjective problem. So this oscillation should be minimised and to quantify it we propose a new metric.

First we draw the horizontal line corresponding to the mean value of yaw speed during 1 second before the braking (i.e. in figure 1 between time 3 and 4 second). In the following this mean value is called $\dot{\psi}_0$. This line is the dotted line of figure 1 and is called "steady state" in the legend. Then we define two values:

- the positive integral which corresponds to the area between the mean yaw speed line and the actual yaw speed between t_0 and time t_1 when yaw speed first becomes lesser than $\dot{\psi}_0$
- The negative integral which corresponds to the area between the mean yaw speed line and the actual yaw speed between t_1 and time t_2 when yaw speed reaches $\dot{\psi}_0$

The proposed metric is the sum of the absolute values of those two integrals.

In figure 2 with a better regulation of the ESC the oscillation is almost inexistent and both integrals have been significantly reduced. The scale for the yaw speed axis is the same in figure 1 and figure 2 to make the comparison easier.

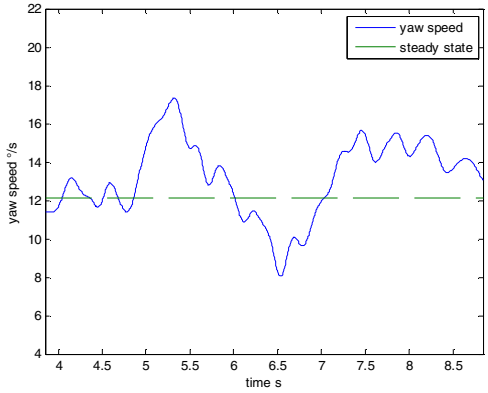

Figure 2: Example of yaw speed time history during a braking in a curve with an improved ESC intervention

2.2 Proposed modification of algorithm

The detection of the instability beginning has not been changed. When the difference between desired yaw speed and actual yaw speed becomes too large the correction is initiated with an open loop brake actuation. This has not been changed and can be seen on figure 1 and 2 where the gradient of yaw speeds is identical at the beginning of the manoeuvre.
In addition lateral acceleration a_y is observed. To be more precise the difference between the measured lateral acceleration and the desired lateral acceleration is calculated. The desired lateral acceleration is obtained with the steering wheel angle and the vehicle speed.
An increasing difference means an increase of side slip angle. If this difference is still increasing during the regulation this means the longitudinal effort on the front outside wheel has to be increased.
When the increase of side slip is stopped the pressure is kept constant if the steering wheel angle is constant or modulated according to this latter value if it changes until actual yaw speeds reaches the desired yaw speed.

3. POWER OFF IN A CURVE

This case is significant to test an ESC as there is no action on the brakes. So the action is typical of an ESC and is not possible with an ABS. For this test the initial

radius is 100 m and we test vehicle speed from 80 km/h up to the maximum of the car with increment of 5 km/h.

3.1 Desired improvement

To determine the vehicle behaviour the ESC measures the yaw speed and the lateral acceleration. There is no direct measurement of the side slip, this value as to be determined. If the increase of the side slip is a slow one, it is difficult for the ESC to detect this increase. This can lead to a big side slip angle and in our opinion this is a problem as we found the slip angle is a cause of driver's stress.
According to [6], 47% of the drivers do not make any action to avoid the accident. So we should not wait for a driver action at the steering wheel to limit the maximum of the side slip angle.
We believe the metric is the absolute value of the side slip angle and not the relative increase from the steady state value during the curve before the power off. That is because the stress is related to the absolute value of side slip and not to an increase from the steady state value.
The figure 3 shows an example of a car equipped with an ESC that allows the side slip angle to become large. We call this behaviour the slow side slip default.
The proposed modified algorithm aims at suppressing this default.

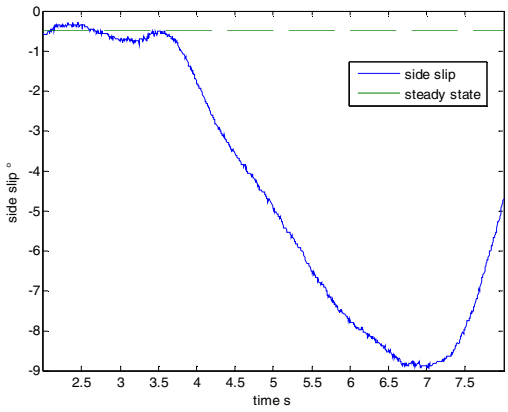

Figure 3: Example of side slip time history during a power off in a curve with the slow side slip default

The figure 4 shows an example of a car equipped with an ESC modified to enhance this behaviour.

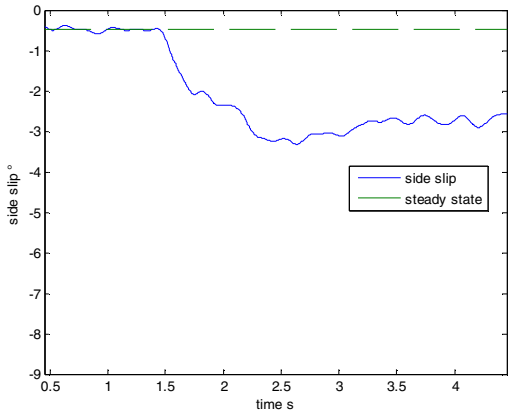

Figure 4: Example of side slip time history during a power off in a curve with correction of the side slip default

To determine the time of intervention of the ESC, it is interesting to look at the yaw speed time history. We can see on figure 5 that the yaw speed decrease begins at 2.07 s. It is important to mention that this decrease is the effect of the ESC intervention. So the initiation and the detection of the side slip is done before. The entire process duration i.e. the detection of the side slip, the decision of ESC intervention and the beginning of side slip increase limitation is around 0.4 second.

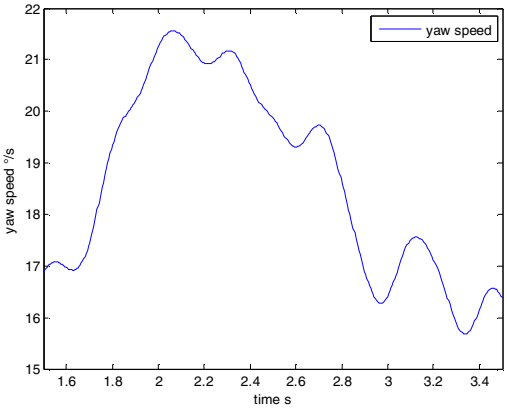

Figure 5: Yaw rate time history during power off in a curve: determination of the ESC intervention

Of course, as shown before with the braking in a curve, we want this ESC intervention to be progressive. This is the reason why the effective limitation of the side slip is obtained around 2.3 second that is 0.6 second after the power off initiation. We do not consider this to be a problem; between the time the first intervention is effective and the effective limitation of side slip, the magnitude of side slip increase is only 0.8° with a maximum at 3.3° for the side slip. All these values are small enough and the driver will not be scared.

3.2 Proposed modification of algorithm

As explained before for the braking in a curve the correction is a several step process. The beginning of the action of the ESP consists in an open loop actuation followed by a closed loop actuation.
All these actions are triggered by specific thresholds. The idea here is to make the thresholds of the closed loop actuation more aggressive as soon as the open loop actuation is initiated. Once the open loop actuation has been initiated there is no risk of undesired correction any more this is the reason why the thresholds are made more aggressive only at this time. Then thanks to these modifications, the closed loop regulation that is more efficient and more comfortable is activated sooner.

4. SEVERE LANE CHANGE MANOEUVRE

4.1. Choice of the test

One of the most popular tests for this situation is ISO 3888-2. Professional test drivers succeed in this test with vehicle speeds as high as 80 km/h. For a normal driver it is not possible to reach such a speed on such a track. The problem of the speed is an important one. In [7] the study of a panel of 72 accident cases shows that when there are multiple actions on the steering wheel the mean speed at the first action on the steering wheel is 88 km/h. Of course to follow the test track described in ISO 3888-2 there are multiple actions on the steering wheel. So this test is not related to real world accidents conditions: the actions on the steering wheel and the speed are not consistent.
Nevertheless as it is practised by a lot of journalists it is one of our test case and we find it interesting to test the rollover resistance.

4.2. The questions to be answered

If there is a risk of rollover, the ESC can activate a dedicated module: the RollOver Mitigation (ROM). To make it simple, this module limits the lateral acceleration when there is a risk of rollover. On the one hand, if a given car presents a risk of rollover this module must be fit in because it is an improvement of the safety. On the other hand, if the car does not present a risk it is better not to install this module to avoid any risk of undesired lateral acceleration limitation.
For this reason we need a process to determine if there is a risk of rollover or not

4.3. Process to determine if there is a risk of rollover or not

When one must answer this question two main difficulties are present:

- The great number of load cases to be tested
- The need for safe experiment

To obtain safe tests the cars are equipped with outriggers during rollover test sessions. The main drawback of this equipment is the bias it introduces in the inertia and the load distribution. How can we say that when car does not roll over with outriggers it will not without and vice versa? In order to answer this question we developed the process described in figure 6.
Of course, during the high dynamics tests, the ESC's regulations change the behaviour of the car. So the simulations need the ESC's regulations. This is the reason why we make these simulations with a Hardware In the Loop (HIL) test bench. For the correlation between simulation and measurement, we check the errors of dynamics variables of the body: yaw and roll velocity, roll and pitch angle, heave, side slip angle; accelerations and suspension movements. In addition, we check that the instant of activation of ESC are the same for real and virtual testing.

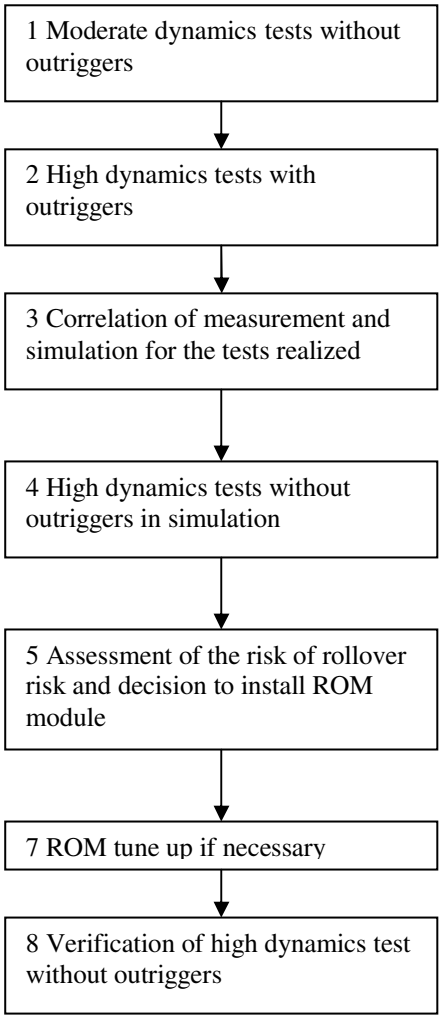

Figure 6: process to determine if the ROM is necessary

But only one problem has been addressed so far: the need for safe tests without bias in inertia or load distribution.
Once this process was initiated we decided to use it to reduce the number of load cases to be tested. The corresponding process is described in figure 7

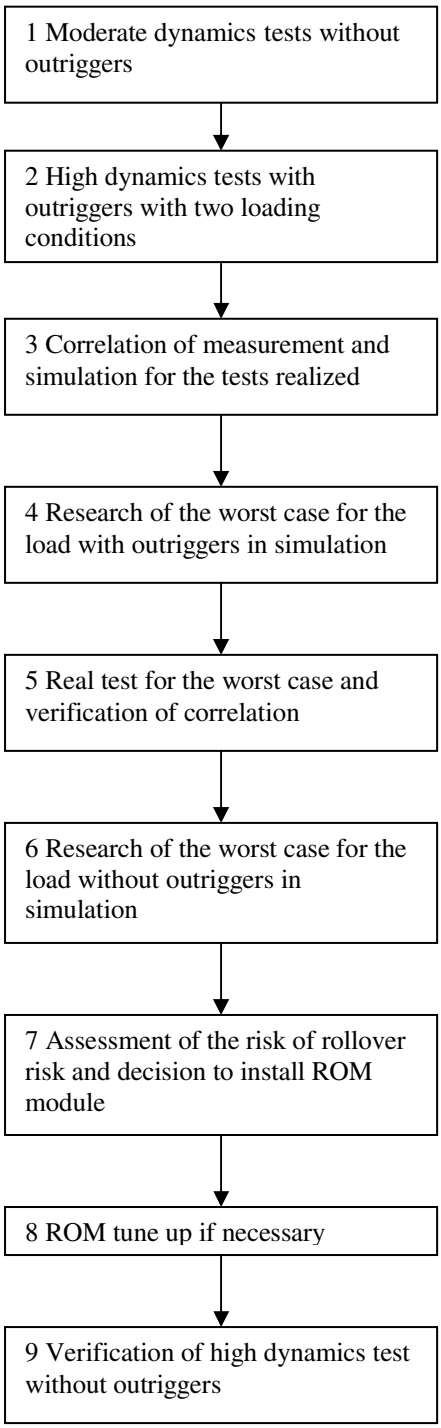

Figure 7: process to determine if the ROM is necessary with reduction of the load cases to be tested

The idea was to add "an optimisation" to find the worst case: the one with the higher risk of roll over during the step of simulation (4 and 6). The worst case is the one with the smallest load on the internal wheels or the case with two wheels lift up with the smallest speed in the test.

It is difficult to obtain a good correlation between simulation and measurement for high dynamics manoeuvres, this is the reason why we believe step 5 is useful. It enables to verify the correlation is still effective for the worst case.
One of the events that may lead to rollover is a contact of one rim with the ground. The described process is also useful to avoid this contact.

5. PROCESS TO AVOID THE CONTACT OF THE RIM ON THE GROUND

5.1. Michelin tire testing method principle

Testing tyres on a bench in conditions as close as possible to those encountered during high dynamics manoeuvres (e.g. up to rim contact) is not possible for evident safety reasons. A method to test tyres with minimal rim clearance has been developed. Because relation between rim clearance and load can not be presupposed, the bench is directly commanded in loaded radius mode. Appropriate loaded radius is deduced from target rim clearance and relation between rim clearance and loaded radius.

5.2. Test definition

For a given tire, the maximum loaded radius (e.g. free radius) and the minimum one (e.g. corresponding to minimum rim clearance allowed by bench or tire depending on conditions) are determined as functions of camber angle, tire dimensions (width, aspect ratio and internal diameter), rim dimensions (width, diameter, side height) and tire sectional thicknesses (summit, sidewall). From these functions, slip angle sweep sequences with various deflections objectives (and corresponding rim clearances) are defined with speed, pressure and camber effects.

5.3. Loaded radius formula

Usual acquisition channels are saved during testing (e.g. forces, torques, angles, speeds, pressure and loaded radius) and post-processed to fit a simplified loaded radius formula:

$$\begin{aligned} R_L = &\left(k_{0_0} + k_{0_V}.V + k_{0_P}.P\right) + |\gamma|.k_\gamma \\ &+ F_Z.\left(k_{Z_0} + k_{Z_V}.V + k_{Z_P}.P\right) \\ &+ |F_Y|.\left(k_{Y_0} + k_{Y_V}.V + k_{Y_P}.P\right) \end{aligned}$$

With V the speed in kph and P the pressure in bars.

Figure 8 shows the loaded radius measurement and fit during the measurement protocol.

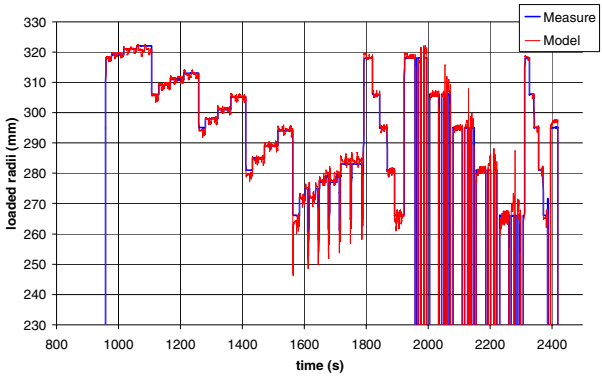

Figure 8: Loaded radius fitting quality

5.4. Rim clearance prediction

To define the test and to use the loaded radius model for rim clearance prediction, the relation between the previous has to be described according figure 9:

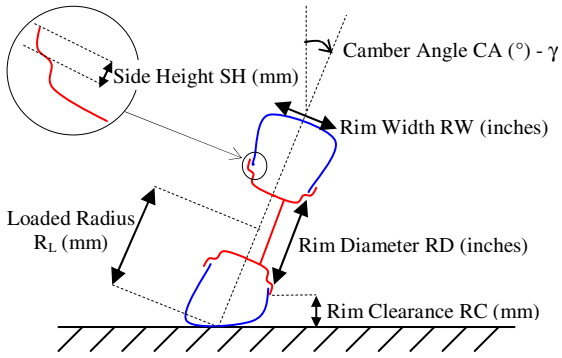

Figure 9: Rim clearance to loaded radius relation

$$RC = \left(R_L - \frac{RD}{2}.25{,}4 - SH \right).\cos(\gamma) - \frac{RW}{2}.25{,}4.\sin(|\gamma|)$$

5.5. Evaluation of the tyre loading conditions during high dynamics manoeuvres

When there is a risk to get a contact of the rim on the ground it not possible to make a measurement with a dynamometer wheel. These equipments are too expensive to take such a risk.
The idea is to make measurements with dynamometer wheels only during the test of step 1 of figure 7: the low dynamics tests. Then the correlation between the tests and the simulations of step 3 is also checked for the tyre efforts.

Then we assume the verification of the dynamics variables of the body : yaw and roll velocity, roll and pitch angle, heave, side slip angle, accelerations and suspension movements during the high dynamics manoeuvres is sufficient to validate the tyre efforts during these manoeuvres.

So we can use the tyre efforts obtained during the simulations as the loading case to be introduced in the formulae to check if there is a risk of contact or not.

5.6. Tire dimension effect example during high dynamics manoeuvres

As an example, 3 tires of different dimensions have been measured, fitted and their models used to replay the typical manoeuvre.
Figure 10 shows the results of the computed rim clearances.
Data show that tire dimension 215/55R16 has more rim clearance during simulated avoidance manoeuvre than tire dimension 215/50R17 and even more than tire dimension 215/45R18. Results have proofed to be consistent with on track tests made to check vehicle behaviour under high dynamics manoeuvres with the different tire dimensions.

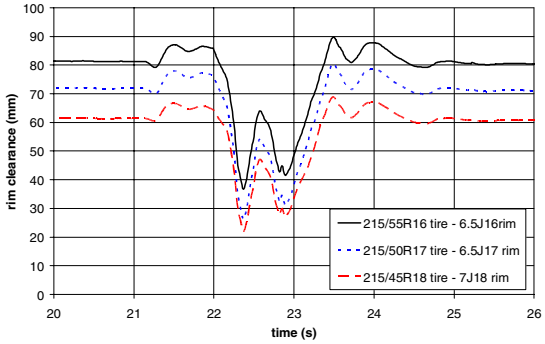

Figure 10: Computed rim clearances for 3 tires

5.7. Effect of longitudinal force on loaded radius

Indoor combined measurements have revealed that the perturbations introduced by the application of a longitudinal force are small. The effects of the ESC and ROM on loaded radius are so not requesting the Fx force knowledge but only the modifications on Fy and Fz forces, camber angle and speed. And the rim to ground distance is not impacted by the actions of the ESP and ROM as much as mainly Fx force is modified.

CONCLUSIONS

Accidents data analyses introduce classes of accident situations for which the ESP is pertinent. In this paper three situations are shown: braking in a curve, power off in a curve and severe lane change. Example of ESP enhancement are given for each test respectively a regulation that will improve the diver comfort and reduce trajectory deviation, a limitation of the side slip increase for a better stability and a reduction of the stress of the driver and a method to decide if the rollover protection module has to be install or not.
A method to determine if a contact of the rim on the ground is possible that uses mainly test bench measurement is proposed.

REFERENCES

[1] Aga M., Okada A. (2003) Analysis of vehicle stability control (VSC)'s effectiveness from accident data. ESV paper 541. 18th ESV Conference, Nagoya, 2003

[2] Tingvall C., Krafft M., Kullgren A., Lie A. (2003) The effectiveness of ESP (Electronic Stability Programme) in reducing real life accidents. ESV Paper 261. 18th ESV Conference, Nagoya 2003

[3] Unselt T., Breuer J., Eckstein L., Frank P. (2004) Avoidance of "loss of control accidents" through the benefit of ESP.
FISITA Conference, Barcelona, 2004

[4] Yves Page, Sophie Cuny (2004) Is ESP effective on French Roads? 1st International ESAR (Expert Symposium on Accident Research)

[5] Fenaux E. (2003) Proposition of a method to evaluate active safety handling qualities. ESV Paper. 18th ESV Conference, Nagoya 2003

[6] Lechner D., Van Eslande D. (1997) Comportement du conducteur en situation d'accident, Ingénieurs de l'automoblile, 1997

[7] Thomas C., Hermitte T., Perron T.((1999) Driver action during real world pre-crash phases, JSAE Spring Convention Proceedings, n°15, 1999

.

EFFECTS OF THE PROCESS OF REAR TIRE DELAMINATION ON VEHICLE STABILITY

David A. Renfroe, Ph.D., P.E.
H. Alex Roberts
David Beltran
The Engineering Institute, LLC.
United States
Paper Number 07-0142

ABSTRACT

The effects of the delaminated tire after a tread separation event on the handling of a vehicle have been well documented. However, the period when the tire is delaminating, which can last from about one and one half to many seconds, can pose a serious threat to vehicle stability depending on the duration of the delamination process, the design of the rear suspension of the vehicle, and the speed at which the delamination commences. This paper will present the results of testing where a delaminating tire results in a bump on the tire and a subsequent loss of control even with expert drivers. Similar vehicles were tested under a controlled environment to determine that the cause of the loss of control is axle tramp induced by the bump frequency of the delamination occurring at the natural frequency of the axle/spring (the tire is the dominant spring) system. During this tramping the handling characteristics become severely oversteer. The resulting oversteer has been measured using standard SAE J266 test procedures for various models of vehicles characterized by a Hotchkiss type rear suspension system. Proposed solutions were increasing the tramp damping characteristics of the axle system and/or the addition of dual wheels on certain vehicles. These solutions are examined for their effectiveness. Testing will illustrate how proper shock absorber sizing and placement will have a positive effect on the oversteer situation.

INTRODUCTION

Though public awareness of tire failures and tire delamination events has greatly increased over the last several years, these events are not unanticipated or new to the vehicle dynamics community, tire designers, and others. However, the detrimental effect of a tire delamination event on the vehicle handling is an area that is currently being researched. A further understanding of the dynamics of the interaction of the delamination process and the suspension sub-system will allow vehicle designers to anticipate the adverse effects of this process on vehicle handling and stability and design a system that is more robust and less likely to lose its directional controllability during such a foreseen event.

OVERVIEW

It is rather intuitive to a vehicle dynamicist that the reduced friction associated with a tire that has lost its outer tread belt and is rolling on the steel wires composing the steel belt will have less lateral traction at this location. It is also well understood that with regards to a certain steering wheel angle, this lower lateral traction will lead to an increased slip angle at this corner of the vehicle than would be developed by a non-compromised tire. The terms understeer and oversteer are defined by relative slip angles. If the slip angle generated by the front tires of the vehicle is greater than that generated by the rear, the vehicle is said to be understeer. Alternatively, if the rear slip angle exceeds that of the front, the vehicle is said to be oversteer. A special case can exist where the front and rear slip angles are equal. This situation is known as neutral steer. Using these definitions to analyze a vehicle with a delaminated tire, it can be concluded that if the failure is on the front of the vehicle, the vehicle's understeer will likely be increased, and a delaminated tire on the rear will result in reduced understeer which could transition to oversteer. Dynamic testing has proven that vehicles with delaminated tires are in fact limit oversteer vehicles.

A much less intuitive analysis is required to understand the effects on the vehicle directional control characteristics of a tire in the process of a delamination event. During this process of the tire shedding its outer tread cap, a rotating imbalance is developed and transmitted to the rear suspension system. As the cap separates, the unbonded cap can fold over on itself until it completely separates, or the cap can separate in

pieces leaving some attached to the tire. Either of these situations will cause a lump and a rotating imbalance and result in a cyclic forcing frequency at that tire. It is this approximately one and one half to several seconds duration event with which the research presented in this paper is concerned. During this time, at highway speeds, the previously mentioned vertical oscillations can induce the tramp natural frequency of the rear axle (usually around 10 to 15 Hz). When this occurs, the rear traction is severely compromised. On Hotchkiss type suspensions, as shown below, this tramp mode is transmitted across the rear axle causing both rear tires to intermittently lose traction. Recent vehicles with this type of suspension include SUVs, cargo and passenger vans, and light trucks, among others.

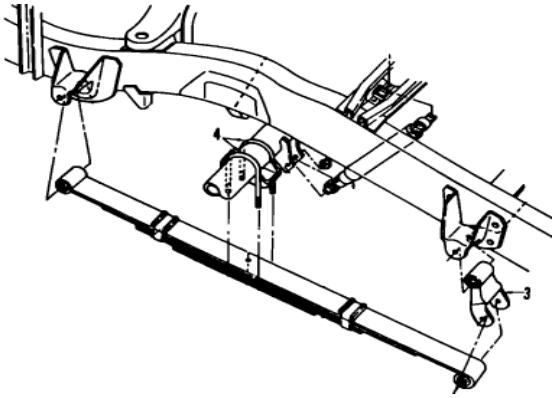

Figure 1. Illustration of Hotchkiss rear suspension.

This paper will discuss testing which has demonstrated that a severe oversteer condition can occur during the delamination event resulting in sudden loss of directional stability.

Nearly all vehicles sold to the public are designed to be steady-state understeer vehicles. Therefore, an understeer vehicle is what the motoring public is accustomed to driving. An understeer vehicle is considered safer for an average driver. An oversteer situation, especially a snap oversteer, creates a dangerous situation for untrained and unsuspecting drivers. An oversteer vehicle actually over responds to driver inputs, by steering more than the steering wheel angle and vehicle geometry would predict. Thus, it is vital for vehicles to be designed to remain controllable during a tire delamination event and not suddenly become a highly oversteer condition. The research presented here not only demonstrates the oversteer associated with tire delamination events, but also outlines design principles that significantly reduce or even eliminate the oversteer during the delamination event.

TESTING BY THE ENGINEERING INSTITUTE

Testing Protocol

All testing conducted referenced "SAE J266, Steady State Directional Control Test Procedures for Passenger Cars and Light Trucks." The test method followed was the constant radius test. In this test, the vehicle is driven on a constant radius circle at a slowly increasing speed. As the lateral acceleration on the vehicle increases, the driver is to apply appropriate steering to keep the vehicle following the path.

The test is analyzed by plotting the wheel angle (steering wheel angle divided by the steering ratio) against the lateral acceleration. The slope of the curve gives the understeer/oversteer gradient. The curve is not linear, and the gradient is often reported at low lateral accelerations, referred to as the linear range, and at the limits of tire adhesion, referred to as the limit range. The standard units for the understeer/oversteer gradient are degrees per g. A positive number is usually reserved for understeer; whereas, a negative slope indicates that the vehicle is oversteer. Figure 2 shows a typical understeer/oversteer plot for a vehicle with linear range and limit understeer.

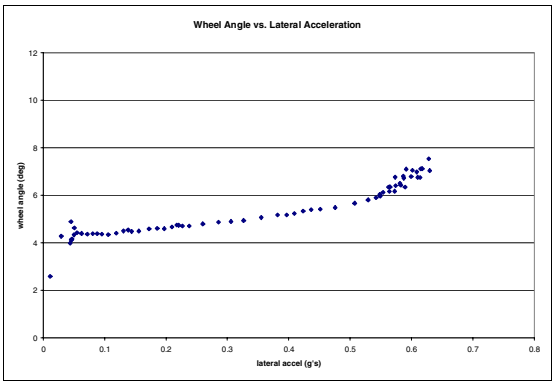

Figure 2. Exemplary understeer/oversteer plot for an understeer vehicle.

To simulate the cyclic input, tread pieces were either vulcanized or bolted to the outer surface of the tire. For the circle testing, 3 tread pieces were bolted around the circumference of the tire

at 120 degree intervals. This was done in order to induce the tramp mode frequency at speeds attainable in the circle test. A frequency of 10 to 15 Hz would occur at speeds of 60 to 70 mph with a single lump generated by a delaminating tire. The design of the SAE J266 maneuver limits the maximum attainable speeds to much less than this. The maximum attainable speed is a function of the size of the test circle and the vehicle design. For a vehicle with a lateral handling limit of 0.75 g's being driven on a 130 foot radius circle, the maximum attainable velocity as predicted by (Equation 1) is 38 mph.

$$A_y = \frac{v^2}{r} \qquad (1).$$

Therefore, in order to simulate the 10 to 15 Hz input at a relatively safe speed attainable in a constant circle test, the three lumps were applied to reduce the speed by a factor of 3, approximately 20 to 23 mph. Examples of the lumped tires prepared for testing are seen in Figures 3 and 4.

Figure 3. Prepared tire with bolted lumps.

Figure 4. Prepared tire with vulcanized lumps.

General Testing Results

The test vehicles were all linear and limit understeer in their standard configuration with the exception of the fully loaded passenger van discussed later. However, testing demonstrated that the vehicles are all severely oversteer in a range of frequencies at and around the tramp mode natural frequency of the rear suspension system. The data plots during the oversteer condition are characterized by a wide band of data points indicating that the steering necessary to remain on the path was widely varied and unpredictable.

Another commonality between the vehicles tested besides all being Hotchkiss rear suspensions is a relatively far inboard placement of the shock absorbers on the axle as exemplified by Figure 5. This significantly reduces the effective tramp damping at the wheels. Since the input responsible for exciting the tramp mode natural frequency is coming from the tire, it was theorized by Kramer [Kramer, 1996] that greater effective damping at the tire would help control the motions of the tire and axle and decrease the induced oversteer.

Figure 5. Hotchkiss rear suspension system showing shock placement.

Aftermarket externally adjustable shock absorbers with high levels of damping were purchased to test the theory that greater damping on the rear axle would reduce the oversteer condition. Also, where possible, the shock absorbers were moved farther outboard to increase their effective damping rate. In addition, an alternative suspension system consisting of a rocker pivot arm amplifying the damping via a mechanical advantage was designed and tested. Testing demonstrated that tuning the effective damping could have beneficial effects on the vehicle handling. Figure 6 is a damping plot for the aftermarket shock absorbers.

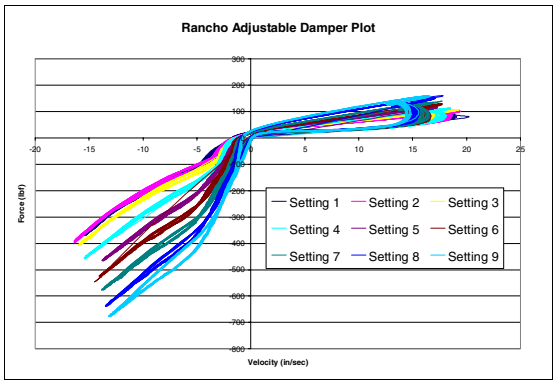

Figure 6. Damping plot for adjustable damping shock absorbers.

Detailed Testing Results

Sport Utility Vehicle Testing – The first testing into the effects of the lumped tire on directional stability involved a sport utility vehicle (SUV). Since the initiation of this test program, various sport utility vehicles and configurations have been tested. All tested vehicles share a similar rear suspension design and share design similarities with regards to the relative placement of the rear shock absorbers. Each vehicle tested demonstrated understeer characteristics in the standard configuration, 'as-designed' state. However, the addition of the lumped tire drastically altered the handling characteristics of the vehicle by inducing oversteer at low lateral accelerations.

Figures 7 and 8 show exemplar data plots resulting from standard configuration testing of two SUVs. The positive slope of each curve is indicative of an understeer characteristic. The understeer gradient for SUV 1 is around 2.8 degrees/g for the range of 0.2 to 0.4 g's and is approximately 2.6 for SUV 2.

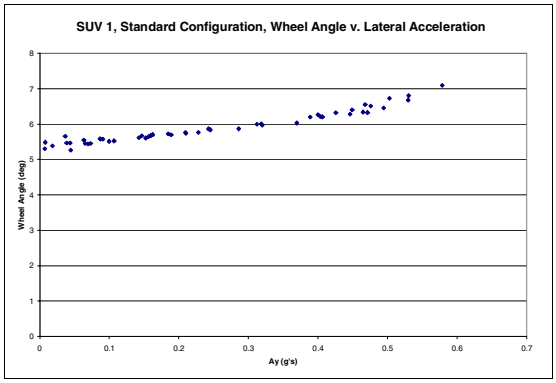

Figure 7. Data plot for SUV 1 standard configuration testing.

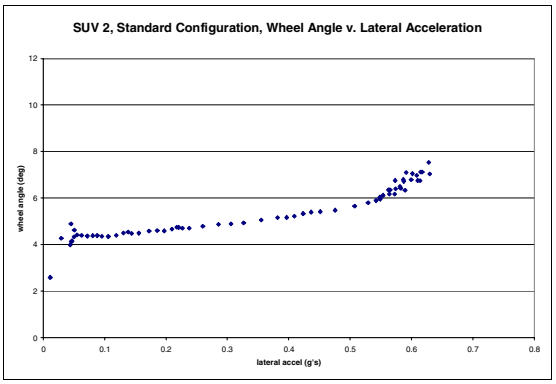

Figure 8. Data plot for SUV 2 standard configuration testing.

The following figures graphically illustrate the striking difference encountered when the vehicles were tested in the presence of the lumped tire. The negative slopes are indicative of an oversteer condition. Since the oversteer occurs at low lateral accelerations, it can be concluded that the oversteer could be induced even with minor steering inputs in a real-world driving situation.

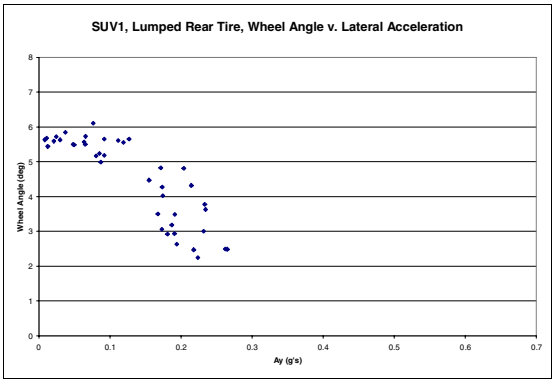

Figure 9. SUV 1 data plot resulting from testing with the lumped tire.

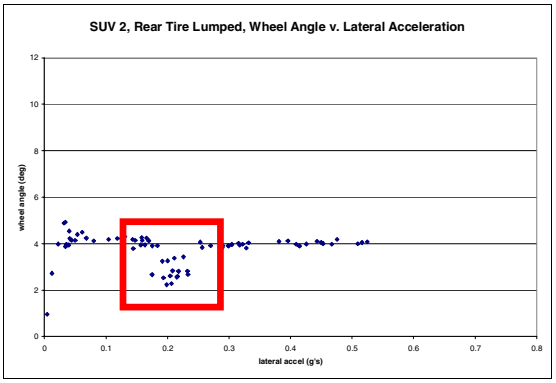

Figure 10. Lumped tire test data plot for SUV 2 with region of oversteer boxed in red.

Figure 10 demonstrates how the oversteer is most pronounced at input frequencies near the rear axle tramp resonant frequency. An accelerometer mounted on the rear axle indicated that the forcing frequency at the rear axle was around 13 to 14 hertz at the time the vehicle is oversteering. It is noteworthy that the vehicle was basically neutral steer (slope = 0) on either side of this frequency band.

Adjustable shock absorbers were installed on both SUVs. This allowed damping to be set to levels greater than possible with the original replacement shock absorbers. Also, new shock mounts were fabricated and installed allowing the shock absorbers to be moved as far outboard as possible. The increased damping improved the directional stability of both vehicles with the lumped tire. SUV 1 remained an understeer vehicle in the lumped tire testing, and SUV 2 exhibited basically neutral behavior. In both cases, the test driver commented that the vehicles were predictable with the damping modifications; a characteristic that was lacking in the lumped tests with the standard vehicle configuration.

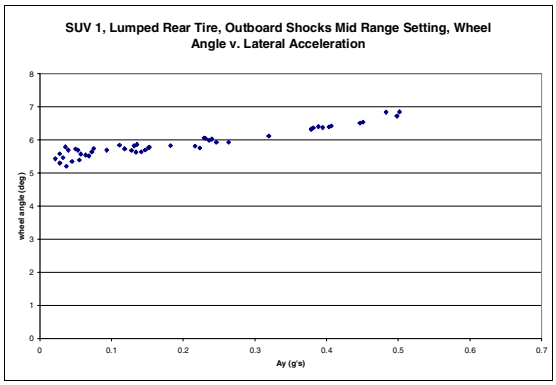

Figure 11. Data plot of lumped tire testing from SUV 1 with outboard mounted higher damping shock absorbers.

Figure 12 shows the effects of the outboard mounted dampers on SUV2. As mentioned, there was a marked improvement in the handling with this set-up.

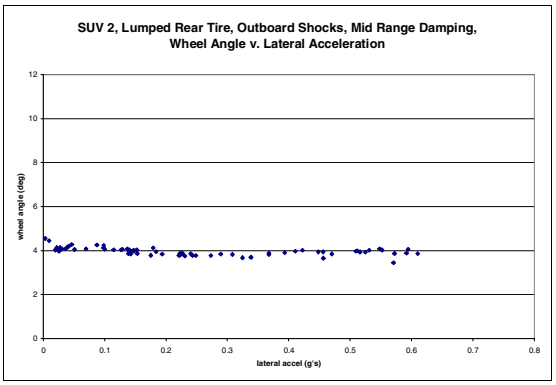

Figure 12. Data plot from SUV 2 outboard shocks lumped tire testing.

15 Passenger Van Testing – Similar testing was conducted on a 15 passenger van. A difference between the van tested and the SUV is that at the heavily loaded (near gross vehicle weight) condition, the van is a limit oversteer vehicle. This condition arises from a center of gravity (CG) shift that accompanies the loading. With the test loading simulating occupants, the CG moved upward and rearward. Static measurements have shown that the upward shift can be between 1 and 2 inches. The longitudinal shift is considerably more. This is due to the design characteristic of the van tested that places a significant amount of the loading behind the rear axle. Static measurements have demonstrated a longitudinal shift rearward of the CG of as much as 17 to 20 inches. Even in the unloaded condition, data scatter is seen at the limits of lateral adhesion, and the driver said the vehicle felt very much on the edge of transitioning to oversteer. However, in the fully loaded testing, the vehicle spun-out at the limit due to its oversteer characteristic.

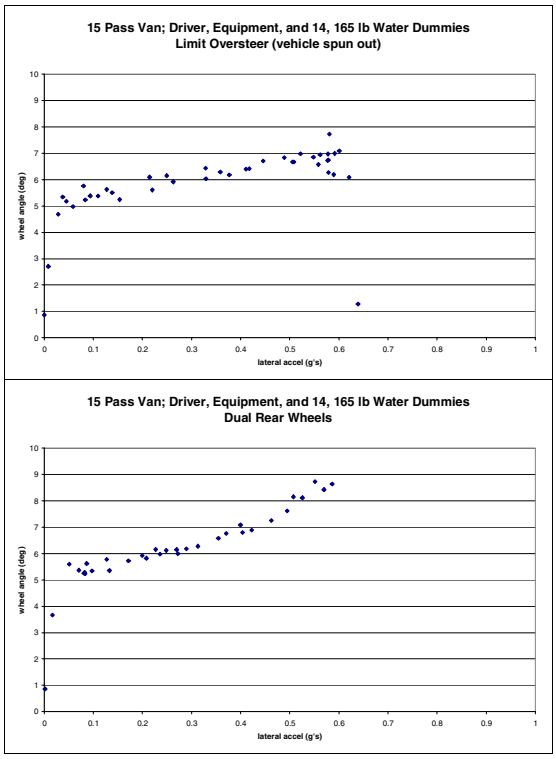

Figure 13. Data plot comparison of standard configuration GVW 15 passenger van testing without (top) and with dual rear wheels.

A method to improve these undesirable handling traits is the addition of dual rear wheels to the van. The dual wheels effectively widen the rear track of the vehicle while simultaneously increasing the lateral grip available at the rear of the vehicle relative to the front. Therefore, in terms of the previous discussion regarding slip angles and oversteer, the slip angle of the rear is reduced relative to the front; thus, promoting an understeer situation. The dual wheels also have a positive effect on transient oversteer.

Not only did the dual rear wheels eliminate the oversteer in a standard test, they also allowed the vehicle to remain understeer when one of the dual wheels was detreaded to the steel belts. This indicates that this vehicle will be understeer before and after a tire delamination.

However, lumped tire testing with this van demonstrated that the van will be oversteer at low lateral accelerations and that the oversteer is much more prominent during the delamination process. The initial round of testing on this van did not test increased damping. An alternative damper mount is currently being designed to mount to this vehicle to allow greater effective damping at the wheels. This future testing will be reported in subsequent publications.

The lumped tire plots for the clockwise and counterclockwise tests are below.

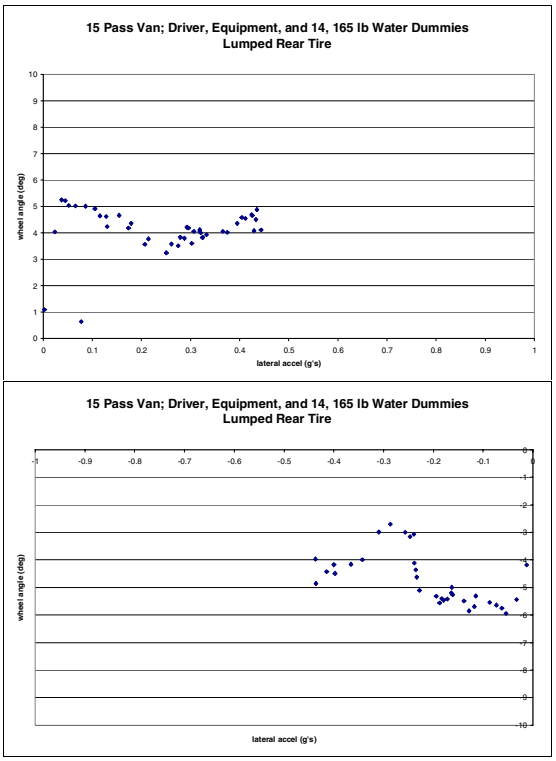

Figure 14. Data plots of lumped tire testing for the 15 passenger van.

<u>Light Truck Testing With Lumped Tires</u> – All vehicles discussed pose a special dilemma when evaluating the effects of a cyclic input into the rear axle and ways of reducing this effect. However, this is especially true with light trucks with heavy duty cargo and towing capacities. Each class of vehicle discussed is designed with the ability to carry relatively large payloads. This means that the load on the rear axle can vary greatly depending on the loading. Light trucks have the greatest variance in that with the unloaded condition, there is relatively little weight on the rear axle; and with loading, it is the rear axle carrying most of the weight. The rear suspension systems on these vehicles has to be designed to be able to accommodate the heavy loading, creating a stiffly sprung system. At unloaded conditions this creates a basically rigid system leading to wheel and axle hop. With the wheel hopping, the rear sprung and unsprung systems are coupled and moving as a single unit. Therefore, the shock absorbers are

not being activated and cannot be used as effectively to control the oversteer condition.

A heavy duty ¾ ton truck was tested in various configurations. It was tested unloaded, with a 1400 cargo load behind the axle, and pulling a heavy equipment trailer loaded with a Bobcat skid steer and sweeper attachment. The trailer as loaded had a tongue weight of 1200 lbs. Each load configuration was tested with OEM replacement shock absorbers mounted at the standard mounts and was tested with adjustable shock absorbers mounted on a pivoting lever arm.

The lever arm was designed such that the attachment point to the axle was as far outboard as possible. In addition, a mechanical advantage of 1.5 was incorporated into the design. This system resulted in variances in the damping ranging from fairly soft to basically rigid by adjusting the damper dial settings from 1 to 9. Figure 15 shows the pivoting lever arm and attachments.

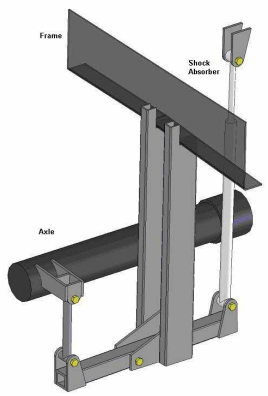

Figure 15. Illustration of pivoting lever arm shock mount.

The figures below show the oversteer associated with the lumped tire testing for the vehicle with no cargo load. For this testing, the lumped tire was placed on the left rear. The first figure shows the clockwise test. With the lumped tire mounted on the left rear, it is on the outside of the turn for the clockwise test and on the inside for the counterclockwise test. Notice the wide scatter in the data. This is indicative of widely varying driver steering inputs. The driver was not able to anticipate the vehicle responses to the steering input and was constantly having to input steering corrections. It is obvious from both the slope of the graphs and the data scatter that this configuration is highly unstable.

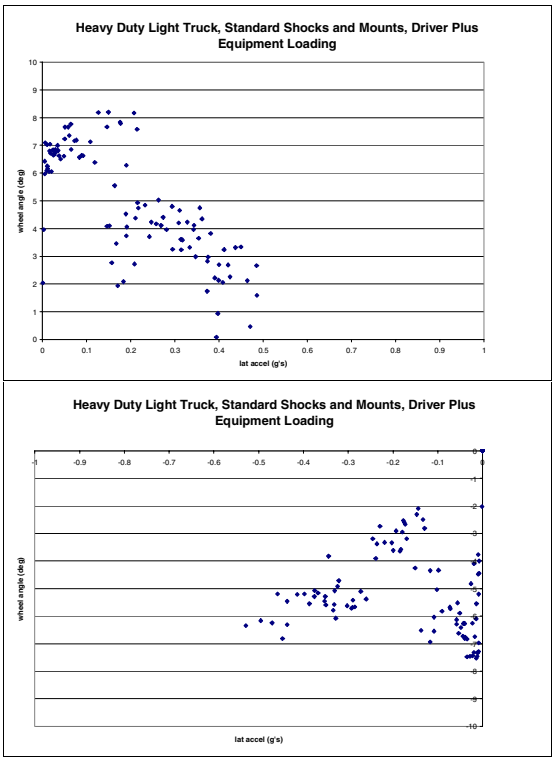

Figure 16. Heavy duty light truck unloaded tests results for the clockwise (top) and counterclockwise test.

The results of the testing with the lever arm and the shock setting 5 are shown for comparison (clockwise test shown first).

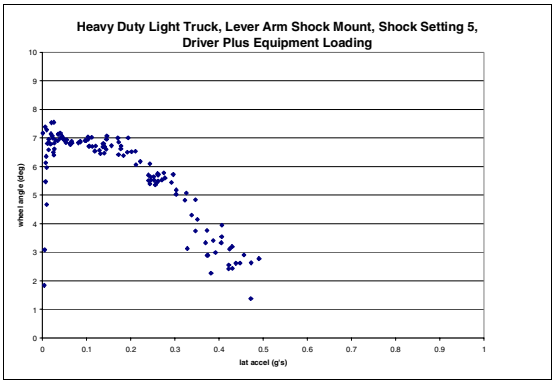

Figure 17. Test Results for the unloaded testing with lever arm shock mount with setting 5 damping (clockwise).

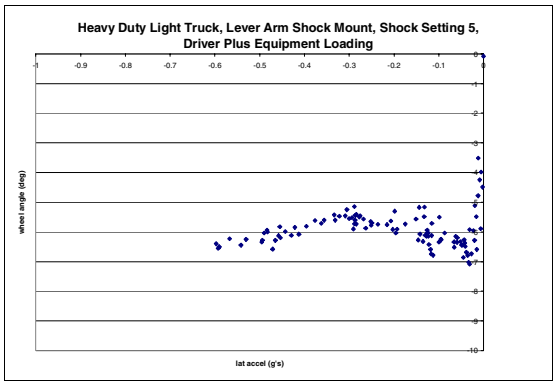

Figure 18. Test results for the unloaded condition with lever arm shock mounts and adjustable shocks setting 5.

Though the general trend of the negative slope is unchanged in this clockwise test, there is much less scatter in the data. This indicates that the driver was able to predict the response of the vehicle and input the appropriate steer to remain on the path with less varied steering wheel angles. The driver stated that the vehicle felt much more controllable in this situation, even though the gradient from each test is similar. A marked improvement is seen in the counterclockwise testing. The driver's feeling during this testing was that the vehicle was near neutral steer and directionally stable.

With the rearward biased cargo load and the standard shocks and mounts, the vehicle was still very unpredictable and unstable as seen below. The top plot shows the clockwise test with the lumped tire on the outside of the turn, and the bottom plots shows the results of the testing with the lumped tire on the inside of the turn (counterclockwise).

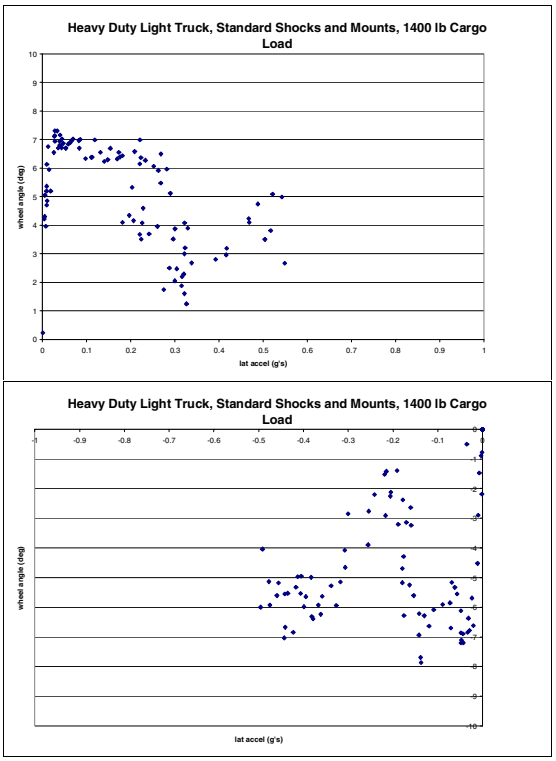

Figure 19. Standard vehicle set-up testing with 1400 pound cargo load.

Again, a dramatic increase in the controllability and predictability of the vehicle was seen in the alternative design shock mount testing, even with the damping on the shock set as low as possible. This is graphically represented below.

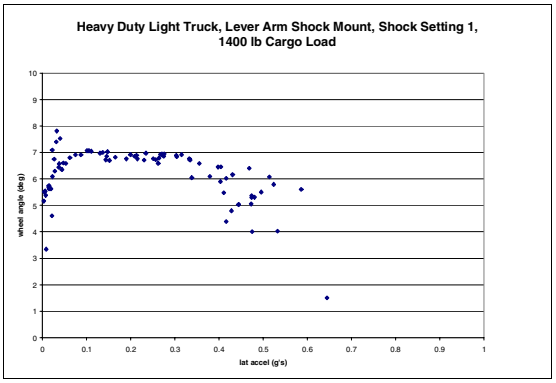

Figure 20. Lever arm shock testing setting 1 with 1400 lb cargo load (clockwise)

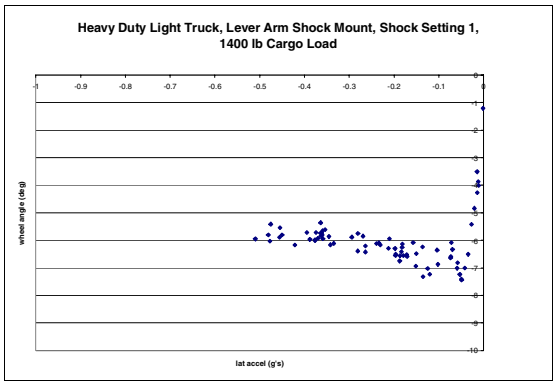

Figure 21. Lever arm shock mounts with shock setting 1 and 1400 lb cargo load.

The final four plots (lumped together as Figure 22) compare the loaded trailer testing with the standard mounts and shock absorbers to the testing with the alternative design. Again, the alternative design greatly improved the handling, especially with the lumped rear tire on the inside of the turn. The top two graphs are the standard configuration clockwise and counterclockwise test, respectively, and the bottom two are the plots for the pivoting lever arm testing.

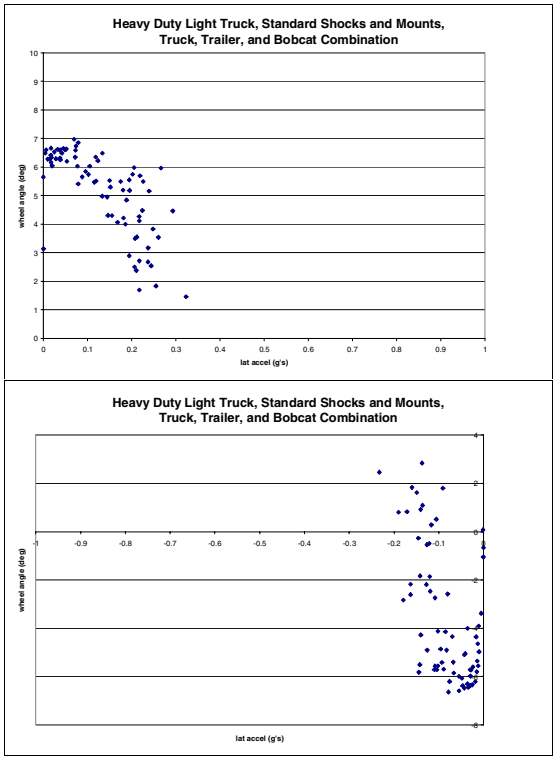

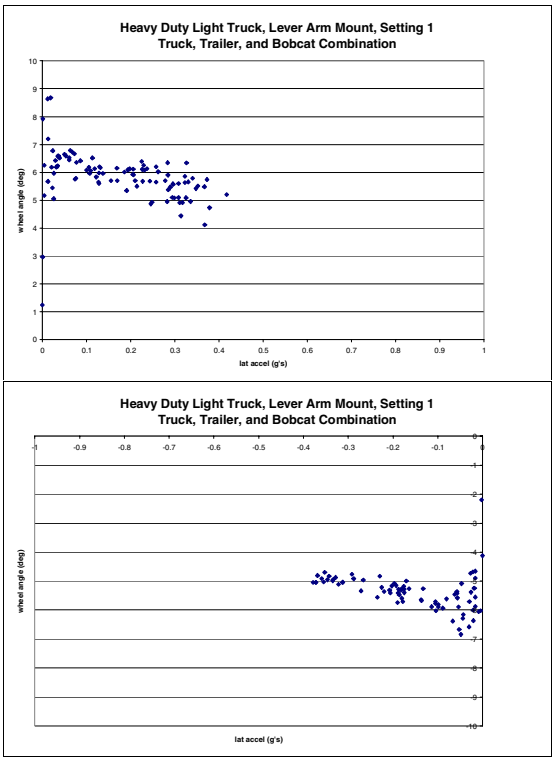

Figure 22. Lumped tire testing results for truck and trailer combination.

CONCLUSIONS

In conclusion, testing has demonstrated the effects of a cyclic input on the suspension systems tested. Cyclic inputs near the tramp mode natural frequency result in a highly uncontrollable vehicle response characterized by severe oversteer even in the quasi-static SAE J266 Steady-State Directional Control Test.

The results of this testing can be extrapolated to real-world highway speed tire delamination events and clearly reveal what a dangerous situation this is for these vehicles traveling at highway speeds.

Testing has also revealed the positive effects of suspension tuning on the controllability of these vehicles during the process of a tire delamination.

REFERENCES

About.com, Hotchkiss Suspensions http://autorepair.about.com/library/glossary/bldef-190.htm, About, Inc, 2007.

Arndt, M.W., Rosenfield, M., and Arndt, S.M., "Measurement of Changes to Vehicle Handling Due to Tread-Separation-Induced Axle Tramp", 2006-01-1680, Society of Automotive Engineers, 2006

Blundell, M., Harty, D., The Multibody Systems Approach to Vehicle Dynamics, Elsevier Butterworth-Heinemann, Linacre House, Jordan Hill, Oxford OX2 8DP, 2004.

Dixon, J. C., Tires, Suspension and Handling 2nd ed., Society of Automotive Engineering, 1996.

Gillespie, T. D., Fundamentals of Vehicle Dynamics, Society of Automotive Engineers, 1992.

Kramer, Kenneth D., Janitor, William A., Bradley, Lawrence R., "Optimized Damping to Control Rear End Breakaway in Light Trucks," Society of Automotive Engineering, Paper Number 962225, 1996.

Milliken, W. F., Milliken, D. L., Race Car Vehicle Dynamics, Society of Automotive Engineering, 1995.

Society of Automotive Engineers, "SAE J266: Steady State Directional Control Test Procedures for Passenger Cars and Light Trucks," Society of Automotive Engineers, 1996.

REAL-WORLD ASSESSMENT OF RELATIVE CRASH INVOLVEMENT RATES OF CARS EQUIPPED WITH ELECTRONIC STABILITY CONTROL

Pete Thomas,
Richard Frampton
Vehicle Safety Research Centre,
Loughborough University, UK

Paper 07-0184

ABSTRACT

This report has evaluated the reduction in crash involvement of cars equipped with Electronic Stability Control (ESC) systems. The evaluation has been conducted for all crashes as well as for a variety of road and loss of control conditions. In addition, a study of ESC benefits in terms of crash costs and accidents prevented has been undertaken. The results show that ESC effectiveness is 3% in crashes of all severity. Serious crashes are 19% lower compared to non-ESC cars and fatalities 15% lower. The potential annual savings in accident costs for a 100% take up of ESC amounts to 588 million pounds by preventing some 5212 crashes. Overall, ESC has shown worthwhile reductions in both accident frequency and cost across a wide variety of crash situations.

INTRODUCTION

In order to effectively direct future policy-related improvements in vehicle design it is important to gain feedback on previous changes to vehicle design. The development of secondary safety technologies is bases on a sound knowledge of vehicle structure and restraint system design and human bio-mechanics. However when intelligent technologies are intended to prevent crashes occurring there are factors which are less well known. Electronic stability control systems have been developed to increase the level of control over vehicle dynamic performance. Comparison of steering wheel heading and front wheel direction allows over-steer or under-steer to be identified and corrected by applying braking on the appropriate wheel. While these systems demonstrate good levels of performance under test conditions their use in the real-world can involve the possibility that other confounding factors may reduce the effectiveness. Examples include the possibility that drivers may change their driving style in response to the increased capability of the system, that real-world driving conditions may be different from the tests or that the electromechanical systems may not function in the manner observed in tests. It is therefore essential to evaluate the performance of new systems once they are on the road.

Several authors have analysed the crash rates of cars equipped with ESC to compare with non-ESC vehicles. These values vary significantly and are listed below in Table 1

Table 1:.
Summary of ESC effectiveness studies

Study	Approach	Crash type	Effecti-veness
Sferco[1]	Predicted influence	Fatal crashes	34%
	Predicted influence	Serious crashes	19%
Langwieder [2]	Predicted effectiveness	Skidding crashes	60%
Becker [3]	Measured effectiveness	All crashes	45%
Aga and Okada [4]	Measured effectiveness	Single vehicle	35%
Tingvall[5]	Measured effectiveness	All crashes	22%
	Measured effectiveness	Wet/icy roads	17%
Farmer[6]	Measured effectiveness	Single vehicle	41%
	Measured effectiveness	Multi-vehicle	0%
Dang[7]	Measured effectiveness	All car crashes	30%
	Measured effectiveness	All SUVs	67%
Thomas[8]	Measured effectiveness	All crashes	3%

It is clear from Table 1 there is no standard way of describing the effectiveness of a system and this means it is difficult to compare results. The only firm conclusion is that ESC systems appear to uniformly give a positive contribution to crash prevention but it is not clear what that level should be nor under what conditions. Thomas (2006) analysed the Great Britain casualty data for the years 2002 to 2004 and concluded the overall reduction of crash involvement of cars equipped with ESC was 3%. This result was substantially lower than the experience of other countries and against this background it was decided to re-

evaluate the GB results using accident data gathered in the years 2002 - 2005.

METHODOLOGY

Crashes that occur in Great Britain resulting in injury and reported to the police are recorded on the national register known as Stats19[9]. The data for 2002-2005 were matched to vehicle licensing information so that car make, model, variant and year of manufacture was known. Information on ESC fitment was matched in using data from the Glass's Guide Checkbook, 2005[10]. A subset of this data was selected to include all injury accidents in which a car was involved. Crashes where a pedestrian, motor cycle or bicycle was involved were excluded. This is because these vulnerable road users tend to dominate the injury severity of the crash.

The analysis uses a case-control method based on the induced exposure method (Evans, 1986 [11]). Case vehicles were defined as those known to be equipped with ESC. A comparable group of control vehicles not fitted with ESC were also defined. These were, in general the previous version of a case vehicle. The make and model of case and control vehicles are shown in appendix B. There were 10,475 case vehicles and 41,656 control vehicles in the dataset. This represents a 21% increase in ESC equipped cars compared with the earlier study.

The case control method also requires vehicle manoeuvres to be separated into those where ESC may have an effect and those where no ESC effect is assumed. Table 1 shows how these case and control manoeuvres were defined.

Table 2

Case and Control Manoeuvres

Control Manoeuvre (no ESC effect assumed)	Other Manoeuvre (ESC effect possible)
Reversing	U turn
Parked	Turning left
Waiting to go ahead but held up	Turning Right
Stopping	Changing lane to left
Starting	Changing lane to right
Waiting to turn left	Overtaking moving vehicle on it's offside
Waiting to turn right	Overtaking stationary vehicle on it's offside
	Overtaking on nearside
	Going ahead left hand bend
	Going ahead right hand bend
	Going ahead other

Using the case-control method, cars in the sample were distributed between the four case control categories shown in table 3.

Table 3.
Case and Control Contingency Table

	Control Manoeuvre (assumed no ESC effect)	Other Manoeuvre (ESC effect possible)
Case Vehicle (ESC)	N_{00}	N_{01}
Control vehicle (no ESC)	N_{10}	N_{11}

The method then calculates the odds of a case vehicle being involved in either of the two crash types (1) and the odds ratio is used to compare the two groups of cars (2). The effectiveness of ESC is defined in (3) and the standard deviations are calculated as shown in (4).

(1) $\text{Odds}_{ESC}\ (\text{Control/Case}) = N_{00}/N_{01}$

(2) $\text{Odds ratio} = (\text{Odds}_{ESC}/\text{Odds no}_{ESC}) = N_{00}/N_{01}\ N_{11}/N_{10}$

(3) $\text{Effectiveness}_{ESC} = (1 - \text{Odds ratio})100\%$

(4) $SD = \text{Odds ratio} \times \exp\left(\sqrt{\left[1/N_{00} + 1/N_{10} + 1/N_{01} + 1/N_{11}\right]}\right)$

RESULTS

The reductions in crashes for severity groups is shown in Figure 1. Overall cars with ESC fitted were involved in 7% fewer collisions than non-ESC cars. Fatal crashes were reduced by 25% although this was non-significant and the serious injury group decreased by 11%.

Figure 1.
Reduction in crashes with ESC

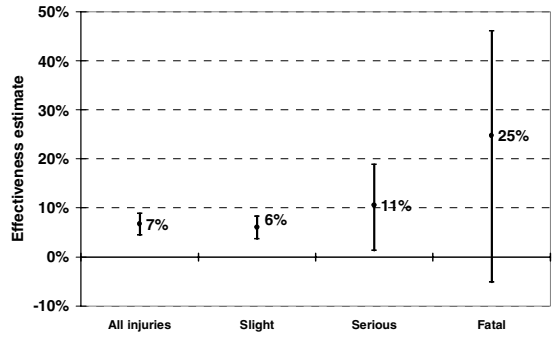

The UK car fleet includes 26,000,000 cars and each year 2,500,000 new cars enter the fleet. Based on the conservative assumption there were no ESC cars on UK roads in 2005 Figure 2 shows the increasing proportion in the fleet that is expected to be ESC equipped if all new cars from 2008 were ESC equipped.

Figure 2.
Projected fleet penetration of ESC equipped cars

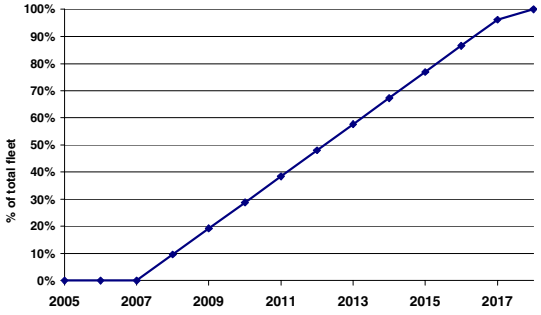

The projection indicates that effectively full fleet penetration would be achieved by 2018.

The projected casualty and financial savings can be projected based on the fleet penetration information and also on the true casualty numbers of occupants in cars. The UK, like many other countries has declining numbers of traffic casualties Table 4 shows the average annual reduction since the current baseline values of the 1994-8 average. Fatal casualty numbers have reduced by a mean of 0.5% each year while the drop for all casualty severities is 1.2%pa.

Table 4.
Mean annual casualty reduction over 1994-8 baseline

Total car occupants	1994-8 average	2005	Mean annual decline from 1996
Killed	1,762	1,675	0.5%
Serious	21,492	12,942	4.0%
Slight	180,034	163,685	0.9%

Figure 3 shows the result of combining the existing casualty reduction rates with the increasing fleet penetration of ESC equipped cars to estimate the reduction in total casualties due to the increasing ESC numbers in the fleet. The figure also shows the financial savings based on the standard UK model using willingness to pay methods.[12].

Figure 3.
Annual casualty and financial savings with ESC

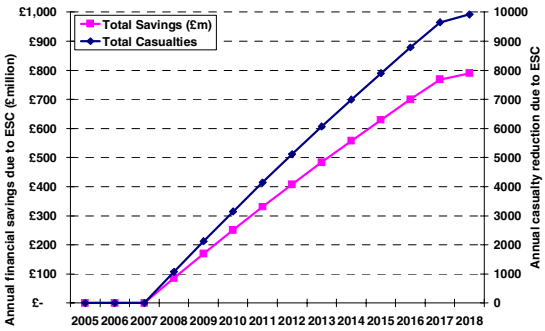

When full fleet penetration is achieved by 2018 ESC systems are projected to be reducing total casualties by 9919 each year, including 388 fatalities, compared to the baseline of no ESC in the fleet. The value of these savings, taking account of the different costs for each severity level, equal £790 million (€1,100 million) each year (2005 prices).

Table 5 shows the projected numbers of each injury category in 2008 and 2018 when all cars in the fleet are expected to be equipped with ESC for the two groups assuming there is no further increase in ESC equipped cars and assuming that all new cars from 2008 will have ESC.

Table 5.
Casualty reduction projections

	Total without further ESC		
Year	**Slight**	**Serious**	**Fatal**
2008	159305	11450	1650
2018	145535	7613	1569

	Reduction with ESC		
Year	**Slight**	**Serious**	**Fatal**
2008	919	116	39
2018	8732	799	388

Figures 4 to 6 show the effectiveness of ESC according to different road surface conditions.

Figure 4.
ESC Reduction for Wet Road Surfaces

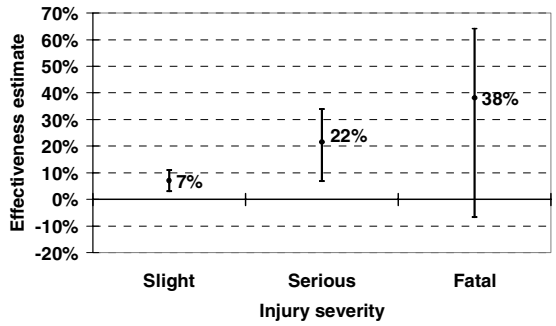

Figure 5.
ESC Reduction for Dry Road Surfaces

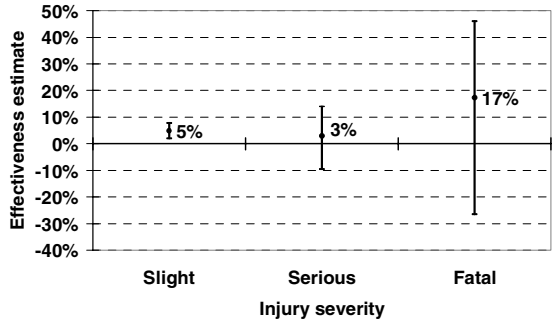

Figure 6.
ESC Reduction for Snowy and Icy Road Surfaces

The overall reduction of crashes for ESC equipped cars on dry road surfaces was 5%, on wet roads it was 9% and on snow or icy surfaces it increased to 20%. On all road conditions the reductions were greater for the more severe injury outcomes although there were insufficient cases to form an estimate of fatal crashes on snow and icy surfaces. Despite the greatest effectiveness of ESC `being observed under the more adverse road conditions these were seldom associated with crashes in the GB data. Figure 7 shows the frequency with which these conditions were associated with crashes in the accident data..

ESC EFFECTIVENESS IN SKIDDING AND ROLLOVER Skidding or rollover generally indicate a loss of control situation. The incidence of these factors in the crash sample is shown in figure 7 and the changes in crash involvement of ESC equipped cars is shown in figures 8 and 9. Figure 7 shows that the majority (78%) of crashes did not involve skidding or overturning. Skidding alone occurred in 16% of crashes and overturning was rare in only 5% of crashes.

Figure 7.
Distribution of Skidding and Overturning

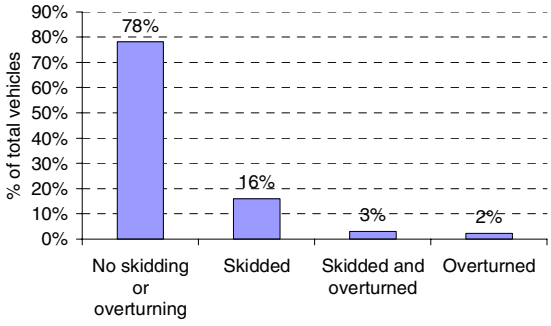

Where skidding alone was involved ESC equipped cars were 23% less likely to be involved in crashes of all severities. The corresponding value for overturning crashes was higher at 36%. Figures 8 and 9 also indicate that ESC was beneficial in

serious injury crashes showing effectiveness values of 33% for skidding related events and 59% for overturning crashes. Values for fatalities are not shown for either condition due to very wide error bands and low numbers of cases.

Figure 8.
ESC reduction in Skidding Related crashes

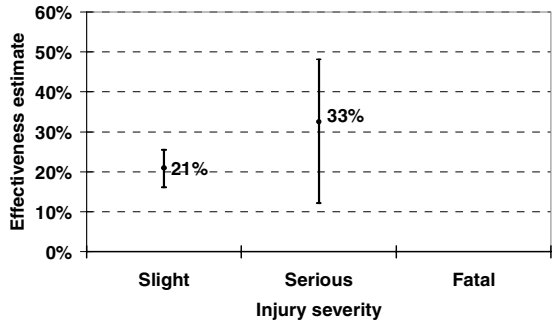

Figure 9.
ESC Reduction in Overturning Crashes

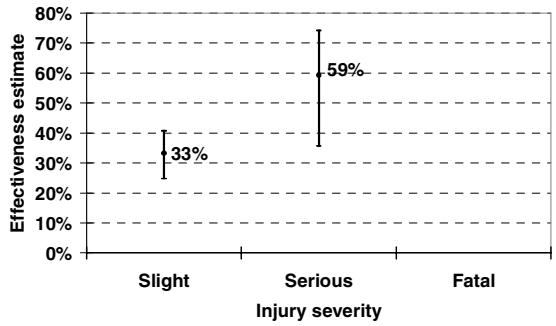

ESC EFFECTIVENESS IN SINGLE VEHICLE CRASHES Single vehicle crashes are those that involve only one vehicle but may involve a pedestrian. The crashes analysed here do not include pedestrians because of their domination of the crash severity outcome. Figure 10 shows the distribution of single vehicle compared to multi vehicle crashes. Crashes involving only one vehicle are in the minority at 8%. Figure 11 shows effectiveness rates for cars equipped with ESC in single vehicle crashes. Overall effectiveness is 27% dropping to 17% for slight crashes. The high value for serious crashes (91%) should be viewed with caution as it is based on only 1 control vehicle and 2 case vehicles in a control manoeuvre situation while no vehicles were present in that situation for fatal crashes.

Figure 10.
Numbers of Vehicles Involved in Crash

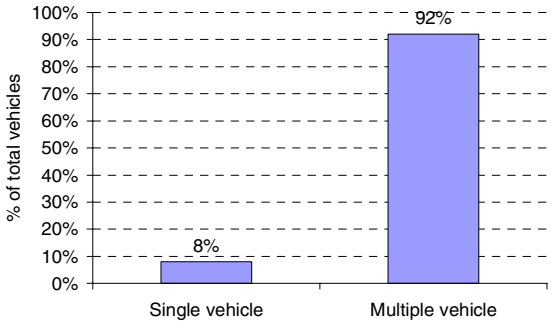

Figure 11.
ESC Reduction in Single Vehicle Crashes

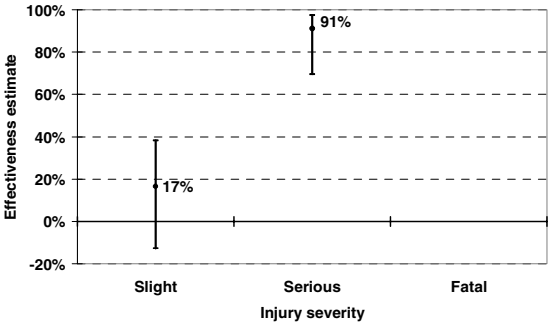

ESC EFFECTIVENESS AND GENDER Figure 12 shows the distribution of driver gender in the sample. Males are in the majority at 70%. For males, ESC showed an effectiveness of 7% for all severities of crash. Figure 13 shows an increasing ESC effectiveness with injury severity. 6% for slight injury, 10% for serious injury and 48% for fatals. For females (figure 14), overall effectiveness was 5% and the values for slight and serious crashes were not significantly different to those for males 4% and 15% respectively. The value for female fatalities was not significant due to small case numbers.

Figure 12.
Distribution of Driver Gender

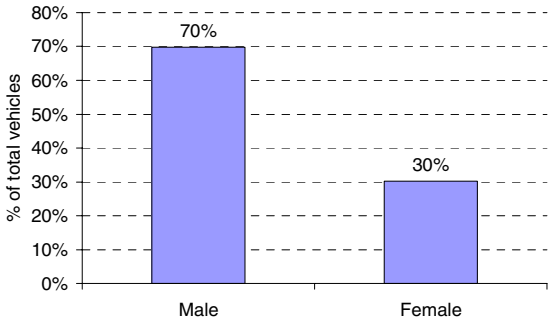

Figure 13.
ESC Reduction in Cars with Male Drivers

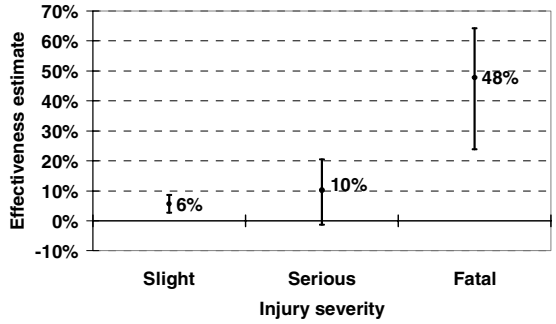

Figure 14.
ESC Reduction in Cars with Female Drivers

ESC EFFECTIVENESS IN FRONT AND SIDE IMPACTS The GB national casualty dataset includes an assessment of first point of impact on the vehicle. Figure 15 shows that 47% of all vehicles sustained an impact to the front and 21% to the side. The case vehicles with ESC had a 10% lower rate of frontal collisions and a 9% lower rate of side collisions. So there was very little difference in overall effectiveness between front and side collisions.

Figure 15.
First Point of Impact to Car

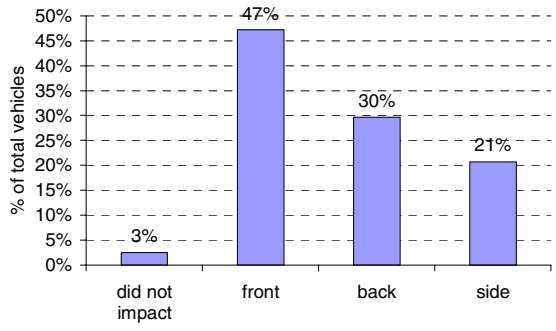

Figures 16 and 17 suggest that ESC may be more effective in side crashes when serious injury occurs. ESC equipped cars were involved in 22% fewer crashes in side impact compared to 2% in frontal crashes. Confidence limits for fatalities were large and negative for both impact types making effectiveness rates non significant.

Figure 16.
ESC Reduction in Front Collisions

Figure 17.
ESC Reduction in Side Collisions

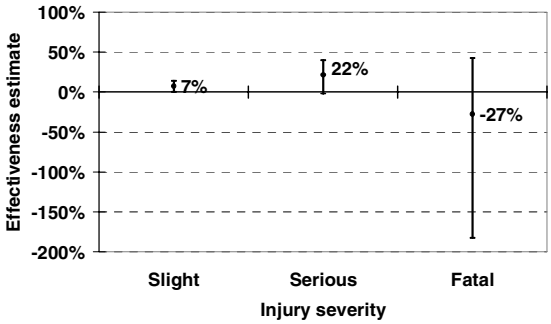

DISCUSSION

This analysis demonstrates that cars equipped with ESC are involved in significantly fewer crashes than similar cars without ESC . The overall reduction on GB roads was 3.1% corresponding to 9,000 fewer crashes each year with a corresponding cost to GB of £559,773,000 at 2004 rates. Under adverse road conditions the effectiveness is greater rising to 25% on snow or icy roads although such crashes only account for 2% of GB crashes.

LIMITATIONS

There are limitations to this analysis since there may be other significant differences in handling between case and control vehicles in addition to ESC systems. If these changes also improve the dynamic behaviour of the vehicle then the effectiveness of ESC alone would tend to be over-estimated. Additionally the chances of crash involvement will also be dependent on driving behaviour; if the case vehicle is a model preferred by drivers with lower risk acceptance the vehicles will not be exposed to comparable driving situations and again the effectiveness of ESC will tend to be over-estimated. This analysis has selected control cars that are as similar as possible to the case cars in order to minimise these effects but they can not be completely avoided. On the other hand the mis-classification of ESC equipped cars, whether in the case or control groups will tend to under-estimate the effectiveness of ESC. The matching of the ESC equipped data is dependent on

an accurate definition of the vehicle model. The matching has been done to the limits of the available data, on the basis of the make, model, variant, engine size and year of manufacture, but there may be a small number of cars misclassified. Kreiss et al[13] have shown that the effect of mis-classification is to consistently under-estimate the effectiveness of ESC so the effectiveness rates reported in this analysis have to be considered to be minimum values although it is expected that the opportunity for mis-classification has been small.

SUMMARY

One of the largest datasets of ESC equipped cars available has been analysed for this case-control study. It has shown that in general ESC equipped vehicles have a lower crash involvement rate and these are particularly high under adverse road surface conditions but there are classes of car and types of accident where benefits are reduced or negative. The results show that ESC effectiveness is 7% in crashes of all severity. Serious crashes are 11% lower compared to non ESC cars and fatalities 25% lower. The potential savings in accident costs for a 100% take up of ESC amounts to some £790 million pounds annually by preventing some 9919 crashes. Even at a 50% take up the saving amounts to some £395 million.

ESC appears to offer additional benefit in adverse road conditions. Overall effectiveness was estimated as 20% for icy conditions and 9% for wet conditions compared to 5% for dry roads. In terms of serious crashes however, ESC effectiveness appears even more pronounced, 22% for wet roads compared to 3% for dry. Skidding and overturning crashes are typical situations on bends when the driver enters too quickly and attempts to steer. The study suggests a high ESC effectiveness. 23% in all skidding related crashes and 36% in all overturning crashes. The corresponding values for serious crashes are 33% and 59% respectively.

There appears to be little difference in ESC effectiveness depending on whether a male or female is driving.

Effectiveness in serious side crashes is much higher (22%) compared to that in serious frontal crashes (2%). This is in line with work by Reiger et al (2005) which suggests that ESC preferentially prevent side impacts since they are more likely to involve loss of control. Single vehicle crashes are also those where ESC is often supposed to have a significant effect. Compared to non-ESC cars, 27% fewer ESC vehicles were involved in all single vehicle crashes compared to 7% for multi and single vehicle crashes taken together. Unfortunately case numbers did not allow a reliable assessment of ESC contribution to the reduction in serious single vehicle crashes.

Overall, ESC has been seen to show worthwhile reductions in both accident frequency and cost across a wide variety of crash situations. There are however, a number of factors to consider when interpreting these results.

Levels of ESC effectiveness in international studies are in many cases different, usually higher, than those seen in this study. This could be due to a different variety of road, driving and weather conditions as well as to differences in classification of crash severity and vehicle manoeuvres. It is therefore important that any decisions over mandatory fitting of ESC systems be taken on the basis of their overall effectiveness across a range of traffic environments.

The case-control method compares ESC and non-ESC cars in total and hence compares all the differences between case and control cars. It has been hypothesized that as all ESC cars have ABS systems, this may be the only reason for the differences in crash involvement. It is unlikely that this is the case as previous studies of ABS systems have shown the effects of ABS to be small Evans (1998) and Broughton (2002).

One important factor to consider when viewing results of this study is the part played in injury reduction due to improvements in passive safety of the cars. Generally, the cars in the control group were all equipped with airbags and structural improvements compared with cars designed before the introduction of the EU front and side impact Directives but there may have been further improvements introduced at the same time as ESC systems. There is no indication that passive safety improvements change driving behaviour that would influence the risk of crash involvement but the improvements could be expected to change injury outcomes. Whilst the reductions in killed and seriously injured occupants will represent the combined effects of reduced crash involvement and reduced injury risk, a passive safety system would be expected to give the same protection on a wet as a dry road under the same crash conditions yet there are very different risks of fatal and serious crashes in the data reported here. Although it was not possible to quantify the effects of passive safety improvements, the results in this study are considered largely to be a measure of improvements in handling performance – mostly ESC.

Every effort was made to compare cars that were as similar as possible so that the major difference was ESC fitment. It is possible that a few were misclassified, however, Kreiss et al (2005) have shown that the effect of misclassification will be to consistently underestimate the effects of ESC. It is

also likely that many crashes with slight injuries are not reported to the police as is the case with damage only events. In addition, we cannot tell how many crashes were avoided completely by the operation of ESC. In those respects, any estimates of ESC effectiveness shown in this study should be viewed as conservative.

The Great Britain national casualty data used in this analysis provides one of the largest samples of ESC equipped cars but further methodological procedures may be required to fully isolate the crash reduction benefits of the system.

ACKNOWLEDGEMENTS

The author would like to thank the DfT for the use of the STATS19 data which provides a very valuable resource to examine the effectiveness of active safety systems. Marianne Page and Lucy Rackliff prepared the background literature for this work.

REFERENCES

[1] Sferco R, Page Y, Le Coz J, Fay P (2001) "Potential effectiveness of the electronic stability programs (ESP) – what European field studies tell us". 17th International Technical Conference on the Enhanced Safety of vehicles. Paper 2001.S2 – 0 – 327, June 4-7, 2001.

[2] Langwieder K., Gwehenberger J., Hummel T., Bende J. (2003). Benefit Potential of ESP in REAL Accident Situations Involving Cars and Trucks. ESV-paper No. 150. 18th-ESV-Conference, Nagoya, (Japan).

[3]Becker, H. et al.: Großzahlenmaterial, "In-Depth" Erhebungen und Einzelfallanalyse, Werkzeuge zur Verbesserung der Fahrzeugsicherheit im Volkswagenkonzern (Large number material, in-depth studies and single case analysis – tools for improvement of vehicle safety at Volkswagen Group). 1. Dresdner Tagung, „Verkehrssicherheit inter-disziplinär", 27.-28. June 2003 (in German).

[4] Aga and Okada (2003) "Analysis of vehicle stability control (VSC)s effectiveness from accident data" Paper no 541, Proceedings of the 18th International technical Conference on the Enhanced Safety of Vehicles. NHTSA, Washington DC.

[5] Tingvall C, Krafft M, Kullgren A, Lie A. (2004) "The effectiveness of ESP (electronic stability programme) in reducing real life accidents" Swedish National Road Administration, paper number 261. Traffic Injury Prevention, vol 5, pp 37 – 41

[6] Farmer, Charles M (2004), "Effect of electronic stability control on automobile crash risk", Traffic Injury and Prevention 5: 317 – 325, 2004

[7] Dang, Jennifer N (2004), "Preliminary results analyzing the effectiveness of electronic stability control (ESC) systems", National Highway Traffic Safety Administration, US Department of Transport, September 2004. Report number DOT-HD-809-790

8 Thomas, P. (2006) 'Crash involvement risks of cars with electronic stability control systems in Great Britain, *Int. J. Vehicle Safety*, Vol. 1, No. 4, pp.267–281.

[9] Road Casualties Great Britain 2005, The Stationery Office, September 2005

[10] Glass's Guide Car Checkbook 2005.

[11] Evans L. Double paired comparison – a new method to determine how occupant characteristics affect fatality risk in traffic crashes. Crash Analysis and Prevention, Vol 18 No 3, pp 217-227, 1986.

12 Highways Economics note No 1. 2005 Valuation of the Benefits of Prevention of Road Accidents and Casualties. UK Department for Transport, London 2007

[13] Kreiss J-P, Schüler L, Langwieder K. The Effectiveness Of Primary Safety Features In Passenger Cars In Germany. ESV Conference paper no 05-0145 Washington 2005.

QUANTITIVE MEASURE OF TRANSIENT OVERSTEER OF ROAD VEHICLES

David A. Renfroe
Paul T. Semones
Alex Roberts
Engineering Institute, LLC.
United States
Paper Number 07-0217

ABSTRACT

When discussing oversteer of a vehicle, reference is made to results of the SAE J266 circle test or gradually increasing steer test. However, these tests demonstrate the vehicle's characteristics at a quasi-static condition and do not consider the dynamic effects of the moment of inertia of the vehicle or of the wheelbase and tire characteristics during yaw accelerations occurring in transient maneuvers. Frequently, there are discussions of the transitional effects on oversteering of the vehicle and reference may be made to the radius of gyration squared versus the product of the front and rear distances from the axles to the CG. This particular relationship, however, assumes that the tire lateral capabilities on the front and the rear are the same. This paper will discuss the comparison of the "Ackermann yaw rate" versus the measured yaw rate in transient steer maneuvers such as the step steer. The Ackermann yaw rate will be the yaw rate developed if the vehicle were to track exactly along the direction that the wheels are pointing. If this theoretical yaw rate is compared to the measured yaw rate, a vehicle's transitional handling characteristics can be quantified. An example where there has been considerable discussion is with the 15-passenger van. Loss of control of these vans, attributed to oversteer when attempting an accident avoidance maneuver, has been discussed extensively by government and private groups. That oversteer occurs even though these vans exhibit understeering characteristics when tested with the J266 protocol up to a transition to oversteer at the vehicle's lateral adhesion limit. The technique described here allows the transitional oversteer characteristic of any vehicle to be quantified. This will help to explain and quantify the characteristic causing loss of control of these vans and other similar vehicles.

INTRODUCTION

Recent discussion concerning 15-passenger vans states that these vehicles are oversteer at higher lateral accelerations [NHTSA, 2004]. However, testing of a 15-passenger van, using the SAE J266 circle test, illustrates that these vehicles are definitely understeer up to the limit of lateral acceleration where they transition to oversteer (see *Figure 1*).

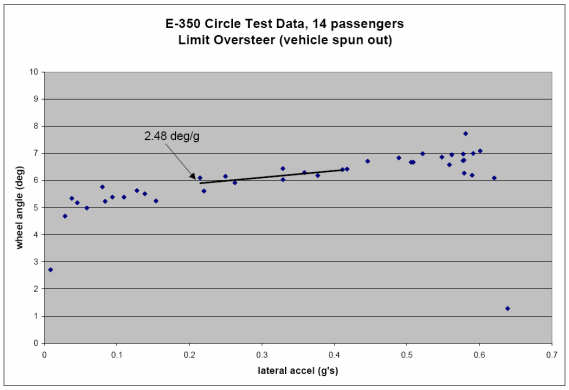

Figure 1. Steer angle versus lateral acceleration for Ford E-350.

Nevertheless, it continues to be asserted that these vehicles are oversteer, and in defense of this claim, driving a fully loaded van certainly feels unstable and there is a tendency to wander on some models. The reason that a 15-passenger van does not oversteer in this quasi-static circle test is that the moment of inertia of the cargo box is not affecting handling during that maneuver, since there is very little or no angular acceleration during the maneuver. Even though the center of gravity moves rearward as the load of the van increases, the force on the rear tires also increases which will increase their lateral load handling capacity. Also, with the large rear overhang, as the load moves beyond the rear axle the front axle actually begins to unload. This would tend to cause the front end to drift out in the circle test, causing classic understeer.

However, during the transitional phase of a turn, the vehicle has a yaw acceleration. Once the yaw rate approaches the Ackermann yaw rate as defined by the steering angle, velocity, and wheel base (see *Equation 1*), the angular inertia of the vehicle tends to cause the vehicle to overshoot the Ackermann yaw rate. This overshoot is what is felt by the driver and is in fact an instability.

In an attempt to quantify this instability as a form of oversteer, measured yaw rate will be compared to an ideal yaw rate or "Ackermann yaw rate." The Ackermann yaw rate (AYR) is the theoretical ideal. This would be the yaw rate that would occur with no lateral slip in the tire. The AYR would be strictly a function of the wheel base (W), steering angle (A), and velocity (V).

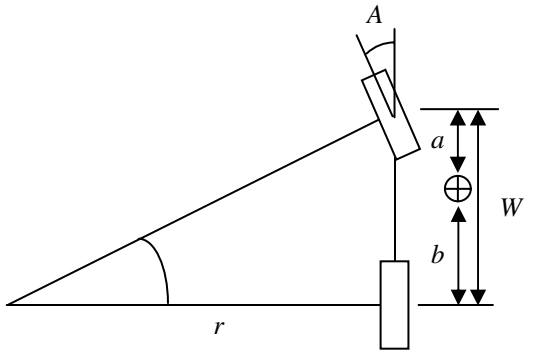

Figure 2. The bicycle model in a constant radius turn.

The resulting function would be:

$$AYR = \frac{V \cdot \tan(A)}{W} \qquad (1.)$$

The actual (i.e., measured) yaw rate can then be compared to this AYR to quantify the transitional oversteer or understeer of the vehicle by observing the undershoot or overshoot of the measured yaw rate to the AYR. Since most maneuvers are conducted with a dropped throttle resulting in a decreasing velocity during the maneuver, the AYR can be calculated and plotted over time with respect to the measured velocity of the vehicle. Such a comparison of the theoretical to the actual yaw rates has been discussed previously by Ellis [Ellis, p. 162, 1969] and Blundell [Blundell, p. 411, 2004]. When discussing the comparison of the ideal path and the actual path a car takes including any transient effects, Ellis states, "The actual path will not be coincident with the ideal path due to the finite response times of the car, but the divergence can be measured as a lateral displacement or path error and a difference in heading angles, the course error." Blundell calls the Ackermann yaw rate the idealized or geometric yaw rate and provides his definition of understeer as the geometric yaw rate divided by the actual yaw rate. When this quotient is less than 1 the vehicle is oversteering. Stonex described the same method of observing transient understeer and oversteer in his paper published in 1940 [Stonex, 1940]. Using these definitions the handling characteristic of vehicles will be investigated for the transient reaction of a maneuver to determine what is occurring with the vehicle versus what a driver may be feeling. Generally, the characteristic that will contribute to a transient oversteer will be the yaw radius of gyration versus the wheel base. Dixon quantifies this relationship as

$$ab < k^2 \qquad (2.)$$

where a is the distance from the center of gravity (CG) to the front wheels, b is the distance to the rear wheels from the CG, and k is the radius of gyration about the z axis [Dixon, p 469]. He says, "If $ab<k^2$, it [the rear slip angle] will initially develop in the wrong direction and will undergo a reversal before reaching steady state." The results of this testing will illustrate this effect. To correct for this problem Dixon states that moving the wheels out to the corners increases the ab of the vehicle and therefore the vehicle becomes more agile. Similar observations were made in the 1930's by Olley and reported in a 1962 monograph published at General Motors, then published for the public in 2002 [Milliken, p. 250, 2002]. He said, "What is clear is that, for positive ['good' or 'desirable'] handling – without 'faking' the geometry by exaggerated roll understeer at the rear tires – it is essential to have an adequate wheelbase, and that this should give a k^2/ab ratio considerably less than 1.0."

Another way of reducing the transient oversteer of the vehicle is to increase the lateral stiffness of the rear tires. In the case of the 15-passenger van, this can be done by installing dual tires. These effects will also be illustrated.

TRANSIENT OVERSTEER IN J-TURN MANEUVERS

A J-Turn is a standard maneuver used to test for the transient response of a vehicle to a step input. For any dynamic system, the response to a step input is observed by measuring the rate that the system approaches the steady state condition. In this case, that steady state condition is defined by the steering angle of the front wheels. Response time and overshoot are typical observations for dynamic systems. One can describe a system by the length of time it takes for the response to approach the steady state, the magnitude of the overshoot or the number of oscillations around the prescribed steady state condition of the new trim of the system. *Figure 3* illustrates a typical underdamped dynamic system with significant overshoot.

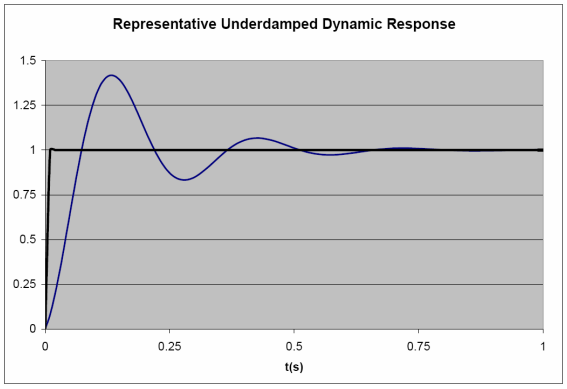

Figure 3. Typical dynamic response to a step input.

However, in a standard J-Turn the response will not be an approach to a horizontal line on a graph. Yaw rate versus time during a typical sub-limit (low speed) J-Turn would step up to the AYR determined by the steering angle, wheel base and velocity, then decrease with time as the velocity decreases as shown in *Figure 4*.

In a standard 35 mph J-Turn test with 300 degrees of steering input, the steering input graph will appear as shown in *Figure 5*. For the particular case shown, a J-Turn test utilizing a 2001 Ford E-350 15-passenger van, the yaw rate response is shown in *Figure 6*.

Upon gross comparison of the two curves, the vehicle's yaw rate response actually appears to undershoot the expected steady-state response to a typical step input. However, in the above case, velocity falls off to zero after four seconds because the J-Turn test protocol involves a sudden reduction of accelerator input to zero simultaneously with the steering input. Thus, the vehicle coasts to a near stop (and approximately zero measurable yaw rate) a few seconds after the steering is applied.

When this linear deceleration throughout the J-Turn maneuver is accounted for, it becomes clear that the yaw rate response in the particular case shown at right is in fact a transient overshoot of the ideal yaw rate expected from the twin step inputs of steering and accelerator release. For, while the steering is a classic step input, the ideal yaw rate will actually be a declining curve as velocity bleeds off to zero.

Oversteer is evident after about 2.7 seconds in *Figure 7*, as the measured yaw rate exceeds the ideal yaw rate expected from the steering input and deceleration. It could be argued that the vehicle is always transiently oversteering in this case if the slope of the Ackermann yaw rate versus time is compared to the converging slope of measured yaw rate versus time.

In this particular case, there was no tipping or significant loss of contact between tires and the ground as the vehicle oversteered.

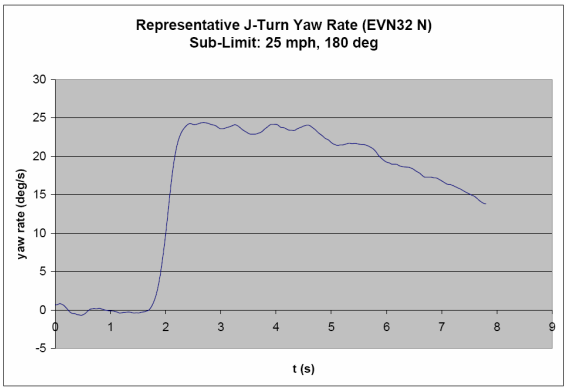

Figure 4. Measured yaw rate versus time in a low-speed J-Turn.

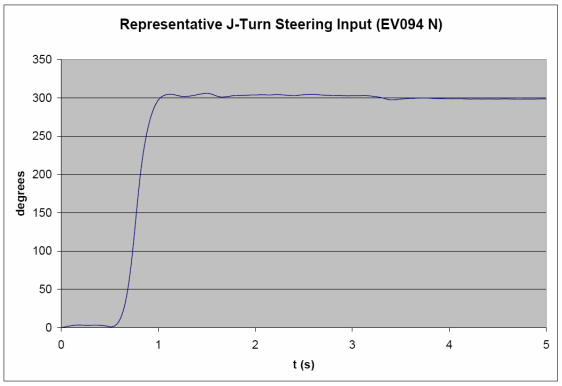

Figure 5. Representative J-Turn Steering Input.

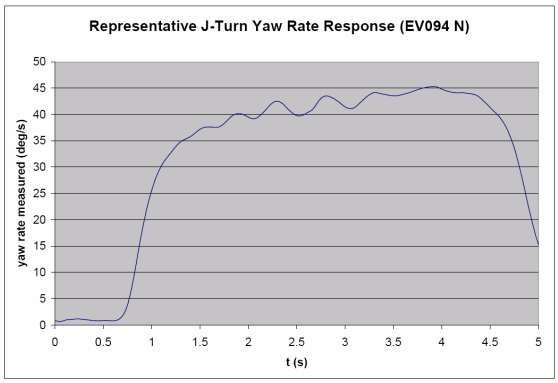

Figure 6. Typical yaw response observed with a loaded 15-passenger van.

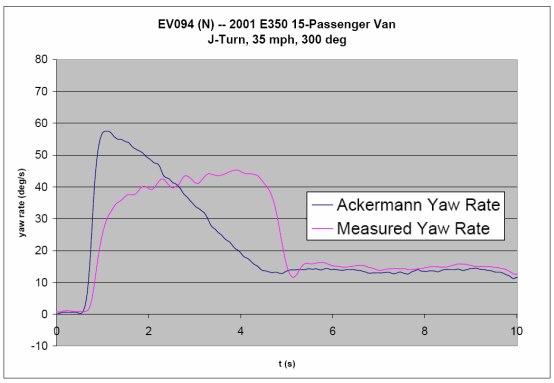

Figure 7. AYR versus Actual yaw rate. (Data from same test as shown in *Figures 5* and *6*.)

TRANSIENT OVERSTEER IN RAPID REVERSAL MANEUVERS

Transient oversteer behavior was analyzed in several rapid reversal steering tests conducted with Ford E-350 15-passenger vans. All tests were conducted featuring initial left turns followed rapidly by right steering inputs, and frame-by-frame video analysis was conducted to match vehicle behavior (such as incidence of wheel lift or outrigger contact) with recorded data to determine whether vehicle events were occurring during phases of oversteer or understeer, as plotted from the collected data.

Testing illustrated in *Figure 8* was conducted with an initial velocity of approximately 33 mph and exhibited oversteer in both the left and right steering phases. In the right steer (the second steering phase of the test), the right front wheel lifted off the ground, which would normally cause understeer. However, the van began to oversteer during the first instance of wheel lift.

The test illustrated in *Figure 9* was conducted with an initial velocity of approximately 39 mph and exhibited oversteer in both the left and right steering phases. In the latter phase, the vehicle tipped over and loaded the outriggers. However, the onset of oversteer occurred before wheel lift. Note how the higher speed causes greater transient oversteer.

Testing on a 1997 E-350, illustrated in *Figure 10*, was conducted with an initial velocity of approximately 35 mph and exhibited oversteer in the initial steering phase. In the latter phase, oversteer was also observed after the vehicle had tipped over and loaded the outriggers. (Velocity data was lost after approximately 5 seconds, and thus the Ackerman yaw rate is not shown beyond that point in *Figure 10*.)

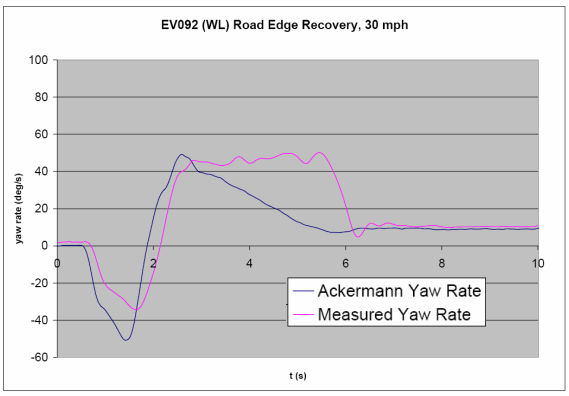

Figure 8. Test 1 – NHTSA Fishhook at 33 MPH.

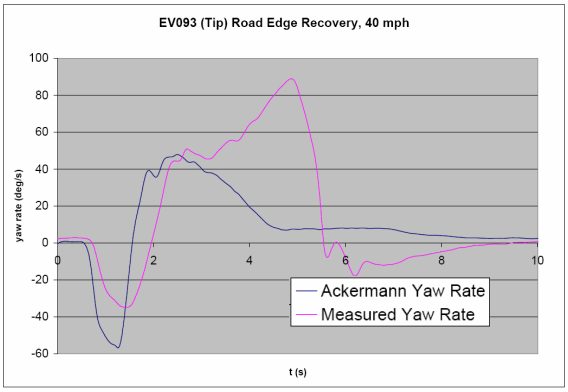

Figure 9. Test 2 – NHTSA Fishhook at 39 MPH.

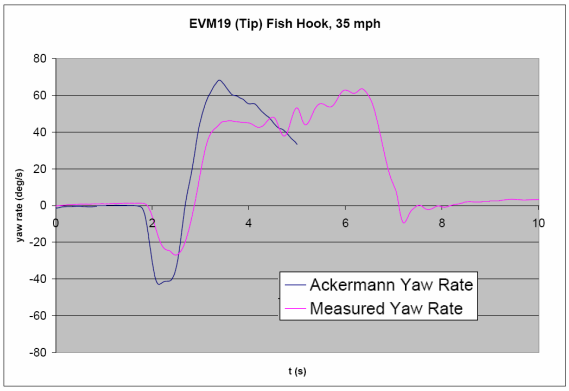

Figure 10. Test 3 – NHTSA Fishhook at 35 MPH. (Velocity data was lost after ~5 s.)

In comparing the three tests, a trend was observed in the relationship between the duration of initial phase oversteer and when the onset of oversteer occurred in the second phase after steering reversal. For the test with the briefest oversteer in the initial left turn, Test 3 (*Figure 10*), oversteer in the second phase did not occur until after the vehicle had already tipped over onto the outriggers and committed to rolling over.

The test with the next longest initial oversteer, Test 1 (*Figure 8*), oversteer in the second phase began earlier, during the first lift of the right front wheel. The test with the longest initial oversteer of the three, Test 2 (*Figure 9*), saw onset of oversteer in the second phase soonest of the three tests, oversteering before any wheel lift had occurred, and the vehicle ultimately tipped over onto its outriggers and committed to roll.

In summary, the trend observed in these three tests showed that the longer the period of initial oversteer, the earlier oversteer would occur in the reverse steer phase. Further frame-by-frame video analysis of available test data would have to be conducted to confirm the general validity of this trend.

EFFECT OF INCREASING LATERAL STIFFNESS OF THE REAR AXLE ON TRANSIENT OVERSTEER

Oversteer/understeer behavior was analyzed on two Fishhook tests conducted with a 1995 Ford E-350 15-passenger van, both before and after the installation of dual wheels on the rear axle to increase the lateral stiffness. Both tests were conducted on the same day with the same vehicle. The first test (see *Figure 11*) was conducted with an initial velocity of approximately 35 mph and involved right-then-left steering inputs. The vehicle exhibited transient oversteer in the initial turn, then in the second turn began to transiently oversteer, lifted the inside wheels and rolled onto the outriggers.

After installation of dual wheels on the rear axle of the test vehicle, a second test (see *Figure 12*) was conducted with an initial velocity of approximately 40 mph, and followed the same Fishhook maneuver as the first test. The vehicle exhibited brief oversteer in the initial turn, but remained well within the understeer range throughout the second phase of the maneuver. The right front wheel lifted off the pavement at least twice during the second phase.

The video frame captures provided in *Figures 11* and *12* represent approximately identical locations on the test track, and demonstrate the significant difference in vehicle behavior before and after installation of dual wheels on the rear axle. The video frame shown of the dual-equipped van in *Figure 12* captures the instant of maximum wheel lift visible in the test, and additional video analysis showed no evidence that the

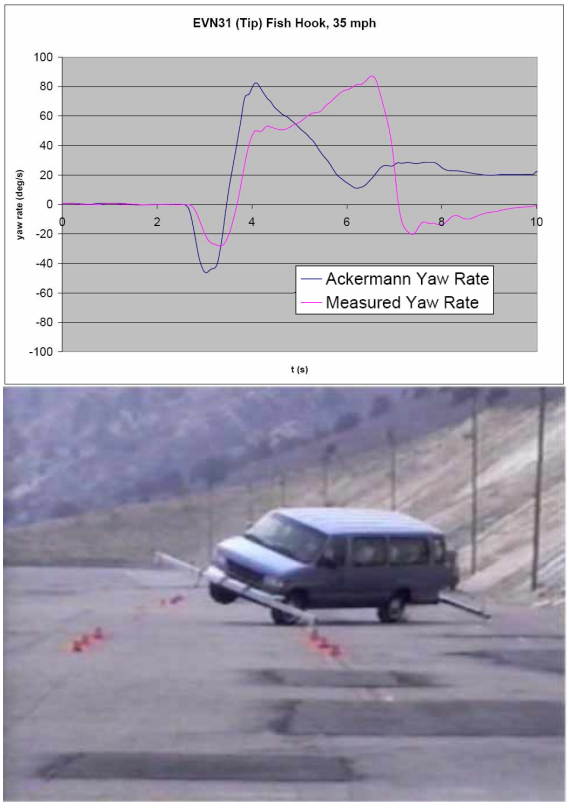

Figure 11. Test 4 – NHTSA Fishhook with unmodified vehicle and single rear wheels.

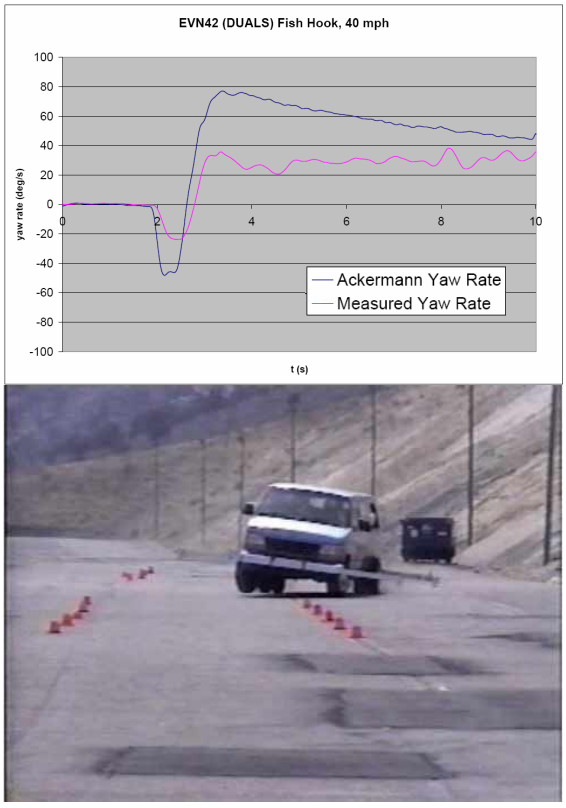

Figure 12. Test 5 – NHTSA Fishhook after installation of dual rear wheels.

right rear tires ever lost contact with the pavement. While the frame provided here appears to show open space between the right rear outer tire and the pavement, frames examined 1/25th of a second before and after the provided frame show the tires apparently in full contact with the pavement.

EFFECT OF FULL LOAD VERSUS LIGHT LOAD

As reported by NHTSA [NHTSA, 2001], the center of gravity of a fully loaded 15-passenger van moves several inches rearward and upward when compared with a lightly loaded (e.g., driver only) condition. The fact that a full load of passengers increases the van's propensity to roll over was demonstrated with two 1995 Ford E-350 15-passenger vans in 40 mph Fishhook Maneuvers. Quasi-static understeer/oversteer characteristics are still shown to be understeer with oversteer at the limit even for the fully loaded van as was shown in *Figure 1*. Here it will be shown the effect of loading the van on the transient oversteer characteristics.

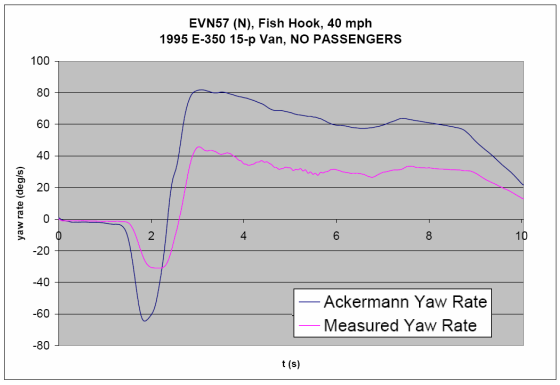

Figure 13. Test 6 – NHTSA Fishhook with vehicle at light loading condition.

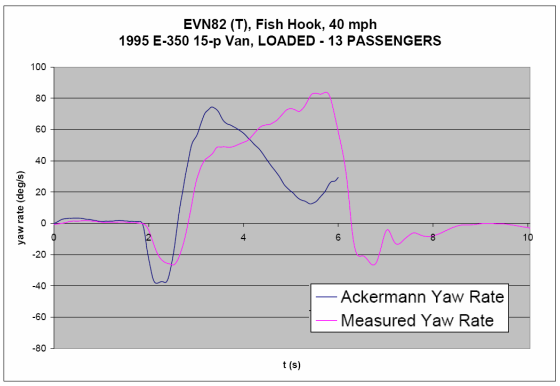

Figure 14. Test 7 – NHTSA Fishhook with full ballast loading. (Velocity data lost after ~6 s.)

In the Fishhook test conducted without passengers, the steering inputs were approximately 270° and 360°, and neither wheel lift nor transient oversteer occurred (see *Figure 13*). In the Fishhook test conducted at this speed and fully loaded with ballast in all passenger positions, the result was tipover and rapid transition to oversteer in a maneuver with steering inputs of approximately 180° and 360° (see *Figure 14*).

A PROPOSAL FOR QUANTIFYING THE TRANSIENT OVERSTEER CHARACTERISTIC

With transient oversteer characteristics now demonstrated as being observable in terms of traditional dynamic system response, a metric for quantifying the magnitude of the characteristic will now be proposed. Over a set of ten tests of Ford E-350 15-passenger vans, the metric shows good correlation to a range of desirable and undesirable vehicle responses.

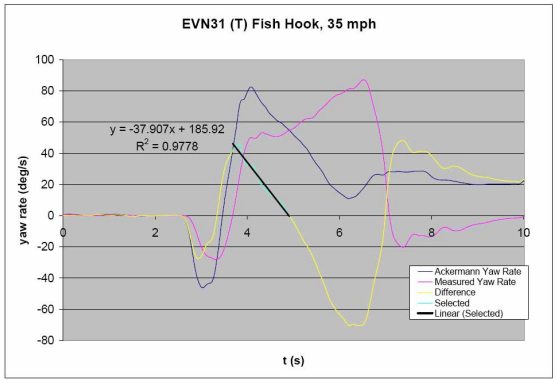

Figure 15. Test 4 (see Figure 11) with transient oversteer metric applied.

The metric is developed by plotting the difference between Ackermann and measured yaw rates. This difference is shown as the yellow plot in *Figures 15-17*. A portion of the difference plot is selected for examination (highlighted in bright blue in the figures) and a linear curve fit applied. As will be explained below, the slope of the examined portion is taken as a transient oversteer metric due to its physical relevancy to vehicle behavior.

In cases of rapid reversal steering maneuvers such as the Fishhook or Road Edge Recovery tests, the examined portion of the difference plot is bounded by two clearly defined points. (See *Figure 15* above.) The first is the point at which the measured yaw rate crosses zero at the start of the second half of the

steering maneuver, or equivalently, the point at which the difference plot equals the Ackermann yaw rate. The second point is defined as the location where the difference curve equals zero, or equivalently, the point at which the Ackermann and measured yaw rate plots intersect (if, indeed, they do).

(For some maneuvers, such as the single J-Turn test evaluated, the first point of interest was simply identified as the peak of the difference curve, since it had no clear intersection with the Ackermann curve. This method is shown in *Figure 16*. For other maneuvers, the second point of interest was identified as the minimum of the difference curve, since it never reached zero, and this method is shown in *Figure 17*.)

In purely theoretical terms, the intersection of the two yaw rate lines represents the switch from theoretical understeer to theoretical oversteer, although it should be noted that the transient oversteer characteristic of the actual vehicle behavior is intrinsic to the entire dynamic response portion of the curve. But in the sense that the difference plot represents the actual vehicle's deviation from the theoretical ideal, the metric proposed here evaluates that portion of the curve that is "understeer": that is, the portion over which the measured yaw rate is less than the Ackermann yaw rate. It is the rate at which this measured yaw rate approaches (and often overshoots) the Ackermann yaw rate that is the fundamental characteristic quantified by this proposed metric.

In a mathematical sense, the slope of the examined portion of the difference curve has units of angular acceleration (deg/s^2), and corresponds to the physical rate of change of the vehicle's yaw angular velocity. Its significance to transient oversteer characteristics and undesirable vehicle responses, such as tipping over, is that it allows transient oversteer to be described as the rate at which a vehicle's yaw response overtakes the declining ideal yaw rate in dropped-throttle, limit steering maneuvers.

In the ten examined E-350 van tests, a high absolute value for the metric (i.e., a steep slope to the examined portion of the difference curve) correlated well to high oversteer and/or rollover to outrigger contact. A low absolute value for the metric (i.e. a shallow slope) correlated to successful tests in which all four of the vehicle's tires remained in contact with the ground.

The values of this transient oversteer metric computed for the ten tests are presented in *Table 1* on the following page. Absolute values ranged from 2.8 to 55.0. All three tests with metrics of 4.9 or less resulted in no wheel lift. All seven remaining tests had metrics of 7.5 or greater, and all but two of those resulted in tipping over. One of the two exceptions resulted in single wheel lift only, and that run had the lowest tested speed (30 mph) of the set. The other exception was the sole J-Turn examined, which did not result in wheel lift, but did result in significant oversteer.

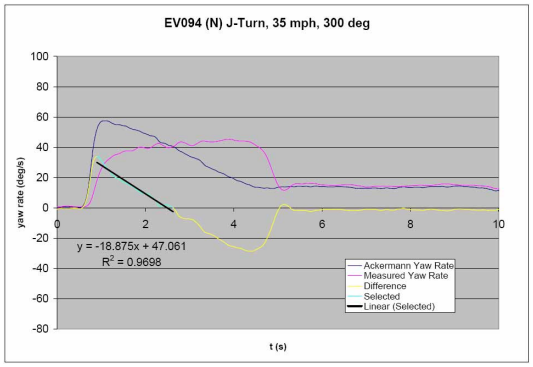

Figure 16. J-Turn test (see Figure 7) with transient oversteer metric applied.

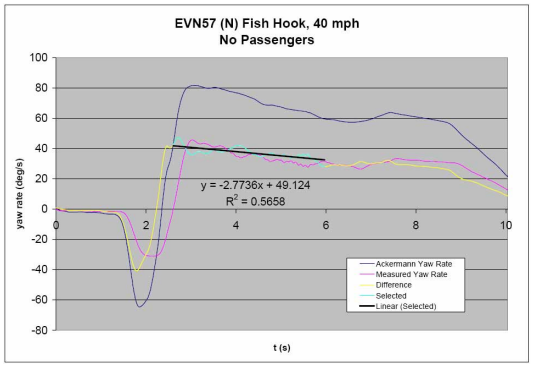

Figure 17. Test 6 (see Figure 13) with transient oversteer metric applied.

The metric correlates well to the loading conditions of the 15-passenger vans tested, confirming the relationship between unsafe vehicle responses and a full load of passengers. Three of the four tests with the lowest metric were those tests with the lowest loading condition – either driver/instruments only or ballast loading short of the full 15-passenger complement. The remaining test was fully loaded but had the modification of dual wheels installed on the back axle, dramatically improving its rollover resistance and minimizing any transient oversteer.

The transient oversteer metric could be only weakly correlated to test speed or maneuver type, but does

suggest that a 15-passenger van's loading condition is a greater influence on rollover propensity than the speed of an emergency steering maneuver.

The results suggest that a metric value between 4.9 and 7.5 represents the boundary between desirable and undesirable vehicle handling response. This value boundary may be particular to the 15-passenger van, whereas other vehicles may have different values for acceptable performance.

CONCLUSION

A simple method for the quantification of transient oversteer has been illustrated. By comparing the theoretical or Ackermann yaw rate to the actual measured yaw rate, the overshoot of a step input or a series of inputs can be analyzed. As has been shown here, when the yaw moment of inertia increases, so does the transient oversteer. As the yaw momentum increases due to vehicle velocity, so does the yaw overshoot. Control of the yaw overshoot to the steering input can be gained by increasing the lateral stiffness of the rear tires as has been predicted in the previous literature. This tool will allow the analysis of testing results to quantify what may have heretofore been heuristic results reported by the drivers of the vehicle and reported as merely a subjective score.

REFERENCES

Blundell, M., Harty, D., The Multibody Systems Approach to Vehicle Dynamics, Elsevier Butterworth-Heinemann, Linacre House, Jordan Hill, Oxford OX2 8DP, 2004.

Dixon, J. C., Tires, Suspension and Handling 2nd ed., Society of Automotive Engineering, 1996.

Ellis, J. R., Vehicle Dynamics, John Ronaine Ellis, London Business Books LTD., 1969.

Milliken, W. F., Milliken, D. L., Chassis Design – Principles and Analysis, Society of Automotive Engineering, 2002.

NHTSA, Research Note: "The Rollover Propensity of Fifteen-Passenger Vans," April, 2001.

NHTSA, "NHTSA Action Plan for 15 Passenger Van Safety," http://www.nhtsa.dot.gov/cars/problems/studies/15PassVans/15passvan.html, 2004.

Stonex, K. A., "Car Control Factors and Their Measurement," Society of Automotive Engineers, December 1940.

Table 1.
Transient oversteer metrics for a suite of 10 steering tests on late model Ford E-350 15-passenger vans.

Test Name	Maneuver	Loading	Speed	Result	Transient Oversteer Metric*
EV093	Road Edge Recovery	Ballast in all positions	40 mph	Tipped	**55.0**
EVN31	Fish Hook	Ballast in all positions	35 mph	Tipped	**37.9**
EV092	Road Edge Recovery	Ballast in all positions	30 mph	Wheel Lift	**31.1**
EVN82	Fish Hook	Ballast in all positions	40 mph	Tipped	**27.7**
EV094	J-Turn	Ballast in all positions	35 mph	(No Lift)	**18.9**
EVM19	Fish Hook	Ballast in all positions	35 mph	Tipped	**17.6**
EVN60	Fish Hook	Ballast in 12 positions	35 mph	Tipped	**7.5**
EVN42	Fish Hook	Ballast in all, DUALS	40 mph	(No Lift)	**4.9**
EVN56	Fish Hook	Driver only	35 mph	(No Lift)	**3.9**
EVN57	Fish Hook	Driver only	40 mph	(No Lift)	**2.8**

*Given in absolute values.
Actual computations result in negative quantities.

OBJECTIVE TEST METHODS TO ASSESS ACTIVE SAFETY BENEFITS OF ESP®

Marcus Nuessle
Ruediger Rutz
Matthias Leucht
Markus Nonnenmacher
Hardy Volk

DaimlerChrysler
Mercedes Car Group
Germany
Paper Number 07-0230

ABSTRACT

Since ABS started in the Mercedes-Benz S-class (W116) in 1978, but mainly by the introduction of ESP® in 1995 in the Mercedes-Benz S-class (W140), Active Safety of passenger cars has been affected by combination of chassis parameters and wheel-brake based systems. Since ESP® has a significant impact on vehicle stability; the evaluation of Active Safety has to be performed in combination with ESP®. Therefore objective tests have been developed to assess the combination of chassis and ESP®. A huge number of tests are used during the development and application of ESP® Systems to vehicle platforms.

Many accident investigations showed an outstanding benefit of ESP® for Active Safety. This raised the interest in objective test methods to assess ESP® performance and finally leads to NHTSA's recently published notice of proposed rulemaking for safety standards for ESP®.

This paper will demonstrate various objective tests and measures for ESP® evaluation. This article will illustrate objective criteria by means of ESP® sub-functions and several operating points (e.g. different speed, lateral acceleration, steering input). The objective behavior of ESP® on high µ will be discussed as well as special demands on low µ.

INTRODUCTION

Current overall ESP® Systems contain several sub-functions to enhance Active Safety in different driving situations. The history of wheel brake-based systems started with braking functions like Anti Lock Brake (ABS). Even to ABS several functions have been added over the last years.

Present systems control the brake balance between front and rear axle by dividing brake force. When it comes to braking in a turn special algorithms are used to maintain yaw stability and provide attainable deceleration. Another part of ABS has the same approach if driver brakes on µ-split. Brake assist recognizes emergency brake situations and supports driver with maximum brake pressure.

The driving functions like traction control represent another category within ESP®. These algorithms assist driver during vehicle acceleration by controlling the maximum wheel slip to maintain stability and if it is driver's intent with achievable lateral acceleration. There are different intervention levels. First engine torque can be adjusted to current driving situation. The second level brakes the driven axle to avoid wheel spin and finally to prevent vehicle spin out it might also be necessary to apply brakes on the front axle to stabilize the vehicle.

The main function of ESP® affects the vehicle dynamics itself. Active yaw control supports driver in situations, where loss of control might occur. In driving situations were vehicle is massive understeering ESP® supports by applying more than one wheel brake to follow driver's intent. Especially vehicles with low static stability factors use additional algorithms to prevent rollover if steering input is very extreme. In these situations ESP® applies vehicles brakes to reduce speed and keep vehicle inside its performance capability.

The sensors and actors of ESP® give the opportunity to implement further functions to enhance Active Safety or to make driving more convenient. In combination with special algorithms ESP® is used to regain stability if a trailer tends to oversteer. Starting on a hill can also be supported be ESP®, if brakes kept applied when the brake paddle is released. Especially in sport utility vehicles ESP® can be used to assist driver in off-road down hill driving by limiting maximum speed and controlling wheel lock.

ACCIDENT STATISTIC

The combination of all ESP® functions increases Active Safety of passenger cars significantly. Investigations of other manufacturers, authorities

and institutions on basis of partly different statistics come to comparable results [Aga, M.; Okada, A. (2003) Dang, J. N. (2004) Farmer, Ch. (2004) IIHS (2005) Tingvall, C. et al. (2003)]. ESP® is therefore a system of outstanding influence on the Active Safety of vehicles. Figure 1 shows this impact on Active Safety as the percentage of driving accidents for Mercedes-Benz and vehicles of other brands. Particularly favored by the steep gradients during the introduction of ESP® in Mercedes-Benz passenger cars, 2002 a decrease of the portion of driving accidents of about 30% could be obtained. These are typically serious accidents with a high number of fatalities and severely wounded passengers. In this area of driving safety, ESP® is effective.

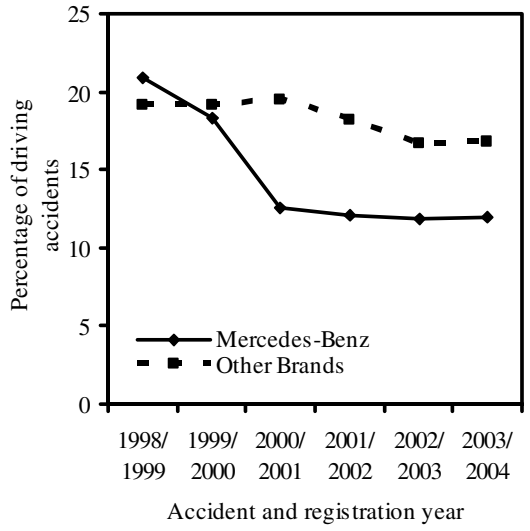

Figure 1: Efficiency of ESP® – accident statistic Mercedes-Benz – Starting 2000 ESP® standard on all Mercedes-Benz Cars – Source: Anonymous sample of data from Federal Bureau of Statistics Germany 1998 – 2004

This retrospective view from accident statistics can not be used for development and ESP® application directly. Therefore other methods have been established in the past and new ones are still in development. Various tests are described in several standards. Mercedes-Benz updated some tests to reflect current requirements of Active Safety. Several maneuvers used by Mercedes-Benz will be discussed.

OJECTIVE ASSESMENT OF ESP®

In the real world there are innumerable different driving situations. ESP® is constantly comparing driver's intent and vehicle reaction. If a difference between drivers intent and vehicle reaction is observed, ESP® reacts and minimizes the deviation. In many cases conflicts between two or even more criteria arise. After deliberating the criteria of these conflicts, targets can be defined for objective assessment.

Traction Control

A basic conflict exists between acceleration and stability of the vehicle. Mercedes-Benz uses objective measurement on high and low µ to provide driver with excellent stability and a predictable driving behavior while offering highest acceleration capability. First the µ-low test is discussed.

µ-low acceleration in a turn - This objective test represents real world turning maneuvers on low µ. On low µ all rear or all-wheel drive vehicles are able to generate power oversteers, if torque or slip on rear axle is not controlled. In this case there is a conflict between traction and stability. Traction Control supervises rear axle slip and can significantly influence stability but also longitudinal acceleration. To provide the customer with highest acceleration and guarantee stability under all circumstances, Mercedes-Benz uses the objective test "drop throttle in a turn on µ-low" to assess this behavior (Figure 2).

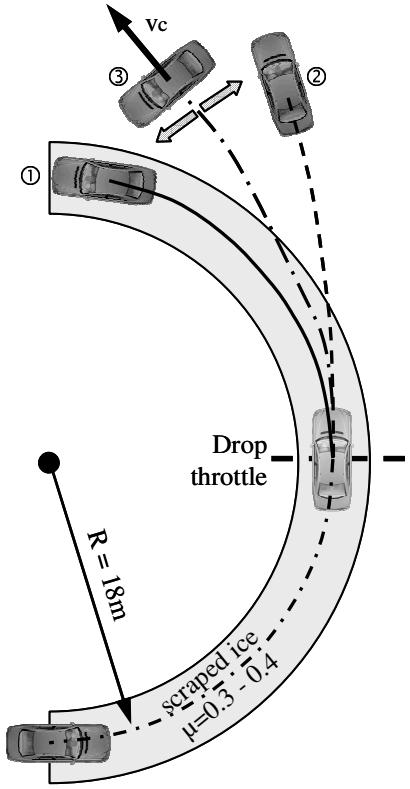

Figure 2: Drop throttle in a turn – ① quasi neural, ② understeering stable, ③ oversteering instable

The initial conditions are adjusted to the coefficient of friction. The maneuver starts with initial steady state cornering on 18 m Radius and a velocity of v = 25 km/h. During this steady state turning accelerator pedal position is immediately increased to a certain level. The rise of accelerator pedal position is stepwise increased until maximum level is reached. All objective measurements must prove at least a certain repeatability level. A significant impact by the coefficient of friction can only be avoided if many measurements on different places are performed. The wheel slip at the drop throttle always polishes the scraped ice surface and has an effect on the result, if a second measurement is performed at the same place. Even with a huge number and attentive execution, level of repeatability is lower than high μ tests.

Data analysis first calculates rise of vehicle course velocity v_c which represents the absolute vehicle velocity along the actual course (see Figure 2). For all data sets the rise of course velocity compared to the initial steady state cornering and rear axel side slip angle two seconds after drop throttle is evaluated. Figure 3 shows the results for three different vehicle setups. The dashed line represents traction control deactivated. The side slip angle increases significantly and loss of control is imminent if velocity rise exceeds 10 km/h. Traction control enhances vehicle stability by controlling the vehicle wheel slip or active brake apply to regain stable conditions. The basic ESP® setup shown in Figure 3 is rather restrictive, only moderate rise of velocity is possible. The optimization of this setup almost allows the same velocity rise as the setup without traction control but on a much higher stability level. The side slip angle at the rear axle does not exceed 10° which is at this speed controllable for any driver.

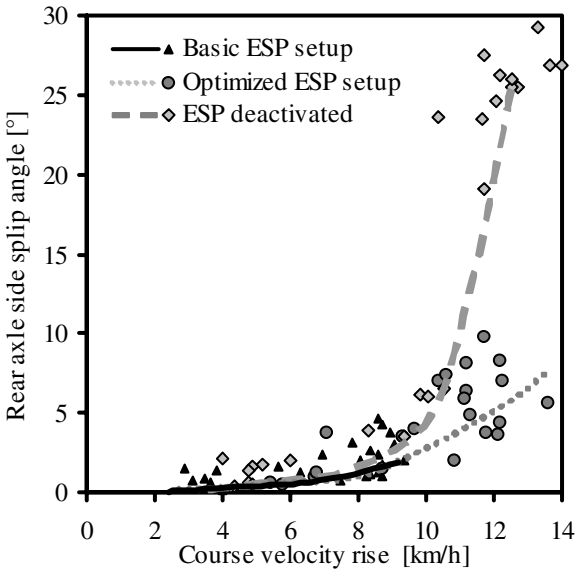

Figure 3: Conflict diagram - drop throttle in a turn

Well attuned traction control systems almost allow the same velocity rise than the vehicle without systems but side slip angle is limited to convenient level. A certain level of side slip is still necessary in order to keep the course of the vehicle on adequate radius. If radius exceeds a certain level, driver will subjectively feel too much understeering.

Acceleration in a turn – A similar test to assess velocity rise and lateral stability is performed on high μ. The initial conditions of the maneuver differ to the test on μ low. The initial radius is reduced to 6.5 m while initial speed v = 25 km/h is the same as on low μ. This leads to higher level of lateral acceleration.

In preliminary tests the maximum rise of velocity is determined. Therefore the vehicle is tested with traction control deactivated. Several tests are performed while at each test the maximum level of the accelerator pedal is increased. Figure 4 shows the velocity rise for the different levels of the accelerator pedal. The maximum velocity rise for the vehicle shown in Figure 4 is reached with accelerator level of 80 percent. Above this level the maximal velocity rise is lower again. If sufficient engine power is available, even on high μ spin out at full throttle is possible. At the test vehicle shown in Figure 4 spin out occurred at almost full throttle. To increase repeatability several test are performed at the accelerator paddle level which provides the maximum velocity rise.

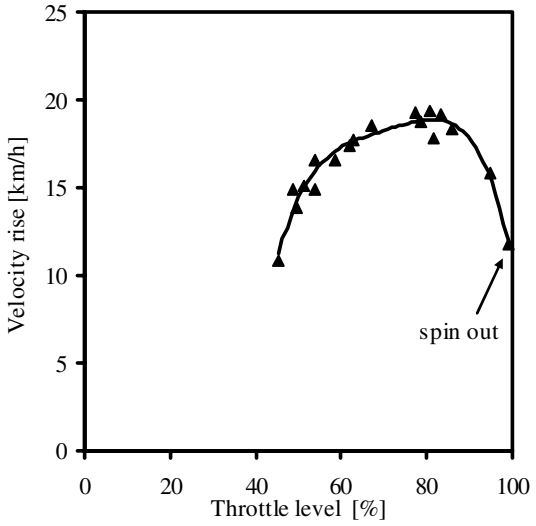

Figure 4: Acceleration in a turn – velocity rise at different throttle levels

The tests where traction control is activated are always performed with full throttle. The exhausting procedure of finding the maximum velocity rise with activated system is so simplified very much. Several tests are accomplished to increase repeatability.

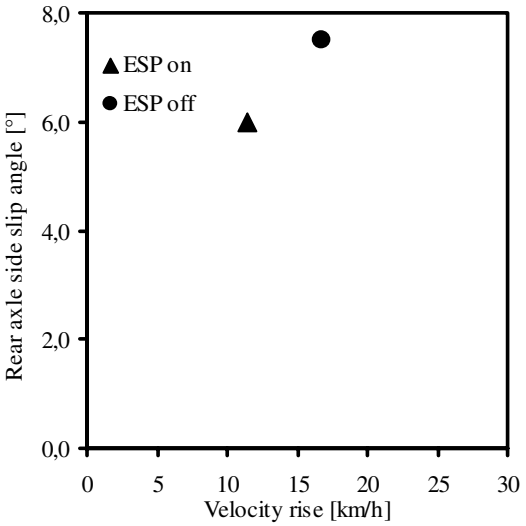

Figure 5: Drop throttle in a turn – maximum velocity rise vs. stability

The summarized results of the conflict velocity rise vs. stability are shown in Figure 5. In this case all measurements with system activated are averaged as well as the measurements with maximum velocity rise and system deactivated. In principle higher velocity rise is possible with traction control deactivated, if driver accelerates by using the optimum accelerator pedal level. Therefore driver needs to control the accelerator pedal to reach this performance and still takes the risk of spinout without ESP®. The velocity rise with traction control activated for the tests shown in Figure 5 is around 70% of the overall maximum level. This velocity rise is reached in a much safer way. Mercedes-Benz uses this test procedure to develop the typical stable and predictable driving behavior.

Vehicle dynamic control

Basically the vehicle dynamic control function builds the core of ESP®. Based on a vehicle model the actual course and driver's intent are compared. The vehicle model uses basically steering wheel angle and vehicle speed to determine driver's intent. Since NHTSA focuses for the evaluation of ESP® systems on the sine with dwell maneuver, this maneuver comes more in focus for ESP® assessment. The conflict between yaw stability and lateral performance is already addressed by this maneuver. Mercedes-Benz uses the sine with dwell maneuver to support application of the dynamic control function.

Especially braking in a turn can lead to an exacting driving situation, if vehicle is running with high speed. In this kind of situations driver needs to be supported. To assess the driving behavior Mercedes-Benz uses the test "braking in a turn at high speed", which will be described next.

Braking in a turn at high speed – Additional to the maneuver braking in a turn, defined in the standard ISO 7975, Mercedes-Benz uses a slightly modified version. In principle all these procedures evaluate conflicting aims between stability and attainable deceleration during the braking. This additional test assesses Active Safety at high speed. Therefore the maneuver starts at a steady–state run at 200 km/h.

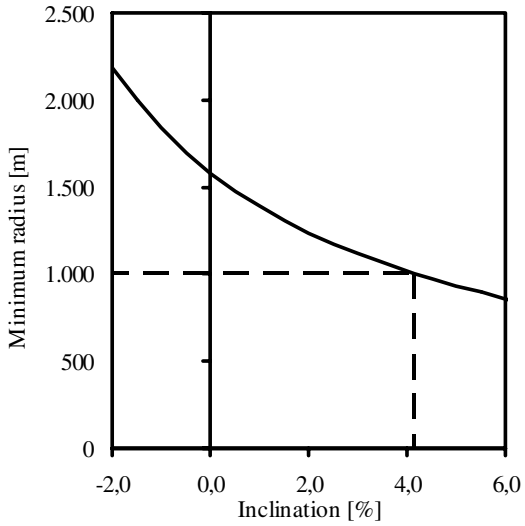

Figure 6: Construction of minimum radius at different inclination for German Autobahn according to RAS-L 1984

The ISO Standard suggests a lateral acceleration of $a_y = 5$ m/s². If this lateral acceleration is used at 200 km/h the vehicle runs on a radius which is typically not used for German Autobahn. The radii on German Autobahns are designed, besides a lot of other parameters, dependant to the inclination (see Figure 6). To reflect a typical German Autobahn profiles the minimum radius is adjusted to R = 1000 m. This leads to a lateral acceleration of $a_y = 3.1$ m/s².

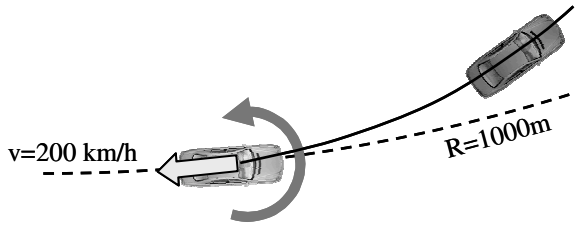

Figure 7: High speed braking in a turn

The brake test starts with the steady-state condition v = 200 km/h and R = 1000 m (see Figure 7). Several measurements at different level of longitudinal deceleration are performed. The deceleration should be kept constant during the single brake maneuver (see Figure 8).

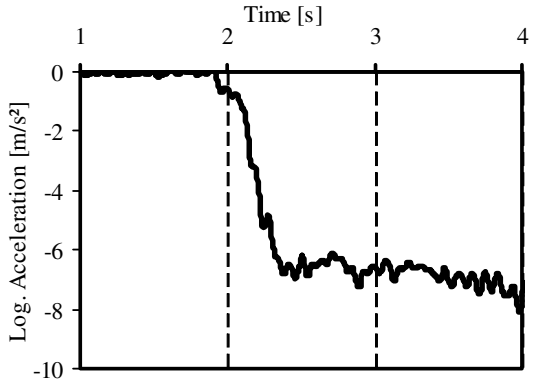

Figure 8: High speed braking in a turn – Example time plot of longitudinal acceleration (brakes applied at t = 2 s).

The yaw reaction is relevant particularly within the first second after the initial brake contact, since the driver, depending on its individual reactivity, compensates course deviations only thereafter. Therefore maximum deviation to the reference of yaw velocity within the first second of brake test is evaluated for every single test (see Figure 9). For this calculation the arithmetic of ISO 7975 is used.

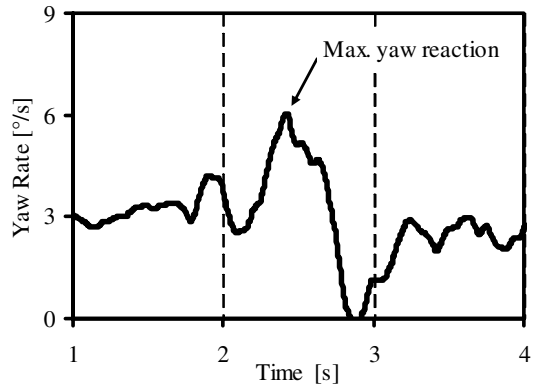

Figure 9: High speed braking in a turn – Example yaw reaction (brakes applied at t = 2 s)

Several braking test on the different deceleration levels and the corresponding yaw reaction is illustrated in Figure 10. Typically these results show the maximum yaw reaction at a deceleration of a_x = 5-7 m/s². Very good car ESP® configurations reach maximum yaw reaction shown in Figure 10.

Physically the yaw velocity as well as the steering wheel angle which are necessary to run with v = 200 km/h on a radius R = 1000 m is quite low. Thus the internal ESP® algorithm also calculates low reference values. Even if the difference between reference and the actual yaw rate is also low, a significant lateral deviation between vehicles course and driver's intent might occur. To support driver in these kind of situation the corner brake control especially controls driver's intent and actual course. To enhance vehicle stability the brake pressure at rear axel is limited to a certain level to increase vehicle stability. Since rear axle does not provide too much brake force the influence of braking distance is not very significant. Brake pressure at rear axle can be increased during the deceleration. If vehicle reaction still is intensive the beginning of the braking maneuver can be influenced to reduce path deviation. Dependent on the corning direction the brake pressure on the front axel is built up slightly asymmetrical. This additional yaw moment works against the vehicle oversteering behavior. Corner brake control enhances vehicle stability and also provides driver maximum deceleration.

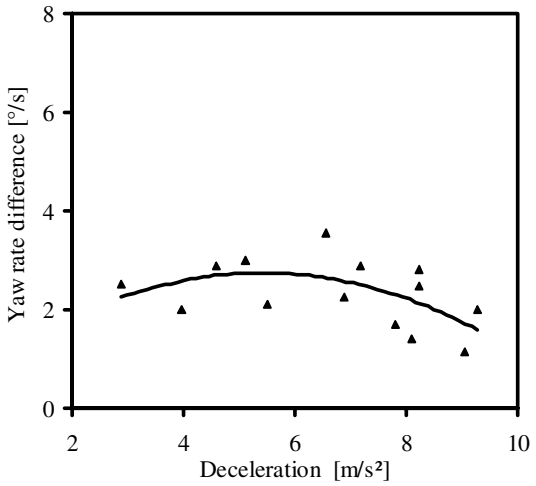

Figure 10: High speed braking in a turn – summarized results

Special functions

Since ESP® becomes more standard in vehicles additional functions are implemented. Some functions make driving more convenient. These kind of functions are not discussed in this paper. Other functions enhance Active Safety.

ESP® Trailer Stabilization is such an additional function. Car-trailer combinations tend to oscillate after excitation from cross-wind, irregular roadway or steering input. The damping of the system decays if speed increases. Therefore the oscillation lasts for a longer period of time if the car-trailer combination is traveling with higher speed. Above the zero-damping speed the oscillations of the rig will not decay anymore (see Figure 11). The level of the zero-damping speed is characteristic for every single car-trailer combination. The mass/inertia moments of the trailer, drawbar length and tires mainly influences the zero-damping speed.

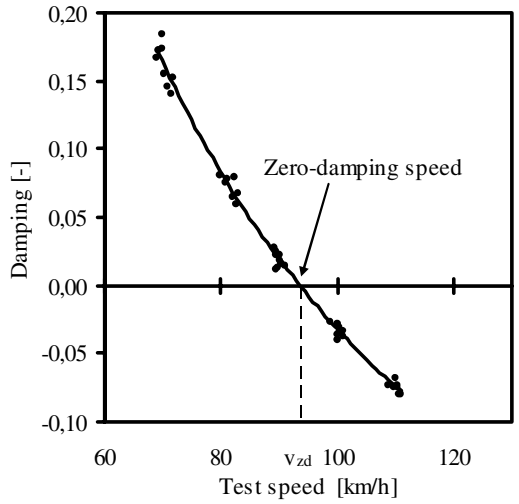

Figure 11: Typical damping of a car-trailer combination at different speed

If a car-trailer combination starts to oscillate at a speed above the zero damping speed, an accident can only be avoided if speed is reduced immediately. After recognizing a car-trailer oscillation situation ESP® Trailer Stabilization applies the brakes of the towing-car to work against the oscillation. This mechanism and reduction of speed increases damping and stabilizes the combination.

A test method to asses the stabilization is illustrated in Figure 12. The driver activates an oscillation of the car-trailer combination by a pulse steer at the towing car. In the first phase of the maneuver the amplitude of the lateral acceleration at trailers center of gravity increases (see Figure 12). After ESP® detects a critical level the brakes are applied in a way that counteracts the oscillation by building up yaw moments in phase with the oscillation. This mechanism additionally damps the oscillation. In this second phase the car decelerates which can be seen in the speed diagram in Figure 12. The speed reduction itself increases the damping of the system and helps to regain stability. This leads to a decay of trailer lateral acceleration amplitudes.

Figure 12 shows two different ESP® setups. The dashed line represents a basic setup. This setup recognizes the trailer oscillation approximately 4 s after the steering input. At this time lateral acceleration already reached 5 m/s², which is a quite high level for trailers. This is already a severe situation; therefore the basic ESP® setup needs to decelerate the car-trailer combination very hard. This test started with an entry speed of almost 120 km/h, after the stabilization of the car-trailer combination the speed was only around 40 km/h. Only if this kind of situation is detected very fast and the braking activations are well controlled the exit speed in this kind of maneuvers remains on adequate level. Nevertheless the exit speed of the maneuver needs to be below the zero-damping speed. Otherwise there is still not enough damping to maintain stability.

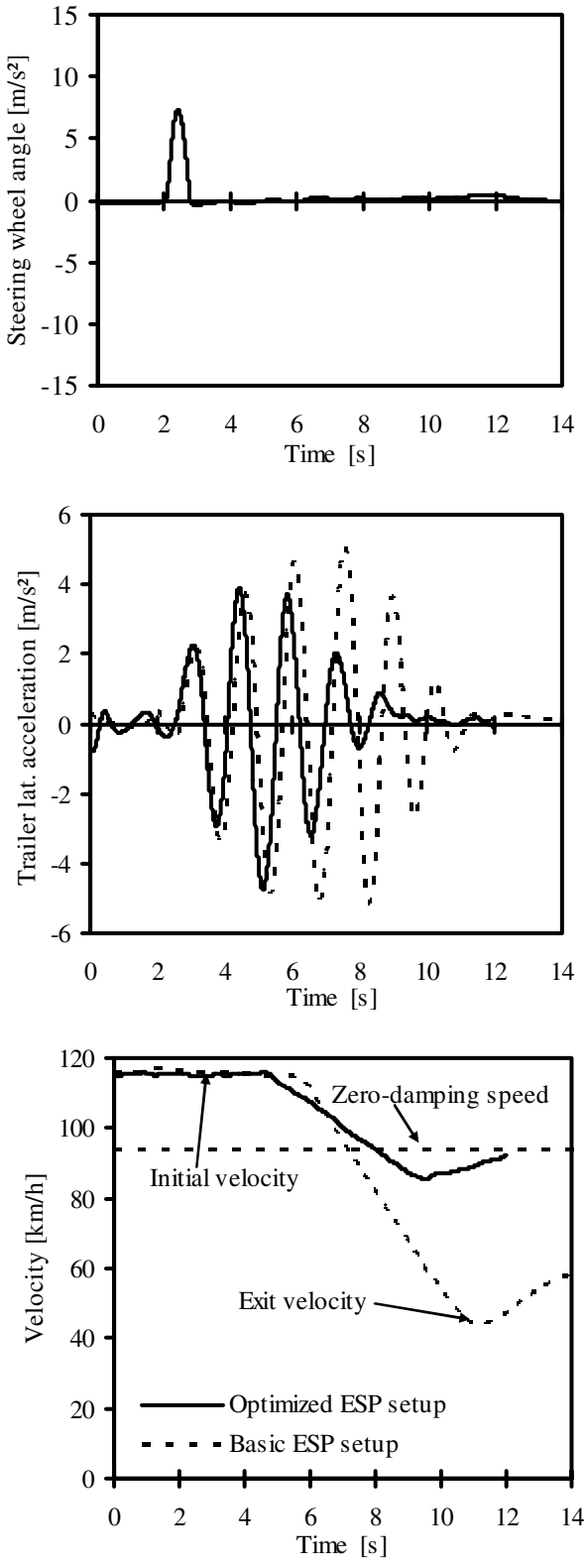

Figure 12: Oscillation and stabilization of a car-trailer combination with different ESP® setups

This conflict of stabilizing and braking the car-trailer combination needs to be assessed during the

application of ESP® Trailer Stabilization. Mercedes-Benz uses for this test the already introduced pulse steer maneuver which is based on the ISO 9815 standard. A preliminary test detects the zero-damping speed of the car-trailer combination without ESP® interaction. For that damping of the combination is determined at different speed levels by the test maneuver. Speed is increased till the zero-damping speed is passed.

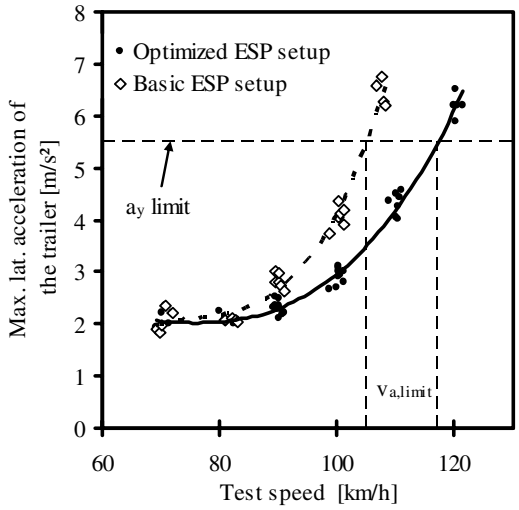

Figure 13: Maximum lateral acceleration of the trailer after pulse input at different speed levels of a car-trailer combination with different ESP® setups

Same test on different speed levels is performed with ESP® interaction. Figure 13 shows the maximum lateral acceleration of the trailer at different speeds and the termination limit. A basic setup which reaches the termination limit at lower speed and an optimized ESP® setup are illustrated. For safety reasons these tests are performed till a certain limit of lateral acceleration of the trailer is reached. Trailers are typically not quipped with high performance tires. This can already at a lateral acceleration level of a_y = 5-6 m/s² lead to a spin out of the trailer. On the other hand trailers with high loading tend to rollover if lateral acceleration overruns this limit.

The speed which reaches the limit of lateral acceleration of the trailer represents a measure for the ESP® Trailer Stabilization performance. This measure is referred to the zero-damping speed to reduce influence of different car-trailer combinations (Equation 1). This stabilization ratio (SR) reflects the stabilization performance of the ESP® Trailer Stabilization.

$$SR = \frac{v_{a,limit}}{v_{zd}} \qquad (1)$$

where

$v_{a,limit}$ is the speed where lateral acceleration of the trailer is equal to the limit

v_{zd} is the zero-damping speed

The second criteria to assess ESP® Trailer Stabilization evaluates velocity drop during the stabilization of the car-trailer combination. Without active mechanisms (e.g. active coupling ball mechanism) a car-trailer combination oscillation above the zero-damping speed can only be stabilized if the speed is reduced immediately. The reduction of speed helps to increase Active Safety in this situation. Of course if the reduction of speed during the stabilization leads to a speed which is way below the common cruise speed inconvenient situation especially for following traffic might occur.

The basic ESP® setup in Figure 12 shows a significant velocity drop during the stabilization. To reduce speed drop during the stabilization phase ESP® Trailer Stabilization needs to detect the trailer oscillation very fast and the application of the ESP® trailer stabilization has to work very efficient. ESP® Trailer Stabilization intervenes by alternating left and right brake application. This intervention lasts for a longer time than conventional ESP® application. This works very efficient against the oscillation of the car-trailer combination. The velocity drop ratio (VDR) assesses the loss of speed. Like the stabilization ratio the velocity drop ratio VDR is also referred to the zero-damping speed (Equation 2) to make different car-trailer combinations more comparable.

$$VDR = \frac{v_{exit}}{v_{zd}} \qquad (2)$$

where

v_{exit} is the speed where the ESP® intervention ends (Figure 12).

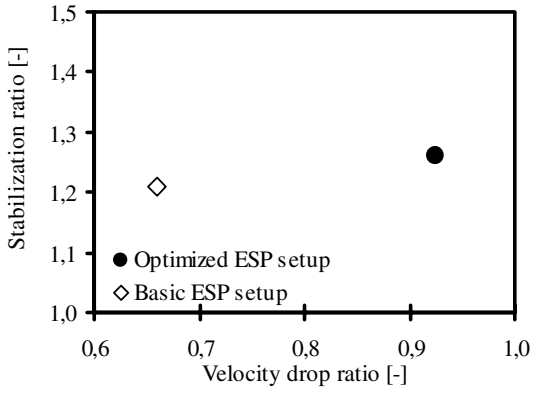

Figure 14: Conflict diagram of stabilization performance and velocity drop of a car-trailer combination with different ESP® setups

The conflict diagram (Figure 14) integrates both criteria. An ESP® setup where the velocity drop ratio is close to VDR = 1 detects trailer oscillation fast and stabilizes the combination quickly.

Nevertheless the VDR needs to be smaller than VDR = 1 (or exit speeds needs to be lower than zero-damping speed) to ensure that the car-trailer combination remains stable even, if the ESP® intervention is terminated.

An ESP® setup were SR > 1 can stabilize car-trailer combination even if the oscillation occurs at speeds above the zero-damping speed. ESP® Trailer Stabilization setups were VDR is close to 1 and SR > 1.2 can be assumed to be well tuned.

SUMMARY

ESP® supports driver in almost every severe driving situation. Several accident statistics show an outstanding reduction of driving accidents. ESP® uses a vehicle model to calculate drivers intend by mainly using steering wheel angle and vehicle speed. These results are constantly compared with the current vehicle course. If a deviation is observed, ESP® will support driver by a specific brake application. The model and several additional features have to be adjusted to the specific vehicle platform. To support and assess this application various maneuvers are used. During application of the system conflicts between several criteria have to be resolved. Several objective tests are used by Mercedes-Benz to support application of the system with objective measures. This paper introduced a selection of these tests. Starting with the driving function, drop throttle in a turn on high and low μ is discussed. This maneuver assesses the conflict between vehicle yaw stability and attainable acceleration. The Active Safety at higher speeds can be evaluated by the test maneuver braking in a turn at high speed. This maneuver focuses on the conflict between vehicle stability and deceleration. The stabilization of a car-trailer combination can be also objectively observed. The optimum ESP® setup must take the stabilization performance as well as the reduction of speed into account.

Of course an ESP® system can not be only attuned by objective testing but a framework is given. Beyond this ESP® application uses single events during subjective pretests or semi-subjective driving to determine the ESP® setup.

REFERENCES

Aga, M.; Okada, A. (2003): Analysis of vehicle stability control effectiveness from accident data, ESV Conference, Nagoya

Dang, J. N. (2004): Preliminary results analyzing the effectiveness of electronic stability control systems, NHTSA DOT HS 809 790

Farmer, Ch. (2004): Effect of Electronic Stability Control on Automobile Crash Risk, IIHS Insurance Institute of Highway Safety, Arlington, Virginia, USA

IIHS (2005): The Risk of Dying in One Vehicle vs. Another, Status Report Vol. 40, No.3, IIHS Insurance Institute of Highway Safety, Arlington, Virginia, USA

ISO 7975 (2006): Passenger Cars - Braking in a turn - open loop test procedure

ISO 9815 (2003): Road vehicles – Passenger-car and trailer combinations – Lateral stability test

Richtlinie für die Anlage von Straßen RAS (1984), Teil: Linienführung (RAS-L), Abschnitt 1: Element der Linienführung

Tingvall, C. et al. (2003): The effectiveness of ESP in reducing real life accidents, ESV Conference, Nagoya

Light Commercial Vehicles – Challenges for Vehicle Stability Control

Dr. rer. nat. E. Liebemann
Dipl. Ing. T. Führer
Dipl. Ing. P. Kröger
Robert Bosch GmbH, Chassis Systems Control
Germany
Paper Number 07-0269

ABSTRACT

The electronic stability program (ESP®) is increasingly finding acceptance in vans and light commercial vehicles (LCV). Nearly all current models, whose gross vehicle weight is generally between 2.8 and 7.5 metric tons, are now available with this active safety system, either as an option or even as standard equipment.

Many studies have now confirmed that ESP® can prevent a vehicle from skidding or rolling over in nearly all driving situations [1, 2]. This is particularly important in the case of vans, since their design and their use leave them with tighter safety margins. Depending on load, the center of gravity shifts, and consequently the risk of rollover may increase. Bosch has developed a system specifically for light commercial vehicles that automatically adapts its control mechanisms to the current situation.

INTRODUCTION

Worldwide traffic is increasing with more and more vehicles on the road. With further economic growth, we will continue to see more increase in mobility and in traffic density throughout the world. The progress of crash energy absorbing car body design and the standard fitting of airbags significantly improved the passive safety especially combined with the use of seat belts (Figure 1).

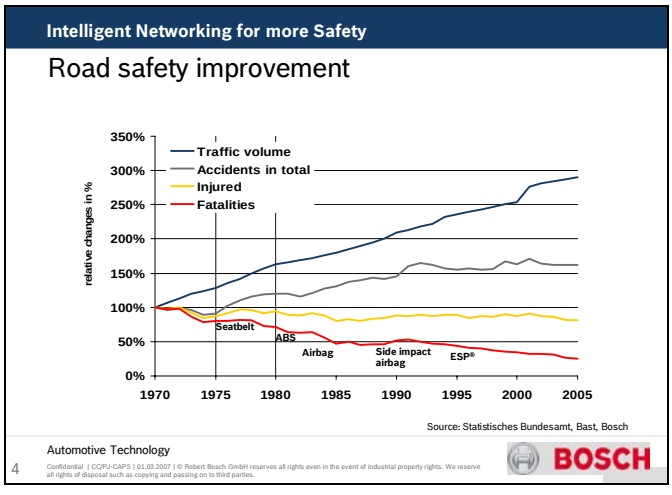

Figure 1. Traffic volume increase and road safety improvement in Germany from 1970 to 2005

But many of the serious accidents happen through loss of control in critical driving situations. When skidding occurs, a side accident is a frequent result. With a reduced protection zone for the occupants compared to front crashes, these accidents show an amplified severity. Especially with vehicles of an elevated center of gravity like vans, sport utility vehicles (SUV) and light commercial vehicles, the loss of control with subsequent skidding may even lead to rollover.

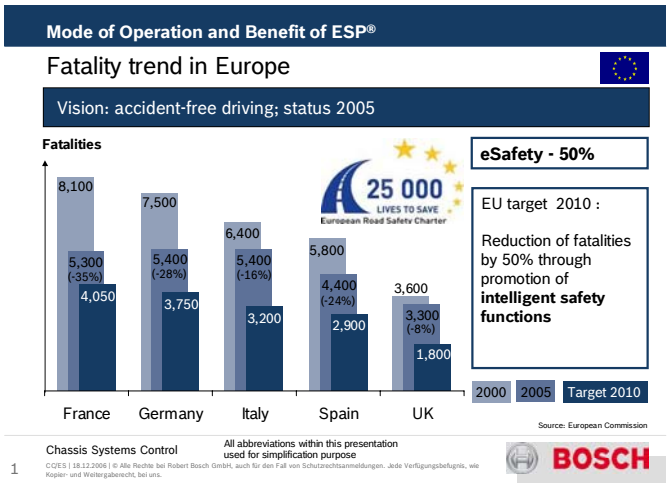

Figure 2. European eSafety initiative of the European Union for 2010 is set to reduce road deaths by 50%

According to accidentology conducted by VW [1], ESP® is considered to avoid 80% of the accidents caused by skidding. VW concludes that the safety benefit of ESP® is even greater than that of the Airbag.

Based on the analysis of Japanese traffic accident statistics, Toyota [2] estimated that the accident rate of vehicles with

ESP® is reduced by approximately 50% for severe single car accidents and reduced by 40% for head-on collisions with other automobiles. The casualty rate of vehicles with ESP® showed approximately 35% reduction for both types of accidents.

Although good progress is shown with a reduction of 21% over the first half decade (Figure 2), the European Union will most likely not achieve the objective. Additional efforts will be required to furthermore enhance the road safety. Bosch supports this with ESP® systems for all vehicle segments including Light Commercial Vehicles (LCV) and furthermore with the combination of active and passive safety systems.

MAIN SECTION

Intelligent safety systems start to support drivers in situations where they are overburdened due to lack of training and driving experience. A study by Prof. Langwieder showed (Figure 3) that in 49% of car-to-car and car-only accidents no braking was applied at all, partial braking was applied in 12% respective 20%, and emergency braking in only 39% respective 31% of the accidents.

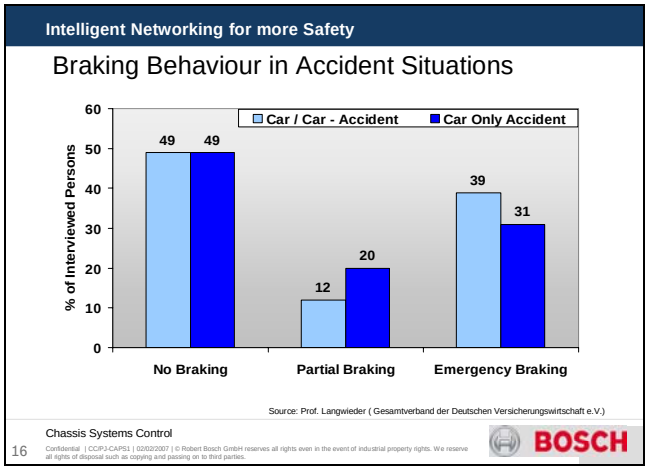

Figure 3. Braking behavior of drivers in car to car and car only accidents in Germany

Although partial braking and to a certain extent emergency braking can be supported efficiently with brake pre-fill and hydraulic brake assist, no braking requires surrounding sensors to enable mitigation functions. First safety systems based on e.g. Radar sensors have already been introduced, supporting partial braking situations with adapted brake assist and brake pre-fill and no braking situations with automated vehicle deceleration.

Still, special emphasize is required to cover the demanding requirements of light commercial vehicles (LCV) and light trucks (LT). For cargo space optimization, LCVs are usually equipped with comparably small wheels. The resulting limitation of brake rotor diameter leads to high pressure ESP® applications with challenging durability requirements.

LT are usually equipped with large wheels allowing remarkable brake sizes with high volume consumption. To ensure full ESP® and rollover mitigation functions and reduced stopping distance, a special brake system design is required. Consequently, Bosch develops the ESP®LT with an optimized

Figure 4. ESP® system for Light Trucks. ESP®LT with optimized motor, pump and valves for improved pressure build-up and better pressure response time during partial braking and ABS intervention; larger accumulator chamber for large brakes with high volume consumption

motor, pump and valves for improved pressure build-up and better pressure response time during partial braking and ABS intervention (Figure 4). Low temperature conditioning is available to ensure full stability performance down to below -25° C. In addition a larger low pressure accumulator chamber is introduced for excellent ABS performance.

Beside typical brake sizes or brake pressure levels, LT and light commercial vehicles share the rather demanding characteristic of high load and mass variances between empty and fully laden vehicle. Specific measures are mandated to ensure full braking, traction and ESP® performance both for the loaded as well as for the empty case. The measure is called Load Adaptive Control or LAC.

LAC – LOAD ADAPTIVE CONTROL

In particular, vehicles with a tare to gross vehicle mass ratio larger than 1.5 such as LCV or LT benefit from LAC. Figure 5 shows the typical load variation for a passenger car compared to a LCV. When the maximum load variance for a car is typically below 40%, it can reach up to 100% and more for a LCV with even stronger relative variations for the Center of Gravity (CoG).

The load configuration has a profound impact on vehicle dynamics. In particular, the load significantly influences:

- braking efficiency incl. ABS- and split-µ performance
- traction efficiency and stability, esp. for vehicles with rear-wheel (RWD) or all-wheel drive (4WD)
- cornering behavior
- rollover tendency

The maximum axle loads are important parameters. They are derived from the mass and longitudinal center of gravity. Since the loading platform tends to be behind engine and passenger compartment, payload mainly increases the rear axle load while only having a minor effect on the front axle load. This also means that front-wheel drive (FWD) vehicles may be as influenced by load changes as RWD and 4WD vehicles.

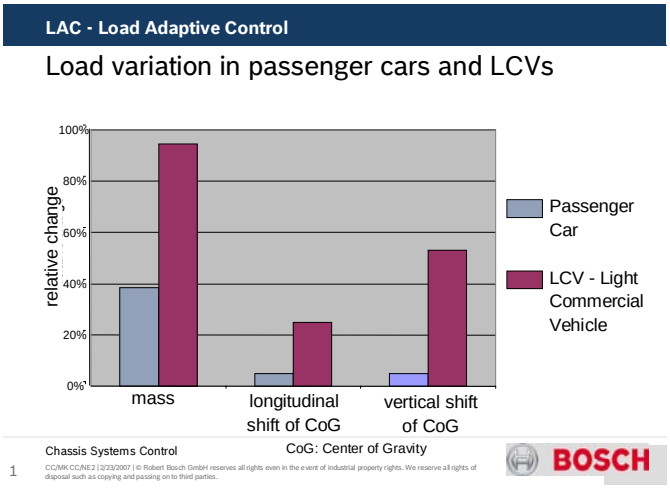

Figure 5. Representative results for relative change of mass, longitudinal and vertical shift of Center of Gravity for empty and loaded cars and LCV

Beside braking and traction performance, different load conditions influence the self-steering and cornering performance of the vehicle. Figure 6 shows the cornering behavior reflected by the yaw gain (according Ackermann) of one and the same vehicle under different load conditions. The empty vehicle shows the expected understeering behavior whereas oversteering is shown with a payload of 1500 kg on the rear axle. A non-adapted target yaw rate would lead to either too early or too late stabilizing interventions.

With LAC, the load impacted characteristic speed is estimated and the target yaw rate and regulating thresholds are adapted accordingly.

The Ackermann yaw gain presumes the free rolling case without longitudinal tire forces. The acceleration causes a pitch effect, thereby shifting load from the front to the rear axle which contributes to increased understeering. The stabilizing effect of traction forces is therefore taken into consideration by LAC.

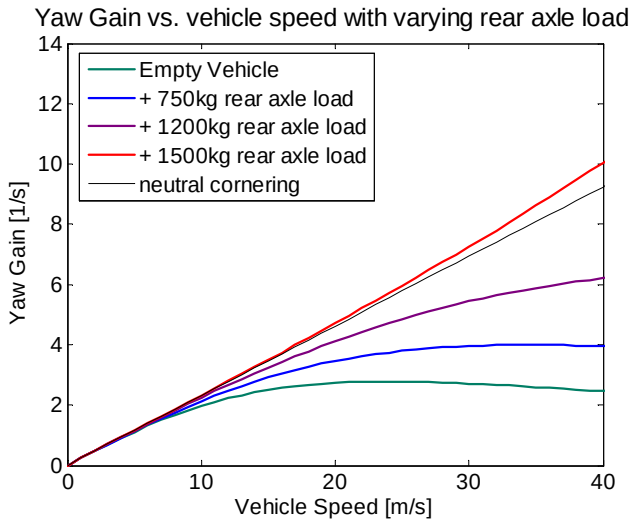

Figure 6. Self-steering and cornering behavior of one vehicle under various load conditions. While the empty vehicle shows the expected understeering, a payload of 1500 kg on the rear axle results in oversteering

LAC consists of algorithms for the estimations of mass, the longitudinal shift of CoG and the change of self-steering behavior reflected by the characteristic speed. The estimation algorithms are centralized while the resulting adaptations are by their nature decentralized and located in various vehicle dynamics modules like the brake slip controller. It is important to note that estimation-based adaptation algorithms need a learning phase, which means that they are never available immediately after key-on. Since estimations will never be 100% accurate, they can only be used to such an extent that a maximum error will not lead to a safety-critical situation. This is to be considered in the FMEA and must be verified in vehicle tests prior to software release.

The following sections describe the positive impact of LAC in different driving situations (for standard ESP® performance and control principles see [3, 4]).

Traction Control and braking performance

The Traction Control System (TCS) determines the target slip depending on the road friction coefficient µ, which is calculated based on the longitudinal and vertical wheel forces. The vertical or normal forces are based on the mass distribution of the vehicle. The high mass variance of LCV in different load conditions would lead to incorrect µ-estimations resulting in inappropriate target slip values. A loaded RWD vehicle during cornering on a low friction surface (i.e. during winter conditions) would estimate a higher µ with the result of excessive wheel slip and the potential of oversteering.

But even with a correct µ estimation, the cornering stability depends on the load and load distribution especially with RWD vehicle. While a vehicle with a low rear axle load may begin to oversteer during acceleration in curves, the loaded vehicle at the same engine torque could still be very stable or even tend to understeer. To adapt for these conditions, ESP®

with LAC calculates an oversteering indicator based on the measured yaw rate compared to the target yaw rate.

With the estimated mass and the longitudinal center of gravity (CoG), the activation thresholds of the rear and front axle torque are adapted. The more the CoG shifts towards the rear axle, the later the torque limitation for the rear brakes will be activated. This results in a more even load distribution between front and rear brakes thereby reducing rotor and pad wear and the risk of fading.

For constantly good braking performance, the actual wheel loads are determined by comparing the braking forces with the prevailing slip values. The higher the estimated wheel loads, the higher the brake controller gains can be selected.

By estimating mass, load distribution, wheel loads and improving the µ-estimation with LAC, the traction and braking stability is optimized for all load conditions.

Fading-detection

Especially with loaded vehicles, fading is more likely to occur. Depending on the design of the front brakes, the dissipated energy may cause excessive brake disc and pad temperatures, leading to fading and - in extreme cases - even to total brake failure. In these cases even high master cylinder pressures will not generate adequate brake torque especially at the front wheels. If front axle fading is detected, the rear axle braking pressure is increased, in case additional rear braking potential is available. Rather than being severely under-braked, the deceleration can be improved and the load on the front brakes reduced.

Load dependent adaptations for split-µ braking

During split-µ braking, different braking forces on the left and right wheels cause a yaw moment which would result in unwanted build-up of body slip angle. With an inappropriate or too late steering correction by the driver, the vehicle might start spinning and potentially rollover in case of vehicles with a high centre of gravity. Therefore the pressure difference between the left and right wheels of one axle is limited to ensure that an average driver can keep control over the vehicle subject to the split-µ caused yaw moment. However, a limit set too low leads to longer braking distance.

Loaded vehicles are more stable during split-µ braking situations than empty vehicles. Therefore, the rear axle pressure difference of a laden vehicle can be increased to higher values at the same stability level. The steering angle information is utilized to adapt the pressure limitation. If small steering angles are sufficient, the rear axle pressure difference is increased and is frozen for large steering wheel angles.

Vehicle dynamics control (VDC)

The changes of self-steering behavior imposed by different loading conditions (Figure 6) are considered by LAC. The VDC activation thresholds to counteract under- and oversteering are adapted as well as the target yaw rate in relation to the Ackermann yaw rate. Prior to or in support of brake interventions, ESP® first adjusts the engine torque to counteract oversteering and severe understeering.

To achieve the required brake slip and the resulting lateral forces in a stability intervention (Figure 7), the brake force must be adapted to the respective wheel load. An empty vehicle requires less brake pressure than a loaded vehicle. Note that the rear outside slip maximum is not changed with LAC.

All these adaptations contribute to optimized stability performance at minimized intrusiveness for the loaded vehicle. Since the payload inflicted changes of the CoG height (Figure 5) can be significant for light commercial vehicles, special considerations are taken for optimized performance in rollover critical situations.

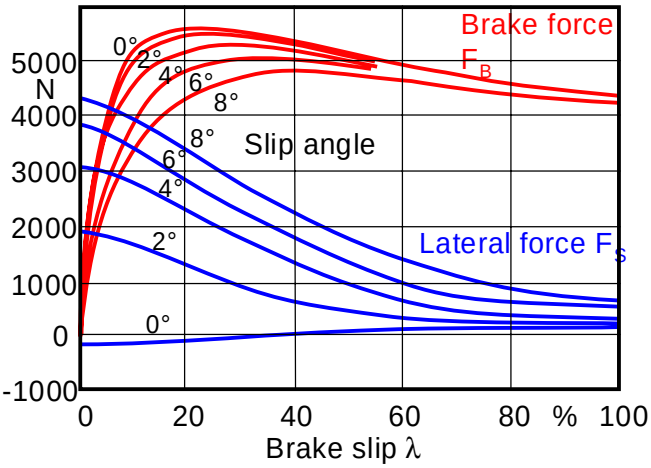

Figure 7. Dependency of lateral forces from longitudinal forces caused by braking for various steering angles. Applying brake pressure controls the maximum possible lateral forces for cornering.

ROLLOVER MITIGATION WITH LAC

By reading in the estimated mass, the ROM ay-dependent activation thresholds can be adjusted. In this way, the activation thresholds can be increased for empty vehicle and lowered for the loaded vehicle, causing later or earlier interventions, respectively. The figure 8 shows how the threshold adaptation works.

In the US, about 10% of all road accidents are non-collision crashes, but approximately 90% of such single-vehicle crashes account for fatalities [5]. SUV, LT as well as LCV with their elevated center of gravity (CoG) show an amplified rollover propensity, which is reflected in their increased rollover rates.

A vehicle rollover occurs when the lateral forces create a large enough moment around the longitudinal roll axis of the vehicle for a sufficient length of time.

Critical lateral forces can be generated under a variety of conditions. The vast majority of rollover crashes take place after a driver lost control over the vehicle. By skidding off the road, the vehicle may get in lateral contact with a mechanical obstacle like a curb, a pot hole or a plowed furrow which yields a sudden large roll moment. This results in a so called tripped rollover in contrast to an un-tripped or friction rollover. The latter takes place on roads during severe steering maneuvers solely as a result of the lateral cornering forces. Although the ratio of un-tripped to tripped rollovers is small, the un-tripped rollovers account for the most severe crashes.

Accident analysis has shown that the ratio of the track width T and the height of the center of gravity h_{CoG} gives a first indication for the rollover propensity of vehicles.

$$SSF = \frac{T}{2 \cdot h_{CoG}} \qquad \text{Static Stability Factor}$$

The SSF is an important parameter affecting vehicle rollover risk and is both relevant for tripped as well as un-tripped rollover. The track width is a fixed parameter while the center of gravity height varies with subject to different load conditions. Through a one rigid body model - which means no distinction between the mass of the chassis and the sprung mass of the vehicle body – the SSF relates geometrical vehicle data to the level of lateral acceleration that will result in a rollover.

A one rigid body model cannot predict time dependent details of an on-road rollover critical situation. For transient maneuvers involving high lateral accelerations, many vehicle design parameters have an effect on the vehicle handling behavior like e.g. front to rear roll couple distribution, roll axis location, tire behavior, suspension characteristics and roll resonant frequency. These handling characteristics significantly influence the ability of the driver to maintain control in an emergency situation.

The load condition influence on the rollover propensity is shown in Figure 8 in a simplified manner for different types of cars and loading conditions. The static stability factor for typical passenger cars is far above the lateral acceleration which can be transferred by the maximum tire grip. This is the reason why passenger cars are usually not subject to un-tripped rollovers even in extreme loading conditions. If the adhesion limit between the tires and the road surface is reached before the lateral acceleration gets rollover critical, the vehicle starts to skid over the front wheels.

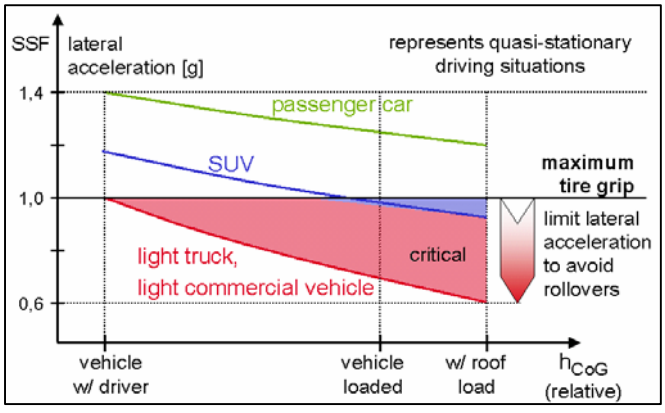

Figure 8. Typical critical lateral accelerations for rollover dependent on loading conditions reflecting different types of vehicles

The situation is different especially for light commercial vehicles, where elevated loading may play a major role.

At the physical limit, the tire behavior is extremely nonlinear and the linearized tire-wheel-brake system is even unstable. As a result, the vehicle may suddenly spin and the driver is caught by surprise.

Changing the direction of the resultant tire forces of individual wheels by specific wheel slip demands applies a stabilizing yaw moment (Figure 7) . Besides standard ESP®, active steering can be used as well to increase the vehicle's tracking stability. Both concepts mentioned as well as Active Roll Control [6] or Electronic Damper Control [7] can in general help to avoid critical situations and as a result indirectly help to reduce the rollover risk.

Besides the classification according to the rollover reason, rollover scenarios can be divided into highly dynamic maneuvers, e.g. obstacle avoidance, or quasi stationary maneuvers like circular driving with steadily increasing steering wheel angle. The latter can arise while driving on a highway exit with excess speed.

The Bosch Rollover Mitigation Functions (RMF) are based on the standard ESP sensor set and provide a scalable structure concerning the determination of rollover critical situations and brake/engine control. Other solutions additionally use a roll rate sensor [8]. Further details on the intervention strategy and functional concepts of the Bosch RMF are described in Ref [9].

The Bosch approach uses only existing sensor signals and estimated values to predict the vehicle's rollover propensity. For example, based on the well-known single-track model, an early lead for a subsequent high lateral acceleration is given by

$$c_{pre} = \dot{\psi} \cdot v_x - a_y \approx -\dot{\beta} \cdot v_x$$

$\dot{\psi}$: yaw rate $\qquad$ v_x : longitudinal velocity

a_y : lateral acceleration $\qquad$ $\dot{\beta}$: change in body slip angle

With a rapid change of body slip angle weighted with v_x, the lateral acceleration will subsequently increase considerably. The general control strategy is to increase brake pressure at the curve outside wheels to realize the brake slip target values. This reduces the lateral forces as well as the longitudinal speed of the vehicle and results in an increased curve radius. Subsequently the track can be regained due to the reduced

speed. In these special situations the brake intervention is usually combined with a cut back on engine torque.

In general, the hydraulic braking system must provide a fast pressure increase over a wide temperature range. For that, the brake tube dimensions, caliper size, and the characteristics of the utilized brake fluid are very important. When a dynamic maneuver is detected, the inside wheel brake on the front axle

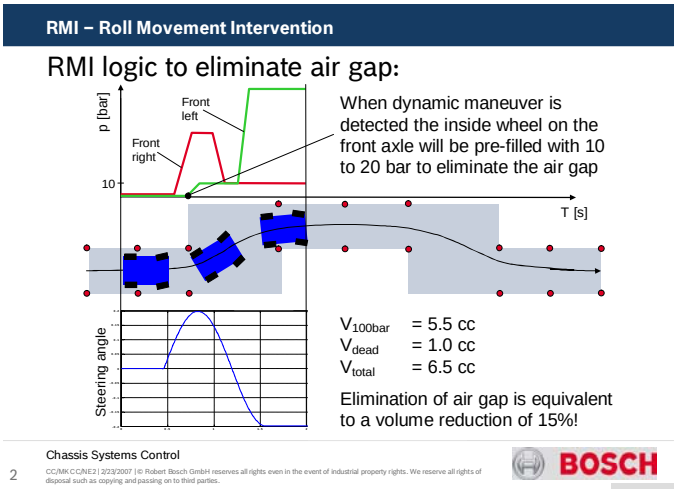

Figure 9. ESP® intervention strategy for increased pressure build-up capability in high dynamic maneuvers requiring Roll Movement Interventions

will be pre-filled with 10 to 20 bar to eliminate the air gap and to cut short on the time needed for a subsequent stability intervention (Figure 9). The elimination of the air gap is equivalent to a volume reduction of approx. 15% depending on the brake design.

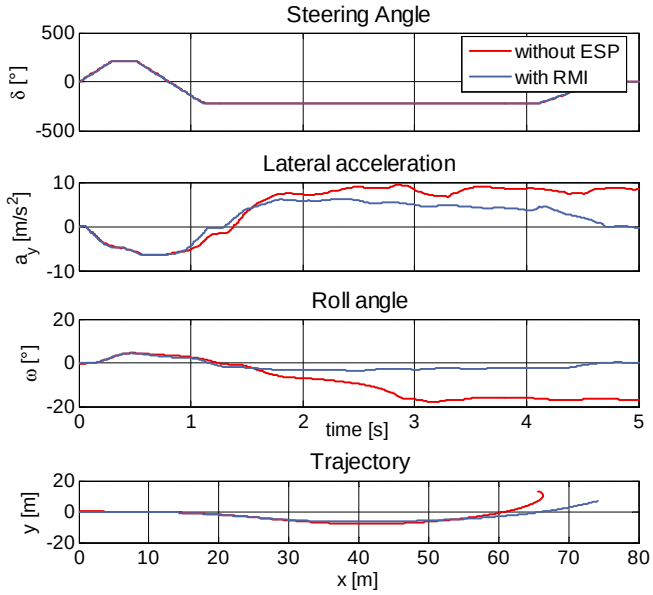

Figure 10. Fishhook maneuver at 80 kph entry speed with a LCV with passenger loads on all seats. Without ESP®, rollover is indicated by two wheel lift off after 2.6 s. With ESP®, the function RMI – Roll Movement Intervention efficiently prevents rollover

The NHTSA fishhook maneuver with a light commercial vehicle is used as an example to illustrate the rollover mitigation function (Figure 10) compared to the same vehicle w/o ESP® support. Entry speed of the maneuver was 80 kph and the vehicle had passenger loads on all seats. The steering input is depicted in terms of steering wheel angle whereas the vehicle reaction is expressed in terms of lateral acceleration and roll angle. During severe steering back a brake torque pre-control at the curve inside wheel is used to eliminate the air gap for reduced pressure build-up time. While the commercial vehicle with ESP® finished the maneuver successfully, it would have rolled over w/o the Roll Mitigation function.

For vehicles with a high variance of the center of gravity height, an adaptive rollover mitigation strategy is designed. It uses the vehicle's mass and the estimated CoG position to adjust the threshold for brake interventions. This ensures timely interventions with the correct intensity and minimized comfort impairment.

TRAILER SWAY MITIGATION

SUV, LCV and LT are frequently used as towing vehicles for trailers. In typical driving situations, external excitations acting on vehicle and trailer will initiate a sway motion which is automatically attenuated. Above a so called "critical velocity", the sway motion will continuously increase and finally result in serious instability. The appropriate driver reaction would be a reasonable deceleration to a speed below the critical velocity, however some drivers even continue to accelerate, which in short term improves the situation but finally results in aggravated sway and loss of control, as soon as the driver releases the accelerator.

The critical velocity is typically in the speed range between 80 kph and 110 kph. It depends on the geometrical dimensions of vehicle and trailer and their specific load distributions. Especially loading behind the trailer axle affects the critical velocity negatively. Thereby the occurrence of a sway motion may be shifted into a speed range, where the driver never

Figure 11. ESP® function "Trailer Sway Mitigation" to counteract sway movement induced by external excitation (e.g. side wind, road bump)

before experienced any stability impairment. The ESP® function "Trailer Sway Mitigation (TSM)" can effectively counteract the sway motion without need for additional sensors.

The trailer sway results in a periodic yaw motion of the towing vehicle, which is easily detected by the yaw rate sensor. In case the critical velocity is surpassed, the sway amplitude will constantly increase (Figure 12 – top). The TSM function continually monitors the amplitude and decelerates the vehicle with automated brake apply in case a threshold amplitude is exceeded (Figure 12 – middle). Since the required speed reduction can be significant, it might result in undesirable braking of following cars or trucks on the same lane.

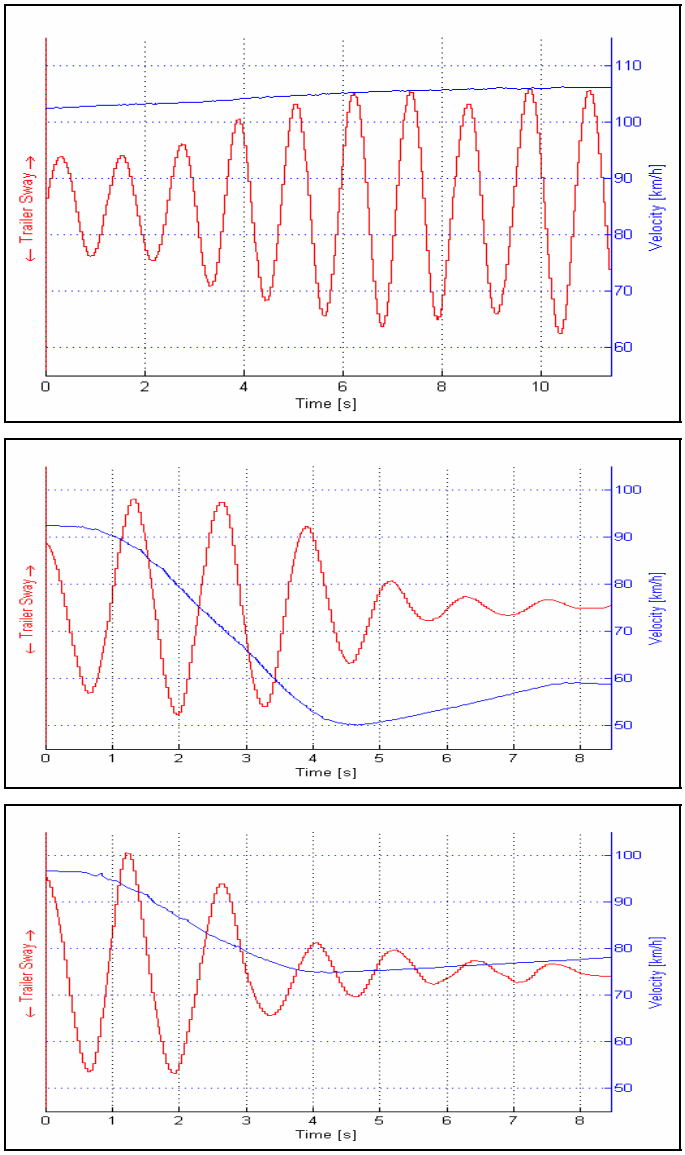

Figure 12. Trailer Sway affects the yaw motion of the towing vehicle. Yaw motion measured with standard ESP® sensor set.
Top: Increasing yaw rate of towing vehicle above critical speed
Middle: Sway damping after symmetrical brake intervention
Bottom: Sway damping after opposite-in-phase brake intervention

The wheel individual brake control of ESP® together with TSM also enables an opposite-in-phase brake intervention with improved efficiency (figure 12 – bottom). The trailer sway is attenuated quickly and the vehicle speed is reduced to just below the critical velocity.

CONCLUSION

The specific characteristics of LCV and LT require special adaptations of stability control due to the load dependent shift of self-steering properties and center of gravity changes. Bosch has developed the Load Adaptive Control that automatically adapts specific ESP® control mechanisms to such changing conditions. In particular, LAC improves the braking efficiency during partial braking as well as in ABS- and split-µ situations. The Drive-away and the overall traction efficiency is improved particularly for RWD and 4WD variants. The stability control is automatically adapted to loading dependent changes of the self-steering properties and the respective cornering behavior. It also supports the driver with an optimized lateral acceleration control to manage rollover critical on-road situations. Together with the TSM function for continually monitoring potential trailer sway, the functional enhancements developed by Bosch ensure that the remarkable safety benefits of ESP® can be fully extended to LCV, LT and heavy SUV.

REFERENCES

[1] Rabe, M.; VW-Research, Germany, 5. Symposium Automatisierungs- und Assistenzsysteme für Transportmittel, Braunschweig, Germany, (17-Feb-2004).

[2] Aga, M.; Okada, A.; Toyota, Japan, Paper No. 541, JSAE Automotive Engineering Exposition, Yokohama, May 2003.

[3] Van Zanten, A. et al.: "Control Aspects of the Bosch-VDC". International Symposium on Advanced Vehicle Control AVEC ' 96, 1996.

[4] Van Zanten, A. T.: "Bosch ESP systems: 5 years of experience". SAE 2000-01-1633, 2000.

[5] National Highway Traffic Safety Administration (NHTSA): Final Policy Statement on NCAP Rollover Resistance Rating, Consumer Information, 2003.

[6] Sampson, D.J.M.: "Active Roll Control of Articulated Heavy Vehicles". Ph.D. thesis, Cambridge University Engineering Department, UK, 2000.

[7] BMW EDC, see http://www.bmw.co.za/Products/FIRST/Active/act-EDC.htm

[8] Brown, T. A. et al.: "Rollover Stability Control for an Automotive Vehicle". US patent No. 6,263,261 B1.

[9] Liebemann, E. et al.: "Intelligent Networking for more Safety. VDM and CAPS – The Combination of Active and Passive Safety Systems", Chassis Tech Munich, 2007

CONTACT

Dr. E. K. Liebemann, Robert Bosch Corporation, Chassis Systems Control, email:

edwin.liebemann@de.bosch.com

ANNOTATION:

All abbreviations within this paper are used for simplification purposes.

DEFINITIONS, ACRONYMS, ABBREVIATIONS

4WD:	Four Wheel Drive
ABS:	Anti-Lock Control
CCC:	Center Coupling Control
CoG:	Center of Gravity
ESC:	Electronic Stability Control (= ESP®)
ESP®:	Electronic Stability Program (= ESC)
FMEA:	Failure Mode Effects Analysis
HBA:	Hydraulic Brake Assist
LAC:	Load Adaptive Control
LCV:	Light Commercial Vehicle
LT:	Light Truck
NHTSA:	National Highway Traffic Safety Administration
RMF:	Rollover Mitigation Function
RMI:	Roll Movement Intervention
ROM:	Rollover Mitigation
RWD:	Rear-Wheel Drive
SSF:	Static Stability Factor
SUV:	Sport Utility Vehicle
TCS:	Traction Control System
TSM:	Trailer Sway Mitigation
VDC:	Vehicle Dynamics Control

BEHAVIOUR OF SUV AND MPV-TYPE VEHICLES IN COLLISIONS WITH ROADSIDE SAFETY BARRIERS

Roy Minton
Richard Cuerden
TRL Limited
United Kingdom

Paper Number 07-0432

ABSTRACT

Roadside safety barriers are designed to deflect errant vehicles back onto the carriageway, preventing them from encountering potentially dangerous off-road hazards or crossing into the opposing carriageway on dual carriageways. However, there are concerns that SUVs and MPVs, by virtue of their greater mass and height, may not be well catered for by the current design of safety barrier, which is tested to withstand an impact with a 1500kg standard car.

An analysis of National accident statistics (all police-reported injury accidents in Great Britain) is presented, which indicates that the occupants of these larger vehicles generally incur less severe injuries than occupants of standard cars. Only a small proportion of road accidents involve barrier strikes, and the involvement of a barrier is associated with increased likelihood of rollover and increased injury severity for occupants of all vehicle types. These increases in rollover incidence and injury severity are found to affect SUVs and MPVs much more than standard cars (rollover incidence rises by factors of 4 for cars, 7 for SUVs and 9 for MPVs).

However, detailed information on a small number of barrier strike accidents involving SUVs or MPVs taken from TRL's in-depth accident databases (10 cases in total) indicates that the barriers themselves may not be to blame. The barriers are found to exceed their design specification in a number of cases, and the cause of the accident is found in several cases to be difficulty in controlling these larger vehicles in extreme situations.

Despite the limitations of a lack of detail in the national accident statistics and a small number of cases for in-depth analysis, this study nevertheless offers a useful insight into an accident scenario in which SUVs and MPVs become less safe for their own occupants than standard cars.

INTRODUCTION

Roadside safety barriers, also known as vehicle restraint systems, are designed to contain errant vehicles, preventing them from encountering potentially dangerous off-road hazards or crossing into the opposing carriageway on dual carriageways. However, there are concerns that Sports-Utility Vehicles (SUVs) and Multi-Purpose Vehicles (MPVs), by virtue of their greater mass and height, may not be well catered for by the current design of safety barrier in the UK, which is tested to withstand a 1500kg standard car impacting at 70mph (112kph) at an angle of 70^{o}.

In terms of sales, the UK market share of SUVs has grown from 3% to 6% over the 15 years from 1990, and that of MPVs has more than doubled to a peak of 22% in 2001, though this has dropped back to 20% in the last few years. However, proportionately more SUVs are involved in accidents, which may imply that there are more of them in the vehicle fleet. This could be explained by the fact that SUV-type vehicles have existed for a long time, whereas MPV numbers are growing from a much smaller base. As a result of this increasing market penetration, any problems associated with the crash characteristics of these vehicle types are likely to grow as time goes on.

We therefore set out to determine the nature of real world crashes involving these larger vehicles, to determine whether differences exist between their crash characteristics and those of standard cars, particularly when vehicle restraints are struck and, if so, to quantify the size of the problem. There is currently a shortage of information on vehicles of this type, which fall somewhere between cars and light goods vehicles (LGVs) in terms of size; indeed, some of the larger MPVs are little more than vans with windows and seats. However, in contrast to LGVs, which generally do not carry passengers, and which tend to be driven by professional drivers, the vehicles of interest are frequently used to transport families, so they have the potential to produce a greater number of casualties in any collision.

MATERIALS AND METHODS

National road accident data for Great Britain (England, Scotland and Wales - GB) were analysed for the years 1995 to 2004 inclusive. All injury road crashes are required to be reported to the police, who compile a standard set of data about the crash circumstances, which is subsequently entered into the national Stats19 database. Only a fairly crude categorisation of vehicle types is possible from this data source, with most SUVs and MPVs being simply classed as "cars". Our analysis subset was therefore defined as "all injury road accidents involving at least one car-type vehicle". It is possible that some SUVs and MPVs may have been miscoded as a non-car vehicle type, and so might be excluded from the subset. However, since the most likely collision partner for any vehicle is a car, a large proportion of these miscoded vehicles would still be included because their collision partners would make the accident eligible.

Using vehicle registration marks (VRMs), this subset can then be linked to the national vehicle registration and licensing database, giving make and model information on the vehicles involved. By comparing this to a standard list of SUV and MPV makes and models drawn up for the purpose (see Appendix, Tables A1 & A2), these vehicle types could be identified in the road accident statistics. This process was not perfect, since errors at the data collection stage, either in recording the VRM, or in mixing up the VRMs between the vehicles in an accident could result in a blank record being returned or even the wrong make and model being assigned. Thus it is sometimes possible to see Porsche Carrera bicycles or Harley Davidson heavy goods vehicles involved in accidents. This problem was found to be worse in some years than others, but as far as could be ascertained, it never affected more than about 0.2% of vehicles. Sometimes the police do not see the vehicle involved and so do not record the VRM. This can happen in hit-and-run pedestrian accidents, where the vehicle is not traced, or possibly in some minor accidents which may only come to the attention of the police when the casualties attend hospital. Even when the linking was successful, the data from the licensing database was sometimes found to be incomplete, with only the make of the vehicle being available, so that it was not possible to say whether this was a standard car or an SUV or MPV. Because of this, five categories of vehicles were recognised in the analysis:

SUV: Make/model data available and identified from Table A1

MPV: Make/model data available and identified from Table A2

Car: Car-type vehicle, make/model data available and not an SUV or MPV

Other car: Car-type vehicle, make/model data not available or incomplete

Other vehicle: Any other vehicle, regardless of whether make/model data was available.

The "Other car" category doubtless contains some SUVs and MPVs, but they are not identifiable.

Another difficulty associated with this linking related to geographical bias. VRM-linked data has not always been available; the process was introduced in the early 1990s, involving data from just a few police force areas, and national coverage was not achieved until 1997. Data in our sample from 1995 and 1996 lacked information from several large urban police force areas and was noticeably anomalous as a result. These years have been excluded from the results presented here. For the remaining eight years, VRM-linked data was available for 80±2% of all accidents.

In each of the years studied, the overall sample sizes were of the order of 250,000 known cars, 6,500 SUVs and 3,500 MPVs.

RESULTS AND DISCUSSION

Driver Characteristics

For cars, the proportion of accident-involved vehicles with male drivers was found to exhibit a slight hint of a downward trend, from 63% to 61% over the study period. Both SUVs and MPVs had slightly higher proportions of male drivers, but with a more pronounced downward trend from 68% to 62%. SUVs were significantly different from cars in this respect in all years. There were also differences in the ages of the drivers, as shown in Figure 1 which, for each of the eight years in the study period, shows the numbers of each accident-involved vehicle type with drivers under 36 years old as a proportion of the total number of accident-involved vehicles of that type in that year:

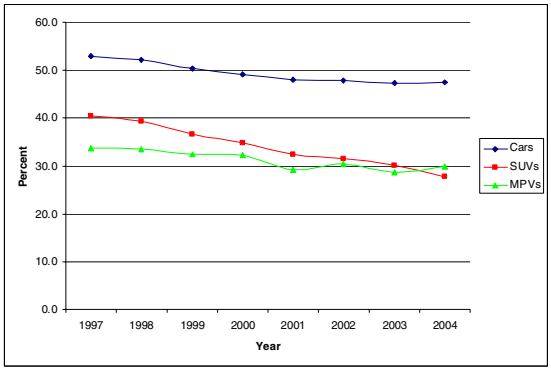

Figure 1. Vehicles with drivers under 36 years old.

The accident-involved car driving population appears to be getting older, with a downward trend in the number of drivers under 36 years old. Reasons for this could possibly include demographic changes in the age structure of the population, an improvement in the accident involvement rate of young drivers, or some other factor. The proportions for SUV and MPV drivers show similar downward trends, converging in 2003/04 at about 20 percentage points lower than cars, with just under 30% less than 36yrs, compared to just under 50% of car drivers. In general, this can probably be explained in terms of the drivers' financial and social situations, with cost and image value probably making a standard car more attractive to a young vehicle buyer. SUVs and MPVs are both significantly different from cars as regards driver age in each of the eight years studied.

Injury Outcomes

Figure 2 compares known standard cars with SUVs and MPVs for each of the eight years considered, with respect to the highest injury severity recorded for the vehicle occupants (vehicles which hit pedestrians are excluded). For each vehicle type, the percentages indicate the number of vehicles with killed or seriously injured occupants as a proportion of all accident-involved vehicles of that type in that year. See Appendix for definitions of injury severity terms.

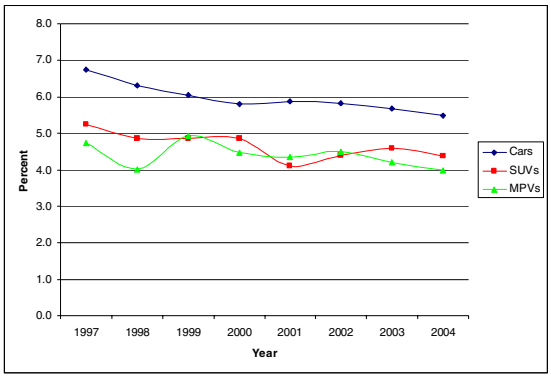

Figure 2. Vehicles with killed or seriously injured occupants.

The well-documented reduction in the rate of killed or seriously injured (KSI) occupants in GB over the study period is quite clear. The KSI rate in SUVs and MPVs is consistently lower than in cars (and this is statistically significant in each of the years considered), giving credence to the widely-held perception that these vehicles are safer for their occupants. Amalgamating the figures for all eight years, the KSI rates for SUVs and MPVs are both about 75% of the KSI rate for cars. The reason for this is probably related to the fact that the most likely collision partner is a smaller, lighter, standard car; incompatibility between cars and SUVs in particular is a well-recognised problem, with cars most likely to come off worse in any collision. This perception could change if the numbers of SUVs and MPVs were to rise to the point where the most likely collision partner is another SUV or MPV. Comparison of the three types of vehicle with respect to the numbers of uninjured occupants confirms that occupants of SUVs and MPVs are more likely to walk away from a crash uninjured than are car occupants.

Accident circumstances

Figure 3 is based on accidents involving pedestrians, where the pedestrian strike was the only impact which the vehicle experienced. Again, for each vehicle type, the figure shows the number of vehicles striking pedestrians as a proportion of all accident-involved vehicles of that type in that year.

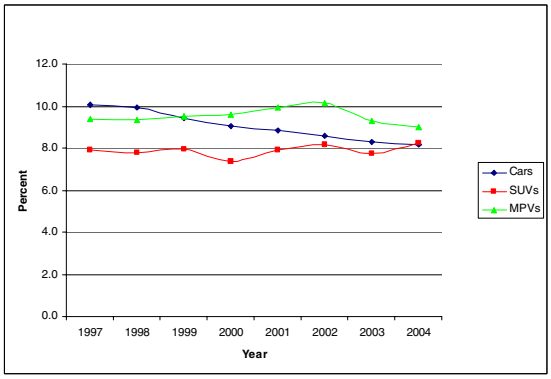

Figure 3. Vehicles in pedestrian accidents (no other vehicle involved).

There is a steady decline over the study period in the proportion which pedestrian/car accidents form of all car accidents, from about 10% to about 8%. Over the same period, pedestrian/SUV accidents as a proportion of all SUV accidents have remained fairly constant at about 8%, while the figures for MPVs have climbed from about 9.5% to 10% before dropping back to about 9% in 2003-04. Overall, the figures for MPVs are consistently higher than those for SUVs, and this may be a reflection of different road environments that these vehicle types are used in. It is interesting that neither SUVs nor MPVs are following the downward trend in pedestrian accidents seen for cars.

Figure 4 compares the three vehicle types with respect to the proportions which are involved in single-vehicle accidents (SVAs). It is interesting that the incidence of SVAs among cars rose by five percentage points to 20% over the eight years studied. Relative to cars, SUVs have historically had a higher proportion of SVAs, though they have

converged over the last three years of the study period. MPVs, on the other hand, show a lower involvement rate in SVAs over the whole eight years, with no indication of likely convergence in the future.

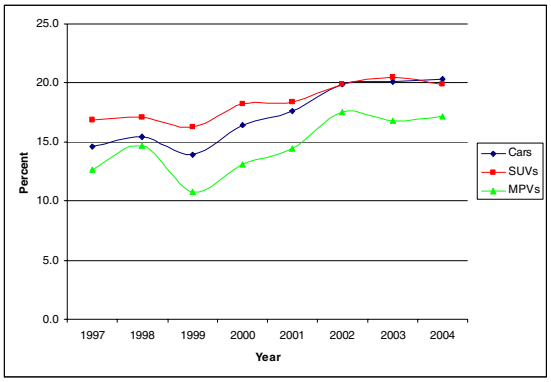

Figure 4. Vehicles in single-vehicle accidents (no pedestrian involved).

Figure 5 looks at vehicles which overturned during the accident. The data available are not sufficiently detailed to enable us to determine whether the rollover occurred before or after the first impact, nor whether the roll was the most injurious event.

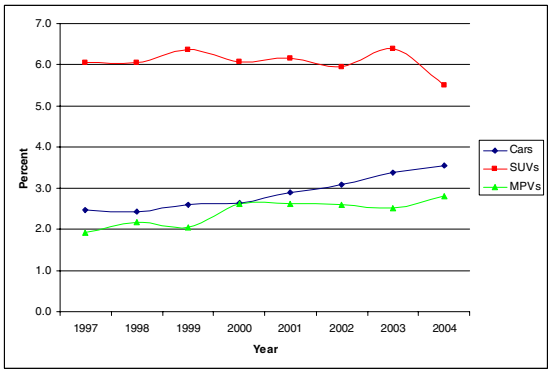

Figure 5. Vehicles overturning.

Clearly, SUVs are roughly twice as likely to overturn in an accident as cars are, although there is a rising trend among cars which is not seen for SUVs. These differences are statistically significant in each of the eight study years. MPVs, on the other hand, are slightly less likely to overturn than cars, but the differences are only significant in the final three years. Table 1 shows how injury outcome is affected by rollover.

Table 1.
Overturning vehicles by occupant injury severity and vehicle type (no pedestrian involved)

Maximum severity in vehicle	Car		SUV		MPV	
	Number	%	Number	%	Number	%
Injured	55973	97.1	3146	95.1	775	95.2
Uninjured	1662	2.9	162	4.9	39	4.8
KSI	12260	21.3	645	19.5	152	18.7
Slight & uninjured	45375	78.7	2663	80.5	662	81.3
Totals	57635	100	3308	100	814	100

Because rollover is a relatively rare occurrence, this table amalgamates the figures from the entire eight year period. Vehicles which struck pedestrians are excluded. Comparing this to Figure 1, we see that the KSI rate for all three vehicle types has, as might be expected, risen. The KSI rate for cars is 21% when rollover occurs, compared to an average of about 6% in Figure 1. However, SUVs and MPVs, are much more badly affected by rollover, with their KSI rates now much closer to those of cars, whereas previously their KSI rates were only about 75% of that for cars.

Figure 6 shows the proportion of vehicles which left the carriageway, either before or after impact. Cars show a rising trend from 2000 on, to such an extent that by 2004 a higher proportion of cars than SUVs leave the carriageway, whereas historically, SUVs were more likely to go off the road. MPVs appear to be much less likely to leave the carriageway than either cars or SUVs.

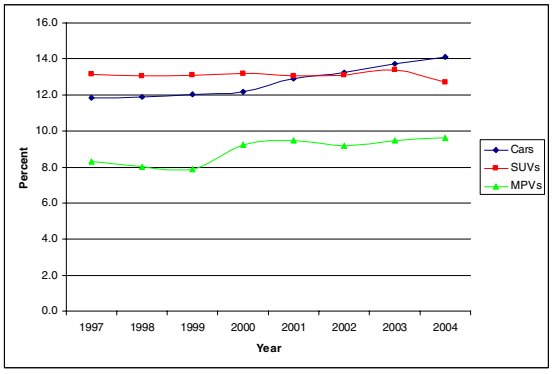

Figure 6. Vehicles leaving the carriageway.

The data available includes details of the objects struck by vehicles which left the carriageway. Although some 13% of cars and SUVs leave the carriageway, only about 10% strike anything in the process. Similarly, only about 7% of all MPVs strike anything off the carriageway. Table 2 gives details of the off-carriageway objects struck, using amalgamated data from all eight years.

Table 2.
Vehicles by Off-Carriageway Object Struck and Vehicle Type

Object struck	Car		SUV		MPV	
	Number	%	Number	%	Number	%
Road sign/signal	16514	8.5	359	7.1	180	9.0
Lamp post	20421	10.5	316	6.3	172	8.6
Telegraph pole	7022	3.6	162	3.2	60	3.0
Tree	28182	14.5	693	13.7	276	13.7
Bus stop/shelter	1220	0.6	20	0.4	10	0.5
Central barrier	14813	7.6	453	9.0	210	10.5
Road side barrier	14512	7.5	391	7.8	174	8.7
Submerged	225	0.1	7	0.1	2	0.1
Entered ditch	17473	9.0	638	12.7	216	10.8
Other object	73802	37.9	1986	39.4	701	34.9
Not coded	567	0.3	16	0.3	7	0.3
Totals	194751	100	5041	100	2008	100

The two barrier categories (central and road side) together account for about 15% of the off-carriageway objects struck by cars, the proportions being somewhat higher for SUVs and MPVs. Overall, however, less than 1.5% of all accident-involved vehicles strike safety barriers. This is a fairly small proportion, but Tables 3 and 4 demonstrate that barrier strikes, while being associated with significantly worse outcomes for all vehicle types, have a particularly adverse effect on SUVs and MPVs.

Table 3.
Vehicles by overturning, barrier contact and vehicle type

Vehicle overturning	Car		SUV		MPV	
	Number	%	Number	%	Number	%
No barrier strike						
Overturn	57879	2.9	3316	6.1	818	2.5
No overturn	1966998	97.1	51442	93.9	31761	97.5
Total	2024877	100	54758	100	32579	100
Barrier strike						
Overturn	3213	11.0	348	41.2	88	22.9
No overturn	26112	89.0	496	58.8	296	77.1
Total	29325	100	844	100	384	100

Table 4.
Vehicles by occupant injury severity, barrier contact and vehicle type

Vehicle overturning	Car		SUV		MPV	
	Number	%	Number	%	Number	%
No barrier strike						
KSI	109880	6.0	2327	4.6	1278	4.4
Slight & uninjured	1725611	94.0	47975	95.4	28094	95.6
Total	1835491	100	50302	100	29372	100
Barrier strike						
KSI	3566	12.2	134	16.0	45	11.7
Slight & uninjured	25570	87.8	703	84.0	339	88.3
Total	29136	100	837	100	384	100

The top half of table 3 is similar to Figure 5, and shows SUVs being more than twice as likely as cars to roll over in accidents generally, with MPVs being slightly less likely than cars to roll. The lower half of the table is based on the subset of vehicles which struck barriers, and shows a more than three-fold increase in rollover incidence for cars. This is likely to be related to the fact that

barriers are generally installed on high-speed roads, where any impact is more likely to result in the vehicle overturning. However, the figures for SUVs and MPVs indicate that these vehicle types are much more badly affected in these circumstances, with rollover incidence increasing by factors of nearly 7 for SUVs and 9 for MPVs. These differences are statistically significant for all three vehicle types.

We have already seen (Table 1) that the KSI rate is particularly badly affected by rollover for SUVs and MPVs. Table 4 gives the injury outcome data for vehicles striking barriers, whether they overturned or not. Again, this uses amalgamated data from all eight years, and excludes vehicles striking pedestrians.

The top half of Table 4 gives information similar to that in Figure 2 – that is, the KSI rate for SUVs and MPVs is about 75% of that for cars. The lower half of the table gives the results for barrier strike crashes and shows that, in these circumstances, SUVs become significantly less safe than cars in terms of the KSI rate, while MPVs become only slightly safer than cars. These results are consistent with Tables 1 and 3 above, where overturning was shown to have a disproportionately deleterious effect on injury outcome for SUVs and MPVs compared to cars, and the incidence of overturning was also shown to be disproportionately higher for SUVs and MPVs when a barrier was involved.

CASE STUDIES

In addition to the analysis of national statistics presented above, a small number of police reports on cases where an SUV or MPV had hit a barrier were available for detailed study. These cases were drawn from a collection of some 30,000 police reports on fatal accidents held by TRL, spanning the years 1986 to 2005. Table 4 indicates that there were 179 KSI cases over the study period, and of these, 23 involved a fatality. The police reports on ten of these cases were available. The results of these case studies, in most cases, indicated that the barriers themselves were not the cause of the problem. In a number of cases, the barriers out-performed their specification in retaining these heavier vehicles on their own carriageway. There was no compelling evidence to indicate that the barriers were instrumental in causing the vehicles to roll over. In a number of cases, the barrier strike was only a glancing blow, and the loss of control and rollover could be attributed to over-reaction by the driver in terms of steering input in an attempt to regain the carriageway proper. In other cases, the vehicle was already completely out of control before the barrier strike. High speed was a factor in most of the cases, and the overall conclusion was that the problem lay in drivers' inability to control their vehicles at high speeds in extreme situations.

Only one case gave cause for concern. Here a stepped approach to a barrier was felt to have been instrumental in launching an SUV over the barrier into the opposing carriageway. This occurred despite the barrier being higher than normal specification would allow. It may be that such a stepped approach would be better avoided if possible.

CONCLUSIONS

1. There are significant differences between SUVs and MPVs and cars in terms of their accident characteristics. These can be summarised as follows:

a. SUVs and MPVs are slightly more likely to be driven by males than cars are, and the average age of these drivers is significantly greater than that of car drivers.

b. MPVs are more likely than cars to have accidents involving pedestrians. SUVs have historically shown the opposite tendency, but they have converged with cars in this respect recently. MPVs are less likely than cars to have single-vehicle accidents, but both cars and MPVs show a rising trend over time. SUVs have historically been more likely than cars to be involved in SVAs, but again they have converged in recent years.

c. Occupants of Group vehicles are significantly less likely to be killed or seriously injured and more likely to be uninjured compared to car occupants.

d. SUVs are significantly more likely to overturn during an accident than are cars. MPVs in recent years have shown a slight tendency in the opposite direction.

e. Historically, SUVs have been more likely than cars to leave the carriageway, but a rising trend among cars has resulted in the opposite being the case in recent years. MPVs are significantly less likely to leave the carriageway than is the case for cars.

f. Less than 1.5% of all the accident-involved vehicles studied hit safety barriers when they leave the carriageway.

g. Barrier impacts are associated with increased incidence of rollover and higher injury severity outcome for all vehicle types, but disproportionately so for SUVs and MPVs.

2. Analysis of a small sample of cases from TRL's Fatal Accident File collection has indicated:

a. In most of the crashes the barrier out-performed its specification in terms of the mass of the striking vehicle and the speed and angle of approach.

b. It appears that the increased injury severity associated with SUVs and MPVs involved in barrier strikes may be a function of difficulties in controlling these vehicles in extreme situations, regardless of whether or not they struck a barrier. In several cases the barrier merely contained an already out-of-control vehicle.

c. Only one case gave cause for concern. Here a stepped approach to a barrier was felt to have been instrumental in launching an SUV over the barrier into the opposing carriageway. This occurred despite the barrier being higher than normal specification would allow. This was more a shortcoming in the associated infrastructure than in the barrier itself.

ACKNOWLEDGEMENTS

The authors wish to acknowledge the support of the UK Highways Agency in carrying out this project, which was funded under the Framework Project Task Number 3/372-R37.

Police fatal accident reports are supplied to TRL Limited on a routine basis by most police forces in England and Wales when they are no longer required for legal processes. Their collection and cataloguing is funded by the United Kingdom Department for Transport (DfT) (Road Safety Division).

Summaries of National Stats19 injury accident data are published annually by the United Kingdom Department for Transport (DfT) in the Road Casualties Great Britain series.

APPENDIX

Police Injury Severity – In this paper, the UK government's definitions of injury severity (Fatal (Killed), Serious or Slight) are used.

'Fatal' injury includes only those where death occurs in less than 30 days as a result of the accident. Fatal does not include death from natural causes or suicide.

Examples of 'Serious' injury are:
- Fracture of bone
- Internal injury
- Severe cuts
- Crushing
- Burns (excluding friction burns)
- Concussion
- Severe general shock requiring hospital treatment
- Detention in hospital as an in-patient, either immediately or later
- Injuries to casualties who die 30 or more days after the accident from injuries sustained in that accident

Examples of 'Slight' injuries are:
- Sprains, not necessarily requiring medical treatment
- Neck whiplash injury
- Bruises
- Slight cuts
- Slight shock requiring roadside attention

Table A1.
SUV Makes and Models

Make	Model	Make	Model
Acura	MDX	Mazda	Tribute
ARO		Mercedes	G-Class
Asia	Rocsta	Mercedes	ML-Class
BMW	X5	Mitsubishi	Challenger
Cadillac	Escalade	Mitsubishi	Montero
Chevrolet GMC	Blazer	Mitsubishi	Pajero
Chevrolet GMC	Silverado	Mitsubishi	Pajero Io
Chevrolet GMC	Tahoe	Mitsubishi	Pajero Mini
Chevrolet GMC	Vega	Mitsubishi	Pajero Pinin
Daewoo	Korando	Mitsubishi	Shogun
Daewoo	Musso	Mitsubishi	Shogun Pinin
Daihatsu	Fourtrak	Mitsubishi	Shogun Sport
Daihatsu	Sportrak	Nissan	Navara
Daihatsu	Terios	Nissan	Patrol
Dodge (USA)	Durango	Nissan	Safari
Dodge (USA)	Ram	Nissan	Terrano
Ford	Explorer	Nissan	X-Trail
Ford	F150	Porsche	Cayenne
Ford	Maverick	Rover	Range Rover
Ford	Ranger	Ssangyong	Korando
Honda	CR-V	Ssangyong	Musso
Honda	HR-V	Ssangyong	Rexton
Hyundai	Santa Fe	Subaru	Forester
Hyundai	Terracan	Subaru	Legacy Outback
Infiniti	QX4	Suzuki	Escudo
Isuzu	Bighorn	Suzuki	Grand Vitara
Isuzu	Mu	Suzuki	Jimny
Isuzu	Trooper	Suzuki	Samurai
Jeep	Cherokee	Suzuki	SJ
Jeep	Grand Cherokee	Suzuki	Vitara
Jeep	Wrangler	Tata	Safari
Kia	Sorento	Toyota	4Runner
Kia	Sportage	Toyota	Harrier
Land Rover	109	Toyota	Hilux
Land Rover	110	Toyota	Landcruiser
Land Rover	127	Toyota	Landcruiser Amazon
Land Rover	88	Toyota	Landcruiser Colorado
Land Rover	90	Toyota	Rav4
Land Rover	Defender	UMM	
Land Rover	Discovery	Vauxhall	Frontera
Land Rover	Freelander	Vauxhall	Monterey
Land Rover	Range Rover	Volkswagen	Touareg
Lexus	RX300	Volvo	XC90

Table A2.
MPV Makes and Models

Make	Model	Make	Model
Chrysler	Grand Voyager	Mitsubishi	Space Star
Chrysler	PT Cruiser	Mitsubishi	Space Wagon
Chrysler	Town & Country	Mitsubishi	Town Box
Chrysler	Voyager	Nissan	Almera Tino
Citroen	Berlingo	Nissan	Prairie
Citroen	C8	Nissan	Serena
Citroen	Synergie	Opel	Agila
Citroen	Xsara Picasso	Opel	Zafira
Daewoo	Tacuma	Peugeot	806
Daihatsu	Delta	Peugeot	807
Daihatsu	Grand Move	Peugeot	Partner Combi
Daihatsu	Move	Renault	Avantime
Fiat	Doblo	Renault	Caravelle
Fiat	Multipla	Renault	Espace
Fiat	Ulysse	Renault	Grand Espace
Ford	Fiesta Courier	Renault	Kangoo
Ford	Focus	Renault	Megane Scenic
Ford	Galaxy	Seat	Alhambra
Ford	Tourneo	Seat	Terra
Honda	Odyssey	Suzuki	Wagon R+
Honda	Shuttle	Toyota	Avensis Verso
Honda	Stepwagon	Toyota	Corolla Verso
Honda	Stream	Toyota	Estima
Hyundai	Atoz	Toyota	Granvia
Hyundai	Matrix	Toyota	Ipsum
Hyundai	Trajet	Toyota	Lucida
Kia	Carens	Toyota	Picnic
Kia	Sedona	Toyota	Previa
Mazda	MPV	Toyota	Space Cruiser
Mercedes	Vaneo	Toyota	Yaris Verso
Mercedes	V-class	Vauxhall	Agila
Mitsubishi	Chariot	Vauxhall	Meriva
Mitsubishi	Delica	Vauxhall	Sintra
Mitsubishi	Dion	Vauxhall	Zafira
Mitsubishi	Minica	Volkswagen	Caravelle
Mitsubishi	Mirage	Volkswagen	Microbus
Mitsubishi	RVR	Volkswagen	Sharan
Mitsubishi	Space Runner	Volkswagen	Touran

LATERAL FORCES ON HEAVY TRUCKS – CONTRIBUTIONS FROM WIND

Dr. Frank Wilson
Dr. Eric Hildebrand
Transportation Group
University of New Brunswick
Canada
Paper Number 07-0444

ABSTRACT

A tractor semi-trailer unit equipped with on-board instrumentation that measured speed, lateral accelerations, and the roll angle of the vehicle was driven around a test site (inter-change ramp) under varying wind conditions. A portable weather station was installed in the centre of the test track. The rollover threshold of the truck was calculated based on the characteristics of the vehicle and then compared with the lateral accelerations measured on the test vehicle. An analysis of the data indicated that there existed significant differences in lateral accelerations under scenarios of varying wind speeds, verifying that wind can contribute to rollover. An analysis of the rollover threshold revealed that the lateral accelerations experienced by the truck were often greater than the rollover threshold for brief periods of time. The time periods were not sufficiently long enough to cause rollover of the vehicle.

The research demonstrated that the technique developed on this project could be used to determine the safe speed for heavy trucks operating on specific sections of the roadway.

INTRODUCTION

The main objective of this research was to determine how lateral forces are affected by wind as a heavy truck traverses a highway curve or interchange loop-ramp. The procedure developed for this research was unique compared with other procedures for testing lateral accelerations or forces in that a truck was maneuvered around a curve a number of times, under varying wind conditions and vehicle speeds. The design of this experiment was such that a statistical analysis of the vehicle's dynamic responses could be carried out based on various wind conditions. The experiment also demonstrated a new approach for determining the maximum safe speed for trucks on highway curves based on the geometric characteristics and wind conditions.

TRUCK ACCIDENT CHARACTERISTICS

Commercial trucks make up a significant portion of the traffic stream on many highways in North America. In the United States in 1999, there were nearly eight million registered heavy vehicles, which accounted for 3.5 percent of the registered vehicle fleet. In addition, the average miles traveled per truck (26,014 miles) was more than double the average mileage for passenger vehicle (11,888 miles) in 1999 (1). In terms of safety, four percent of the 11 million accidents in the United States in 2001 were caused by commercial trucks. In total, trucks accounted for eight percent of all vehicles involved in fatal crashes, but only four percent of vehicles involved in injury and property damage only crashes (1). These figures suggest that while truck accidents occur less frequently than other types of vehicles, many of these accidents are more severe.

Large trucks were involved in 18,000 rollover events in the United States, of which, 622 were fatal crashes (1). Eleven thousand of the rollover events resulted in injury, indicating that the injury occurrence in a rollover is high (61%) compared to total truck accidents (21%). Combination trucks accounted for 11,000 of all heavy truck crashes while single-unit trucks accounted for 7,000 crashes (1).

In Canada, there are fewer heavy vehicles than in the United States. In 2000, there were approximately 661,000 heavy trucks (straight trucks and combination trucks with weights greater than 4,500kg) (2), of which, 528 were involved in fatal collisions. This represents about

12 percent of all fatalities on the road (2). In total, truck rollovers account for 13 to 38 percent of all truck accidents, and of these, between 40 and 60 percent occur on highway interchange ramps (3).

BACKGROUND

Variables that contribute to truck rollovers can be divided into four categories – vehicle characteristics, highway features, environmental and human factors. In many cases, truck rollovers are caused by excessive speed as trucks negotiate short radius curves on highway ramps. Hildebrand and Wilson (4) studied in detail 53 heavy freight vehicle collisions between 1993 and 1996 in New Brunswick. In 15 cases, rollover was the initial factor in the incident and more than a third of these occurred on highway ramps. Excessive speed was the main contributing factor causing five of the accidents, and in the sixth case, speed and load shift combined to cause the accident. Other vehicle characteristics, besides speed, that affect a vehicle's rollover threshold include the height to the center of gravity, type of suspension, and track width. Highway features that commonly contribute to rollover accidents include posted speed limits, curve radii and lengths, super-elevation, and deceleration lane widths. Human factors encompass the characteristics of the driver's control of the vehicle. Environmental factors include wind force and direction as well as rain, snow, ice, etc.

The effect of wind on the stability of heavy vehicles is an important safety consideration and the primary focus of this research project. For the most part, limited research has been undertaken on this topic, although it has been noted to be a critical safety factor in areas with frequent high winds, or in areas prone to strong gusts. In Atlantic Canada, the Confederation Bridge between New Brunswick and Prince Edward Island, the "Wreckhouse" area in western Newfoundland and the Tantramar Marshes in New Brunswick are three examples of areas where wind often plays a critical role in the stability and safety of heavy vehicles. These areas are frequently closed to truck traffic due to wind conditions. Two of these sites are in close proximity to the study area for this research project.

When a truck negotiates the curves or ramps on a highway, wind may play a considerable role in causing the vehicle to rollover at lower speeds than expected, or it may be responsible for preventing rollover when it might have occurred at higher speeds. In the case of a truck traveling around a curve, a strong gust of wind from the inward side (coming from the centre of the curve) may provide the extra force required at the critical moment to cause the overturning forces to exceed the resisting forces, resulting in rollover. On the other hand, a gust of wind from the outward side (coming from outside of the curve) may provide a counter-force that helps resist the overturning forces.

There are many mathematical models and computer simulations that are used to estimate the dynamic responses and rollover thresholds of heavy vehicles. These include the:

- PHASE-4 computer program developed by the Texas Transportation Institute and the Texas State Department of Highways and Public Transportation (5).
- University of Michigan Transportation Research Institute (UMTRI) model (6).
- Linear yaw plane model (7).
- TBS model (7).
- Static roll model (7).

Most of the previous research has involved modeling or tilt-table tests. This study was directed to obtain over-the-road measured results. This provided a means for researchers to compare actual field condition data with the theoretical results.

Figueredo (8) designed a data acquisition system to collect field data on lateral acceleration experienced by the vehicle, roll angle of the trailer, and the vehicle speed. The purpose of this project was to equip a five-axle-tractor-semi-trailer with instrumentation that would measure the dynamic forces exerted on a vehicle in transit, and to use this data to determine the lateral forces experienced by the vehicle while moving around a curve. The testing process took place over 1,110 km of highway between Moncton, New Brunswick and North Sydney, Nova Scotia. From this study, it was found that:

- the Data Acquisition System (DAS) provided an acceptable method of collecting dynamic characteristics of a heavy vehicle while in motion.
- that it provided a high level of accuracy of the

recorded data.
- the data can be used to determine the dynamic stability of a vehicle in motion.

METHODOLOGY

In order to measure the dynamic forces acting on a heavy vehicle while in motion, several pieces of equipment were required. Figuereo's (8) Data Acquisition System (DAS) was used to collect data on lateral forces experienced by the vehicle, roll angle of the trailer, and vehicle speed. Wind conditions (i.e. speed and direction) were measured using a weather station that was positioned near the test ramp.

The Data Acquisition System DAS-P1000 uses a set of sensors and a central processing unit to collect the dynamic response characteristics of the tractor-semi-trailer while in motion. Its features include:

- central processing unit.
- three tri-axial accelerometers.
- steering wheel optical sensor.
- roll angle sensor.

The three tri-axial accelerometers measured the lateral, vertical, and longitudinal accelerations on the truck while in motion. One was placed at the top of the rear of the trailer, another near the fifth-wheel assembly, and the third in the cab of the truck. The steering wheel optical sensor provided a measure of the steering angle of the truck at any given instant and was attached to the steering column. The radar gun was used to collect the actual speed data of the truck, and was placed in the cab of the truck, aimed towards the road. The roll angle sensor located on the roof on the centerline of the rear of the trailer measured the vertical displacement of the top of the truck, which was used to measure the roll angle of the trailer. The central processing unit was a PC-based system that collected the data at 1/5 second intervals.

The weather station was used to measure the wind speed and direction near the ramp. A simple vane-and-cup anemometer was used, and combined with a data logger, measured the wind speed and direction at 1 second intervals.

The site selected for this research was near Moncton, New Brunswick, at the interchange between Route 2 (Trans Canada Highway) and Route 15. The eastbound-to-northbound ramp was utilized for vehicle testing as shown in Figure 1. The vehicle was instrumented, and testing took place between October 2003 and March 2004. A total of 54 test runs were completed over four separate days. The same vehicle was used for all of the runs to normalize for the effects of vehicle characteristics on lateral acceleration. The driver was required to follow the yellow edge line as closely as possible to control for human factors as the vehicle traveled along the ramp. The testing occurred over several months because of the need to coordinate the availability of all personnel with the days when the wind conditions satisfied the testing criteria and roads were clear of ice and snow.

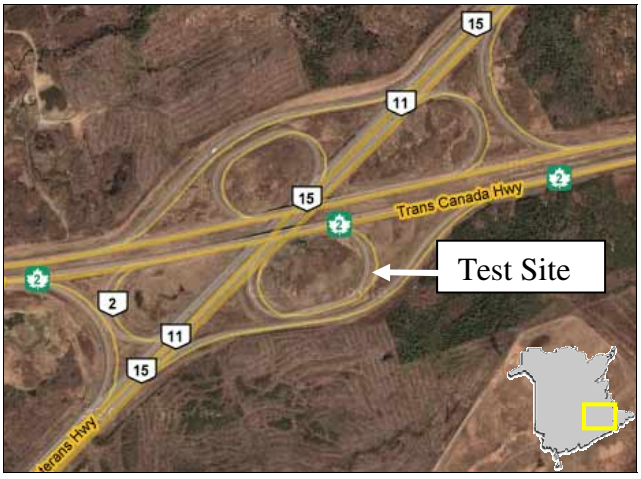

Figure 1. Loop ramp test site.

There are a number of reasons why this location was selected as the test site. First, the ramp has a history of rollover accidents, which was approximately two times the rate on adjacent ramps in the area. Anecdotal evidence indicates that the ramp can be challenging for trucks to maneuver because of its configuration. The ramp has two curves connected by a tangent. The curve at the entry to the ramp has a radius of 90m and a length of 314m. A tangent with a length of 108m follows this curve. The second curve at the end of the tangent has a radius of 80m and a length of 182m. While traveling along the first curve, an unfamiliar driver is generally cautious, and traverses the curve at a reasonable speed. On the subsequent tangent, the driver tends to accelerate, assuming the controlling curve has passed. Additionally, the tangent consists of a small down grade, which may add to the vehicle speed. When the driver enters the second curve, the speed is often greater than the speed through the first curve. This second curve has slightly smaller radius than the first, which causes an increased chance of vehicle rollover. The speed posted at the beginning of the first curve was 50 km/h. After the testing was completed, the speed posted at the beginning of the ramp was reduced to 40 km/h. A second posting of 40 km/h was posted at the mid-point of the tangent.

The second reason this ramp was chosen was because of the openness of the area. The area around the interchange is relatively clear of obstructions such as trees or buildings. In addition, the openness of the area results in sustained high winds that can be measured and used in determination of the effect of wind on truck rollover. The openness also allowed for an unobstructed view of the entire site.

TESTING

The trials were performed to determine the impact of lateral forces exerted by the wind on a heavy vehicle as it traveled around a highway ramp. A summary of the testing times and weather can be found in Table 1. Results were reported for 50 out of the 54 test runs because data were not accurate from four of the test runs due to instrumentation errors.

Table 1.
Testing Conditions

	Date	Number of Runs	Wind Condition
Day 1	November 15, 2003	14	Calm (≤8.8 km/h)
Day 2	November 16, 2003	5	Calm (≤8.8 km/h)
Day 3	December 11, 2003	12	Moderate (8.8 to 19.0 km/h)
Day 4	March 25, 2004	19	Strong (≥19.0 km/h)

The trials were made at varying speeds, with attempts to hold truck speeds constant at 35, 45, and 55 km/hr. However, the actual speeds of each run varied somewhat as the curves were traversed.

ANALYSIS

Data on the dynamic behavior of the truck was collected for each trial run. In order to study rollover potential, the lateral accelerations were examined. A typical lateral acceleration plot is shown in Figure 2.

The elements of Figure 2 are as follows:

A – The truck enters the curve to the right and the lateral accelerations to the left begin to increase.

B – The average maximum lateral acceleration peaks.

C – On the tangent, the lateral acceleration begins to decrease as the truck exits the curve and lateral acceleration approaches base conditions.

D – On the second curve, the lateral accelerations once again begin to rise and reach a peak value.

E – At the end of the second curve, a small peak in lateral accelerations can be experienced, most likely due to a combination of speed increase and the "sudden snap" noted by drivers.

F – When the truck enters Highway 15 North, the lateral accelerations begin to recede.

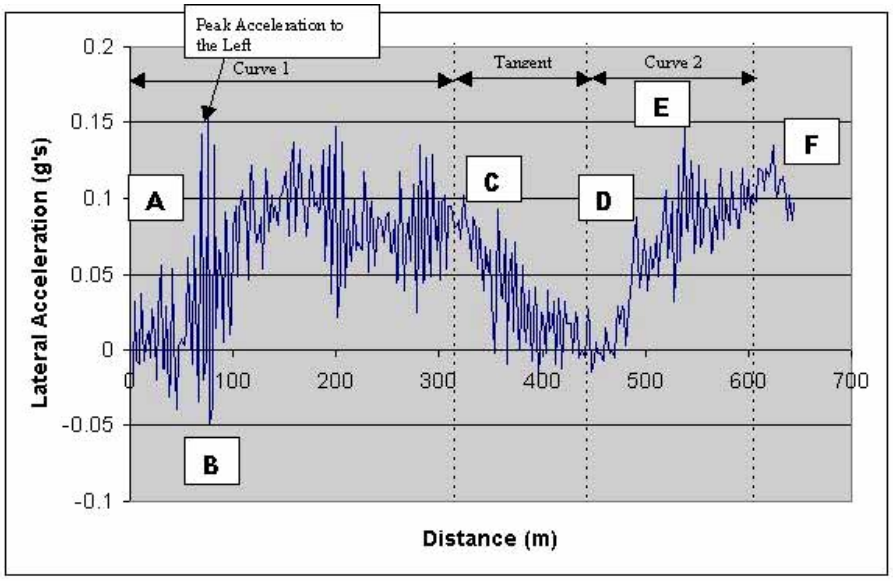

Figure 2. Lateral accelerations through test site.

Each run was analyzed by determining the peak lateral accelerations the trailer and the truck experienced. To determine the contribution of the wind forces on lateral accelerations, each run was categorized based on vehicle speed and wind speed. The average peak lateral accelerations for the runs in each group were calculated and a comparison made between the different groups. The lateral accelerations (Ax) in bold text in Table 2 indicate the average maximum lateral acceleration recorded by each accelerometer for the various wind and truck speeds. The second row (Vt) in each group of vehicle speeds represents the average truck speed for the group. The third row (Vw) represents the average wind speed for the group. The final row (N) indicates the number of observations in the group. Each observation corresponds with a ramp run, and was sorted based on the position on the ramp, i.e. curve 1 or curve 2.

TABLE 2.
Lateral Accelerations

Vehicle Speeds (km/h)	Test Results	Curve 1			Curve 2		
		Wind Speed (km/h)			Wind Speed (km/h)		
		0-8.8	8.9-18.9	>19.0	0-8.8	8.9-18.9	>19.0
<42	**Ax (g's)**	**0.157**	**0.222**	**0.291**	**0.187**	**0.229**	**0.281**
	Vt (km/h)	35.7	39.7	38.8	36.4	39.0	39.8
	Vw (km/h)	4.6	14.1	21.6	5.3	16.1	23.1
	N	5	5	4	5	3	4
42-49	**Ax (g's)**	**0.233**	**0.264**	**0.362**	**0.269**	**0.327**	**0.370**
	Vt (km/h)	44.1	45.7	46.1	44.1	47.8	46.8
	Vw (km/h)	3.0	14.1	21.4	3.6	16.2	21.3
	N	5	2	10	7	7	5
>49	**Ax (g's)**	**0.306**	**0.331**	**0.409**	**0.337**	**0.366**	**0.397**
	Vt (km/h)	51.4	53.9	51.4	52.6	54.8	52.1
	Vw (km/h)	3.6	15.5	21.2	3.9	15.7	21.4
	N	6	7	6	6	6	7

where:
Ax = equals lateral force on vehicle (g's).
V_t = average speed of test vehicle (kph).
V_w = average speed of wind (kph).
N = number of runs in sample.

Figures 3 and 4 illustrate the trends in the lateral accelerations on curves one and two, respectively, by classes of wind speed. Each series plotted represents varying vehicle speed.

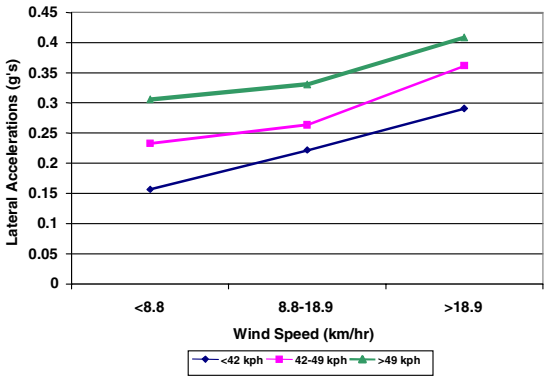

Figure 3. Maximum lateral accelerations by wind speed on curve 1.

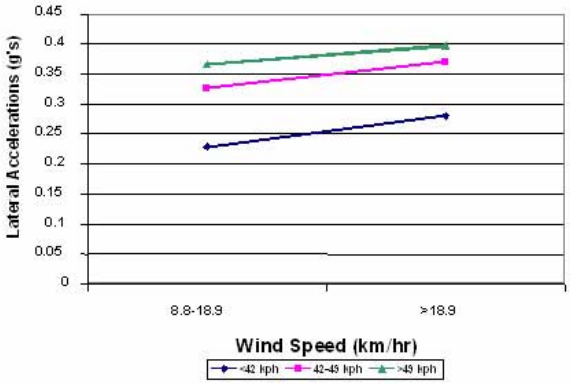

Figure 4. Maximum lateral accelerations by wind speed on curve 2.

The lateral accelerations were compared statistically to determine if wind speed and vehicle speed have an effect on the lateral forces measured. The Student's t-test for the comparison of means assuming unequal variances was used for the analysis. A summary of the tests for significance results is presented in Table 3.

Table 3.
Tests of Significance for Trailer Accelerometer

Vehicle Speed (kph)	Wind Speed Class (kph)	Significant Difference?	
		Curve 1	Curve 2
<42	0-8.8 vs. 8.9-18.9	Yes	Yes
	8.9-18.9 vs.> 19.0	Yes	Yes
42-49	0-8.8 vs. 8.9-18.9	Yes	Yes
	8.9-18.9 vs.> 19.0	Yes	Yes
>49	0-8.8 vs. 8.9-18.9	Yes	Yes
	8.9-18.9 vs.> 19.0	Yes	Yes

For each vehicle speed category, the low and middle wind speeds and the middle and high wind speeds were compared. For each curve and for each vehicle speed, it was determined at the 95 percent confidence level that as wind speed increased so did the lateral accelerations.

The roll threshold for the truck was also calculated using the static roll model and compared to the peak lateral accelerations experienced by the truck. Table 4 lists the values for the determination of the rollover threshold for this truck.

The truck rollover threshold varies between 0.47 and 0.54 g's for the test unit, depending on superelevation development and trailer roll angle. The maximum average lateral accelerations found to occur on the truck were 0.409 g's and 0.397 g's for curve 1 and curve 2. This indicates that the empty unit experienced lateral forces that were 86 and 74 percent of the rollover threshold for the vehicle.

Table 4.
Rollover Threshold

Values for Static Roll Model Calculation	Curve 1	Curve 2
Track Width (m)	2.0	2.0
Maximum roll angle of the trailer (degree)	20	11
Lateral shift of the centre of gravity of the trailer (m)	0.44	0.24
Height of Centre of Gravity of Truck (m)	2.0	2.0
Roll Centre Height (m)	0.78	0.78
Maximum Superelevation	0.07	0.08
Rollover Threshold (g's)	0.473	0.539

During the testing, there were individual lateral force events that actually resulted in the rollover threshold being exceeded. The results for day 4, run 3 (D4R3) are shown in Figure 5. The plot of peak accelerations shows two events that exceeded the calculated rollover threshold (with lateral accelerations of 0.582 g's and 0.492 g's compared to the rollover threshold of 0.473g's). These events were spikes in the lateral accelerations and may have been caused by a strong gust of wind or other external road factors. Baker and Reynolds (9) estimated that in order for rollover to occur, the rollover threshold must be exceeded for more than 0.5 seconds (10). The duration of these peaks were short enough (<0.2 seconds) that the vehicle did not enter a roll condition before the vehicle experienced forces below the roll threshold. However, the results show that wind gusts of a longer duration could have caused the vehicle to roll.

CONCLUSIONS

This research investigated the impact that wind has on heavy truck rollover. It was found that wind does compound the lateral forces experienced by a truck, even when the wind speed is not extreme. The additional lateral forces results in net changes to effective lateral accelerations thereby compromising roll stability of the unit.

The maximum wind speed observed during these tests was approximately 28 kph, which was not perceptible to the driver. In strong winds, when a driver can feel the wind blowing against the truck, the lateral forces would be expected to be much higher. By investigating how a seemingly imperceptible wind increase can increase the lateral forces experienced by a truck, design guidelines and speed signing can be adjusted to improve the safety of vehicles operating on highway curves and ramps. This research confirmed that the procedures developed in this project, using an improved data acquisition system, could be adopted to evaluate wind forces on heavy trucks. The tests developed as part of this research could be used to recommend speed advisories on interchange ramps and other curves on a highway system.

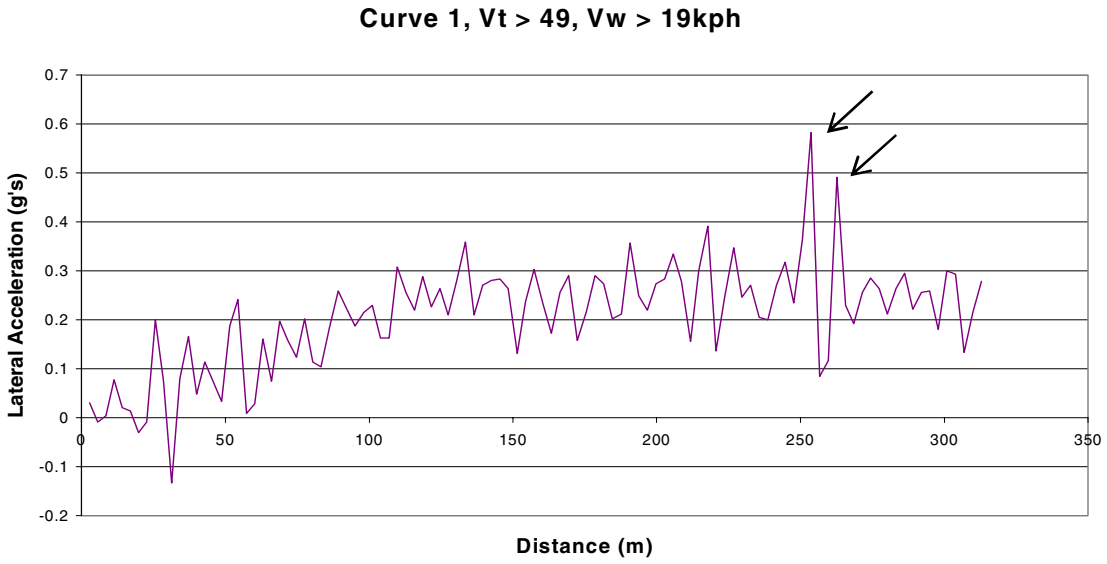

Figure 5. Lateral Accelerations for Test on Day 4, Run 3.

RECOMMENDATIONS

From the research it was found that similar methods could be utilized to further the understanding of the impact of wind forces on truck rollover. Lateral accelerations could be measured on trucks in other high-risk areas, such as Prince Edward Island's Confederation Bridge, using a data acquisition system similar to the one developed in this study. The impact of wind speeds could then be determined by combining the results of the dynamic characteristics of the truck with wind data from weather stations. Results such as those presented in Table 2 and Figures 2 and 3, would assist operators in better managing traffic in these high-risk areas. If further testing of this type is considered, it is recommended that the data acquisition system on the truck be improved by adding:

- A GPS unit to log the truck position, speed and direction.
- An on-board anemometer to measure wind speed and direction.
- Pressure sensors to measure the wind force on the sides of the truck.

ACKNOWLEDGEMENTS

The authors would like to acknowledge the contributions made to this project by the National Science and Engineering Research Council of Canada, GW Driver Training School and technicians of the University of New Brunswick, Department of Civil Engineering. Without their support, this research would not have been possible.

REFERENCES

1. U.S. Department of Transportation. *Traffic Safety Facts* 2000*; Large Trucks.* Publication DOT HS 809 325.NHTSA, U.S. Department of Transportation, 2000.

2. Transport Canada. *Canadian Motor Vehicle Traffic and Collision Statistics*; 2001. Publication ISBN 0-662-67110-4. Transport Canada, 2003.

3. Wang, J and Council, FM. Estimating truck-rollover crashes on ramps by using a multistate database. *Truck Safety Research*; Journal of the *Transportation Research Board, No. 1686,* TRB, National Research Council, Washington, D.C., Dec. 1997, pp. 39-45.

4. Hildebrand, Eric D. and Wilson, Frank R. The Development and Intermediate Findings of a Level III Heavy Truck Collision Study. In *Transportation Research Board,* No. 1595, TRB, National Research Council, Washington, D.C., Dec. 1997, pp. 39-45.

5. Perara, H.S., Ross, H.E. Jr., Humes, G.T. Methodology for estimating safe operating speeds for heavy trucks and combination vehicles on interchange ramps. In *Transportation Management, HOV Systems, and Geometric Design Effects. No. 1280,* TRB, National Research Council, Washington, D.C., 1990, pp. 208-215.

6. Bedard, Jean T. *Vehicle Rollover Threshold Evaluation: An Assessment of Computer Simulation Models. Vehicle Weights and Dimensions Study.* Roads and Transportation Association of Canada. Vol. 12, 1986.

7. Wong, J. Y. and El-Gindy, M. *A Comparison of Various Computer Simulation Models for Predicting the Lateral Dynamic Behaviour of Articulated Vehicles. Vehicle Weights and Dimension Study.* Vol. 16. Roads and Transportation Association of Canada.

8. Figueredo, Garcia, L. Analysis of the Dynamic Response of Heavy Trucks on Highway Curves Under Actual Operating Conditions. *Thesis submitted for a degree of Doctor of Philosophy in Engineering, University of New Brunswick.* 374pp, 2001.

9. Baker, CJ, and Reynolds, S. Wind-induced accidents of road vehicles. *Accident Analysis & Prevention.* Vol. 24 No. 6, 1992, pp. 559-575.

10. Baker, CJ. High sided articulated road vehicles in strong cross winds. *Journal of Wind Engineering and Industrial Aerodynamics.* Vol. 31, 1988 pp. 67-85.

LIGHT VEHICLE ESC PERFORMANCE TEST DEVELOPMENT

Garrick J. Forkenbrock
Patrick L. Boyd
NHTSA
United States
Paper Number 07-0456

ABSTRACT

On September 18, 2006 the National Highway Traffic Safety Administration (NHTSA) announced a proposal that would require installation of electronic stability control (ESC) as standard equipment on all light vehicles by model year 2012 [1]. The decision to mandate ESC required that NHTSA develop an ESC compliance test and evaluation criteria. This paper describes the proposed test maneuver and discusses the methods proposed to interpret the data generated by that maneuver.

NHTSA's ESC proposed compliance test maneuver, the Sine with Dwell, was used to produce all the data described in this paper. This maneuver is based on a single cycle, 0.7 Hz steering input, with a 500 ms pause between the third and fourth quarter cycles. Output from Sine with Dwell tests is used to evaluate both the lateral stability and responsiveness of ESC-equipped light vehicles.

NHTSA proposes acceptable lateral stability be assessed with two performance criteria, intended to encourage yaw rate to decay in a controlled manner. These criteria compare the yaw rates measured 1.0 and 1.75 seconds after completion of the maneuver's steering inputs to the first local yaw rate peak produced after the second steering reversal. These "yaw rate ratios" must be less than or equal to 35 and 20 percent, respectively.

To ensure that a balance between lateral stability and the ability of the vehicle to effectively respond to the driver's inputs is maintained, NHTSA has proposed a responsiveness metric supplement that used to assess lateral stability. The proposed metric is based on vehicle lateral displacement calculated 1.07 seconds after initiation of the maneuver's steering inputs.

INTRODUCTION

As part of a comprehensive plan for reducing the serious risk of rollover crashes and the risk of death and serious injury in those crashes, NHTSA has proposed a new Federal motor vehicle safety standard (FMVSS). FMVSS No. 126, Electronic Stability Control Systems, would require ESC systems on passenger cars, multipurpose passenger vehicles, trucks and buses with a gross vehicle weight rating of 4,536 Kg (10,000 pounds) or less [1].

Preventing single-vehicle loss-of-control crashes is the most effective way to reduce deaths resulting from rollover crashes. This is because most loss-of-control crashes culminate in the vehicle leaving the roadway, which dramatically increases the probability of a rollover. Based on the best available data drawn from crash data studies, NHTSA estimates that the installation of ESC will reduce single-vehicle crashes of passenger cars by 34 percent and single vehicle crashes of sport utility vehicles (SUVs) by 59 percent, with a much greater reduction of rollover crashes. NHTSA estimates that ESC has the potential to prevent 71 percent of the passenger car rollovers and 84 percent of the SUV rollovers that would otherwise occur in single-vehicle crashes.

NHTSA estimates ESC will save 5,300 to 9,600 lives and prevent 156,000 to 238,000 injuries in all types of crashes annually once all light vehicles on the road are so equipped. The Agency further anticipates that ESC could substantially reduce the more than 10,000 deaths each year on American roads resulting from rollover crashes (by 4,200 to 5,500).

Manufacturers equipped about 29 percent of model year (MY) 2006 light vehicles sold in the U.S. with ESC, and intend to increase the percentage to 71 percent by MY 2011. As proposed, FMVSS No. 126 requires installation of ESC in 100 percent of light vehicles by MY 2012 (with exceptions for some vehicles manufactured in stages or by small volume manufacturers).

SINE WITH DWELL TEST MANEUVER

All tests described in this paper were performed with a test maneuver known as the 0.7 Hz Sine with Dwell maneuver (referred to as simply the "Sine with

Dwell" for the remainder of this paper). Considerable effort was used to select this maneuver from a comprehensive group of twelve other candidates. However, for the sake of brevity this paper will only discuss details pertaining to the Sine with Dwell. A detailed discussion of the maneuver selection process is available in [2,3].

As the name implies, the Sine with Dwell maneuver is based on a sinusoidal steering input. Specifically, a single cycle input is performed at a frequency of 0.7 Hz, with a 500 ms pause between completion of the third quarter cycle and initiation of the fourth quarter cycle, as shown in Figure 1.

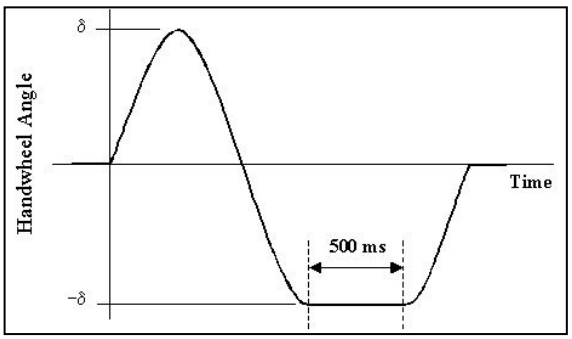

Figure 1. Sine with Dwell steering profile.

To begin the maneuver, the driver accelerates the vehicle to a speed of approximately 52 mph, at which point the throttle is released and a programmable steering controller is engaged. Once the vehicle has coasted down to a speed of 50 mph, the steering machine automatically executes the steering wheel angle profile previously shown in Figure 1.

Since the maneuver entrance speed is always 50 mph, increasing the magnitude of the steering wheel angles is used to increase maneuver severity. This is accomplished by multiplying the steering wheel angle capable of producing a lateral acceleration of 0.3g during Slowly Increasing Steer testing ($\delta_{0.3g}$) by a series of scalars [4]. The steering wheel angles nominally begin at $1.5*\delta_{0.3g}$, and are increased in increments of $0.5*\delta_{0.3g}$ until a termination criterion has been satisfied. For the data discussed in this paper, four termination conditions were used:

- The final heading angle of the vehicle, measured four seconds after completion of the Sine with Dwell steering input, was 135 degrees or more.

- A steering wheel angle of $6.5*\delta_{0.3g}$ or 270 degrees is used (whichever was greater) without the final heading angle of the vehicle reaching 135 degrees.

- Simultaneous wheel lift of the inside front and rear tires ≥2.0 inches occurred during any test.

- Rim-to-pavement contact and/or tire debeading occurred during any test.

Note: these conditions differ slightly from those actually proposed for FMVSS No. 126 as they were used for maneuver development purposes.

Sine with Dwell tests are performed with left-right and right-left steering. To produce the data featured in this paper, tests were performed with ESC fully enabled, then fully disabled on the same tire set. Additionally, if a vehicle offered an additional driver-specified ESC setting, it was evaluated with a second tire set. The proposed FMVSS No. 126 would only require Sine with Dwell tests be performed with ESC fully enabled.

LATERAL STABILITY

NHTSA believes a vehicle equipped with an effective ESC system should not spinout during any Sine with Dwell test performed with the system fully enabled. Unfortunately, while the term "spinout" is easy for most people to visualize, it is a somewhat ambiguous description of an excessive oversteer event. Therefore, before a means of quantifying lateral stability could be identified (i.e., for use in a compliance test), an objective definition of what NHTSA means by "excessive oversteer" needed to be determined.

Note that ESC systems are designed to mitigate excessive over- *and* understeer. However, the Sine with Dwell maneuver and performance criteria described in this paper were specifically developed to facilitate the evaluation of excessive oversteer only. NHTSA is presently performing ESC understeer mitigation research; however results from these tests are not yet available.

Definition of an Excessive Oversteer Model

To quantify excessive oversteer, the output of a logistic regression model, based on the SAS Genmod procedure, was used. Specifically, this model describes how well the percent of the vehicle's second peak yaw rate (subsequently referred to as the

yaw rate ratio, or "YRR"), measured at different time intervals occurring after completion of the maneuver's steering inputs would predict the trial outcome, represented by a binary response variable. In the case of the excessive oversteer model, the binary variable was taken to be whether the heading angle of the vehicle, measured four seconds after completion of the maneuver's steering inputs, was greater than or equal to 90 degrees from the initial path; yes or no. Separate analyses were performed for fifteen different instants in time, beginning at the instant the maneuver's steering inputs were complete (t_0), and continuing in 250 ms increments from t_0 to t_0 + 4 seconds. These instants are referred to as the times after completion of steer, or COS.

Figure 2 summarizes the ability of a particular YRR and time after completion of steer (subsequently referred to as "YRR and COS combination" for brevity) to predict if the vehicle would be expected to satisfy NHTSA's definition of spinout. The color of each cell describes the confidence intervals associated with each YRR and COS combination.

A dark green cell indicates a model using that cell's particular YRR and COS combination is 95 percent confident the vehicle will not achieve a final heading angle greater than 90 degrees. For these cells, the Chi-Squared probability statistic is less than 0.05, and both confidence interval boundaries are lower than the 95th percentile confidence level (i.e., excessive oversteer is predicted less than 5 percent of the time).

The light green region indicates it is unlikely that the vehicle will exhibit excessive oversteer. For these cells, the Chi-Squared probability statistic is less than 0.05, but at least one of the confidence interval boundaries are outside of the 95th percentile confidence level.

The yellow cells represent regions of uncertainty, where the Chi-Squared probability statistic is greater than 0.05, and the confidence interval boundaries are both less than and greater than 50 percent. This implies the model cannot predict whether the vehicle will exhibit excessive oversteer or not.

The pink cells indicate if the vehicle will likely exhibit excessive oversteer. For these cells, the Chi-Squared probability statistic is less than 0.05, but at least one of the confidence interval boundaries are outside of the 95th percentile confidence level. From a statistics stand point, the pink regions are conceptually equivalent to the light green regions, however the physical meaning is different.

Finally, a red cell indicates a model using that cell's particular YRR and COS combination is 95 percent confident the vehicle will exhibit excessive oversteer. For these cells, the Chi-Squared probability statistic is less than 0.05, and both confidence interval boundaries are greater than the 95th percentile confidence level.

Application of Excessive Oversteer Model Output

The primary reason for developing a metric to evaluate lateral stability was to provide the Agency with a means of objectively ascertaining whether a vehicle's ESC is capable of mitigating excessive

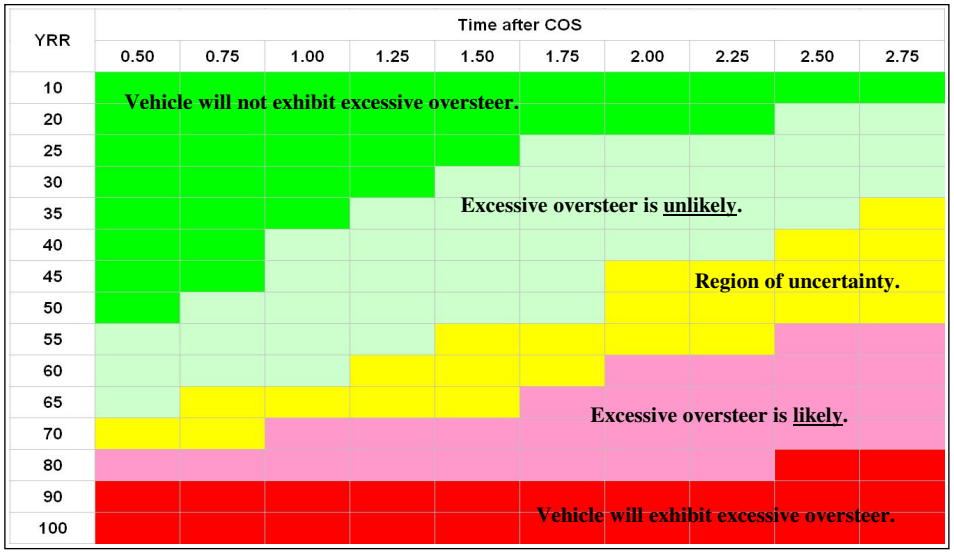

Figure 2. YRR confidence interval based spinout predictions.

oversteer. Therefore, the data contained in Figure 2 provided a valuable way to define lateral stability thresholds. Since the YRR and COS combinations shown in the dark green cells indicate the likelihood of a vehicle exhibiting excessive oversteer is less than five percent, and that the light green cells indicate the likelihood of exhibiting excessive oversteer is greater than five percent but less than 50 percent, NHTSA researchers decided the dark green YRR and COS combinations that define boundary between the dark and light green regions provided the best combination of prediction certainty and meaningfulness[1].

To assess how each YRR and COS combination defining the boundary between the dark and light green regions were able to define a minimum lateral stability threshold, data collected during evaluation of 24 diverse light vehicles were considered. The YRRs of each vehicle were calculated, and plotted as a function of time after completion of steer. Data from fully enabled and fully disabled ESC tests were used. Additionally, data collected during tests performed with two vehicles in partially disabled ESC modes were included.

Yaw Rate Ratio (YRR) Selection

Review of the data produced by the previously mentioned 24 vehicles showed considerable differences between the yaw rate responses of the vehicles evaluated with fully enabled and fully disabled ESC. The differences were particularly pronounced at 1.5 to 1.75 seconds after COS, where the yaw rates of the vehicles equipped with fully enabled ESC systems had decayed to approximately zero while those associated with the fully disabled tests remained quite high.

To identify which of these two times after COS provided the better discriminatory capability, additional data were considered. The larger data set, comprised of 62 light vehicles, ultimately revealed the time of 1.75 seconds after COS was able to most clearly distinguish the lateral stability of vehicles with ESC from those not so equipped (represented by the fully disabled ESC configuration).

[1] If a threshold based on a particular YRR and COS combination is too conservative, the ability of the lateral stability metric to define acceptable ESC performance is compromised. In such as case, even a vehicle with a poorly performing ESC may pass the minimum performance criterion.

Although use of the YYR at 1.75 seconds after COS possessed good discriminatory capability, NHTSA researchers believed that metric alone would do little to require a vehicle's yaw rate to decay in a controlled and predictable manner (since only one threshold would need to be satisfied and it occurred nearly 2 seconds after the maneuver had been completed). Therefore, a second YRR performance threshold was deemed necessary; one that occurred as soon after completion of steer as possible, but late enough to still provide good discrimination between vehicles with and without ESC. Based on consideration of all available test data, NHTSA ultimately decided a metric based on the YRR 1.0 seconds after COS would meet the two requirements and effectively augment the later value, as indicated in Figure 3.

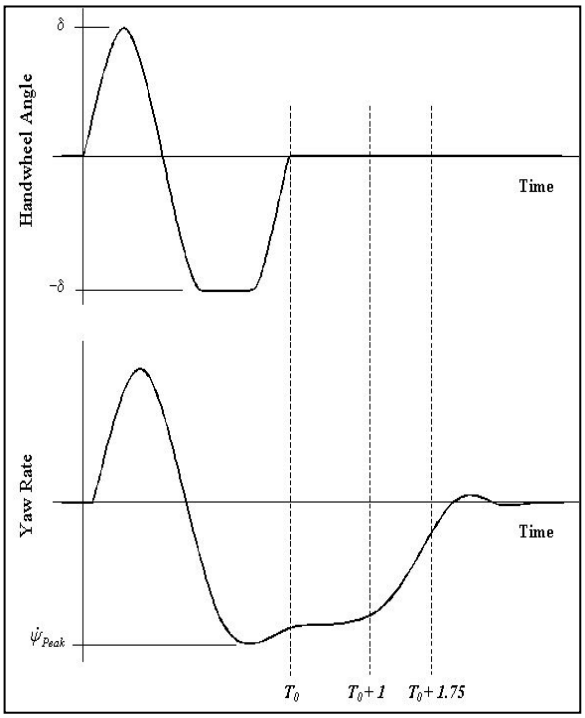

Figure 3. Steering wheel position and yaw rate information used to assess lateral stability.

Once the two time intervals after COS had been established, determination of the YRR performance thresholds associated with each time were required. To establish these criteria, NHTSA researchers used the output of the SAS model presented previously in Figure 2. At 1.0 seconds after COS, the model was 95 percent confident that light vehicles will not exhibit excessive oversteer if the YRR is 35 percent or less. At 1.75 seconds after COS, the model was 95 percent confident that light vehicles will not exhibit

excessive oversteer if the YRR is 20 percent or less. These thresholds define what NHTSA researchers believe the minimum levels of acceptable lateral stability for an ESC-equipped vehicle should be. A formal definition of the lateral stability performance criteria is provided below.

Criteria #1:

$$Percent\ \dot{\psi}_{Peak,COS=1.0\,sec} \leq 35\%$$

where,

$$Percent\ \dot{\psi}_{Peak,COS=1.0\,sec} = 100 * \left(\frac{\dot{\psi}(t_0 + 1.0)}{\dot{\psi}_{Peak}} \right)$$

Criteria #2:

$$Percent\ \dot{\psi}_{Peak,COS=1.75\,sec} \leq 20\%$$

where,

$$Percent\ \dot{\psi}_{Peak,COS=1.75\,sec} = 100 * \left(\frac{\dot{\psi}(t_0 + 1.75)}{\dot{\psi}_{Peak}} \right)$$

In both criterion,

$\dot{\psi}_{Peak}$ = first local yaw rate peak produced after the second steering reversal

$\dot{\psi}(t_0 + x)$ = yaw rate at x seconds after completion of a maneuver's dynamic steering inputs

Ability of Contemporary Vehicles to Satisfy the Proposed Lateral Stability Criteria

Figures 4 and 5 provide lateral stability results for the various YRR and COS combinations for a larger population of 62 vehicles, including very large pickups, and a stretched limousine (238.2 inch wheelbase). Left-right and right-left steering tests are shown, respectively. Test vehicles evaluated with fully enabled ESC are presented in green and fully disabled ESC tests are shown in red. The partially disabled ESC mode results for a 2005 BMW M3, 2006 BMW 525i, 2005 Chrysler 300C, 2005 Infiniti Q45, 2005 Nissan 350Z, 2005 Mercedes SLK350, and a 2006 Porsche Boxster are provided in yellow. Finally, results produced during BMW 525i tests performed with fully disabled active steering and fully disabled ESC are shown in blue.

Of the 58 *ESC-equipped* vehicles used to develop the lateral stability criteria discussed in the previous section, only the performance of a 2006 BMW 525i would be unable to satisfy both conditions when evaluated with ESC fully enabled.

RESPONSIVENESS

The data shown in Figures 4 and 5 clearly indicate ESC can offer tremendous improvements in lateral stability. However, NHTSA believes these benefits should not come at the expense of a vehicle not being able to sufficiently respond to the driver's steering inputs. An extreme example of this could potentially be having an ESC lock both front wheels as the driver begins an abrupt obstacle avoidance maneuver. Assuming the road is reasonably level, and the surface friction is uniform, it is very likely the wheel lock would suppress any tendency for the vehicle to spinout or rollover. However, having the wheels lock would also prevent the vehicle from responding to the driver's steering inputs. This would cause the vehicle to plow straight ahead and collide with the obstacle the driver was trying to avoid. Clearly, this is not a desirable compromise.

To ensure that a balance between lateral stability and the ability of the vehicle to effectively respond to the driver's inputs is maintained, NHTSA researchers believe a "responsiveness" metric must supplement the lateral stability criteria established by the Agency.

Responsiveness Metric Evaluation Criteria

NHTSA researchers considered a wide variety of metrics capable of quantifying responsiveness. Some were developed by NHTSA, others by vehicle dynamics experts outside of the Agency [5,6]. The candidate responsiveness metrics included methods based on the vehicle's ability to achieve lateral displacement, lateral acceleration, lateral velocity, and/or sideslip. Some metrics were comprised of a single evaluation criterion, while others incorporated multiple factors into a single composite metric. However, one commonality shared by each candidate was that they all used data produced during the same Sine with Dwell test series used to assess lateral stability. Also, since the later part of the maneuver is what excites the vehicle's tendency toward oversteer, each metric only used data produced by the first half cycle of the Sine with Dwell's steering inputs (i.e., the "obstacle avoidance" component of the maneuver).

When evaluating the various responsiveness metric candidates, NHTSA researchers considered the following factors: (1) face validity, (2) objectivity, and (3) ease of computation. In the context of

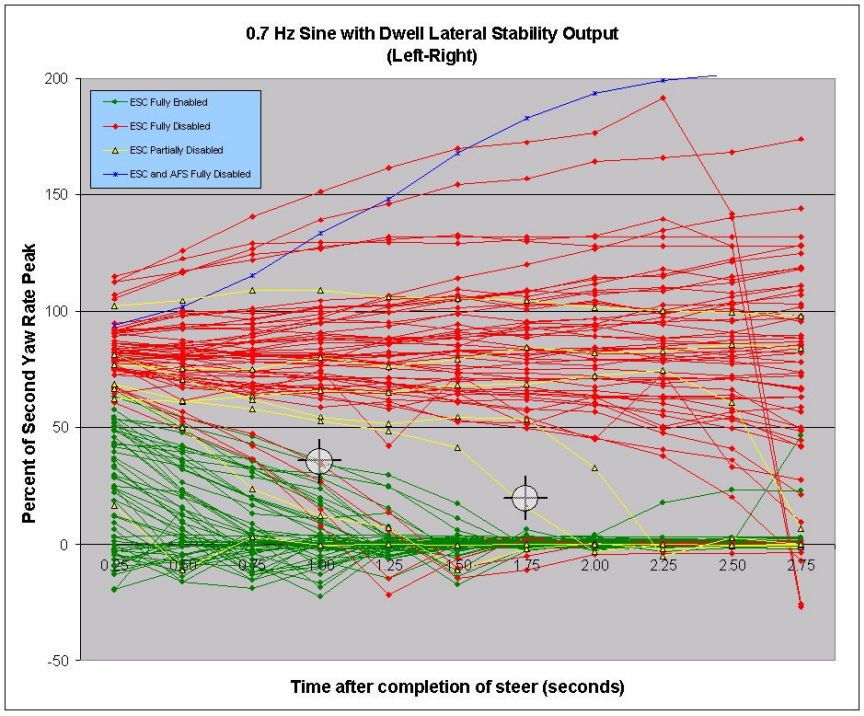

Figure 4. Yaw rate ratio plotted as a function of time after completion of steer for tests performed with left-right steering. NHTSA's proposed lateral stability thresholds are indicated by the two black crosshairs. Results from 62 vehicles are shown.

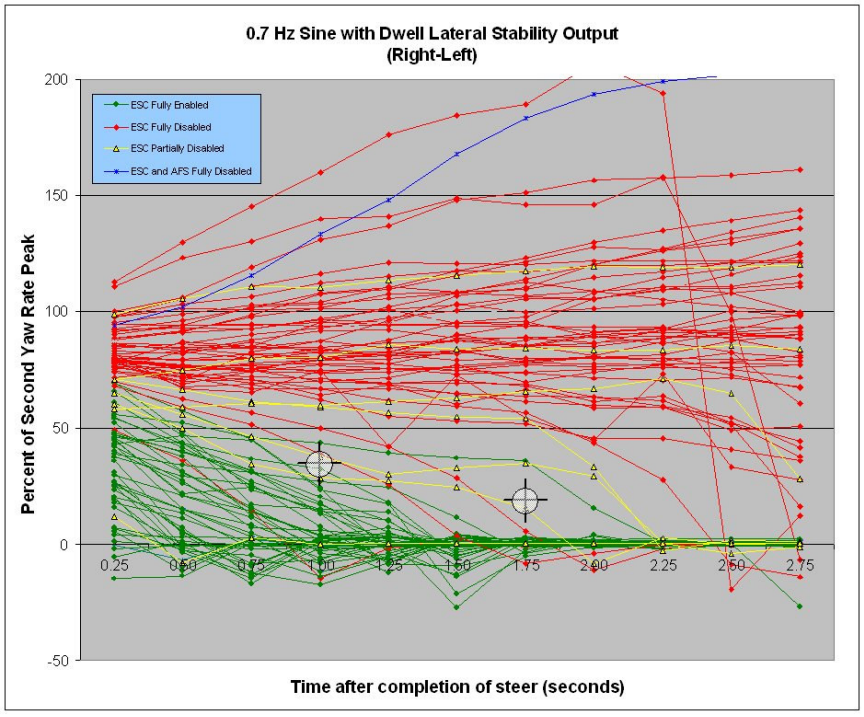

Figure 5. Yaw rate ratio plotted as a function of time after completion of steer for tests performed with right-left steering. NHTSA's proposed lateral stability thresholds are indicated by the two black crosshairs. Results from 62 vehicles are shown.

responsiveness, these factors may be defined as follows:

Face validity. This refers to the real world relevance of the metric. A responsiveness metric with high face validity relates well to situations encountered on public roadways. High face validity increases the ability of the Agency to explain the metric's meaning to the general public.

Objectivity. A good responsiveness metric should be able to consider the performance of all light vehicles equally. This is difficult given the diversity of the vehicles sold in the United States. The output of a robust responsiveness metric should allow NHTSA to directly compare the performance of all light vehicles with good discriminatory capability.

Ease of Computation. Although this attribute is of less importance than the other two, it is of practical significance to NHTSA and the automotive industry. A metric based on data that are difficult and/or time consuming to collect is generally less appealing than one requiring simple analytical techniques.

For sake of brevity, only those responsiveness metrics based on lateral displacement are discussed in this paper. Of the many responsiveness metrics considered, NHTSA believes those based on lateral displacement are the most appealing since they have the most obvious and direct relation to obstacle avoidance.

Multiple metrics based on lateral displacement were explored, differing only in when the measurement occurred in time. Specifically, metrics based on when overall maximum lateral displacement occurred, at 1.0 and 1.75 seconds after COS (i.e., the times used in the assessment of lateral stability), at the completion of the initial steer (i.e., the first quarter-cycle), and at completion of the second steer (i.e., the third quarter-cycle) were used. In the context of responsiveness, lateral displacement was defined as the perpendicular distance of the vehicle's center of gravity from a line defined by the vehicle's initial heading (i.e., before the test maneuver was initiated). If a maneuver was performed with left-right steering, lateral displacement to the driver's left was measured. If right-left steering was used, the lateral displacement to the driver's right was measured.

Maximum Lateral Displacement

While a responsiveness metric that simply considers the vehicle's maximum lateral displacement possesses high face validity, it was found to suffer from low discriminatory capability. There was significant variability in the longitudinal positions (measured from initiation of the steering wheel input) of the vehicles at the instant maximum lateral displacement was recorded. NHTSA researchers believe a vehicle that achieves its maximum lateral displacement with a short longitudinal displacement (i.e., earlier in time) should be deemed more responsive that a vehicle requiring a longer longitudinal distance. However, a responsiveness metric based on maximum lateral displacement would be unable to differentiate such vehicles.

The discriminatory capability of the maximum lateral displacement metric is a significant problem; however it is not the metric's only shortcoming. For some vehicles, such as the 2006 Mercedes ML350 evaluated during this research, maximum lateral displacement may be indeterminate. In some instances, the vehicle may effectively respond to the "avoidance" component of the maneuver's steering input, but not to the later "recovery" phase, a response often associated with the aggressive braking present during roll stability control (RSC) intervention. For some vehicles, RSC intervention remains engaged past the point in the maneuver where effective steering may occur. In these instances, the heading angle of the vehicle may not change much beyond that established with the initial steering input, causing lateral displacement to increase over time. By impeding the ability for the vehicle to respond to the recovery input, the responsiveness of the vehicle is clearly reduced. However, if maximum lateral displacement is used to quantify responsiveness, the vehicle would receive a very favorable assessment – the maximum lateral displacement is limited only to the duration of the sampling interval used for data collection.

Figure 6 helps to explain this phenomenon by presenting the lateral positions of two vehicles, a 2006 Mercedes ML350 and 2005 BMW M3, over time. Both tests were performed with ESC fully enabled using peak steering wheel angles of approximately 230 degrees. The BMW M3 achieved a maximum lateral displacement of 17.1 feet (5.2 m), 108 feet (32.9 m) after initiation of the maneuvers steering inputs. With the Mercedes ML350, a peak lateral displacement is never established. For this vehicle, lateral displacement continues to increase up to the point data collection is terminated, approximately 6 seconds after initiation of the maneuver's steering input.

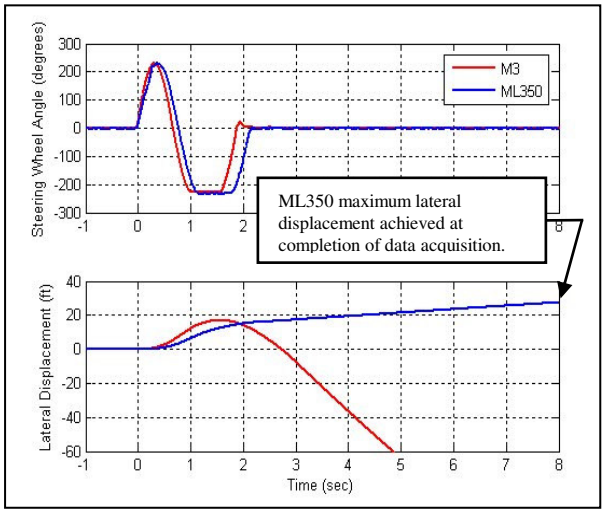

Figure 6. 2006 Mercedes ML350 and 2005 BMW M3 lateral displacements observed over time.

For the reasons discussed in this section, the contradictory, unrepresentative results produced from the maximum lateral displacement responsiveness metric were deemed unacceptable and alternative metrics were explored.

Lateral Displacement at 1.0 and 1.75 seconds after Completion of Steer

For each test, performed with every vehicle, maximum lateral displacement (when it could be accurately determined) was achieved before the 1.0 and 1.75 seconds after completion of steer data points. Since the intent of the responsiveness metric was to consider the vehicle's reaction to the avoidance component of the maneuver's steering input, but not to the later recovery phase, use of these times was deemed inappropriate. As such, the idea of assessing lateral displacement at 1.0 and 1.75 seconds after completion of steer was abandoned.

Lateral Displacement at Completion of the Initial Steer

A second attempt to use lateral displacement to define responsiveness used the lateral displacement measured at completion of the initial steering input. Unlike the previously described technique, where lateral displacements measured at 1.0 and 1.75 seconds after completion of steer were found to occur too late in the maneuver to quantify responsiveness, lateral displacement measured at completion of the initial steer proved to be too early.

Since all Sine with Dwell tests were performed with a commanded frequency of 0.7 Hz, completion of the initial steer occurs approximately 357 ms after initiation of the maneuver's steering inputs. Perusal of the test data indicated this interval is so short that the vehicles are not given sufficient time to generate significant lateral acceleration and, consequentially, lateral displacement. Due to the low magnitude of the responses, and the similarity among all vehicles considered, NHTSA researchers ultimately concluded the lateral displacements output with this analysis technique offer little practical insight into light vehicle responsiveness. For these reasons, the concept of measuring lateral displacement at completion of the first steering input was discarded.

Lateral Displacement at Completion of the Second Steer

Having defined instants in time that occurred both too early and too late to be used for the effective quantification of light vehicle responsiveness, NHTSA researchers surmised the instant the completion of the second steering input occurred would likely provide more useful lateral displacement data. During a September 7, 2005 briefing to NHTSA, the Alliance of Automobile Manufacturers announced their considerable and collective responsiveness research had lead them to the same conclusion, indicating that times much beyond completion of the second steering input may result in a metric with considerable disparity [6]. This is because the test data showed the overall maximum lateral displacements always occurred after completion of the second steering input, often during or slightly after the 500 ms pause that immediately followed its occurrence.

Theoretically, completion of the 0.7 Hz Sine with Dwell second steering input should always occur 1.07 seconds after initiation of the maneuver's first steering input. However, the inability of a vehicle's power steering system to keep the actual steering input in phase with the programmable steering machine's commanded input (a phenomenon known as power steering "pump catch") can affect when completion of the second steering input actually occurs. Regardless of whether it is the intention of the vehicle manufacturer or not, the inability of the power steering system to keep up with the demands of the Sine with Dwell maneuver is somewhat common, especially when large steering wheel angles and rates are used.

For this reason, consistently determining when the instant completion of the second steering occurs can be difficult. Not only can pump catch affect the

phasing of the actual versus commanded inputs, but many times the transition from completion of the second steering input to the Sine with Dwell's 500 ms pause is not crisp. Rather, the steering inputs in this region are smoothed as the steering machine attempts to overcome the increased torque demand imposed by pump catch. When considering the resulting data in post-processing, this can contribute to disparity in how and/or when completion of the second steering input is reported. Practically speaking, this makes the reporting of lateral displacement at the same instant in time, an attribute intended to consider the performance of all light vehicles fairly and objectively, impossible.

To avoid this complication, analyzing lateral displacement data a specific point in time (i.e., independent of actual steering wheel position) in the vicinity of the completion of the second steering input was recommended [6]. Since 1.07 seconds after initiation of the maneuver's first steering input represents the theoretical instant completion of the second steering input should occur, this time was suggested. NHTSA researchers believe this is a very reasonable approach, and lateral displacement at 1.07 seconds after initiation of the maneuver's first steering input provides an excellent way of quantifying light vehicle responsiveness. Figure 7 summarizes this analysis technique.

A Simplified Approach to Measuring Lateral Displacement

Use of the lateral displacement at 1.07 seconds after initiation of steer represents the best way to quantify light vehicle responsiveness known to NHTSA. To provide the data necessary for this metric, NHTSA has had to record vehicle position over time using GPS-based measurements. Once the raw data have been collected, they are corrected with a differential post-processing technique and carefully synchronized with the other test data (collected on a second in-vehicle computer). Although this method is capable of producing highly accurate vehicle position data, the acquisition and manipulation of these data are time consuming and expensive.

One practical way to avoid the burden imposed by the use of GPS to measure lateral displacement is to calculate it via double integration of lateral

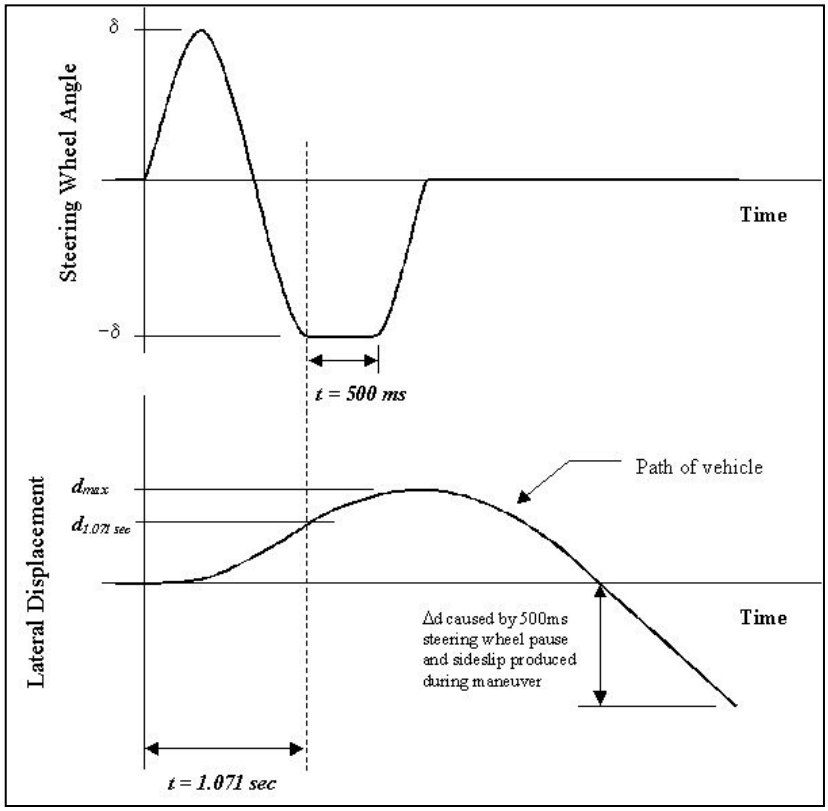

Figure 7. NHTSA's measure of light vehicle responsiveness. Steering wheel angle and lateral displacement data are used for this metric.

acceleration [6]. Although this process is not recommended as a general practice because small errors in zeroing, etc. can produce large errors in calculated displacement over time (see Figure 8), a responsiveness metric based on data 1.07 seconds after initiation of the maneuver's first steering input only requires lateral acceleration be integrated over a short time interval. Therefore, it was expected there would be good agreement between calculated and measured lateral displacements.

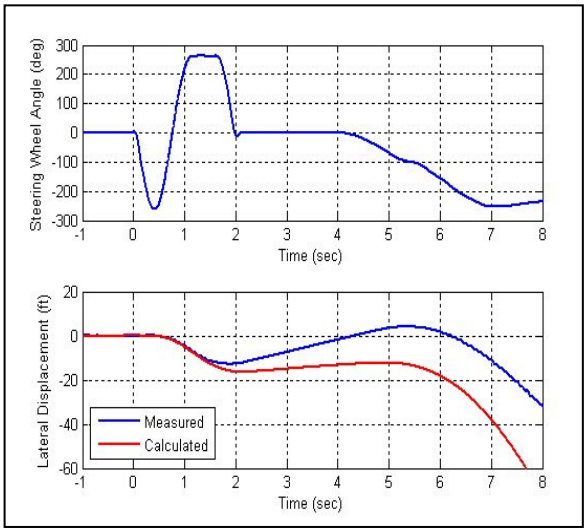

Figure 8. Comparison of measured and calculated lateral displacements over time.

After comparison of GPS-based lateral displacement measurements and those calculated via the careful double integration of lateral acceleration data, NHTSA researchers concluded: (1) measured and calculated lateral displacements are comparable 1.07 seconds after initiation of the maneuvers' steering inputs, and (2) use of a calculated lateral displacement 1.07 seconds after initiation of the maneuvers' steering inputs is an acceptable way by which it may be quantified. **Note:** Careful zeroing for offset and drift greatly improved the accuracy of calculated lateral position. For this reason, NHTSA researchers zeroed the lateral acceleration data before and after the first integration, and then again after the final integration.

Proposed Responsiveness Thresholds

Figure 9 shows the lateral displacements calculated from lateral acceleration data collected 1.07 seconds after initiation of the maneuvers' steering inputs. This figure presents the entire suite of data collected during evaluation of 62 light vehicles. All steering scalars and ESC configurations are represented, as are both directions of steer. Most passenger cars, wagons, minivans, and SUVs are shown in black. All pickups are shown in white. A series of left-right tests performed with a 2004 GMC Savana 3500 15-passenger van, when tested with ESC fully enabled, is shown in blue. The lateral displacements calculated for tests performed with a 2005 Jeep Grand Cherokee and 2005 Lincoln Town Car limousine are presented in red and green, respectively. In the case of the Jeep Grand Cherokee, the tests shown in red were performed with ESC fully enabled. The green Lincoln limousine tests were performed without ESC (the vehicle was not so-equipped).

The vehicles shown in Figure 9 were late-model production vehicles, comprised of model years 2002 to 2006, with a diverse range of handling characteristics. The results shown in this figure make good physical sense (e.g., sports cars such as the Porsche Boxster, BMW M3, and Mazda RX-8 are shown to be highly responsive, whereas sport utility vehicles with aggressive RSC systems, large heavy pickups, and the stretched limousine reside at the bottom of the responsiveness scale), and provide the foundation upon which NHTSA ultimately selected its responsiveness performance thresholds.

To ensure that the responsiveness of future vehicles is not degraded much beyond that present in the contemporary population, NHTSA researchers used the data shown in Figure 9 to establish the "Proposed Region of Noncompliance." The intent of this region was to ensure a minimum level of responsiveness is maintained throughout a range of steering wheel inputs attainable by actual drivers in severe obstacle avoidance situations.

As proposed, there are two criteria used to establish the boundaries of the Proposed Region of Noncompliance [7]. The vertical boundaries were used to define the range of steering wheel angles for which lateral displacement capability was to be assessed. The lower bound of this range was taken to be 180 degrees. This value was used since increases in steering wheel angle beyond this magnitude did not typically coincide with significantly more lateral displacement. The upper boundary of steering angle magnitudes was simply the overall maximum used without producing a termination condition for a given vehicle.

The horizontal boundary of the Proposed Region of Noncompliance was created to ensure light vehicle responsiveness was not degraded beyond what the

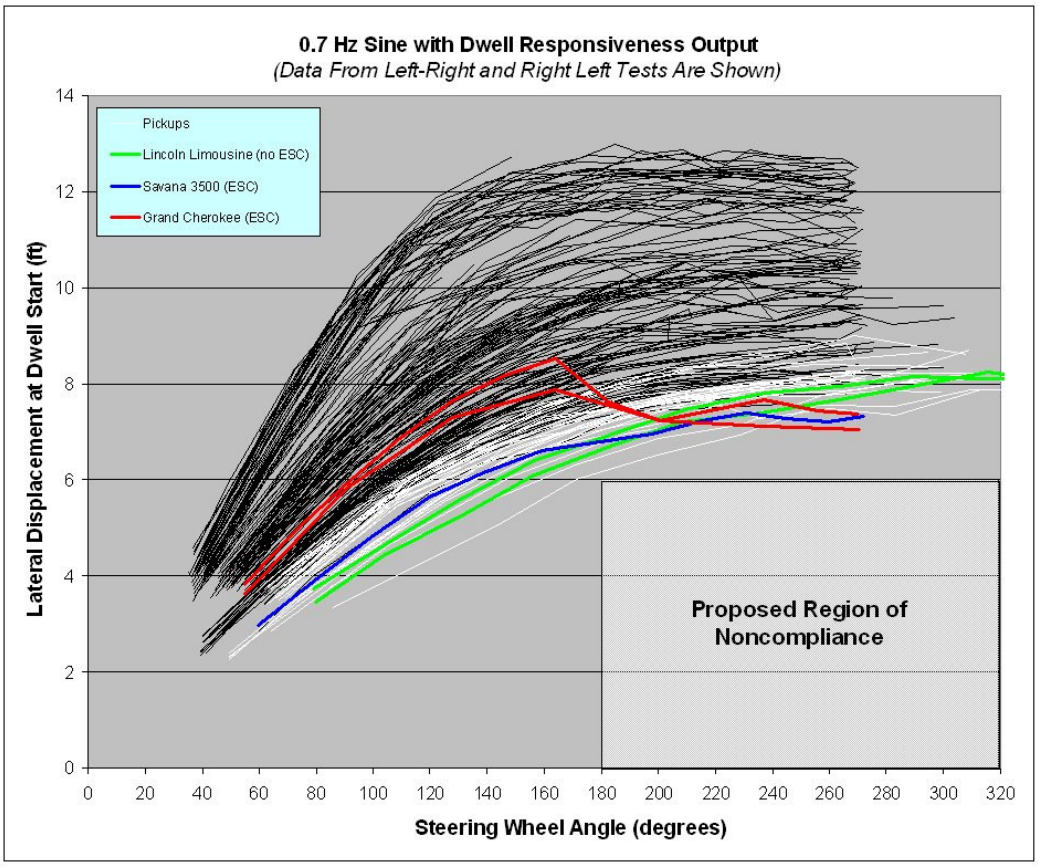

Figure 9. Lateral displacements produced during Sine with Dwell tests.

data presented in this paper have shown to exist for a vast majority of the contemporary light vehicle fleet. NHTSA's research has indicated a minimum lateral displacement of 6.0 feet, (1.83 m) measured 1.071 seconds after initiation of the maneuvers' steering inputs, is a reasonable threshold, as each of the 62 vehicles were able to satisfy this performance criteria, regardless of whether they were equipped with ESC.

CONCLUSIONS

NHTSA's decision to mandate ESC on all light vehicles is expected to have a tremendously positive impact on safety. To facilitate this mandate, development of test procedures and a series of minimum performance criteria to ensure acceptable ESC effectiveness were required. This paper has provided an overview how the performance criteria proposed for FMVSS No. 126 were developed.

NHTSA proposes the Sine with Dwell test maneuver be used to assess ESC compliance on the test track. This maneuver is based on a single-cycle, 0.7 Hz steering input, with a 500 ms pause between the third and fourth quarter cycles. Output from Sine with Dwell tests provides data used to evaluate lateral stability and responsiveness compliance of ESC-equipped light vehicles.

As proposed, acceptable lateral stability requires compliance with two performance criteria, intended to encourage yaw rate to decay in a controlled manner. This is accomplished by comparing the yaw rates measured 1.0 and 1.75 seconds after completion of the maneuver's steering inputs to the first local yaw rate peak produced after the second steering reversal. These "yaw rate ratios" must be less than or equal to 35 and 20 percent, respectively.

To ensure that a balance between lateral stability and the ability of the vehicle to effectively respond to the driver's inputs is maintained, a responsiveness metric supplements that used to assess lateral stability. As proposed, FMVSS No. 126 would require all light vehicles produce a lateral displacement of at least 6 feet (1.83 m), assessed 1.07 seconds after initiation of the maneuver's steering inputs

ACKNOWLEDGEMENTS

The authors of this report would like to express their appreciation for the tremendous efforts and insightful contributions of our colleagues within NHTSA; Devin Elsasser, Bryan O'Harra, Robert Jones, and Larry Jolliff from the Transportation Research Center; and members of the Alliance of Automobile Manufacturers' non-linear handling working group.

REFERENCES

[1] See Docket Number NHTSA 2006-25801

[2] Forkenbrock, Garrick J., Elsasser, Devin H., O'Harra, Bryan C., "NHTSA's Light Vehicle Handling and ESC Effectiveness Research Program," ESV Paper Number 05-0221, June 2005.

[3] Forkenbrock, Garrick J., Elsasser, Devin H., O'Harra, Bryan C., "Development of Electronic Stability Control (ESC) Performance Criteria," DOT HS 809 974, September 2006.

[4] Forkenbrock, G.J., O'Harra, B.C., Elsasser, D., "A Demonstration of the Dynamic Tests Developed for NHTSA's Light Vehicle Rollover Research Program – Phase VIII of NHTSA's Light Vehicle Rollover Research Program," NHTSA Technical Report, DOT HS 809 705, August 2004.

[5] See Docket Number NHTSA 2004-19951-17

[6] See Docket Number NHTSA 2004-19951-21

[7] See Docket Number NHTSA 2006-25801-1

LANE DEPARTURE WARNING SYSTEM RESEARCH AND TEST DEVELOPMENT

Frank S. Barickman
National Highway Traffic Safety Administration
Larry Smith
Robert Jones
Transportation Research Center, Inc.
United States of America
Paper number 07-0495

ABSTRACT

According to Traffic Safety Facts 2005 [1], single-vehicle crashes resulted in over 58% of all vehicular fatalities on the nation's roadways during that year. Of these fatal crashes, almost 15,000 occurred either off of the roadway or on the shoulder. The National Highway Traffic Safety Administration has recognized that technologies such as electronic stability control and other emerging safety technologies can potentially reduce a great number of these fatal crashes.

One emerging technology that the National Highway Traffic Safety Administration believes may have great potential to save lives is lane departure warning. These systems assist the driver by providing a warning (passive or active) that their vehicle is about to depart the road lane. The actual number of lives saved would depend upon the effectiveness of the lane departure warning system.

This paper will discuss both the past and present research that has been conducted by the National Highway Traffic Safety Administration. It will give a general overview of the performance and potential safety benefits of the technology. Information on the type of sensors and performance testing to evaluate lane departure warning systems will be presented, including examples of them. Data from past field operational tests and test track research documenting system performance will be shown.

INTRODUCTION

The National Highway Traffic Safety Administration (NHTSA) has long recognized that single-vehicle road departure (SVRD) crashes lead to more fatalities than any other crash type [2]. Lane departure warning (LDW) was a key technology identified at the start of the Intelligent Vehicle Highway System (IVHS) program that could potentially reduce the number of fatalities and injuries associated with SVRD [3]. Based on 1991 General Estimate System and Fatal Accident Recording System data, Wang and Knipling reported that SVRD crashes accounted for almost 1.3 million of the 6.11 million police reported crashes and about 37.4% of all fatal vehicle crashes [2].

Since that time, NHTSA has continued to study the SVRD problem to increase the understanding of the crash problem and to help foster the development of this crash avoidance technology. In the mid and late 1990s, NHTSA developed performance guidelines to eliminate and mitigate road departure crashes [4]. This work ultimately specified performance guidelines for both a LDW system and a curve speed warning (CSW) system. Pomerleau also estimated that approximately 10% of all passenger vehicle road departure crashes can be prevented with LDW technology [4].

In a more recent effort as part of the Intelligent Vehicle Initiative program, NHTSA completed a road departure crash warning system (RDCWS) field operational test (FOT). The RDCWS FOT studied both a lateral drift warning system and a CSW system in an operational test environment. The study observed 78 subjects' driving behavior for 1 month: 1 week baseline without the RDCWS enabled and 3 weeks with the RDCWS enabled. The study found that the LDW function had three major influences on the subjects [5]:

- Turn signal usage per mile driven increased by 9%. (Note, that the system suppressed warnings when the turn signal was activated.)
- The standard deviation of lane position was decreased significantly.
- Vehicles returned to the lane of travel quicker after being issued an imminent alert as compared to lane excursions during the baseline week.

As part of the FOT, the Volpe Center served as the independent evaluator for the project. In a presentation about the preliminary RDCWS findings [6], it was reported that the RDCWS with full deployment and availability could result in 34,000 to 82,000 fewer lane departure crashes.

Crash statistics show that over time, SVRD crashes have remained the largest category of crashes that result in fatalities. From the crash problem description described by Wang and Knipling in 1994, a similar problem remains today as documented by Traffic Safety Facts 2005 (approximately 40%). Data from the FOT demonstrates that this technology has the potential to reduce SVRD crashes.

PERFORMANCE TEST EVALUATION

LDW can be effective in preventing lane departure crashes because the technology can prevent the vehicle from departing the lane by either warning the driver or actively controlling the vehicle. Similarly, ESC is effective in preventing lane departure crashes because the technology can either limit a vehicle's tendency to oversteer, thus preventing it from spinning out of control or mitigate excessive understeer, thereby preventing a vehicle from "plowing" off the road in a sharp curve. Whereas ESC systems assist drivers who do too much steering in a lane departure event, LDW systems assist drivers that do not steer by alerting them. These systems function at opposite ends of the crash spectrum.

LDW systems have recently been introduced as original equipment on late model vehicles in Japan, Europe, and North America. Unfortunately, it is still too early to support any traditional benefit analysis (crashes before technology vs. crashes after technology) due to low market penetration. However, many have been trying to understand if benefits can be estimated through performance tests and objective test development.

In an effort to understand how LDW systems can potentially reduce SVRD crashes, NHTSA has been studying current LDW technology. For an LDW system to reduce crashes, it must operate at a certain level of performance under varying conditions. The purpose of this testing was to identify what objective test procedures could be used to measure the performance of LDW technology.

Exisiting Objective Performance Tests

During recent years, NHTSA researchers and others have been developing performance tests, specifications, and operational requirements for LDW technology. In some cases, these procedures and/or guidelines have been developed for specific programs such as the RDCWS FOT, but in general many of the concepts they test or specify are very similar. The following list of performance tests was reviewed:

1. Recommendations for Objective Test Procedures for Road Departure Crash Warning Systems [7]
2. ISO/CD17361 Lane Departure Warning Systems [8]
3. Development of Test Scenarios for Off-Roadway Crash Countermeasures Based on Crash Statistics [9]
4. Run-Off-Road Collision Avoidance Using IVHS Countermeasures [4]
5. Concept of Operations and Voluntary Operational Requirements for LDWS On-board Commercial Motor Vehicles [10]

Items 1 and 2 in the above list specify detailed test procedures on how LDW performance testing can be conducted. A variety of test scenarios, conditions, and detailed procedures are defined. Item 3 recommends a series of more abstract tests that can be performed to assess LDW performance based on developing tests from statistical crash data. Najm suggests that 96.3% of all road departure crashes stem from just six conflict scenarios [9]. Items 4 and 5 do not necessarily define performance tests, but provide performance specifications and operational requirements that should be met by an LDW system.

A detailed summary comparing and contrasting the above listed efforts is beyond the scope of this paper, but there are many common concepts that are recommended to be tested. They all indicate that an LDW system should be able to function using different roadway delineations. These include both solid and dashed lines, yellow and white lines, and raised pavement markings. They all recommend (or suggest demonstrating via a test) that LDW warnings should be issued for straight roads (>1000m radius of curvature) and curves (various radius of curvature 50m to 1000m) within some time frame (or distance) of the lane marking at a variety of road departure rates. The lateral departure rates vary from 0.1 to 0.8 m/s. Some of the other common concepts include a minimum operational speed (and/or test-specific speeds), tests to determine if the warning is suppressed by turn signal usage, and environment conditions for the tests.

Test Vehicle and Measures

For this testing, a passenger car was instrumented for data collection. The test vehicle was purchased with original equipment (OE) lane departure warning system (LDW) that provided an audible and visual warning when the vehicle departs the lane. Also included on the platform were an aftermarket (AM) LDW and a low-cost lane position measuring system (LPMS) [11].

Both the OE and AM LDW systems use a forward looking video camera. Both systems issue auditory and visual warnings to the driver to indicate lane departure. For this study, a detailed analysis of the user interface was not appropriate. The output signals were used as a means to indicate lane departure electronically. The primary measures that were collected are defined in Table 1.

Raw measurement data were not available from the OE LDW sensor. Derived measures such as warning time onset and lane line crossing had to be determined by fusing the OE LDW departure flag (i.e. data channel marker) with other data. To compute warning time measures, time synchronized video data were manually compared to the onset of the departure flag from the OE LDW. Other metrics for the OE LDW were calculated by comparing the data from the other two sensors and/or the event button and monitoring the output response of the OE LDW system. Unfortunately, the ability to determine if the LDW is tracking the roadway line (availability) cannot be completely assessed this way, but positive warning rates can be calculated (i.e. if we know a lane line boundary was crossed, did the OE LDW warn or not?).

Derived performance measures for the AM LDW were calculated using the lateral position and lane width channels as measured from the sensor. Lane departures and warning times were calculated by comparing the lane bust measure to the AM LDW warning flag. Data from the point of interest (POI) button and other sensors were also compared to ensure that a lane bust actually occurred. For consistency, warning times were also compared manually to the video data. Availability was measured by monitoring the lane position confidence channel.

TABLE 1.
Primary measures collected by the onboard data acquisitions for testing.

System	Measure Description	Units	Sample Rate
OE LDW	Departure Flag	On/Off	30 Hz
AM LDW	Lateral Position	Meters	5 Hz
AM LDW	Lane Width	Meters	5 Hz
AM LDW	Lateral Velocity	M/sec	5 Hz
AM LDW	Line Type	Solid / Dashed / Unknown / None	5 Hz
AM LDW	Lateral Position Confidence	Percent	5 Hz
AM LDW	Warning Flag	On/Off	5 Hz
LPMS Left	Lateral Dist to Left Line	Meters	30 Hz
LPMS Right	Lateral Dist to Right Line	Meters	30 Hz
GPS Position	High Accuracy Position	Northings and Eastings	10 Hz
POI Button	Point of Interest (Experimenter Flag)	On/Off	30 Hz
Video Left	Left Down Looking Video	N/A	30 Hz
Video Right	Right Down Looking Video	N/A	30 Hz
Video Fwd	Forward Looking Video	N/A	30 Hz

Test Track Testing

Performance testing for each system was conducted at the Transportation Research Center, Inc. (TRC) in East Liberty, OH. Tests were conducted to assess how the systems generated warnings on both straight road segments and curves.

The first test was conducted on the straight section of the Winding Road Course (WRC) at the TRC. This test is very similar to the ISO repeatability test and the NIST lateral drift on a straight road test. The purpose of the test is to assess when warnings are given with respect to departing the lane and how repeatably the warnings are issued. To conduct the

test, cones mark two different approach angles leading up to a lane line. Using GPS measurements, results are recorded by comparing the vehicle position at the time of the warning to the position of the painted road marking.

A rectangular course was marked 188m long by 3.6m wide, with one long edge of the rectangle being a solid painted line as can be seen in Figure 1. Cones were placed on the solid line at the entry, 54m, and 188m from the entry point. An additional cone was placed 3.6m from the painted line to denote the width of the course. The driver was responsible for aligning the cone 3.6 m out from the painted line with one of the cones at 54m and 188m, depending on desired approach rates. Two calculated angles were used to achieve the two approach rates of 0.3 m/s and 0.8 m/s at the controlled vehicle forward speed of 74 KPH. The exact distance from the painted line to the vehicle at the time the LDWS alarm sounded was determined from GPS data.

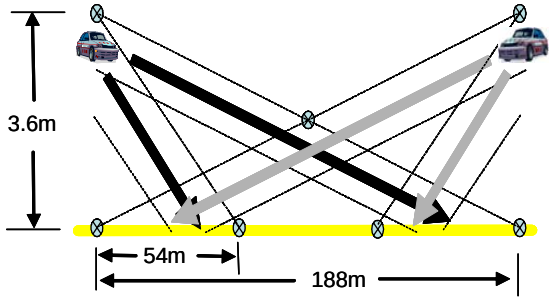

Figure 1. Layout of the straight lateral drift warning scenario (not to scale).

The purpose of the second test was to determine the timeliness and repeatability of the warning during a slow drift while in a curve. A figure displaying the general test scenario is shown in Figure 2. This is similar to the ISO warning generation test and the NIST curved road lateral drift test. The ISO document prescribes that this test be performed in a curve of radius 500m ±50m. No such curve was found in any available test facilities. The warning generation test was attempted on a curve with a radius of 110m, the largest un-banked curve available on TRC property for this test.

The objective of this test was to achieve two different approach rates relative to the lane markings, in two different directions through the curve, and to depart the roadway on both the left and right side of the of lane. On a straight section of the roadway approaching the curve, the vehicle is accelerated to 74 KPH. While in the curve, lane changes are performed at an approximate lateral velocity of 0.3 m/sec and 0.8 m/sec. The exact distance from the painted line to the outside edge of the vehicle at the time the LDWS alarm sounded was determined from GPS data.

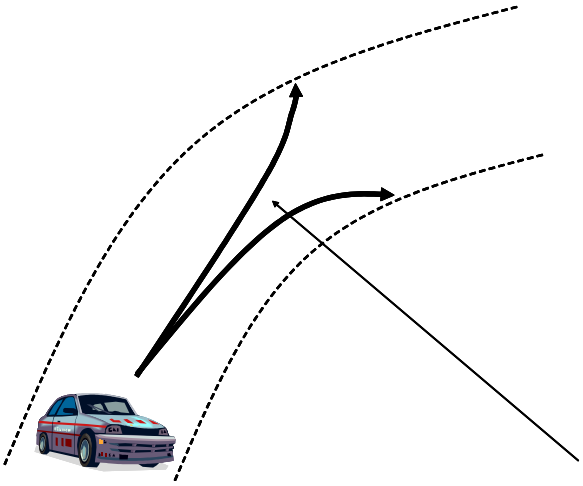

Figure 2. Layout of the curve lateral drift warning scenario.

In the ISO test document, a false alarm test is described. The false alarm test was conducted on the skid pad at the TRC. Straight lanes with painted lines approximately 2km long and 3.6m wide are available. The test was conducted with the car driven directly down the center of the lane. No lane crossings are performed. The objective of the test is to ensure that no false alarms are generated.

Performance Testing Results

The summary results from this testing can be seen in Table 2. Overall, both the OE LDW and the AM LDW systems were able to perform quite well in these tests.

One problem discovered during testing was that the AM LDW was not operating in a warning-enabled state during the lateral drift test in a curve. Although the sensor was functioning (i.e. lateral position was being output) through the curve, the warnings were suppressed because the initial approach did not have lane lines. If the AM LDW senses that there are no lane lines present for some period of time, the system enters a mode where warnings are suppressed. Once the system senses good quality lines for some time

period, it automatically enables itself and is able to present warnings to the driver. In the real world, this is done to prevent false alarms; however, from a test standpoint, this can be a problem when using a limited area.

TABLE 2.
Results of the performance testing conducted on the test track.

#	Description	OE LDW			
		Low Lateral Velocity		High Lateral Velocity	
		L	R	L	R
1	Straight Lateral Drift Warning	Pass	Pass	Pass	Pass
2	Curve Lateral Drift Warning	Pass	Pass	Pass	Pass
3	False Alarm Test	Pass			
#	Description	AM LDW			
		Low Lateral Velocity		High Lateral Velocity	
		L	R	L	R
1	Straight Lateral Drift Warning	Pass	Pass	Pass	Pass
2	Curve Lateral Drift Warning	N/A	N/A	N/A	N/A
3	False Alarm Test	Pass			

Both systems were able to correctly generate warnings during the straight lateral drift warning test. Warnings were issued within the given window specified by the ISO test procedure under both lateral drift rates. The alerts were issued within the 'on time' rating as calculated by the NIST test procedure. They were issued prior to the latest warning line and after crossing the earliest warning line determined by the lateral drift velocity. Finally, warnings were issued in a repeatable manner by both systems during all tests.

The OE LDW system was able to pass the curve lateral drift warning tests. Warning generation tests were within the window of the pass criteria set by the ISO test procedure. Warnings were issued prior to the latest warning line and after crossing the earliest warning line determined by the lateral drift velocity. Repeatability was a little more variable than the straight lateral drift tests. It is believed that the variability was caused by the test driver since it is difficult to create the lane departure scenario in the same manner on a curve (i.e., its harder to judge where you cross the lane boundaries on a curved section of road vs. crossing a lane line while driving straight.). Warnings were issued but were sometimes outside of the ISO set +/- 30cm zone for each test group.

Both systems were able to pass the ISO false alarm test. This test is very easy to implement and run, but it may be too simple to yield valuable data. Neither of the systems tested issued a false alarm (i.e., a warning from the LDWS without a lane departure or near-departure).

Functional Testing

Functional testing was performed to determine how the systems functioned under real-world road conditions. This testing is similar to what Najm describes as system robustness testing. The tests are performed on roads that are very similar to the types of roadways described in the crash statistics. Since the tests are conducted on public roadways, the external test conditions cannot be tightly controlled, but they do provide a reasonable amount of variability that may be experienced in the real world.

Functional testing was conducted on State roadways around the Marysville, Ohio area. The roads have a posted speed limit of 72-88kph, are non-freeway / two lanes, rural, and mostly straight with some curves. The road markings appear to be in good condition based on human visual perception. On the right hand side of the road, the edge is delineated by a constant white line. The left or center line of the roadway is delineated by yellow solid and/or dashed lines. The road can further be characterized by mentioning that the surroundings are mostly agricultural and sparsely populated with rural housing.

The test consisted of multiple drives over time. The testing took place over multiple days and is done at different times of the day. During each drive, the experimenter would regularly but randomly depart the roadway as many times as they could on both the left and right sides of the road. The experimenter would indicate a road departure by pressing the POI button every time the vehicle departed the lane. Data were recorded both manually and electronically, recording if the LDW system(s) issued a warning to the driver.

One of the important aspects of functional testing is to negate environmental conditions over time. To negate environmental conditions, tests using the same roadways were conducted over multiple days, times, weather, and lighting conditions. Tests were also conducted using a "double-back" route, where the route return trip is the same route but in the opposite direction, thus having the sensor face 180 degrees from its initial trip. It is believed that the environmental effects are negated using this method because performance can be shown over a period of time verses any one instantaneous moment. The fact that weather, traffic, sunlight, etc. are constantly changing can be negated if performance is consistently poor or good over a given section of roadway.

Functional Testing Results

The results of the functional testing are displayed in Table 3. The results are for a total of 12 test drives. At first look when evaluating the overall performance of both systems, the results are comparable with both systems performing in the 80 – 85% range. One important note is that the systems both operationally perform differently. This is evident in the number of departure attempts. The OE LDW is capable of warning the driver constantly when speeds are over 70kph. The AM LDW is not capable of warning constantly. The AM LDW system suppresses warnings for 5 seconds after it issues a warning. This limits the overall number of departures that can be accomplished during the same segment. This operational difference also makes the AM LDW departure attempts a subset of the OE LDW departure attempts.

Looking at the individual segments, performance differences become more obvious. The OE LDW system performs above 95% of the time on every segment but one, which brings down its overall average. The AM LDW does not perform as high as the OE LDW but never performs lower than 63% (10% higher than the worst OW LDW performance).

The other interesting observation from the data is that the OE LDW's worst performing section is the AM LDW's best performing section. It is unclear as to why this phenomenon was observed. Again, all of these roadway segments had lane markings that looked average or better and they all looked visually very similar. Tests were also conducted using both systems at the same time. Since the AM LDW was able to perform quite well, it is hard to suggest that there is a particular problem with this segment.

TABLE 3.
Results of the functional testing conducted on public roadways.

Segment	Description	OE LDW		
		Depart	Warn	%
A	TRC Property	106	105	99.1%
B	TRC Gate to Raymond	501	476	95.0%
C	Raymond to SR 31	287	284	99.0%
D	SR 31 to SR 4	520	277	53.3%
E	SR 4 South of SR 347	449	431	96.0%
Totals		1863	1573	84.4%
Segment	**Description**	**AM LDW**		
		Depart	**Warn**	**%**
A	TRC Property	39	32	82.1%
B	TRC Gate to Raymond	441	369	83.7%
C	Raymond to SR 31	264	167	63.3%
D	SR 31 to SR 4	457	419	91.7%
E	SR 4 South of SR 347	381	286	75.1%
Totals		1582	1273	80.4%

DISCUSSION

Unfortunately, detailed data for the OE LDW were not available for this testing. Only the basic inputs (we departed a lane) and outputs (the LDW system warned) were known for testing. If other data such as lateral position within the lane, lane width, line marking type, and measurement confidence were known, a better understanding of why the OE LDW performed poorly during section "D" of the functional test might be known. Looking at the performance from the AM LDW was not helpful since it seemed to perform the best in this section.

Overall, looking at the performance of the AM LDW, the data generally suggest that the sensor sometimes had trouble tracking the roadway markings. This was indicated in the data as either low confidence or the absence of a lane boundary being sensed. This has been discussed by others as "availability".

Similar conclusions were found in the RDCW FOT where they identified that availability was, perhaps, the most important issue in LDW. They found that lane marking quality, camera obstructions, roadway contamination (water, glare, snow, salt, etc.), and ambient lighting conditions can impede the ability of the system to correctly track the lane.

CONCLUSIONS

Assessment of LDW systems is a challenge. There are many external influences that can cause problems and degrade the performance of the system. Although it may be important to characterize the functional characteristics of an LDW system, simply completing performance tests on a test track may not be enough to gain insight into the real-world effectiveness of an LDW system. From the results of this study, it is believed that existing objective test procedures do not adequately characterize real-world performance. Both the OE LDW and AM LDW systems performed quite well during the test track scenarios; however, both systems had various problems when tested on public roadways.

A functional performance test may provide better operational insight about the performance of an LDW system. Using this methodology, external influences can be minimized and real world performance can be measured. Since both systems essentially passed test track testing, it appears both systems are equal in performance. However, when comparing data from the functional test, it becomes obvious that the two systems perform quite differently.

The idea of a functional performance test is quite new, and there are many problems with the concept. One challenge is to make this test repeatable so that similar results can be obtained from any group of similar roadways. Another problem is that roadways are constantly changing over time. Even using the same roadways, the results may differ with the same system. A third challenge for this testing is developing pass/fail criteria for the test. Is it acceptable for an LDW system to perform above 90% and then have a section where it performs at only 50%? Or is it better to have a system that performs at above 80% under all conditions? To help understand these issues and answer these questions, additional testing needs to be completed.

REFERENCES

1. National Center for Statistics and Analysis. *Traffic Safety Facts 2005.* U.S. Department of Transportations, National Highway Traffic Safety Administration.

2. Wang, J., Knipling, R. R. *Single Vehicle Roadway Departure Crashes: Problem Size Assessment and Statistical Description.* DOT HS 808 113, March 1994.

3. Mironer, M., Hendricks, D. *Examination of Single Vehicle Roadway Departure Crashes and Potential IVHS Countermeasures.* DOT HS 808 144, August 1994.

4. Pomerleau, D., Jochem, T., Thorpe, C., Batavia, P., Pape, D., Hadden, J., McMillian, N., Brown, N., Everson, J., *Run-Off-Road Collision Avoidance Using IVHS Countermeasures.* DOT HS 809 170, December 1999.

5. LeBlanc, D., Sayer, J., Winkler, C., Ervin, R., Bogard, S., Devonshire, J. Mefford, M., Hagan, M., Bareket, Z., Goodsell, R., and Gordon, T. *Road Departure Crash Warning System Field Operational Test: Methodology and Results.* UMTRI 2006-9-1, June 2006.

6. Wilson, B. Road Departure Crash Warning System: Preliminary Results of the Independent Evalution. http://www.itsa.org/itsa/files/pdf/RDCW Volpe Evaluation.pdf. ITS America: Public Meeting on the Benefits of Advanced Crash Avoidance Systems. April 2006.

7. Szabo, S., Norcross, R., *Recommendations for Objective Test Procedures for Road Departure Crash Warning Systems.* NISTIR 7288, February 2000.

8. ISO Draft International Standard. *Intelligent Transport Systems – Lane Departure Warning Systems – Performance Requirements and Test Procedures.* Working Document N123.33. ISO/CD17361. Committee ISO/TC204/WG14. June 2003.

9. Najm, W., Koopermann, J. Boyle, L, and Smith, D. *Development of Test Scenarios for Off-Roadway Crash Countermeasures Based on Crash Statistics.* DOT HS 809 505, September 2002.

10. Houser, A., Pierowicz, J., Fuglewicz, D. *Concept of Operations and Voluntary Operational Requirements for Lane Departure Warning System*

(LDWS) On-board Commercial Motor Vehicles. FMCSA-MCRR-05-005. July 2005.

11. Barickman, F., Stoltzfus, D. *A Simple CCD Based Lane Tracking System.* Society of Automotive Engineers. 1999-01-1302. March 1999.

A REPEATABILITY EXAMINATION OF NHTSA'S PROPOSED FMVSS 126 ESC EVALUATION METHOD AND METRICS

Kenneth J. Boyd
Ford Motor Co., United States
John A. Carriere
General Motors Corp., United States
Gene R. Lukianov
DaimlerChrysler AG, United States

Paper Number 07-0501

ABSTRACT

NHTSA's proposed FMVSS 126 ESC evaluation method and performance requirements are repeatedly tested by three vehicle manufacturers and NHTSA using two vehicle configurations, five test sites (tracks) and three temperature ranges. The results are examined to determine the sources of variability. Conclusions are presented on the variation of observed results. The initial experiment was designed considering directional stability metrics. The scope of the study was later expanded to include the responsiveness metric.

INTRODUCTION

In June, 2005, NHTSA employed subjective evaluation techniques that identified two vehicle configurations representing "diminished ESC performance" that defined NHTSA's subjective threshold for acceptable vehicle directional stability performance. One configuration was slightly above this threshold (Threshold+) and the other was slightly below this threshold (Threshold-). These subjective assessments were later confirmed by NHTSA's investigation of stability using a statistical model [1]. Sine with Dwell tests [2] were conducted on these "diminished mode ESC" vehicle configurations as part of the Phase 2a research [1]. Note that these vehicle configurations in the variability study represent "diminished mode ESC performance". The baseline calibrations of these vehicles are shown in Figure 1 by the light blue-gray lines with the round event markers. It can be seen that the normalized yaw rate response of the baseline calibrations return to the desired zero state more quickly than response of the respective diminished mode calibrations indicating a significant improvement in directional stability.

A designed experiment was constructed that allowed the investigation of the vehicle directional stability metrics for sensitivity to track, sensitivity to temperature, and testing variability [3]. This involved repeated tests of the aforementioned threshold vehicle configurations at different test sites and within different temperature ranges. The performance results (test metrics) would be useful for examining the variability of metrics described in the FMVSS 126 NPRM [4] used to characterize vehicle directional stability performance near the threshold of acceptance.

Testing of the vehicle configurations was conducted between August, 2005 and March, 2006 in order to accommodate testing and shipping logistics and to allow for testing within the desired temperature ranges. Figure 1 provides a comparison of the normalized yaw rates (yaw rate divided by the second peak yaw rate) for the threshold vehicle configurations versus the entire population of vehicles measured. It can be seen that the threshold configurations form a "boundary" of the ESC ON and ESC OFF configurations.

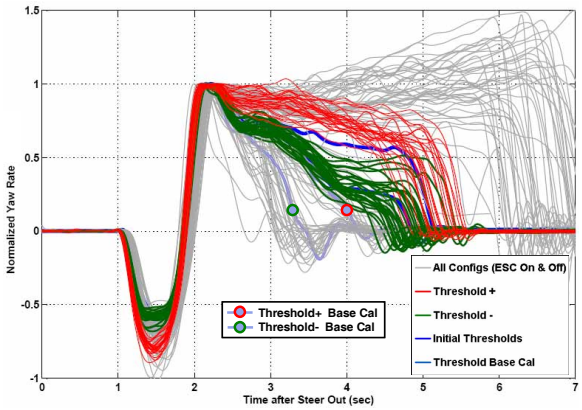

Figure 1. Rationale for configurations selected.

After completion of the aforementioned study, focus shifted to determining the variability for vehicle responsiveness metrics near the threshold for acceptable vehicle responsiveness. The best method to analyze the variation of responsiveness as it pertains to the proposed acceptance criteria is to measure a small number of vehicles whose

responsiveness performance is near the acceptance criteria at a number of different tracks and temperatures. As there was not time available to collect this data, the next best method is to examine the variability of responsiveness of the two configurations used in the stability variability study [5]. The Threshold+ configuration is one of the most responsive (approximately 98th percentile) of vehicles tested to date, while the Threshold- configuration represented the ~50th percentile for responsiveness.

Although the study included a number of directional stability and responsiveness metrics, the scope of this paper is limited to the metrics proposed by NHTSA in the FMVSS 126 NPRM.

DESCRIPTION OF EXPERIMENT

The experiment was designed to execute a test series on each of the two threshold vehicle configurations to determine the variability at five different test tracks. The tracks were chosen in different parts of the United States since tracks tend to be built using local materials. The tracks were located in Arizona, California, Michigan, Ohio, and South Carolina. Aerial photographs of each track are shown in the Appendix. The dates for testing at each location were chosen, based on historical data, to achieve ambient temperatures in the desired temperature range. The experiment was also designed to conduct a test series on the two vehicle configurations at the same test track to determine the effects of testing at three different temperature ranges: Cold (~30 deg F), Medium (~60 deg F), and Hot (~90 deg F).

A test series consisted of four repetitions of the Sine with Dwell maneuver and the associated Slowly Increasing Steer maneuver; once in the early morning and once in the afternoon of each day for two days. This protocol was designed to generate test data at the temperature extremes of each test day. New tires were installed on the vehicle before each Slowly Increasing Steer/Sine with Dwell test combination to minimize the effect of tire wear on the results.

The test matrix for track effect and for temperature effect can be seen in Tables 1 and 2 respectively. The **Threshold+** configuration was labeled **M32** and the **Threshold–** configuration was labeled **302**. These descriptors will be used interchangeably throughout this paper. Note that there were 56 Sine with Dwell tests conducted in total: 28 on the M32 configuration and 28 on the 302 configuration. The initial tests of the M32 and 302 configurations conducted by NHTSA in the spring, 2005 can also be included for comparison purposes. The same vehicles were used, although the tires used in the initial tests were not from the same lot purchased for the repeatability study.

Note that the track sensitivity study only included the Medium temperate range data. The temperature sensitivity study for each vehicle configuration included the data from a single track at which the vehicle was tested at all three temperature ranges (MI for the 302 configuration, and OH for the M32 configuration).

Table 1.
Track Effect Test Matrix

Test Series	Config.	Test Track	Temp.	Tester	Temp or Track Effect
1	302	MI	Hot	GM	Temp
2	M32	OH	Hot	NHTSA	Temp
5	302	OH	Med.	NHTSA	Track
6	M32	MI	Med.	GM	Track
3	302	MI	Med.	GM	Temp / Track
4	M32	OH	Med.	NHTSA	Temp / Track
7	302	SC	Med.	NHTSA	Track
8	M32	SC	Med.	NHTSA	Track
9	302	CA	Med.	Ford	Track
10	M32	CA	Med.	Ford	Track
11	302	AZ	Med.	DCX	Track
12	M32	AZ	Med.	DCX	Track
13	302	MI	Cold	GM	Temp
14	M32	OH	Cold	NHTSA	Temp

Table 2.
Temperature Effect Test Matrix

Test Series	Config.	Test Track	Temp.	Tester	Temp or Track Effect
1	302	MI	Hot	GM	Temp
2	M32	OH	Hot	NHTSA	Temp
5	302	OH	Med.	NHTSA	Track
6	M32	MI	Med.	GM	Track
3	302	MI	Med.	GM	Temp / Track
4	M32	OH	Med.	NHTSA	Temp / Track
7	302	SC	Med.	NHTSA	Track
8	M32	SC	Med.	NHTSA	Track
9	302	CA	Med.	Ford	Track
10	M32	CA	Med.	Ford	Track
11	302	AZ	Med.	DCX	Track
12	M32	AZ	Med.	DCX	Track
13	302	MI	Cold	GM	Temp
14	M32	OH	Cold	NHTSA	Temp

Assumptions

A number of assumptions were made in order to conduct the experiment and interpret the results:

- The two test vehicles are not changing during the experiment
- The variation in instrumentation and measurement systems (between the three manufacturers & NHTSA) is small compared to the variation in a test vehicle configuration

As the scope of the project expanded to determine the variability of the responsiveness metric, further assumptions were necessary:

- The variability in responsiveness of vehicle configurations well above the responsiveness performance requirement is similar to the variability of vehicles configurations near the responsiveness performance requirement when considering the following components of variability:
  - Track sensitivity
  - Temperature sensitivity
  - Run-to-run variability
- The diminished ESC modes of these vehicle configurations have no significant effect on the variability of responsiveness

Factors Not Controlled In This Experiment - It should be noted that brake temperatures and ESC algorithm changes with driving history and ignition resets were not controlled in this experiment; however it is unlikely that these factors had an effect on the results.

TEST RESULTS AND ANALYSIS

Graphical and statistical techniques were used to analyze the data and examine variability. Yaw Rate Ratio (YRR) and normalized yaw rate, the yaw rate divided by the second peak yaw rate, are used interchangeably in this paper.

Graphical Analysis

Graphical analysis was used to examine vehicle performance characteristics for major trends and to highlight variation of performance between vehicles and test conditions of interest. Graphical analysis provides an overall perspective of vehicle performance and provides direction for further statistical analysis.

Graphical analysis included:

- Plots of metrics versus time
- Cross plots of metrics and test variables
- Plot groupings for key variables such as track and temperature categories

Stability and Responsiveness metrics were examined graphically to identify overall patterns.

Stability Metrics - Yaw Rate Ratio vs. time was examined for both vehicle configurations at the five tracks and the three temperature ranges. Comparison of YRR vs. time illustrates the difference in yaw rate ratio decay between the two vehicle configurations. M32 yaw rate ratio (Figure 2) continues at a higher level and for a longer period of time than the 302 yaw rate ratio (Figure 3). This graph provides a sense of the difference in the magnitude of vehicle yaw that continues after the steering is returned to straight ahead. This data also provides an indication of performance variation between tracks.

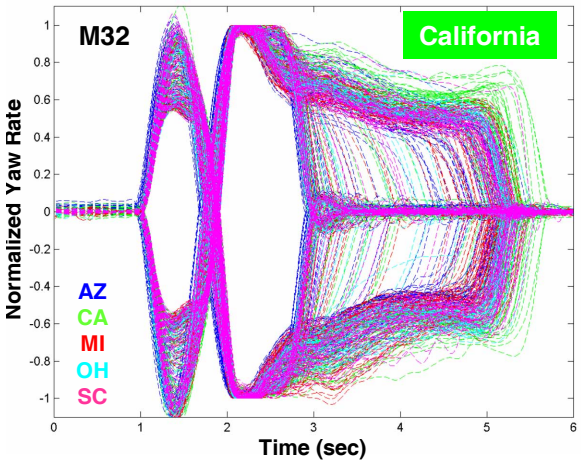

Figure 2. M32 YRR track sensitivity.

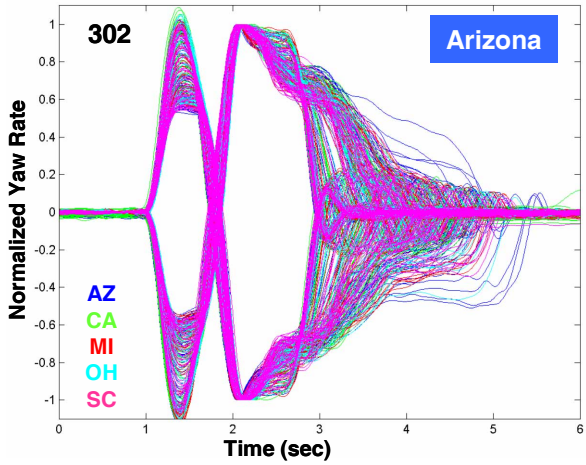

Figure 3. 302 YRR track sensitivity.

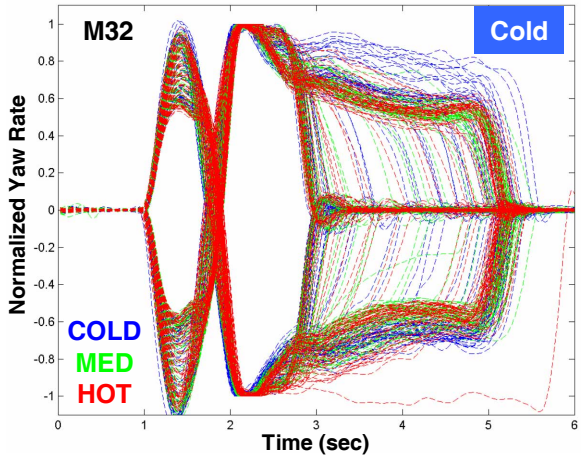

Figure 4. M32 YRR temperature sensitivity.

Examination of YRR vs. time for temperature variation indicates that the M32 configuration

(Figure 4) has a performance shift at Cold temperature that merits further examination. The 302 data (Figure 5) does not exhibit similar temperature sensitivity.

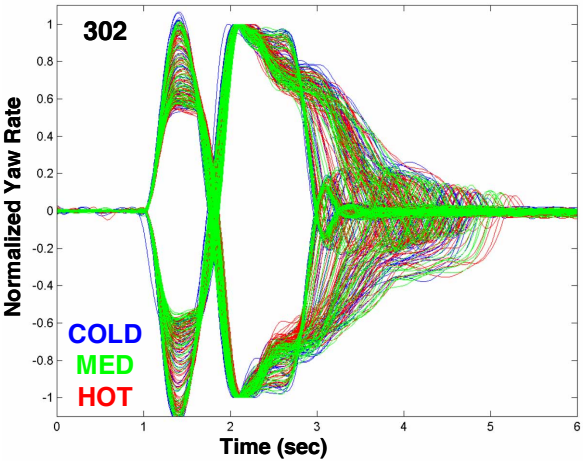

Figure 5. 302 YRR temperature sensitivity.

Plotting Peak YRR at particular times after end of steer versus all steering increments and then sorting by tracks, directions, and temperatures allows a closer examination of Yaw Rate Ratio variations.

The discussion which follows uses the following convention to denote the stability metrics in the FMVSS 126 NPRM:

YRR1 is the Yaw Rate Ratio 1.00 second after end of steer

YRR175 is the Yaw Rate Ratio 1.75 second after end of steer

Figure 6 shows that variation in YRR1 due to tracks is clearly observable for configuration M32.

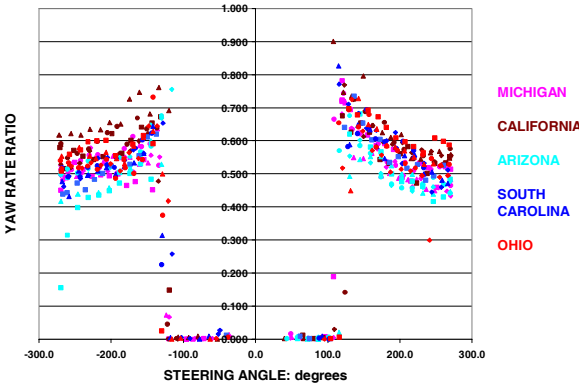

Figure 6. M32 YRR1 vs. steering angle: track sensitivity.

Figure 7 shows the temperature sensitivity in YRR1 for configuration M32.

Figure 8 shows variation in YRR175 due to tracks is observable in configuration M32.

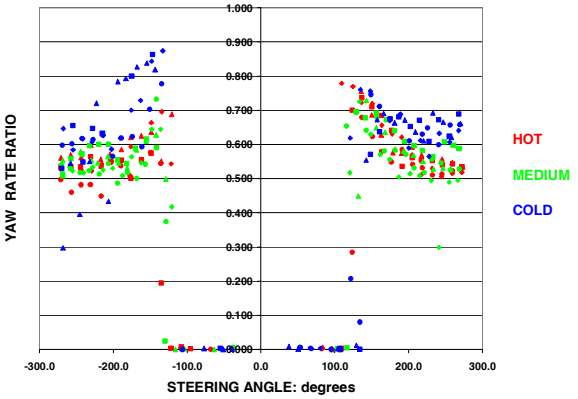

Figure 7. M32 YRR1 vs. steering angle: temperature sensitivity.

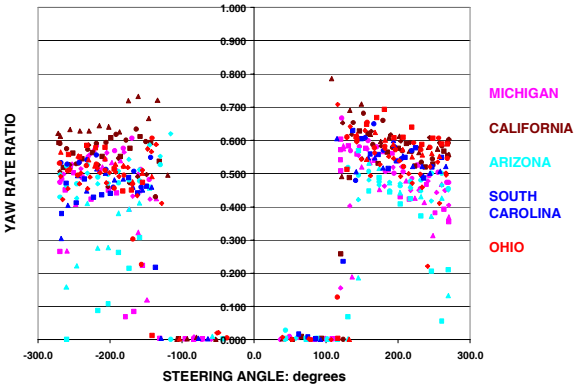

Figure 8. M32 YRR175 vs. steering angle: track sensitivity.

Figure 9 shows temperature sensitivity in YRR175 for the Cold temperature range in configuration M32.

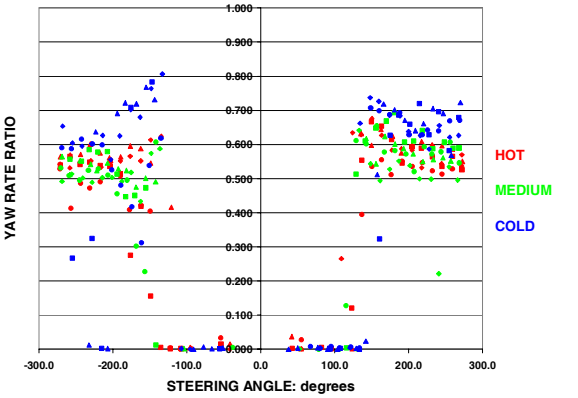

Figure 9. M32 YRR175 vs. steering angle: temperature sensitivity.

Figures 10 through 13 show the YRR metrics for configuration 302. It can be seen that configuration 302 has significantly lower yaw rate ratios compared to M32.

Track variation in YRR1 is difficult to observe, although Arizona appears to have higher than typical variation as seen in Figure 10.

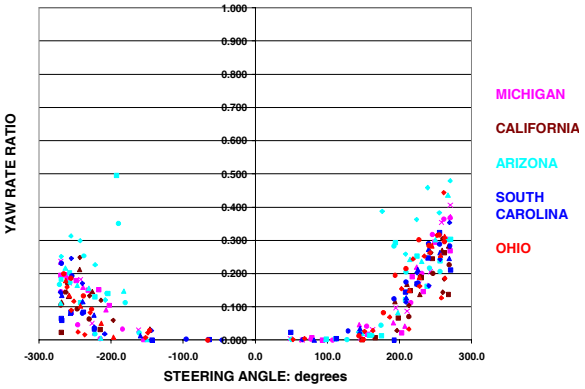

Figure 10. 302 YRR1 vs. steering angle: track sensitivity.

Temperature sensitivity is difficult to observe in configuration 302, as shown in Figure 11.

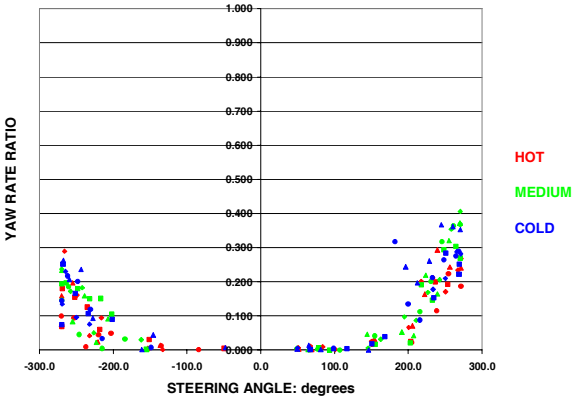

Figure 11. 302 YRR1 vs. steering angle: temperature sensitivity.

Trace amounts of yaw rate ratio are apparent at 1.75 seconds for configuration 302, as illustrated in Figures 12 and 13. Since vehicle yaw is basically complete 1.75 seconds after steer out, it is not surprising that track and temperature sensitivity is difficult to observe.

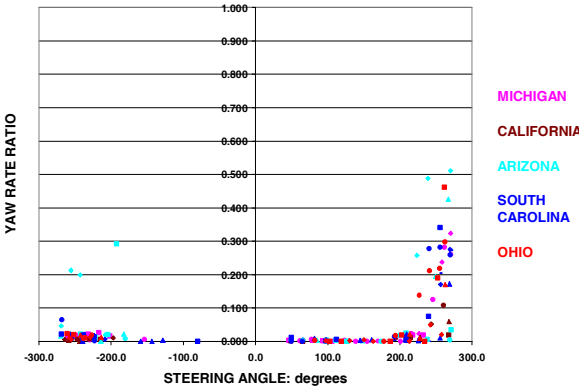

Figure 12. 302 YRR175 vs. steering angle: track sensitivity.

Graphical review of YRR for configurations M32 and 302 suggests that the M32 yaw rate ratio performance may show track and temperature sensitivity, while the 302 YRR performance is less likely to exhibit track and temperature sensitivity.

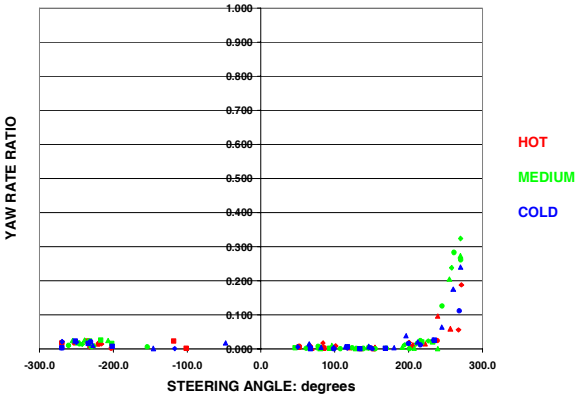

Figure 13. 302 YRR175 vs. steering angle: temperature sensitivity.

Responsiveness Metric – NHTSA's proposed vehicle responsiveness metric, the minimum lateral displacement observed at steering wheel angle amplitudes greater than or equal to 180 degrees (Min Dy) was calculated for the test configurations. Min Dy versus steering wheel angle was examined graphically and reviewed for run-to-run, track, and temperature variation:

Figure 14 shows variation due to tracks for configuration M32.

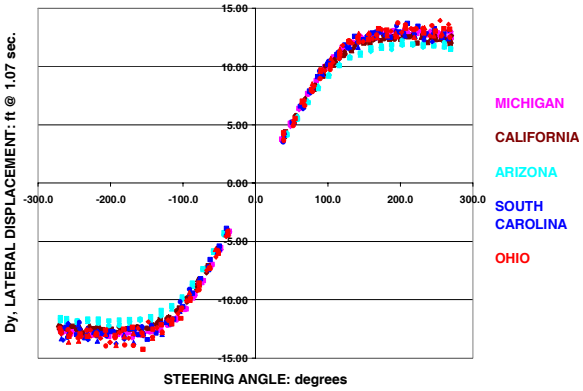

Figure 14. M32 Responsiveness vs. steering input: track variation.

Figure 15 shows that there may be some temperature sensitivity for configuration M32.

Figure 16 shows little variation due to track for configuration 302.

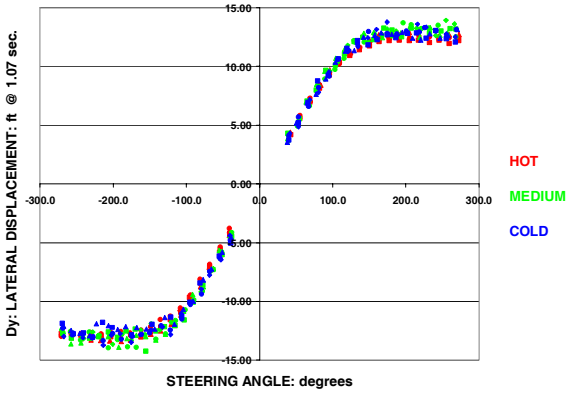

Figure 15. M32 Responsiveness vs. steering input: temperature variation.

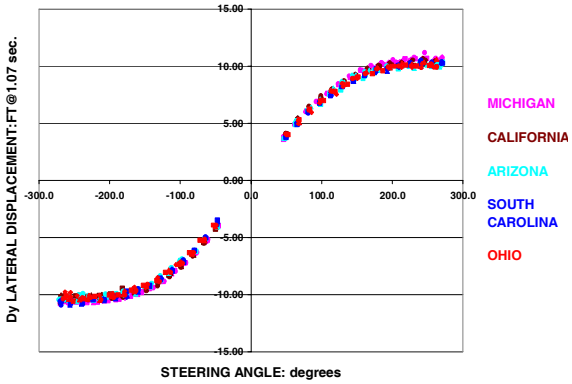

Figure 16. 302 Responsiveness vs. steering input: track variation.

Figure 17 shows some temperature sensitivity for configuration 302.

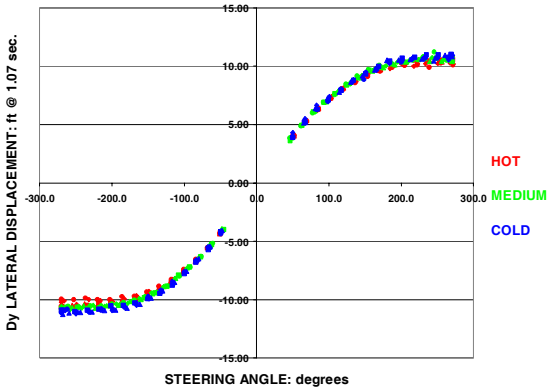

Figure 17. 302 Responsiveness vs. steering input: temperature variation.

Graphical review of the responsiveness plots for possible track and temperature sensitivity reveals probable track and temperature sensitivity for M32 and probable temperature sensitivity for 302. Statistical analysis was used to further quantify these sensitivities to track and temperature.

Statistical Methods

The statistical analysis techniques used in this variability study are described in this section. The detailed results generated by these methods are found in the section discussing a specific metric and in the VARIABILITY RESULTS SUMMARY section.

The analysis methods used in this study consisted of:

- Signal to Noise Ratios
- Confidence Interval Comparison
- Temperature Sensitivity
- Analysis of Variance (ANOVA)
- Pooled Standard Deviation

Different methods for combining standard deviations were also investigated.

Signal to Noise Ratio Calculations – Signal to Noise Ratio (S/N) is a good indicator of the robustness and discrimination capability of a given metric. A higher value is better. The ratio is calculated by dividing the difference between the metrics of each of the two vehicle configurations by the noise in the data.

$$S/N = 2\frac{|\mu_1 - \mu_2|}{CI_1 + CI_2} \qquad (1).$$

Where

μ_1 is the average of vehicle configuration 1's data for the considered runs

μ_2 is the average of vehicle configuration 2's data for the considered runs

CI_1 is the width of the 90% confidence interval for vehicle configuration 1's considered runs

CI_2 is the width of the 90% confidence interval for vehicle configuration 2's considered runs

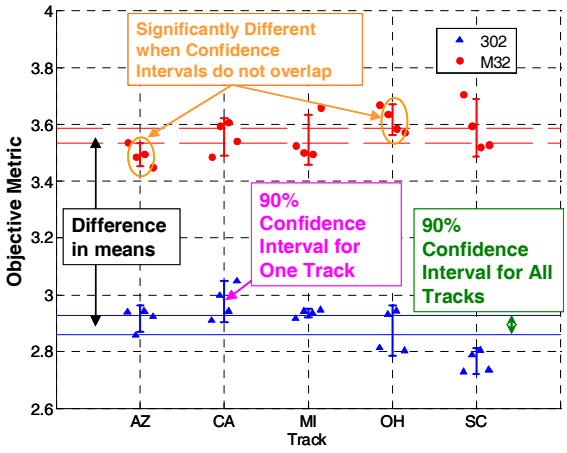

Figure 18. Example of elements of S/N calculation.

Confidence Interval Comparison – Using the sensitivity to track as an example, if variability were zero, it would be possible to get the same result at any track. One comparison metric is the number of times two tracks are statistically different (i.e. 90% confidence intervals do not overlap). This is shown in Figure 18. For five tracks, there are ten possible track pairings. Since there are two vehicle configurations, there are 20 possible track-by-vehicle pairings. A smaller number of non-overlapping pairs are preferred because the overlap shows that the results are track independent.

Pooled Standard Deviation – Since there are some statistically significant track differences, the run-to-run variation was calculated using a pooled standard deviation, where the variation about the mean of each vehicle at each track was summed so that track differences are not included in the run-to-run variability.

Variability due to tracks can be estimated by averaging all four test sequences at each track to get an average value for that track. Considering each vehicle separately, this collapses the data down to 10 values (5 tracks x 2 vehicles). Since the vehicles are statistically significantly different, the pooled standard deviation was calculated using 2 means (1 for each vehicle).

Temperature Sensitivity – The experiment was designed to examine tests conducted in three temperature ranges: Cold, Medium, and Hot by testing at three different times of year. Temperature sensitivity was examined using both the temperature category and the continuous range of temperature.

Once the sensitivity of a metric to temperature has been established, it is useful to know how significant the change due to temperature is compared to typical values of the metric. One method to answer this question is to consider a ΔT defined as the temperature change needed to make the metric change equal to the difference between the two vehicle configurations.

$$\Delta T = \frac{(M_1 - M_2)}{S} \qquad (2).$$

Where

M_1 is the metric value of vehicle configuration 1. This is calculated by doing a linear fit of the metric versus temperature and evaluating the linear fit at 50 deg F

M_2 is the metric value for vehicle configuration 2 at 50 deg F

S is the slope of the metric with respect to temperature

Metrics with higher ΔT values would rank vehicles more consistently across a broader range of temperatures. Temperature sensitivity is only calculated for a vehicle configuration when the slope (S) is statistically significant

Figure 19 shows a typical temperature sensitivity plot. In this case, only the slope for vehicle 302 is statistically significant, and it would take a 489 deg F temperature change to span the gap between the two vehicles at 50 deg F.

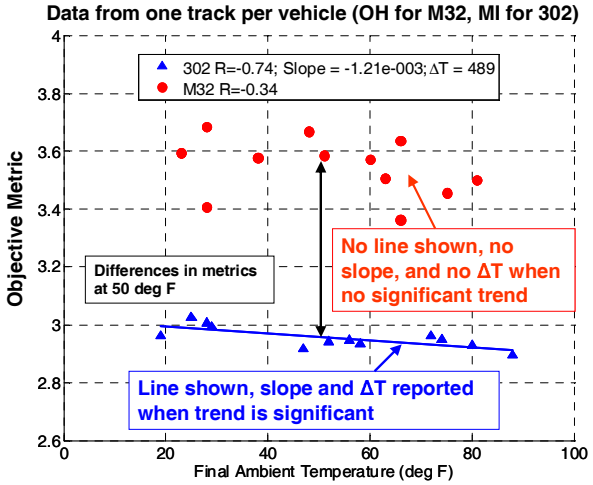

Figure 19. Example of Temperature Sensitivity method .

Another method for understanding the significance of temperature sensitivity is to multiply the sensitivity times the range of allowable temperatures so that the relative change in a metric due to temperature can be compared to the changes due to track and run-to-run variability.

Analysis of Variance – Results were calculated using DEXPERT, an expert system for the design and analysis of experiments [6]. Studies to investigate the effects of track and temperature range were conducted. The track sensitivity study only used the medium temperature range test configurations as they were common for every track. The temperature study used the MI track for the 302 configuration and the OH track for the M32 configuration, as these pairings consisted of testing each configuration over all three temperature ranges.

The components of variability that can be estimated from the structure shown in Table 3 are:

- Vehicle configuration, either 302 or M32
- Location, either MI, OH, SC, CA, or AZ
- Vehicle by Location interaction
- Time of Day, either AM or PM
- Vehicle by Time of Day interaction

- Location by Time of Day interaction
- Vehicle by Location by Time of Day interaction
- Day within Vehicle-Location combination
- Time of Day by Day within Vehicle-Location combination

Table 3.
Track Effect Design Structure

	300C										M3									
	MI		OH		SC		CA		AZ		MI		OH		SC		CA		AZ	
	D1	D2	D3	D4	D5	D6	D7	D8	D9	D10	D11	D12	D13	D14	D15	D16	D17	D18	D19	D20
AM	x	x	x	x	x	x	x	x	x	x	X	x	x	x	x	x	x	x	x	x
PM	x	x	x	x	x	x	x	x	x	x	X	x	x	x	x	x	x	x	X	x

The structure of the temperature sensitivity experiment shown in Table 4 is similar to the track sensitivity experiment except that instead of track, temperature is used. It should be noted that there is a confounding effect caused by the fact that configuration 302 was tested in MI and M32 was tested in OH. The results show that these tracks have similar characteristics, so the confounding effect is small.

Table 4.
Temperature Effect Design Structure

	300C						M3					
	Hot		Med		Cold		Hot		Med		Cold	
	D1	D2	D3	D4	D5	D6	D7	D8	D9	D10	D11	D12
AM	x	x	x	x	x	x	x	x	x	x	x	x
PM	x	x	x	x	x	x	x	x	x	x	x	x

The components of variability that can be estimated from the structure shown in Table 4 are:

- Vehicle configuration, either 302 or M32
- Temperature Range, either Hot, Medium, or Cold
- Vehicle by Location interaction
- Time of Day, either AM or PM
- Vehicle by Time of Day interaction
- Location by Time of Day interaction
- Vehicle by Location by Time of Day interaction
- Day within Vehicle-Location combination
- Time of Day by Day within Vehicle-Location combination

The ANOVA results are shown in the variability results summary section.

Yaw Rate Ratio 1 sec after Steer-Out (YRR1)

Figure 20 illustrates the normalized yaw rate responses for the variation study configurations versus a large number of test configurations conducted by NHTSA and the Alliance [1, 2, 7, 8]. Note that the initial test of the Threshold- configuration represented the central tendency of that configuration while the initial test of the Threshold+ configuration represented the lower boundary of that configuration.

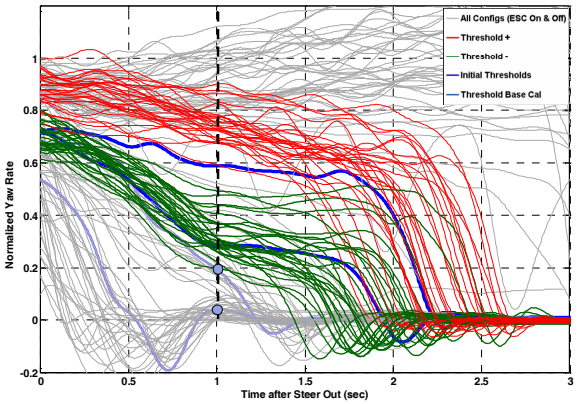

Figure 20. YRR1 variability configuration results vs. tested population.

The results in Figure 21 indicate good discrimination as there is no overlap in the YRR1 metric between the Threshold- and Threshold+ configurations.

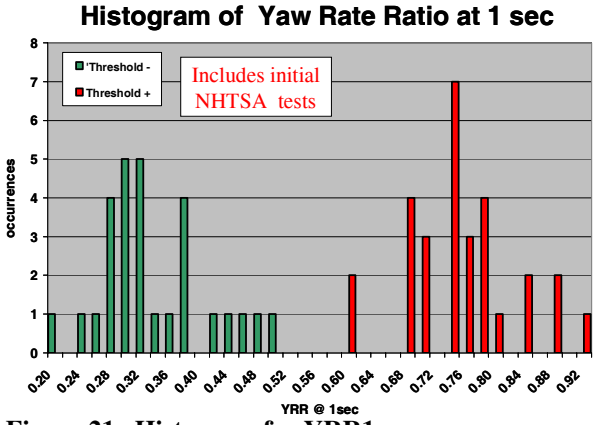

Figure 21. Histogram for YRR1.

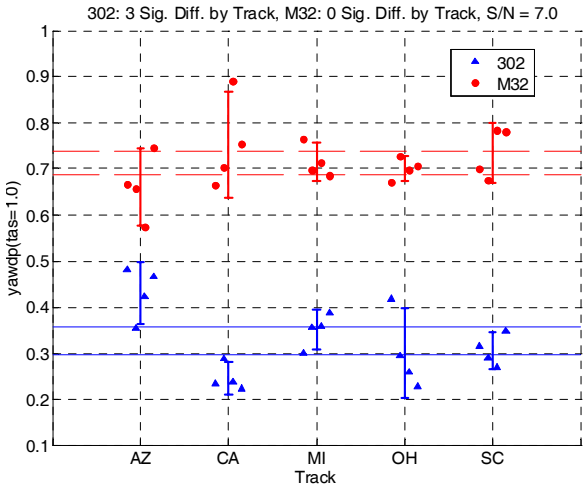

Figure 22. Three Track Differences for YRR1.

Figure 22 shows the yaw rate ratio measurements for each track. Configuration 302 shows three significant differences by track (CA different than MI, CA different than AZ, and AZ different than SC). The

pooled standard deviation for run-to-run variability is estimated at 0.06. The standard deviation for the tracks is estimated at 0.05.

Figure 23 shows the YRR1 versus temperature. Only vehicle M32 showed a statistically significant temperature sensitivity of 0.0022 /deg F. At higher temperatures the yaw rate at 1 second decayed more quickly.

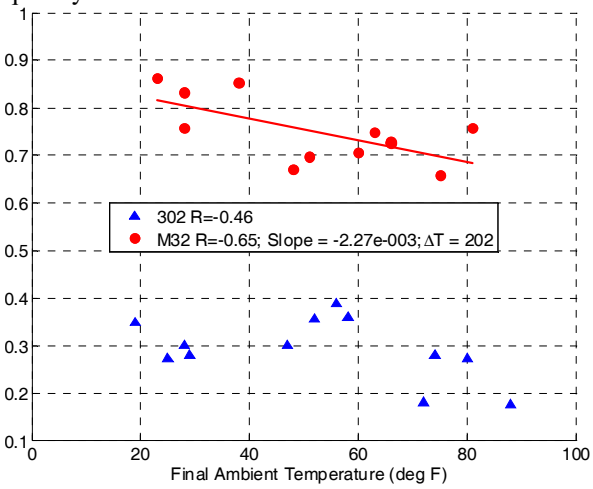

Figure 23. Temperature Sensitivity for YRR1.

Yaw Rate Ratio 1.75 sec after Steer-Out (YRR175)

Figure 24 illustrates the normalized yaw rate responses for the two vehicle configurations versus a large number of test configurations tested previously by NHTSA and the Alliance [1, 2, 7, 8]. Again, the initial test of the Threshold- configuration represented the central tendency of that configuration while the initial test of the Threshold+ configuration represented the lower boundary of that configuration for this performance metric.

The results in Figure 25 indicate reasonable discrimination capability as that there is no observed overlap in the YRR175 metric between the Threshold- and Threshold+ configurations. Although there is no observed overlap, the largest value for the Threshold- configuration is only marginally smaller than the smallest value for the Threshold+ configuration indicating that there would be a statistical overlap.

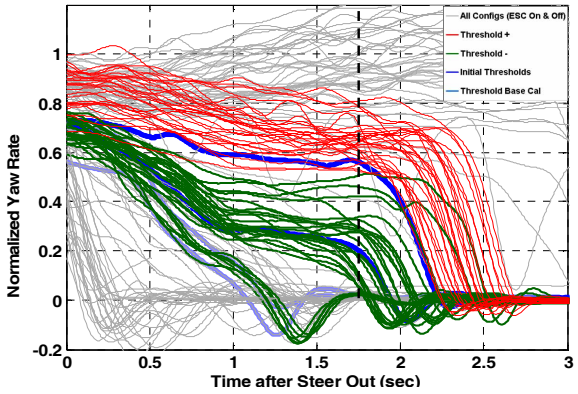

Figure 24. YRR175 variability configuration results vs. tested population.

Also note the bimodal nature of the Threshold- configuration. One central tendency is at 4 to 6 percent, and the other central tendency is at 28 to 30 percent. The cause for this result is not known, but it is hypothesized that the response of the vehicle may be near a threshold level of the ESC algorithm.

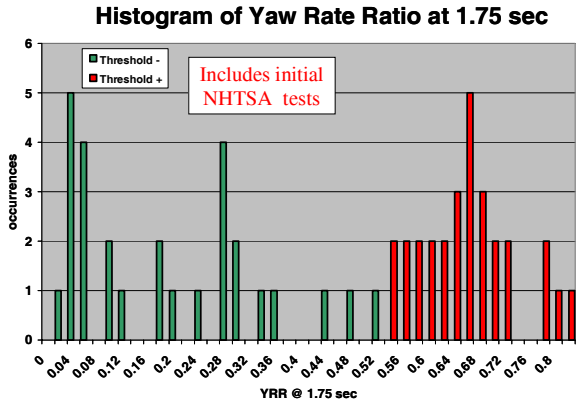

Figure 25. Histogram for YRR175.

Figure 26 shows the YRR175 for all the tracks. For each vehicle there are 3 significant track differences. The pooled standard deviation for the tracks is 0.08 and for run-to-run it is 0.11. Note that variability for YRR175 is higher than that for YRR1 because the YRR versus time curve (see Fig. 20) for configuration M32 is relatively steep near 1.75 seconds and therefore small differences in time to return to zero can result in large differences in YRR.

The temperature sensitivity for YRR175, seen in Figure 27, is similar to that for YRR1; only configuration M32 has a statistically significant slope. The temperature sensitivity of YRR175 is 0.0028 /deg F.

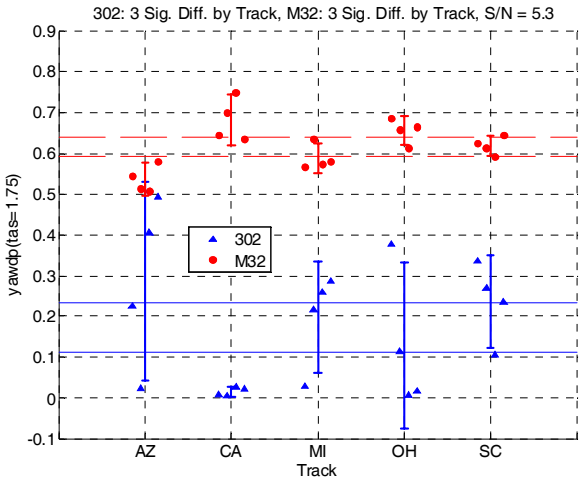

Figure 26. Six Track Differences for YRR175.

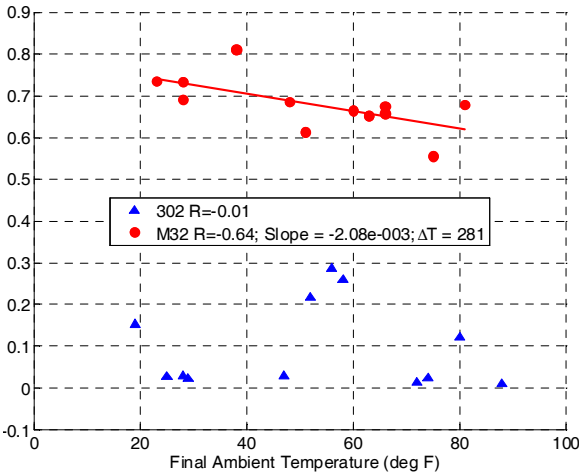

Figure 27. Temperature Sensitivity for YRR175.

RESPONSIVENESS TEST RESULTS

Figure 28 illustrates the lateral displacement response characteristics for the variation study configurations compared to a large number of vehicle tests conducted by NHTSA and the Alliance [1, 2, 7, 8].

The minimum lateral displacement observed at steering wheel angle amplitudes greater than or equal to 180 degrees (Min Dy), was calculated at the 90% confidence level and examined for track, temperature, and run-to-run sensitivities.

Ten significant track differences were observed in the proposed responsiveness metric, Min Dy. The range of track averages observed for Min Dy was 1.05 ft for configuration M32 and 0.55 ft. for configuration 302. This range is approximately ±5% of the overall mean.

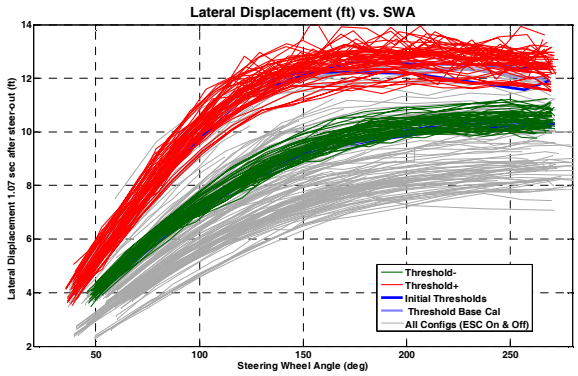

Figure 28. Responsiveness of M32 and 302 configurations vs. tested population.

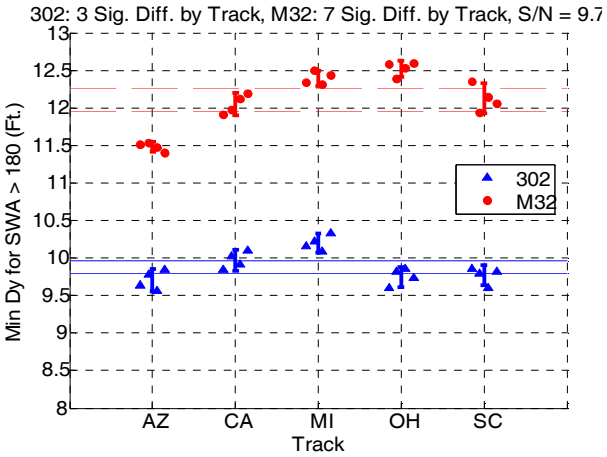

Figure 29. Track Sensitivity of Responsiveness (Min Dy).

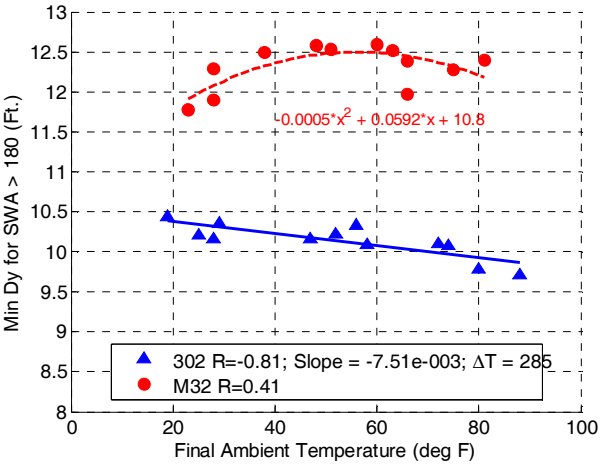

Figure 30. Min Dy temperature sensitivity.

Different patterns of temperature sensitivity were observed for M32 and 302 responsiveness metrics shown in Figure 30. The M32 exhibits a quadratic behavior with a peak in the mid-range of temperature. Configuration 302 exhibits linear behavior and is more responsive at lower temperatures. These same trends were noted in the graphical examination.

Configuration M32 was equipped with high-performance tires. High-performance tires are known to be sensitive to cold temperatures because the higher glass transition temperature of high-performance tire compounds results in lower adhesion at low temperatures. The data for configuration 302 is more typical of all season tires and is consistent with testing observations made during fishhook and other nonlinear vehicle handling tests.

This data indicates that testing variability can be reduced by narrowing the allowable temperature range, especially for vehicles equipped with all season tires.

Further investigation at a constant steering wheel angle, such as at 180 degrees, may shed light on vehicle, track, temperature, and run-to-run variation without the confounding effect of sorting by Min Dy, which occurs at steering angle input greater than 180 degrees.

Run-to-run Variation

Data acquired to assess track sensitivity was used to assess the run-to-run variation caused by random variation in the vehicle, instrumentation, and random variation in the specifics of a particular track (i.e. surface contamination, wind speed and direction, etc.). Track sensitivity can be estimated by pooling the standard deviations calculated for each series of four runs are summarized in Table 5. Pooling can be by configuration and for both configurations

Table 5.
Summary of Standard Deviations for Min Dy

Medium Temperature Only						
	AZ	CA	MI	OH	SC	Pooled
302	0.07	0.31	0.11	0.13	0.11	0.17
M32	0.06	0.13	0.08	0.07	0.18	0.12
					Pooled Run-to-Run	0.14
					Temperature Compensated Pooled Run-to-Run:	0.12

The standard deviations of the Medium temperature data are similar, so the data was combined to calculate the pooled standard deviation. The pooled standard deviation for run-to-run variation is calculated to be 0.12 feet or approximately 1.3% of the overall mean of Min Dy.

Since all the Medium temperature range data was not collected at the same temperature, statistically significant temperature sensitivities were removed before calculating the temperature-compensated, pooled run-to-run standard deviation.

VARIABILITY RESULTS SUMMARY

A summary of the FMVSS 126 proposed stability and responsiveness metrics for the two threshold vehicle configurations are shown in Table 6. The bimodal nature of the YRR175 metric for configuration 302 can be seen in the differences between the median and mean values. Also note the minimum values of Min Dy for both configurations (9.43 feet and 11.42 feet) are significantly larger than the proposed minimum required value of 6 feet.

Table 6.
Overall Summary of FMVSS 126 Metrics

	YRR @ 1 sec	YRR @ 1.75 sec	Min Dy @ swa>=180 deg (ft)
Median - **302**	**0.30**	**0.17**	**9.87**
Mean - **302**	**0.33**	**0.18**	**9.95**
St Dev	**0.07**	**0.15**	**0.28**
St Dev as % of mean	24%	88%	3%
Max	0.49	0.51	10.46
Min	0.20	0.02	9.43
Range	0.30	0.49	1.02
Range as % of mean	97%	289%	10%
Median - **M32**	**0.73**	**0.64**	**12.21**
Mean - **M32**	**0.74**	**0.65**	**12.12**
St Dev	**0.07**	**0.08**	**0.36**
St Dev as % of mean	9.8%	11.6%	3.0%
Max	0.90	0.81	12.60
Min	0.59	0.53	11.42
Range	0.31	0.28	1.18
Range as % of mean	42%	43%	10%

The standard deviations for the FMVSS 126 proposed performance metrics calculated using both the ANOVA and pooled standard deviation methods are shown in Table 7. The results from these two analysis methods show similar trends, except for temperature, where the data was treated differently. The temperature data in the ANOVA was segregated by temperature range and the temperature data in the Pooled method was the observed temperature at end of test.

Table 7.
Variability of Metrics

	ANOVA			POOLED		
Metric	YRR1	YRR175	min Dy SWA ≥ 180 deg (ft)	YRR1	YRR175	min Dy SWA ≥ 180 deg (ft)
Track (1σ)	0.05	0.06	0.40	0.05	0.08	0.31
Run-to-Run (1σ)	0.05	0.08	0.14	0.06	0.11	0.12
Temperature (1σ)	0.04*	0.03*	0.21*	0.12**	0.15**	0.41**

* 1 standard deviation in tested range
** worst case change over a range of 54 degrees F (104-50)

Tables 8 and 9 summarize the percent contribution of each factor in the experiment for each performance metric. The percent variation is given by:

$$\% \, Variation = \frac{V_{component}}{V_{total}} \quad (3).$$

Where

$V_{component}$ is the variation in the performance metric from the component examined

V_{total} is the total variation in the performance metric

Factors that Contribute to Variability

Table 8 shows the contribution of the track-related factors and their interactions (up to 3-way) on performance metrics. It can be seen that the effects of track itself are not present for the YRR metrics, but are present in the Min Dy metric. All metrics show the significant interaction of track sensitivity with vehicle configuration.

Table 8.
Percent Contribution for Track Study

	YRR @ 1 Sec	YRR @ 1.75 Sec	Min Dy for swa ≥ 180 deg	Legend
Vehicle (V)	91	82	94	90% Confidence
Location (L)	0	0	2	
V x L	5	5	3	75-90% Confidence
Time of Day (t)	0	0	0	
V x t	0	0	0	Comparison Only
L x t	0	0	0	
V x L x t	0	0	0	No Statistical Difference
Day (D)	0	7	0	
t x D	4	6	0	
Error	-	-	1	

Table 9.
Percent Contribution for Temperature Study

	YRR @ 1 Sec	YRR @ 1.75 Sec	Min Dy for swa ≥ 180 deg	Legend
Vehicle (V)	94	92	94	90% Confidence
Temperature (T)	1	1	1	
V xT	3	3	2	75-90% Confidence
Time of Day (t)	0	0	0	
V x t	0	0	1	Comparison Only
T x t	0	0	1	
V x T x t	0	0	0	No Statistical Difference
Day (D)	0	0	0	
t x D	2	4	0	
Error	-	-	1	

Table 9 shows the contribution of the temperature range-related factors and their interactions (up to 3-way) on performance metrics. It can be seen that the effects of temperature are present, but are overshadowed by the interaction of temperature sensitivity with vehicle configuration.

Robustness of Metrics to Variability

Table 10 summarizes robustness of the performance metrics to variability as assessed by the following measures:

- Signal/Noise Ratio
- Variance Ratio
- Number of Significant Track Differences
- Temperature Sensitivity

The various indicators for robustness show similar trends for the two YRR metrics. YRR1 appears to be more robust. It has a higher signal-to-noise ratio, a higher ratio of vehicle variance to random error, lower track sensitivity and similar temperature sensitivity.

The trends are mixed for Min Dy. Min Dy exhibits the highest values for signal-to-noise and variation ratio. This is confirmed by noting it has the lowest standard deviation as a percentage of the mean in Table 6. However, Min Dy is the most sensitive metric to different tracks.

YRR and Min Dy temperature sensitivity metrics can not be compared directly because the differences in responsiveness between the two configurations are much larger than the differences in stability.

Table 10.
Robustness to Variability Indicators

Metric Name	S/N	$\sqrt{s^2 Vehicle / s^2 Random}$	# Sig. Track Differences	302 ΔT	M32 ΔT
YRR1	**7.0**	**4.3**	**3**	**----**	**207**
YRR175	**5.3**	**3.6**	**6**	**----**	**196**
Min Dy for swa ≥ 180 deg	**9.7**	**9.5**	**10**	**285**	**----**

CONCLUSIONS

Similar variability findings were obtained using both ANOVA and pooled standard deviation techniques.

In all cases the individual variability components of the performance metrics are in the neighborhood of 3 to 5 percent of the differences seen between the two vehicle configurations.

Yaw Rate Ratio Metrics

The yaw rate ratio metrics discriminated between the two configurations with little to no overlap between these two vehicle configurations which, as previously noted, are near the proposed stability acceptance criteria for FMVSS 126.

The standard deviations of Yaw Rate Ratio @ 1 second due to track and run-to-run had similar values of approximately 0.05. The variation due to temperature was found to be ~0.12 over a 54 deg F temperature range.

Yaw Rate Ratio @ 1.75 seconds had a track to track standard deviation of ~0.07, a run-to-run standard deviation of ~0.10, and a variation of ~0.15 over a 54 deg F temperature range.

Responsiveness metric

The responsiveness metric discriminated, with no overlap, between these two vehicle configurations. Sensitivities to track and ambient temperature were found that are vehicle dependent.

Responsiveness (Min Dy) has a track-to-track standard deviation of approximately 0.31 feet or 2.8% of the mean. The range of observed Min Dy at five tracks is 10% of the mean. The run-to-run standard deviation is ~0.13 feet or 1.2% of the mean. The temperature sensitivity is 0.41 feet over a 54 deg F temperature range.

ACKNOWLEDGEMENTS

The authors wish to recognize the following organizations for providing testing facilities, test vehicles, engineering data, and logistics support: the Alliance of Automobile Manufacturers, DaimlerChrysler AG, DRI Inc, Ford Motor Company, General Motors Corp., Michelin Proving Ground, and NHTSA VRTC. Thanks also to Garrick Forkenbrock, Riley Garrott, and Andrew Snyder from NHTSA VRTC, Robert Thomas from Ford, and Joe Wolkan from GM for their insight into variability and statistics. The synergy of all those involved made this study possible.

REFERENCES

[1] Forkenbrock, G.J., Elsasser, D. H., O'Harra, B. C., Jones, R. E., "Development of Electronic Stability Control (ESC) Performance Criteria", September 2006, DOT HS 809 974

[2] Forkenbrock, G.J., "NHTSA's 2005 ESC Research Program: A Cooperative Effort", January 6, 2005, NHTSA VRTC presentation

[3] Alliance of Automotive Manufacturers "Variability Test Results Findings", September 21, 2006, In Docket Management System, NHTSA-2006-25801-9, (http://dmses.dot.gov/docimages/pdf98/419488_web.pdf)

[4] Federal Register / Vol. 71, No. 180 / Monday, September 18, 2006 / Proposed Rules, 54749, S5.2

[5] Alliance of Automotive Manufacturers, "Preliminary Alliance ESC NPRM Issues", October 27, 2006, In Docket Management System, NHTSA-2006-25801-31, (http://dmses.dot.gov/docimages/pdf99/430075_web.pdf)

[6] Lorenzen, T.J., Truss, L.T., Spangler, W.S., Corpus, W.T., Parker, A.B., "DEXPERT: an expert system for the design of experiments", Volume 2, Number 2/ June, 1992, Computer Science and Mathematics and Statistics, 47-54

[7] Alliance of Automotive Manufacturers, "Alliance Research of Non-Linear Handling Performance", December 3, 2004, In Docket Management System, NHTSA-2004-19951-1, http://dmses.dot.gov/docimages/pdf90/308904_web.pdf

[8] Alliance of Automotive Manufacturers, "Preliminary Results of ESC Performance Metric Evaluations", June 23, 2005, In Docket Management System, NHTSA-2004-19951-17, http://dmses.dot.gov/docimages/pdf92/337256_web.pdf

APPENDIX A

Test Tracks

Figure A1. TRC Skidpad, 1800 ft. x 1200 ft., East Liberty, OH

Figure A5. Dynamic Research Inc. Skidpad, 800 ft. x 300 ft., Shafter, CA

Figure A2. GM Milford Proving Ground Skidpad, 1600 ft. x 1500 ft., Milford, MI

Figure A3. Michelin Proving Ground Skidpad, 1600 ft. x 400 ft., Laurens, SC

Figure A4. DCX Arizona Proving Ground Skidpad, 1350 ft. x 900 ft., Whitman, AZ

APPENDIX B

Table of Results

Configuration	YRR @ 1 sec	YRR @ 1.75 sec	Min Dy @ swa>=180 deg (ft)	Test Site	Temp Range	Final Temp	Test Org
302 - NHTSA, ESC Int'	0.28	0.16	9.65	TRC	---	55	NHTSA
302 - GM, ESC Int, Hot AM 1 TS-A'	0.20	0.02	10.11	GM MPG	Hot	72	GM
302 - GM, ESC Int, Hot AM 2 TS-C'	0.22	0.02	9.72	GM MPG	Hot	74	GM
302 - GM, ESC Int, Hot PM 1 TS-B'	0.29	0.10	10.09	GM MPG	Hot	88	GM
302 - GM, ESC Int, Hot PM 2 TS-D'	0.29	0.19	9.79	GM MPG	Hot	80	GM
302 - GM, ESC Int, Medium Temp AM 1 TS-A'	0.30	0.03	10.17	GM MPG	Medium	47	GM
302 - GM, ESC Int, Medium Temp AM 3 TS-D'	0.37	0.28	10.23	GM MPG	Medium	56	GM
302 - GM, ESC Int, Medium Temp PM 1 TS-B'	0.37	0.27	10.10	GM MPG	Medium	52	GM
302 - GM, ESC Int, Medium Temp PM 2 TS-C'	0.41	0.32	10.35	GM MPG	Medium	58	GM
302 - NHTSA, ESC Int, SC, Medium Temp AM 1 TS-A'	0.32	0.34	9.80	Lauren SC	Medium	63	NHTSA
302 - NHTSA, ESC Int, SC, Medium Temp AM 2 TS-C'	0.29	0.28	9.77	Lauren SC	Medium	56	NHTSA
302 - NHTSA, ESC Int, SC, Medium Temp PM 1 TS-B'	0.27	0.17	9.57	Lauren SC	Medium	60	NHTSA
302 - NHTSA, ESC Int, SC, Medium Temp PM 2 TS-D'	0.35	0.28	9.80	Lauren SC	Medium	64	NHTSA
302 - DCX, ESC Int, AZ, Medium Temp AM 1 TS-A'	0.49	0.29	9.77	DCX APG	Medium	79	DCX
302 - DCX, ESC Int, AZ, Medium Temp AM 2 TS-C'	0.35	0.02	9.70	DCX APG	Medium	74	DCX
302 - DCX, ESC Int, AZ, Medium Temp PM 1 TS-B'	0.44	0.43	9.71	DCX APG	Medium	68	DCX
302 - DCX, ESC Int, AZ, Medium Temp P M 2 TS-D'	0.48	0.51	9.86	DCX APG	Medium	65	DCX
302 - Ford, ESC Int, Medium Temp AM 3 TS-D'	0.26	0.02	9.43	DRI	Medium	65	Ford
302 - Ford, ESC Int, Medium Temp PM 1 TS-B'	0.30	0.11	10.04	DRI	Medium	56	Ford
302 - Ford, ESC Int, Medium Temp AM 1 TS-A'	0.28	0.06	9.93	DRI	Medium	72	Ford
302 - Ford, ESC Int, Medium Temp PM 2 TS-C'	0.26	0.05	10.11	DRI	Medium	77	Ford
302 - NHTSA, ESC Int, OH, Medium Temp AM 1 TS-A'	0.44	0.46	9.60	TRC	Medium	61	NHTSA
302 - NHTSA, ESC Int, OH, Medium Temp AM 2 TS-C'	0.32	0.30	9.87	TRC	Medium	57	NHTSA
302 - NHTSA, ESC Int, OH, Medium Temp AM 1 TS-B'	0.31	0.17	9.87	TRC	Medium	68	NHTSA
302 - NHTSA, ESC Int, OH, Medium Temp AM 2 TS-D'	0.26	0.05	9.76	TRC	Medium	72	NHTSA
302 - GM, ESC Int, Cold Temp AM 1 TS-A'	0.28	0.03	10.46	GM MPG	Cold	28	GM
302 - GM, ESC Int, Cold Temp PM 2 TS-C'	0.32	0.11	10.36	GM MPG	Cold	19	GM
302 - GM, ESC Int, Cold Temp PM 1 TS-B'	0.37	0.24	10.45	GM MPG	Cold	29	GM
302 - GM, ESC Int, Cold Temp AM 2 TS-D'	0.29	0.03	10.23	GM MPG	Cold	25	GM
Average	**0.33**	**0.18**	**9.95**				
St Dev	0.07	0.15	0.28				
M32, ESC MTrack Mode'	0.59	0.54	11.57	TRC	---	44	NHTSA
M32-NHTSA, ESC MTrack Mode, OH, Hot AM 1 TS-A'	0.74	0.67	11.95	TRC	Hot	66	NHTSA
M32-NHTSA, ESC MTrack Mode, OH, Hot PM 1 TS-B'	0.68	0.56	12.22	TRC	Hot	75	NHTSA
M32-NHTSA, ESC MTrack Mode, OH, Hot AM 2 TS-C'	0.76	0.64	12.52	TRC	Hot	63	NHTSA
M32-NHTSA, ESC MTrack Mode, OH, Hot PM 2 TS-D'	0.78	0.68	12.33	TRC	Hot	81	NHTSA
M32-GM, ESC MTrack Mode, Medium AM 1 TS-A'	0.78	0.60	12.35	GM MPG	Medium	65	GM
'M32-GM, ESC MTrack Mode, Medium PM 1 TS-B'	0.74	0.67	12.50	GM MPG	Medium	69	GM
'M32-GM, ESC MTrack Mode, Medium AM 2 TS-C'	0.72	0.58	12.32	GM MPG	Medium	59	GM
'M32-3-GM, ESC MTrack Mode, Medium PM 2 TS-D'	0.68	0.57	12.45	GM MPG	Medium	69	GM
M32 - NHTSA, ESC Int, OH, Medium Temp AM 1 TS-A'	0.70	0.69	12.51	TRC	Medium	48	NHTSA
M32 - NHTSA, ESC Int, OH, Medium Temp PM 1 TS-B'	0.73	0.65	12.42	TRC	Medium	66	NHTSA
M32 - NHTSA, ESC Int, OH, Medium Temp AM 2 TS-C'	0.73	0.62	12.50	TRC	Medium	51	NHTSA
M32 - NHTSA, ESC Int, OH, Medium Temp PM 2 TS-D'	0.73	0.64	12.60	TRC	Medium	60	NHTSA
M32 - NHTSA, ESC Int, SC, Medium Temp AM 1 TS-A'	0.73	0.63	12.37	Lauren SC	Medium	60	NHTSA
M32 - NHTSA, ESC Int, SC, Medium Temp PM 1 TS-B'	0.69	0.65	11.95	Lauren SC	Medium	59	NHTSA
M32 - NHTSA, ESC Int, SC, Medium Temp AM 2 TS-C'	0.83	0.61	12.16	Lauren SC	Medium	52	NHTSA
M32 - NHTSA, ESC Int, SC, Medium Temp PM 2 TS-D'	0.77	0.71	12.04	Lauren SC	Medium	64	NHTSA
M32-Ford, ESC MTrack Mode, Cool AM 1 TS-A'	0.67	0.63	11.92	DRI	Medium	65	Ford
M32-Ford, ESC MTrack Mode, Cool PM 1 TS-B'	0.73	0.68	11.99	DRI	Medium	67	Ford
M32-Ford, ESC MTrack Mode, Cool AM 2 TS-C'	0.90	0.79	12.14	DRI	Medium	77	Ford
M32-Ford, ESC MTrack Mode, Cool PM 2 TS-D'	0.77	0.65	12.21	DRI	Medium	55	Ford
M32 - DCX, ESC Int, AZ, Medium Temp AM 1 TS-A'	0.68	0.57	11.52	DCX APG	Medium	69	DCX
M32 - DCX, ESC Int, AZ, Medium Temp PM 1 TS-B'	0.68	0.53	11.55	DCX APG	Medium	71	DCX
M32 - DCX, ESC Int, AZ, Medium Temp AM 2 TS-C'	0.60	0.53	11.48	DCX APG	Medium	70	DCX
M32 - DCX, ESC Int, AZ, Medium Temp PM 2 TS-D'	0.76	0.62	11.42	DCX APG	Medium	77	DCX
M32 - NHTSA, ESC Int, OH, Cold Temp AM 1 TS-A'	0.86	0.78	11.77	TRC	Cold	23	NHTSA
M32 - NHTSA, ESC Int, OH, Cold Temp PM 1 TS-B'	0.78	0.71	12.27	TRC	Cold	28	NHTSA
M32 - NHTSA, ESC Int, OH, Cold Temp AM 2 TS-C'	0.84	0.77	11.90	TRC	Cold	28	NHTSA
M32 - NHTSA, ESC Int, OH, Cold Temp PM 2 TS-D'	0.87	0.81	12.50	TRC	Cold	38	NHTSA
Average	**0.74**	**0.65**	**12.12**				
St Dev	0.07	0.08	0.36				